

RIN

NASA CR-

141743

THE NATA CODE - USER'S MANUAL, Volume II

W. L. Ball and J. M. Yos
Avco Systems Division
201 Lowell Street
Wilmington, Massachusetts 01887

JSC-III02

NAS9-9744
CR -141743

Final Report
Volume II

Prepared for

LYNDON B. JOHNSON SPACE CENTER
Houston, Texas 77058

(NASA-CR-141743) THE NATA CODE; THEORY AND
ANALYSIS. VOLUME 2: USER'S MANUAL Final
Report (Avco Systems Div., Wilmington,
Mass.) 302 p HC \$9.75

N76-21453

CSCL 20D

G3/34 25120 Unclassified

100-30000-
11-3

1. Report No. NASA CR-141743	2. Government Accession No.	3. Recipient's Catalog No.	
4. Title and Subtitle THE NATA CODE - USER'S MANUAL Volume II.		5. Report Date April 1970	
7. Author(s) W. L. Bade and J. M. Yos		6. Performing Organization Code JSC-11402	
9. Performing Organization Name and Address Avco Systems Division 201 Lowell Street Wilmington, Massachusetts 01887		8. Performing Organization Report No. AVSD-0068-75-CR	
12. Sponsoring Agency Name and Address National Aeronautics and Space Administration Lyndon B. Johnson Space Center Houston, Texas 77058		10. Work Unit No.	
		11. Contract or Grant No. NAS9-9744	
		13. Type of Report and Period Covered Contractor Report Final Report	
		14. Sponsoring Agency Code	
15. Supplementary Notes The final report on Contract NAS9-9744 consists of three volumes: Vol. I The NATA Code - Theory and Analysis (NASA CR-141747) Vol. II The NATA Code - User's Manual (NASA CR-141743) (present document) Vol. III The NATA Code - Programmer's Manual (NASA CR-141744)			
16. Abstract The NATA code is a computer program for calculating quasi-one-dimensional gas flow in axisymmetric nozzles and rectangular channels. The flow is assumed to start from a state of thermochemical equilibrium at high temperature in an upstream reservoir. The program provides solutions based on frozen chemistry, chemical equilibrium, and nonequilibrium flow with finite reaction rates. Electronic nonequilibrium effects can be included using a two-temperature model. An approximate laminar boundary layer calculation gives the shear and heat flux on the nozzle wall. Boundary layer displacement effects on the inviscid flow are taken into account. Chemical equilibrium and transport property calculations are provided by subroutines. NATA contains compiled-in thermochemical, chemical kinetic and transport cross section data for high-temperature air, CO ₂ -N ₂ -Ar mixtures, helium, and argon. It provides calculations of the stagnation conditions on axisymmetric or two-dimensional models, and of the conditions on the flat surface of a blunt wedge. The code's primary purpose is to describe the flow conditions and test conditions in electric arc heated wind tunnels. This volume of the final report on NATA is a user's manual for the code. It includes definitions of the inputs and outputs; tabulations and documentation of the pre-coded data on gas models, reactions, thermodynamic and transport properties of species, and nozzle geometries; explanations of diagnostic outputs and code abort conditions; illustrative test problems; and a user's manual for an auxiliary program (NOZFIT) used to set up analytical curvefits to nozzle profiles.			
17. Key Words (Suggested by Author(s)) planetary atmosphere arc-heated wind tunnels nonequilibrium flow thermal nonequilibrium high-temperature air		18. Distribution Statement SINR Subject Category: 54 (Fluid Mechanics and Heat Transfer)	
19. Security Classif. (of this report) Unclassified	20 Security Classif. (of this page) Unclassified	21. No. of Pages 10	22 Price* \$0.75

*For sale by the National Technical Information Service, Springfield, Virginia 22151

NASA -- JSC

PREFACE

NATA is a computer program for calculating steady, quasi-one-dimensional flow of a reacting gas mixture in a nozzle or rectangular channel. It also computes stagnation-point conditions on axisymmetric or two-dimensional models and the conditions on the flat surface of a blunt wedge. The code's primary purpose is the prediction and interpretation of test conditions in arc-heated wind tunnels used for laboratory evaluation of thermal protection materials for reentry vehicles such as the Space Shuttle Orbiter. The theory and analysis underlying the operation of NATA have been documented in Volume I of this report.* The present volume is a user's manual for the code. It defines the inputs and outputs, documents the precoded data on gas species and nozzle geometries, explains the diagnostic outputs, and includes illustrative results from test problems. In addition, this volume contains a user's manual for an auxiliary program (NOZFIT) which can be used to set up nozzle profile curvefits of the form used in NATA. The programming of NATA and NOZFIT is documented in Volume III.**

*W. L. Bade and J. M. Yos, The NATA Code - Theory and Analysis, NASA CR-2547.

**W. L. Bade and J. M. Yos, The NATA Code - Programmer's Manual, NASA CR-141744.

TABLE OF CONTENTS

	<u>Page</u>
1. Introduction.....	1
2. Inputs.....	2
2.1 Format Requirements for Input Cards.....	2
2.2 Input for Air Cases with a Standard Geometry...	8
2.3 General Inputs.....	12
2.4 Input of Gas Species and Reactions.....	36
2.5 Execution Time.....	44
3. Outputs.....	45
3.1 Listings of Input Variables.....	45
3.2 Problem Summary.....	49
3.3 Definitions of Output Identifiers.....	56
3.4 Reservoir Conditions.....	56
3.5 Flow Solutions.....	56
3.6 Model and Wedge Conditions.....	61
3.7 Throat Conditions.....	66
3.8 Informative Messages.....	66
3.9 Transport Cross Section Edit.....	71
3.10 Species Thermal Properties.....	78
4. Pre coded Data.....	79
4.1 Elements.....	79
4.2 Thermochemical Data for Species.....	80
4.3 Data for Reactions.....	121
4.4 Electronic Nonequilibrium Data.....	127
4.5 Standard Gas Models.....	134
4.6 Transport Cross Section Data.....	177
4.7 Nozzle and Channel Geometries.....	165
Appendix A - Reaction Data for the Helium and Argon Models.....	182
A.1 Helium Model.....	182
A.2 Argon Model	207
Appendix B - Diagnostic Messages	226

**CONTENTS
(Continued)**

	<u>Page</u>
Appendix C - Illustrative Test Problems.....	240
Appendix D - User's Manual for the NOZFIT Code.....	267
D.1 Introduction.....	267
D.2 Inputs of NOZFIT.....	267
D.3 Outputs of NOZFIT.....	270
D.4 NOZFIT Test Problem.....	272
References.....	278

LIST OF ILLUSTRATIONS

	<u>Page</u>
1. Input Data for a NATA Job with Three Cases.....	3
2. Listing of Input Cards for Test Problems No. 1 and 1A.....	46
3. NATA Code Output - Listing of Input Variables for Test Problem No. 1.....	47
4. NATA Code Output - Problem Summary for Test Problem No. 1.	50
5. NATA Code Output - Definitions of Output Identifiers.....	57
6. NATA Code Output - Reservoir Conditions for Test Problem No. 1.....	59
7. NATA Code Output - Frozen Solution for Test Problem No. 1.	60
8. NATA Code Output - Equilibrium Solution for Test Problem No. 1.....	62
9. NATA Code Output - Nonequilibrium Solution for Test Problem No. 1.....	63
10. NATA Code Output - Reaction Rate Data for Test Problem No. 1A.....	64
11. NATA Code Output - Model and Wedge Conditions for Test Problem No. 1.....	65
12. NATA Code Output - Equilibrium Sonic Conditions for Test Problem No. 1.....	67
13. NATA Code Output - Area Rescaling Message from Subroutine THRØAT in Test Problem No. 1.....	69
14. NATA Code Output - Freezing of Minor Species Message in Test Problem No. 1.....	70
15. NATA Code Output - Artificial Increase of Rate Constant Message	72
16. NATA Code Output - Transport Cross Section Edit (Input) ...	73
17. NATA Code Output - Transport Cross Section Edit (Edited) ..	76

LIST OF ILLUSTRATIONS
(Continued)

	<u>Page</u>
18. NATA Code Output - Transport Cross Section Edit (Averaged Pair Cross Sections)	77
19. Thermal Properties of e^-	91
20. Thermal Properties of N.....	92
21. Thermal Properties of O.....	93
22. Thermal Properties of Ar.....	94
23. Thermal Properties of N_2	95
24. Thermal Properties of O_2	96
25. Thermal Properties of NO.....	97
26. Thermal Properties of NO^+	98
27. Thermal Properties of N^+	99
28. Thermal Properties of O^+	100
29. Thermal Properties of N_2^+	101
30. Thermal Properties of O_2^+	102
31. Thermal Properties of CO_2	103
32. Thermal Properties of CO.....	104
33. Thermal Properties of CN.....	105
34. Thermal Properties of He.....	106
35. Thermal Properties of C.....	107
36. Thermal Properties of C^+	108
37. Thermal Properties of He^+	109
38. Thermal Properties of Ar^+	110

LIST OF ILLUSTRATIONS
(Continued)

	<u>Page</u>
39. Thermal Properties of He (³ S)	111
40. Thermal Properties of He (¹ S)	112
41. Thermal Properties of He ₂ ⁺	113
42. Thermal Properties of He ₂	114
43. Thermal Properties of CO ⁺	115
44. Thermal Properties of Ar*(m)	116
45. Thermal Properties of Ar*(r)	117
46. Thermal Properties of Ar ₂ ⁺	118
47. Profile for DCA 1.90-cm Throat (NØZZLE=1)	168
48. Profile for DCA 3.81-cm Throat (NØZZLE=2)	169
49. Profile for MRA 5.72-cm Throat (NØZZLE=3)	170
50. Profile for MRA 2.54-cm Throat (NØZZLE=4)	171
51. Profile for EOS 0.81-cm Throat (NØZZLE=5)	172
52. Profile for EOS 1.97-cm Throat (NØZZLE=6)	173
53. Profile for MRA 1.90-cm Throat (NØZZLE=7)	174
54. Profile for MRA 3.81-cm Throat (NØZZLE=8)	175
55. Profile for 10 Nw 5.72-cm Throat (NØZZLE=9)	176
56. Profile for EOS 2.77-cm Throat (NØZZLE=10)	177
57. First Profile for T12 and T22 Channels (NPRØFL=11)	178
58. Second Profile for T12 Channel (NPRØFL=12)	179
59. Second Profile for T22 Channel (NPRØFL=13)	180

LIST OF ILLUSTRATIONS
(Continued)

		<u>Page</u>
60. Momentum Transfer Cross Section for Electron-Helium Collisions	189	
61. Maxwell Averaged Electron-Helium Momentum Transfer Cross Section, $\bar{Q}_{e-He}^{(1,1)}$	190	
62. Reaction Rate for the Collisional De-excitation Process $He(2\ ^3S) + e^- \rightarrow He(1s^2) + e^-$	200	
63. Maxwell Averaged Momentum Transfer Cross Section $\bar{Q}_{e-Ar}^{(1,1)}$ for Collisions Between Electrons and Ground-State Argon Atoms	208	
64. Maxwell Averaged Momentum Transfer Cross Section for Collisions Between Electrons and Metastable $4s\ (^3P_2)$ Argon Atoms	210	
65. Input Data for Test Problems No. 2, 3, 4A, 4B, and 5.....	241	
66. First Page of Problem Summary for Test Problem No. 2	242	
67. Reservoir Condition Output for Test Problem No. 2	243	
68. Flow-Solution Output for Test Problem No. 2.....	244	
69. Problem Summary for Test Problem No. 3 (First Page)	245	
70. Problem Summary for Test Problem No. 3 (Second Page)	246	
71. Problem Summary for Test Problem No. 3 (Third Page)	247	
72. Problem Summary for Test Problem No. 3 (Fourth Page)	248	
73. Problem Summary for Test Problem No. 3 (Fifth Page)	249	
74. Reservoir Condition Output for Test Problem No. 3	250	
75. Output of Nonequilibrium Flow Solution for Test Problem No. 3 (First Page)	251	
76. Output of Nonequilibrium Flow Solution for Test Problem No. 3 (Second Page)	252	

LIST OF ILLUSTRATIONS
(Concluded)

	<u>Page</u>
77. Output of Nonequilibrium Flow Solution for Test Problem No. 3 (Third Page)	253
78. Output of Nonequilibrium Flow Solution for Test Problem No. 3 (Fourth Page)	254
79. Problem Summary for Test Problem No. 4A (First Page)	256
80. Problem Summary for Test Problem No. 4A (Second Page)	257
81. Reservoir Condition Output for Test Problem No. 4A	258
82. Equilibrium Solution for Test Problem No. 4A (First Page) ..	259
83. Problem Summary for Test Problem No. 5 (First Page)	260
84. Problem Summary for Test Problem No. 5 (Second Page)	261
85. Problem Summary for Test Problem No. 5 (Third Page)	262
86. Reservoir Condition Output for Test Problem No. 5	263
87. Nonequilibrium Solution for Test Problem No. 5 (First Page) ..	264
88. Nonequilibrium Solution for Test Problem N . 5 (Typical) ..	265
89. Output of NOZFIT Test Problem (First Page)	273
90. Output of NOZFIT Test Problem (Second Page)	274
91. Output of NOZFIT Test Problem (Third Page)	275
92. Output of NOZFIT Test Problem (Fourth Page)	276
93. Output of NOZFIT Test Problem (Fifth Page)	277

LIST OF TABLES

	<u>Page</u>
I. Data for Elements.....	80
II. Composition Data for Species	85
III. Thermo Fit Data	86
IV. Data for Physical Model	87
V. Degeneracies of Electronic States	88
VI. Energies of Electronic States	89
VII. Spectroscopic Data for Molecules	119
VIII. Reaction System for Air	122
IX. Reaction System for Argon	123
X. Reaction System for Helium	124
XI. Reaction System for Carbon and Argon Species in the Planetary Atmosphere Models	125
XII. Electronic Nonequilibrium Data for Helium Model	130
XIII. Electronic Nonequilibrium Data for Argon Model	131
XIV. e^- -He Momentum Transfer Cross Section	132
XV. e^- -Ar Momentum Transfer Cross Section	133
XVI. Standard Gas Models	135
XVII. Sources of Cross Section Data	149
XVIII. Precoded Data in the TL, ØMEGAL, ASTAR, and BSTAR Arrays.	162
XIX. Thermochemical Data for Helium Species	183
XX. Reaction Rate Parameters for Helium	184
XXI. Thermochemical Data for Argon Species	185

LIST OF TABLES
(Continued)

Page

XXII. Reaction Rate Parameters for Argon	186
XXIII. Low-Lying Excited States of the Argon Atom	213

THE NATA CODE - USER'S MANUAL

By W. L. Bade and J. M. Yos
Avco Systems Division
Wilmington, Massachusetts

I. INTRODUCTION

The NATA code is a computer program for solving problems of steady, quasi-one-dimensional gas flow in nozzles. The code's capabilities, and the theory and analysis underlying its operation, have been documented in the first volume of this report (ref. 1). The present volume is a user's manual for the code. Section 2 is a comprehensive discussion of NATA's inputs. Section 3 defines the normal outputs which present the results of the flow calculations and the calculations of test conditions on models. Section 4 documents the precoded data on gas models, transport properties, and nozzle geometries. Appendix A discusses the reaction data assumed in the electronic nonequilibrium models for argon and helium. Appendix B lists and explains the diagnostic outputs which NATA produces to aid the user in identifying the causes of abnormal conditions and code failures. Appendix C presents the inputs and outputs of test problems which illustrate the code's use and capabilities. Finally Appendix D is a user's manual for the NOZFIT code, a relatively small auxiliary program for setting up nozzle profile curvefits of the form required by NATA.

2. INPUTS

NATA employs a flexible, user-oriented input system called "Namelist", which is a standard feature of the Fortran IV programming language. The format requirements for the input card deck are summarized in Section 2.1. Section 2.2 discusses the few inputs that are required for running most problems of interest to NASA/JSC. Section 2.3 is a complete list of the definitions of all input variables accepted by NATA, except those used to read in the properties of chemical species and the rates of reactions. Input of these types of gas data is discussed in Section 2.4. In this discussion, the reader is assumed to be generally familiar with NATA's capabilities as summarized in the Introduction of Volume I (ref. 1).

Examples of sets of NATA input data for various types of problem, together with portions of the output produced when the code was run with these data, are presented in Appendix C.

2.1 Format Requirements for Input Cards

The input data for a NATA code run are punched on computer cards. The data for each case in the run require a deck of at least four cards, as explained below. The decks for the cases are stacked to obtain the input deck for the entire run or job. The cases are run in the order in which they appear in the job deck, from the top down. Figure 1 illustrates the input data for a job consisting of three cases. In this figure, the data are written* on an 80-column coding form. Each line of the form corresponds to a card in the input deck. Each column corresponds to one of the 80 columns in which data can be punched on a computer card.

*In figure 1, and in the text of this report, the letter O is written Ø to distinguish it from zero (0), and the letter I is written with scrips to distinguish it from the numeral 1.

ORIGINAL PAGE IS
OF POOR QUALITY

FIGURE 1 - INPUT DATA FOR A NATA JOB WITH THREE CASES

STATEMENT NUMBER		FORTRAN STATEMENT		IDENTIFICATION	
1	2	COUNT			
2	3	12 13 14 15 16 17 18 19 20 21 22 23 24 25 26 27 28 29 30 31 32 33 34 35 36 37 38 39 40 41 42 43 44 45 46 47 48 49 50 51 52 53 54 55 56 57 58 59 60 61 62 63 64 65 66 67 68 69 70 71 72 73 74 75 76 77 78 79 80			
SAMPLE CASE Nφ.	1	- FIRST CASE			
\$INPUT					
NΦΞΖΛΕ=1, PRESAI=1.5,	FLΦW=.153,	CXMXI=40.,	TΣΩΙΑΜ=10.,	ΙΑΜΣΕΙF,	ΜΑΝΓΛΕ=1,
ANGLE=10, NKAOLE=1,	RANDLE=.5,	CXMAXI=45,	WXI=1, 2, 5,		3, 5,
4.3, 5.	ISWHAI=1,				
\$END					
SAMPLE CASE Nφ.	2				
\$INPUT					
FLΦW=.236,	TPRNTI=1, E-3				
\$END					
SAMPLE CASE Nφ.	3	(LAST CASE - HENCE ΙΣΩΥΑ=0)			
\$INPUT					
FLΦW=.211,	PRESAI=2.5,	ΙΣΩΥΑ=0			
\$END					

The first card in the input deck for each case may contain any descriptive information desired by the user. This information is reproduced at the head of the printed output for the case. This card may be left blank, if desired; but it may not be left out.

The second card in the deck for each case must contain the following characters:

\$INPUT

in columns 2-7.*

The numerical input data for the case begin on the third card of the deck for the case. As many additional cards may be used as necessary. The data are punched in the form of equations:

variable name = value (1a)

or

array name = list of values (1b)

These equations are separated by commas. Also, the individual values of a list being read into an array are separated by commas. The admissible names for input variables and arrays are listed and defined in Sections 2.2 and 2.3, below.

The following is a condensed summary of the format requirements for the data cards. A more complete discussion may be found in the UNIVAC and IBM Fortran manuals (refs. 2, 3), under "Namelist".

*When the program is run on an IBM 360 system, the \$ is replaced by an EBCDIC ampersand or a BCD + sign.

- (1) The data must be punched in columns 2-80 of the cards; column 1 should be blank.
- (2) There may be no embedded blanks within the field occupied by a variable name or a numerical value (including the sign, if any). With this exception, blanks may be inserted freely to improve legibility and thus facilitate checking the cards.
- (3) The last item on each data card must be a constant (i.e., a value) followed by a comma. On the last data card for a case, the final comma is optional.
- (4) The number of values listed for an array must be less than or equal to the "number of entries" or the product of dimensions given in Sections 2.2 to 2.4.
- (5) The value given for any variable (except a logical variable) may be a number with or without a decimal point, or a number with a decimal followed by an exponent of 10 expressed in "E" notation. For example, 1.23×10^{-5} could be punched as 1.23E-5, and 9.8×10^{23} as 9.8E+23 or 9.8E23. For example, see the input for TPRINTI in figure 1.
- (6) The typing of variables as integer or real (see Section 2.2) is determined by the program. If a number without decimal is provided as input to a real variable, the name-list input system converts it to a real value before storing it. For example, in figure 1, the specification ANGLE = 10 has the same effect as ANGLE = 10.0. If a decimal number is provided as input to an integer variable, the system rounds it down to the next smallest

integer. For example, NANGLE = 1.3 would be equivalent to NANGLE = 1; however, NANGLE = 5.0 might have the effect of NANGLE = 4 on some computer systems where the 5.0 is represented as 4.999999... Thus, the decimal should be omitted in input values to integer variables.

Note: The remaining features (7-10) in the present list are not needed for setting up standard-type cases using the inputs of Section 2.2.

- (7) The input value to a variable typed "logical" (see Section 2.3) may be T for "true" or F for "false". For example, see the input for AAMS in figure 1.
- (8) In an input of array data in the form (lb), if several successive values in the list are equal to the same value v, these values can be given in the form n*v, where n is the number of values equal to v.
- (9) In the case of a multiply dimensioned array, the order in which the values must be listed is determined by the rule that the left-most index varies most rapidly and the right-most index least rapidly. For example, in a doubly dimensioned array such as ISHAPE(J, M), which is dimensioned (12,2), the values must be listed in the order

```
ISHAPE(1,1)
ISHAPE(2,1)
ISHAPE(3,1)

.
.

ISHAPE(12,1)
ISHAPE(1,2)
ISHAPE(2,2)

.
.

ISHAPE(12,2)
```

It is not necessary to set all of the elements of an array in the input list. However, the list in equation (1b) must begin with the first element and must include values for all elements up to the last one to which a value is assigned. For example, in a channel problem with four sections in each profile, the input for ISHAPE might be

ISHAPE = 1,2,2,1, 8*0,1,2,2,1,

The entry 8*0 fills up the elements ISHAPE(5,1), (ISHAPE(6,1),..., ISHAPE(12,1), which are not actually to be used. This entry is required to place the remaining data (1,2,2,1) into the locations ISHAPE(1,2),..., ISHAPE(4,2). If the 8*0 entry were omitted, the second set of data (1,2,2,1) would be loaded into ISHAPE(5,1),..., ISHAPE(8,1), instead. Note that the elements ISHAPE(5,2),..., ISHAPE(12,2) are not referenced in the above list and are not required.

- (10) A single element of an array can be set in the form (la), if the array name is given with its numerical subscripts; e.g., TSHAPE(3,2) = 1.

The last card in the input deck for each case, following the cards containing the data, must be punched*

\$END

in columns 2-5.

The Namelist input system processes the inputs of the form (1) one at a time, as they are encountered in the input deck. Thus, the order in which the input variables are referenced is arbitrary. If a variable is set more than once, the last value read is used by the program. For example, in figure 1, the program would run with CXMAXI = 45. Input variables which are not referenced in the input deck to a case are not changed; the program runs with the values already in storage in these locations. For example, in the second case of figure 1, only FLØW

*If NATA is run on an IBM 360, the \$ is replaced by an EBCDIC ampersand or a BCD + sign.

and TPRNTI are different from the values in the first case. Most of the input variables in NATA are preset to values which are either usually satisfactory or frequently desired, as indicated in Sections 2.2 and 2.3. If these variables are not referenced at all in the input to the job, the program runs with the preset values. This feature reduces the amount of input data required in most NATA runs by orders of magnitude. However, those variables which are not preset (such as the reservoir pressure, PRESAI) must be set in the input to the first case in every job; otherwise, the program would try to run with garbage data left in the computer by the preceding job, or with zero in the case of a computer in which core is cleared before each job.

A few of the input variables can be reset by operation of the code using certain options. Such exceptions to the rule that variables not referenced in the input do not change from case to case will be pointed out in Section 2.3. Examples include NOZZLE, ATPI, ISHAPE, NPRFLS, and IGAS. Apart from changes in IGAS due to automatic air model selection, these exceptions do not arise in jobs containing cases with only a single type of geometry, i.e., channels or nozzles.

2.2 Input for Air Cases with a Standard Geometry

The NATA code contains compiled-in data on the thermochemistry and reaction kinetics of certain gas mixtures (including air) and on the geometries of standard nozzles and channels in use at NASA/JSC. These precoded gas model and geometry data allow the NATA user to run certain standard types of problems by providing input data for just a few variables. The present section lists and defines these key inputs, under the following assumptions:

- (1) the gas is air;
- (2) the flow is confined by one of the available precoded standard nozzles or channels; and
- (3) the reservoir conditions are to be determined from data on the reservoir pressure and the total mass flow.

Sections 2.3 and 2.4 present a more comprehensive discussion of NATA inputs for users desiring to run nonstandard type problems or to use some of the special options which give the code its flexibility.

It is recommended that NATA users employ the input lists given below and in Section 2.3 as checklists in setting up problems.

The table below lists the names and definitions of the key input variables. For each variable, the "number of entries" is the number of numerical values which can be punched on the right hand side of the input equation (1). The preset values are compiled into the program and will be used unless a different value is supplied in the input deck. The abbreviations under "Type" have the following meanings:

R - Real (number containing a decimal point)

I - Integer (number without a decimal point)

<u>Variable</u>	<u>Number</u>	<u>Preset</u>		<u>Definition</u>
<u>Name</u>	<u>of Entries</u>	<u>Values</u>	<u>Type</u>	
PRESAI	1	---	R	Reservoir pressure (atm).
FLØW	1	---	R	Total Mass flow (lb/sec).
NØZZLE	1	0	I	Index of standard nozzles: 1 - DCA nozzle with 1.905 cm (0.75 inch) throat dia- meter 2 - DCA nozzle with 3.81 cm (1.5 inch) throat dia- meter 3 - MRA nozzle with 5.715 cm (2.25 inch) throat dia- meter 4 - MRA nozzle with 2.54 cm (1 inch) throat diameter 5 - EOS nozzle with 0.813 cm (0.32 inch) throat dia- meter

<u>Variable Name</u>	<u>Number of Entries</u>	<u>Preset Value</u>	<u>Type</u>	<u>Definition</u>
				6 - EOS nozzle with 1.968 cm (0.775 inch) throat dia- meter
				7 - MRA nozzle with 1.905 cm (0.75 inch) throat dia- meter
				8 - MRA nozzle with 3.81 cm (1.5 inch) throat dia- meter
				9 - 10 MW (Aerotherm) nozzle with 5.715 cm (2.25 inch) throat diameter
				10 - EOS nozzle with 2.764 cm (1.088 inch) throat dia- meter

Note: DCA, EOS, MRA, and 10 MW are designations for electric-arc gas heaters in use at the NASA/Johnson Space Center Arc Tunnel Facility:

DCA - Dual-Constrictor Arc

EOS - Electro-Optical Systems Heater

MRA - Modified Ring Arc

10 MW - Aerotherm Heater

ICHAN	1	0	I	Index of standard rectangular channels:
				1 - channel with 2.54 x 5.08 cm (1 x 2 inch) throat for DCA (use CXMAXI = 57.)
				2 - channel with 5.08 x 5.08 cm (2 x 2 inch) throat (nominal geometry) for 10 MW heater (use CXMAXI = 100.)

Note: Only one of the inputs, NOZZLE and ICHAN, is used in a given case. For ICHAN = 0, the flow geometry is determined by NOZZLE. For ICHAN > 0, the input data for NOZZLE are both ignored and overwritten, and the flow geometry is determined by ICHAN. If an axisymmetric flow problem follows one or more channel problems in the same job, it is necessary to input ICHAN = 0 and NPRFLS = 1.

<u>Variable Name</u>	<u>Number of Entries</u>	<u>Preset Values</u>	<u>Type</u>	<u>Definition</u>
CXMAXI	1	1.E5	R	Maximum distance beyond throat at which free-stream and model calculations will be done (inches). If CXMAXI is omitted, the calculations will continue until the free-stream temperature drops to 0.4 percent of the reservoir temperature.
TSDIAM(I)	20	1.E20	R	For nozzle flow problems, specified nozzle diameters at which stagnation point of model or leading edge of wedge will be placed for calculations of model test conditions. For channel problems, specified channel widths at which the free-stream flow and conditions on the channel wall will be calculated. Values assumed to be in inches.
KDIM	1	1	I	0 - two-dimensional model geometry 1 - axisymmetric model geometry

Note: The following 5 inputs are needed only if wedge calculations are desired. Wedge calculations cannot be obtained in channel flow problems.

<u>Variable Name</u>	<u>Number of Entries</u>	<u>Preset Values</u>	<u>Type</u>	<u>Definition</u>
NANGLE	1	0	I	Number of angles of attack for wedge.
ANGLE(I)	10	0.	R	Wedge angles of attack (degrees) in ascending order.
NRADLE	1	0	I	Number of leading edge radii for wedge.
RADLE(I)	5	0.	R	Wedge leading-edge radii (inches).
WXI(I)	20	1.E30	R	Distances from leading edge at which conditions on wedge will be calculated (inches).
ISW1A	1	1	I	0 suppresses frozen flow solution.
ISW2A	1	1	I	0 suppresses nonequilibrium flow solution.
ISW3A	1	1	I	0 suppresses equilibrium flow solution.
ISW4A	1	0	I	Must be nonzero if another case follows in the job. Must be 0 for last case.

2.3 General Inputs

The main inputs to the NATA code are read in under the Namelist name INPUT. All of the input variables in this group are defined in the present section. Data for new species and reactions and transport cross section data are read in under other namelist names, as explained in Section 2.4. Problems in which the precoded data for species and reactions are used require only the inputs discussed in the present section.

In the table of definitions below, the input variables are arranged in ten groups, as follows:

- (1) General control variables
- (2) Output controls
- (3) Reservoir conditions
- (4) Geometry
- (5) Gas model
- (6) Test model conditions
- (7) Wedge conditions
- (8) Controls for the flow solution
- (9) Electronic nonequilibrium
- (10) Controls for diagnostic dumps.

The table format is the same as in the preceding section, except that the array dimensions are listed in place of the "number of values". The type designations R for real and I for integer are defined as before; L denotes logical variables, whose admissible values are T for "true" and F for "false".

Group 1: General Control Variables

<u>Variable Name</u>	<u>Dimensions</u>	<u>Preset Values</u>	<u>Type</u>	<u>Definition</u>
ISW1A	1	1	I	Value 0 suppresses frozen solution.
ISW2A	1	1	I	Value 0 suppresses nonequilibrium solution.
ISW3A	1	1	I	Value 0 suppresses equilibrium solution.
ISW4A	1	0	I	Must be nonzero if another case follows in the job. Must be 0 in last case.

General Control Variables (Cont'd)

<u>Variable Name</u>	<u>Dimensions</u>	<u>Preset Values</u>	<u>Type</u>	<u>Definition</u>
ISW6A	1	0	I	If > 0 , only the reservoir conditions and transport properties in the reservoir are calculated. For the value 2, the reservoir transport property calculations are omitted. If < 0 , tables of species thermal properties at temperatures up to the reservoir temp are produced and no flow calculations are done.
<u>Note:</u> ISW6A < 0 should be used together with ISW2B = 1 and input of CTAPI and PRESAI (see Group 3 below).				
ISW1B	1	0	I	If > 0 , an edit of the steps in the transport property cross section calculations is produced before the flow solutions. If < 0 , averaged transport cross sections are also printed for temperatures up to CTAPI and the flow solutions are not computed. If = -1, these cross section data are also punched on cards.
<u>Note:</u> For ISW1B < 0 , also set ISW2B = 1 and read in CTAPI and PRESAI (see Group 3 below)				
ISW3B	1	1	I	If 0, boundary layer on nozzle wall is omitted.
TWALL	1	300	R	Nozzle wall temperature ($^{\circ}$ K)
NTRAN	1	.FALSE.	L	If .TRUE., all transport property, boundary layer, heat flux, and wedge calculations are suppressed.

General Control Variables (Concl'd)

<u>Variable Name</u>	<u>Dimensions</u>	<u>Preset Values</u>	<u>Type</u>	<u>Definition</u>
TST0PI	1	0.	R	Free-stream temperature at which the flow solutions will be terminated ($^{\circ}$ K). For value 0., the case is stopped at 0.004 times the reservoir temperature.
CXMAXI	1	1.E5	R	Distance beyond the throat at which the solutions will be stopped (inches).
READG	1	.FALSE.	L	If .TRUE., data on elements, species, and/or reactions will be read in under the namelist name EINPUT.
READXS	1	.FALSE.	L	If .TRUE., cross section data for transport property calculations will be read in under namelist name TINPUT.

Group 2: Output Controls

The inputs in this group allow some user control of the types and amount of printed output produced by the code.

<u>Variable Name</u>	<u>Dimensions</u>	<u>Preset Values</u>	<u>Type</u>	<u>Definition</u>
ISW6B	1	1	I	Value 0 suppresses output of species mole fractions in free-stream and model point output. Positive value gives mole fraction output every ISW6Bth printed step. Negative value also gives output of reaction rate data every ISW6B th printed step.

Output Controls (Concl'd)

<u>Variable Name</u>	<u>Dimensions</u>	<u>Preset Values</u>	<u>Type</u>	<u>Definition</u>
ISW7B	1	0	I	Value > 0 gives output of the boundary layer parameters $l^*=n$ and $XSN = \bar{n}$.
TPRNTI	1	0.01	R	The free-stream nonequilibrium solution is printed out at temperature intervals greater than or equal to TPRNTI times the reservoir temperature. For TPRNTI = 0., every step is printed.
DATAPE	1	.FALSE.	L	If .TRUE., data are written onto tape 3 for subsequent plotting.
NRECO	1	0	I	Number of records already on data tape at beginning of run.
IRUN	1	0	I	Run Number (for identification).

Group 3: Reservoir Conditions

The variables in this group control the calculation of the gas state in the upstream reservoir. The methods used are explained in Section 6.5 of Volume I (ref. 1).

<u>Variable Name</u>	<u>Dimensions</u>	<u>Preset Values</u>	<u>Type</u>	<u>Definition</u>
ISW2B	1	0	I	If 0, reservoir temperature is computed from reservoir pressure (PRESAI) and mass flow (FL/W). If positive, reservoir temperature (CTAPI) and pressure (PRESAI) are read in. If negative, reservoir temperature and pressure are computed from mass flow (FL/W) and stagnation enthalpy (HSTAG).
PRESAI	1	---	R	Reservoir pressure (atm). Required in input if ISW2B ≥ 0 .

Reservoir Conditions (Concl'd)

<u>Variable Name</u>	<u>Dimensions</u>	<u>Preset Values</u>	<u>Type</u>	<u>Definition</u>
FLØW	1	---	R	Total mass flow (lb/sec) if JDIM = 1 (see under "Geometry"); mass flow per inch (lb/in-sec) if JDIM = 0. (FLØW is required in the input if ISW2B ≤ 0.)
CTAPI	1	---	R	Reservoir temperature (°K). (Required in input if ISW2B > 0.)
HSTAG	1	---	R	Stagnation enthalpy (Btu/lb). (Required in input if ISW2B < 0.)
MFITER	1	1	I	0 value suppresses iteration to take displacement thickness into account in reservoir condition calculations based on mass flow (ISW2B ≤ 0).

**ORIGINAL PAGE IS
OF POOR QUALITY**

Group 4: Geometry

The geometry of a nozzle is specified, in NATA, by describing the nozzle profile. The geometry of a rectangular channel is specified by giving two profiles. There are four optional methods for defining the flow geometry in the input:

- (1) Standard nozzle - ICHAN must be 0, NPRFLS must be 1, NØZZLE must be an integer in the range from 1 to 10, inclusive.
- (2) Standard channel - ICHAN must be 1 or 2.
- (3) Nonstandard nozzle - ICHAN must be 0, NPRFLS must be 1, NØZZLE must be 0, and input data must be provided for DIAM(1), NSECTS(L,1), ISHAPE(J,1), PARAMI(K,J,1), ATPI(J,1), and XZERØI.
- (4) Nonstandard channel - ICHAN must be 0, NPRFLS must be 2, NØZZLE, NPROFL(1), and NPROFL(2) must be 0, and input data must be provided for DIAM(M), NSECTS(L,M), ISHAPE(J,M), PARAMI(K,J,M), and ATPI(J,M) for M = 1 and 2, and for XZERØI and NBL.

The description of nozzle and channel geometries in NATA is discussed in Sections 4.2 and 4.3 of Volume I (ref. 1).

Geometry (Cont'd)

<u>Variable</u>	<u>Preset</u>		<u>Type</u>	<u>Definition</u>
<u>Name</u>	<u>Dimensions</u>	<u>Values</u>		
NØZZLE	1	0	I	Index of standard nozzles:
				0 - nonstandard nozzle
				1 - DCA nozzle with 1.905 cm (0.75 inch) throat dia- meter
				2 - DCA nozzle with 3.81 cm (1.5 inch) throat dia- meter
				3 - MRA nozzle with 5.715 cm (2.25 inch) throat dia- meter
				4 - MRA nozzle with 2.54 cm (1 inch) throat diameter
				5 - EOS nozzle with 0.813 cm (0.32 inch) throat diameter
				6 - EOS nozzle with 1.968 cm (0.775 inch) throat diameter
				7 - MRA nozzle with 1.905 cm (0.75 inch) throat diameter
				8 - MRA nozzle with 3.81 cm (1.5 inch) throat diameter
				9 - 10 MW (Aerotherm) nozzle with 5.715 cm (2.25 inch) throat diameter
				10 - EOS nozzle with 2.764 cm (1.088 inch) throat diameter

Notes: NØZZLE is altered by input of NPRØFI, or by execution of a case involving ICHAN > 0. In cases with NØZZLE = 0, the first 4 characters on the description card at the head of the input data are used as a facility name.

Geometry (Cont'd)

<u>Variable</u>		<u>Preset</u>		<u>Definition</u>
<u>Name</u>	<u>Dimensions</u>	<u>Values</u>	<u>Types</u>	
ICHAN	1	0	I	Index of standard rectangular channels: 0 - not a channel, or nonstandard channel 1 - channel with 2.54 x 5.08 cm (1 x 2 inch) throat for DCA. (Use CXMAXI = 57.) 2 - channel with 5.08 x 5.08 cm (2 x 2 inch) throat (nominal geometry) for 10 MW heater. (Use CXMAXI = 100.)

Note: In channel cases with ICHAN = 0, the second 4 characters on the description card at the head of the input data are used as a channel name.

JDIM	1	1	I	0 - two-dimensional nozzle 1 - axisymmetric nozzle
------	---	---	---	---

Note: A two-dimensional nozzle may be considered as the limiting case of a rectangular channel when one of the channel profiles is at an infinite distance from the channel axis. This limit is of little practical interest. However, JDIM = 0 gives a convenient way of treating the flow in a channel in which two of the walls are straight and parallel, when the boundary layer is neglected (ISW3B = 0).

NPRFLS	1	1	I	Number of profiles: 1 - nozzle 2 - rectangular channel
--------	---	---	---	--

Note: The program sets NPRFLS = 2 if ICHAN > 0.

Geometry (Cont'd)

<u>Variable Name</u>	<u>Dimensions</u>	<u>Preset Values</u>	<u>Type</u>	<u>Definition</u>
NPRØFL(I)	2	0	I	Indices of profiles in a channel; NPRØFL(1) is equivalent to NØZZLE.
				0 - nonstandard profile
				1 to 10 - profiles for standard nozzles (see NØZZLE above)
				11 - profile 1 for T12 and T22 channels
				12 - profile 2 for T12 channel (ICHAN = 1)
				13 - profile 2 for T22 channel (ICHAN = 2)
NBL	1	---	I	Index (1 or 2) of the profile which diverges from the channel axis least rapidly downstream of the throat.
DIAM(M)	2	---	R	For a nozzle, DIAM(1) is the throat diameter (inches). For a channel, DIAM(M) is the throat diameter of the Mth profile for M = 1 and 2 (inches).
NSECTS(L,M)	2 x 2	---	I	NSECTS(1,M) = number of upstream sections in curvefit for Mth profile; NSECTS(2,M) = number of downstream sections in curvefit for Mth profile. For a nozzle, M = 1; for a channel, M = 1,2.

Geometry (Cont'd)

Variable <u>Name</u>	<u>Dimensions</u>	Preset <u>Values</u>	Type	<u>Definition</u>
ISHAPE(J,M)	12 x 2	---	I	Shape index for Jth section of Mth profile: ISHAPE = 1 straight section ISHAPE = 2 circular section convex toward axis ISHAPE = 3 circular section concave toward axis
				<u>Note:</u> ISHAPe is altered by use of NOZZLE > 0 or ICHAN > 0.
PARAMI(K,J,M)	3 x 12 x 2	---	R	Parameters for profile curvefit sections (lengths in centimeter units): For ISHAPe(J,M) = 1, equation of straight profile is $r(x) =$ PARAMI(1,J,M) + PARAMI(2,J,M)*X For ISHAPe(J,M) = 2 or 3, PARAMI(1,J,M) = distance of circle center from axis PARAMI(2,J,M) = X coordinate of circle center PARAMI(3,J,M) = circle radius
ATPI(J,M)	11 x 2	---	R	Downstream boundaries of profile curvefit sections, measured from throat (cm).
				<u>Note:</u> ATPI is altered by use of NOZZLE > 0 or ICHAN > 0.
XZERØT	I	---	R	Nozzle or channel inlet position at which boundary layer is assumed to begin (negative value, measured in inches upstream from throat).

Geometry (Concl'd)

Note: XZERØI is altered by use of NOZZLE > 0 or ICHAN > 0.

Note: A separate program (NOZFIT) is available for computing the inputs PARAMI and ATPI from nozzle or channel design data such as dimensions, angles, and radii of curvature; see Appendix D.

Group 5: Gas Model

NATA provides three methods for input specifications of the composition, thermochemistry and kinetics of the gas mixture:

- (1) Standard gas models - invoked simply by setting IGAS to 1, 2, 3, 4, 5, or 6.
- (2) Standard gas models with altered elemental composition - obtained by setting IGAS = -1, -2, -5, or -6 and specifying the mole fractions of the cold species (QPJ; see Section 4.5). Using this option, the standard air models can be modified to obtain models for (nearly pure) oxygen or nitrogen by setting the mole fraction for the other cold species (nitrogen or oxygen) to a small value. The proportions of CO₂, N₂, and Ar in the planetary atmosphere models can also be changed in this way.
- (3) Nonstandard gas models - specified by setting IGAS = 0 and reading in NCS, JCS, QPJ, ISCI, ISSI, ISRI, ICI, IE, IS, IR, ISATØM, and ISMØL. If species or reactions other than those compiled into the code are desired, they can also be read in as explained in Section 2.4.

The compiled-in species, reactions, and gas models available in NATA are fully described in Section 4.

<u>Variable Name</u>	<u>Dimensions</u>	<u>Preset Values</u>	<u>Type</u>	<u>Definition</u>
IGAS	1	1	I	Gas model index: 0 - nonstandard gas mixture; NCS, JCS, QPJ, ISCI, ISSI, ISRI, ICI, IE, IS, IR, ISATØM and ISMØL must all be speci- fied to the input. 1 - high-temperature air model 2 - moderate-temperature air model

ORIGINAL PAGE IS
OF POOR QUALITY

Gas Model (Cont'd)

<u>Variable Name</u>	<u>Dimensions</u>	<u>Preset Values</u>	<u>Type</u>	<u>Definition</u>
				3 - argon model including electronic nonequilibrium
				4 - helium model including electronic nonequilibrium
				5 - planetary atmosphere model (75% CO ₂ , 20% Ar, 5% N ₂) for use at reservoir temperatures above 7000°K.
				6 - planetary atmosphere model (75% CO ₂ , 20% Ar, 5% N ₂) for use at reservoir temperature below 7000°K

Note: If a negative value of IGAS is specified, then |IGAS| is the index of a standard gas mixture for which the mole fractions of cold species (QPJ) are to be provided in the input.

AAMS	1	.TRUE.	L	Control for automatic air model selection. If IGAS = 1 or 2 and AAMS = .TRUE., NATA resets IGAS to 1 or 2 based on an enthalpy or temperature criterion; for AAMS = .FALSE., the IGAS value specified in the input is used.
NCS	1	---	I	Number of cold species in mixture (≤ 10).
JCS(I)	10	---	I	Indices of cold species in the master list of species*.
QPJ(I)	10	---	R	Mole fractions of cold species in the same order as JCS (must be provided if IGAS ≤ 0).

*See Section 4.2.

Gas Model (Cont'd)

<u>Variable</u>		<u>Preset</u>			<u>Definition</u>
<u>Name</u>	<u>Dimensions</u>	<u>Values</u>	<u>Type</u>		
ISCI	1	---	I		Number of chemical elements in mixture, including e ⁻ if model contains ion species (≤ 10).
ISSI	1	---	I		Number of chemical species in mixture, including e ⁻ if model contains ion species (≤ 20).
ISRI	1	---	I		Number of reactions included in gas model (≤ 64).
ICI	1	---	I		Number of ions in gas model excluding e ⁻ .
IE(I)	10	---	I		Indices of elements present in mixture, in master list of elements;* if electrons are present, they should be the first element.
IS(J)	20	---	I		Indices of species present in mixture, in master list of species.**These species must be listed in the following order: e ⁻ (if present) Neutral species which are stable at low temperatures Other neutral species Ion species
IR	64	---	I		Indices of reactions included, in master list of reactions.***

*See Section 4.1.

**See Section 4.2.

***See Section 4.3.

Gas Model (Concl'd)

Note: If a nonequilibrium flow solution is to be run with the read-in gas model, there must be (ISSI-ISCI) linearly independent reactions in the chemical kinetic model; see Section 7.3.4 of Volume I (ref. 1). The standard gas models all satisfy this requirement.

Variable <u>Name</u>	<u>Dimensions</u>	Preset <u>Values</u>	Type	<u>Definition</u>
ISATØM	1	---	I	Index of atom used for Lewis number calculations, in master list of species.
ISMØL	1	---	I	Index of molecule used for Lewis number calculation, in master list of species.
CTMXXI	1	5000.	R	Temperature ($^{\circ}$ K) above which species thermal properties are computed from the thermo fit for those species for which thermo fits are supplied.
BZERØI	1	0.0	R	Constant in imperfect gas correction; the 0 value suppresses the correction, which is negligible for the conditions in which NATA is normally applied.
INEQVI	1	0	I	0 - equilibrium molecular vibration 1 - molecular vibration frozen at the reservoir temperature

Group 6: Test Model

NATA provides calculations of test conditions on two types of models: blunt bodies (stagnation point only) and wedges. A single set of inputs (XMØDPL, NMØDPT, TSDIAM) controls the positions in the flow at which test conditions are calculated for both types of model. These inputs and the parameters controlling options in the calculations for blunt models are in the present group. The wedge model inputs are in group 7.

Test Model (Cont'd)

In the case of blunt models, the test model position determined by the inputs is assumed to be the location of the model stagnation point. In the case of wedge models, it is assumed to be the location of the leading edge. There are two options for specifying the test model positions:

- (1) A geometric sequence of distances x downstream of the throat from $x = XM\emptyset DP1$ to $x = CXMAXI$.
- (2) The positions at which the nozzle diameter is equal to the input values TSDIAM(I).

These two options operate independently. In channel flow solutions, model condition calculations are not done but extra points in the free stream solutions are inserted at the locations specified by XM \emptyset DP1, NM \emptyset DPT, and TSDIAM, to provide results for comparison with experimental data from pressure taps and heat transfer gages located at known positions on the channel wall.

Regardless of the model-position inputs, no model or wedge calculations are done at positions where the flow Mach number is less than 1.5.

<u>Variable Name</u>	<u>Dimensions</u>	<u>Preset Values</u>	<u>Type</u>	<u>Definition</u>
XM \emptyset DP1	1	1.E20	R	Initial x for model condition calculations, measured in inches downstream of the throat.
NM \emptyset DPT	1	20	I	Number of model points to be placed in a geometric progression from XM \emptyset DP1 to CXMAXI; for NM \emptyset DPT = 1, the model calculation is done at $x = XM\emptyset DP1$.
TSDIAM(I)	20	1.E20	R	In nozzle flow problems, nozzle diameters specifying model positions; in channel problems, specified channel widths at which extra flow calculations are done (inches).
AXIM \emptyset D	1	.TRUE.	L	Value .FALSE. suppresses stagnation point model condition calculations, if only wedge conditions are desired.

Test Model (Cont'd)

<u>Variable Name</u>	<u>Dimensions</u>	<u>Preset Values</u>	<u>Type</u>	<u>Definition</u>
KDIM	1	1	I	Indicator for blunt model geometry: 0 - two-dimensional 1 - axisymmetric
FSTAG	1	1.0	R	Control for normal shock calculations: Negative - frozen shock Zero - equilibrium shock Positive - both frozen and equilibrium shock computed
CATFAC	1	1.0		Catalytic wall parameter ξ for stagnation point heat flux calculations;* 0 for noncatalytic model surface; theoretical upper limit is < 1.
LEWIS	1	1	I	Indicator for use of Fay-Riddell Lewis number factor in stagnation point heat flux calculations: 1 - include Lewis no. factor 2 - omit Lewis no. factor
TMODEL	1	300.	R	Surface temperature at stagnation point on model ($^{\circ}$ K).

*See Section 8.1.2 of Volume I (ref. 1).

Test Model (Concl'd)

<u>Variable Name</u>	<u>Dimensions</u>	<u>Preset Values</u>	<u>Type</u>	<u>Definition</u>
TPLATE	1	300.	R	Flat plate temperature for calculations of heat flux to a flat plate 1 ft from leading edge ($^{\circ}$ K).

Group 7: Wedge Models

Wedge model calculations are done only if the following conditions are satisfied:

- (a) Model positions have been specified by input of XM \emptyset DPL and CXMAXI, or of TSDT?M(I);
- (b) The flow Mach number at the specified model positions is greater than 1.5;
- (c) Positive values have been specified for both NANGLE and NRADLE; and
- (d) Either NWX > 0, or a value has been specified for WXI(1).

The positions along the surface of the wedge at which the conditions are calculated can be specified in two ways:

- (1) Uniform sequence - The inputs WX1, DWX, and NWX determine a uniformly spaced sequence of distances from the leading edge.
- (2) Specified distances - up to 20 arbitrary distances from the leading edge can be specified using the input array WXI.

Both options may be used together, if desired. In all cases, the specified distances from the leading edge are measured along the surface of the wedge (rather than parallel to the direction of the incident flow.)

Wedge Models (Cont'd)

<u>Variable Name</u>	<u>Dimensions</u>	<u>Preset Values</u>	<u>Type</u>	<u>Definition</u>
NANGLE	1	0	I	Number of wedge angles of attack.
ANGLE(I)	10	0.0	R	Angles of attack of wedge surface relative to the direction of incident flow (degrees), in ascending order.
NRADLE	1	0	I	Number of leading edge radii.
RADLE(J)	5	0.0	R	Radii of leading edge (inches).
WXI	1	1.0	R	Distance of the first computation point from the leading edge (inches).
DWX	1	1.0	R	Distance between computation points (inches).
NWX	1	0	I	Number of computation points in uniform sequence.
WXI(I)	20	1.E30	R	Specified distances of computation points from leading edge (inches)
TWEDGE	1	300.	R	Wedge surface temperature ($^{\circ}$ K).
WK	1	1.333	R	Nose drag coefficient for Cheng-Kemp wedge theory; the preset value is for a cylindrical leading edge.
ISW9B	1	0	I	Control for wedge model calculations and output: ≤ 0 = include calculations using unmodified Cheng-Kemp theory ≥ 0 = omit unmodified theory*

*See Section 8.2.4 of Volume I (ref. 1).

Wedge Models (Concl'd)

<u>Variable</u>		<u>Preset</u>			<u>Definition</u>
<u>Name</u>	<u>Dimensions</u>	<u>Values</u>	<u>Type</u>		
With IS9 = ISW9B :					
IS9 = 1 - print shock ordinate y_s					
IS9 = 2 - print nondimensional distance ζ from leading edge					
IS9 = 3 - print both y_s and ζ					

Group 8: Controls for the Flow Solutions

The inputs in this group are control parameters for the frozen, equilibrium and nonequilibrium flow solutions. They are all preset to values which have proven satisfactory in practice, and need be varied only rarely, to treat cases in which the code has failed to produce a satisfactory solution when run with the standard values.

<u>Variable</u>		<u>Preset</u>			<u>Definition</u>
<u>Name</u>	<u>Dimensions</u>	<u>Values</u>	<u>Type</u>		
WSAVE	1	3.0	R		Parameter controlling the averaging distance for the boundary layer correlation parameter, n. Instability due to coupling of the inviscid flow with the boundary layer can be suppressed by reducing WSAVE.*
DELTII	1	0.01	R		Nondimensional temperature decrement used in frozen and equilibrium calculations and in starting the nonequilibrium solution.
DELTXI	1	0.01	R		Initial step size in X for non-equilibrium integration (cm) (may be overruled by code).

*See Section 5.11 of Volume I (ref. 1).

Controls for the Flow Solutions (Cont'd)

<u>Variable Name</u>	<u>Dimensions</u>	<u>Preset Values</u>	<u>Type</u>	<u>Definition</u>
CCHI	1	0.1	R	Criterion value C_x for switch from perturbation technique to numerical integration in non-equilibrium solution; increase to switch farther downstream, decrease to switch farther upstream.*
NQSI	1	4	I	Number of successful integration steps before increasing step size in the nonequilibrium calculation.
TTEST	1	0.05	R	Maximum $ \Delta T/T $ in one step of the nonequilibrium integration; decrease to force a smaller step size.
GTEST	1	0.1	R	Maximum relative species concentration change in one integration step; decrease to force a smaller step size.
HTEST	1	0.01	R	Maximum relative change in the total enthalpy (due to radiative losses) in an integration step.
TETEST	1	0.05	R	Maximum relative change in the electron temperature in an integration step.
QTEST	1	0.1	R	Criterion value for maximum allowable change in the energy transfer to the electron gas during one integration step.
GAMIN	1	10^{-10}	R	Concentration (moles/g) below which a species will be frozen if it decreases so rapidly that it controls the integration step size.

*See Section 7.3.6 of Volume I (ref. 1).

Controls for the Flow Solutions (Co_1'd)

<u>Variable Name</u>	<u>Dimensions</u>	<u>Preset Values</u>	<u>Type</u>	<u>Definition</u>
DCHLL	1	10^{-4}	R	Parameter limiting the initial integration step size to $0.01 \delta \chi_i _{\min} / DCHLL$.
DCHRAT	1	10^{-4}	R	Parameter controlling the artificial increase in reaction rates in the perturbation solution to avoid premature startup of the numerical integration; minimum allowable $ \delta \chi_i _{\min} / \delta \chi_i _{\max}$ value.

Group 9: Electronic Nonequilibrium

The standard models for helium and argon include electronic nonequilibrium effects such as inequality of the electron temperature and gas temperature and nonequilibrium population of electronic excited states. NATA allows nonstandard gas models containing these features to be set up by the user. The inputs in the present group provide the extra gas model data required to specify these effects.

<u>Variable Name</u>	<u>Dimensions</u>	<u>Preset Values</u>	<u>Type</u>	<u>Definition</u>
INT	1	0	I	Indicator for electronic non-equilibrium: 0 - conventional one-temperature gas model Nonzero - two-temperature (electronic nonequilibrium) model
KTF(IR)	25	---	I	Indicator for forward rate constant k_f for IRth reaction in gas model

ORIGINAL PAGE IS
OF POOR QUALITY

Electronic Nonequilibrium (Cont'd)

<u>Variable Name</u>	<u>Dimensions</u>	<u>Preset Values</u>	<u>Type</u>	<u>Definition</u>
				$1 - k_f = k_f(T)$
				$2 - k_f = k_f(T_e)$
				where T = gas temperature, T_e = electron temperature, and the functional dependence of k_f is as given by equation (69) in Section 2.3 of Volume I (ref. 1)
				$3 - k_f = A \left(\frac{T_e}{10^4}\right)^{\eta} (1 - e^{-E_a/R_0 T})$
				$4 - k_f = A \left(\frac{T_e}{10^4}\right)^{\eta} / \max(1, \tau),$
				where $\tau = b n_p R / N_0$
				$5 - k_f = A / \sqrt{R}$

Note: In the standard gas models (IGAS = 1 to 6), the rate formulas indicated by KTF = 3, 4, and 5 are used only in the argon model (IGAS = 3). Note that for KTF = 3, k_f depends on both T_e and T . In the formulas for KTF = 4, 5, R denotes the local nozzle radius (or a corresponding effective value in the case of a channel). Also, n_p is the number density of the atomic species appearing on the product side of the reaction. See Appendix A for a discussion of these rate formulas.

KTR(IR)	25	---	J	Indicator for reverse rate constant k_r for IRth reaction in gas model:
				$0 - k_r = 0$
				$1 - k_r = k_r(T)$
				$2 - k_r = k_r(T_e)$

Electronic Nonequilibrium (Cont'd)

<u>Variable Name</u>	<u>Dimensions</u>	<u>Preset Values</u>	<u>Type</u>	<u>Definition</u>
ITR(IR)	25	---	I	Indicator of rule for partitioning the reaction energy of the IRth reaction; values may be 1 to 6.

Note: In the definitions below, ϵ_f and $-\epsilon_r$ denote the energies gained by the electron gas in N_0 reactions in the forward and reverse directions, respectively, and q_f , $-q_r$ denote the corresponding energies lost by radiation. Also, N_0 = Avogadro's number. The admissible values of ITR correspond to the following relations:*

ITR = 1	$\epsilon_f = -a R_0 T_e$,	$q_f = \epsilon_0 - \epsilon_f$
	$\epsilon_r = q_r = 0$	
ITR = 2	$\epsilon_f = -\frac{3}{2} R_0 T_e$,	$q_f = \epsilon_0 - \epsilon_f$
	$\epsilon_r = q_r = 0$	
ITR = 3	$\epsilon_f = \epsilon_r = q_f = q_r = 0$	
ITR = 4	$\epsilon_f = \epsilon_r = -\frac{3}{2} R_0 T_e$	
	$q_f = q_r = 0$	
ITR = 5	$\epsilon_f = \epsilon_r = \epsilon_0$	
	$q_f = q_r = 0$	
ITR = 6	$q_f = \epsilon_0$	
	$\epsilon_f = \epsilon_r = q_r = 0$	

The application of these reaction energy partition rules to reactions in argon and helium is discussed in Appendix A.

*The formulas for ITR = 2 are a special case of those for ITR = 1. The reasons for this formulation are historical rather than logical.

Electronic Nonequilibrium (Concl'd)

<u>Variable Name</u>	<u>Dimensions</u>	<u>Preset Values</u>	<u>Type</u>	<u>Definition</u>
EPAR(I,IR)	2 x 25	---	R	EPAR(1,IR) = parameter ϵ_0 for the IRth reaction in cal per N ₀ reactions; EPAR(2,IR) = parameter a for the IRth reaction if ITR(IR) = 1.
BPAR	1	---	R	Parameter b for all reactions with KTF = 4.
TLIST(J)	30	---	R	Temperature values for table of elastic collision cross section (°K).
PØM(J)	30	---	R	Elastic collision cross section values Q ^(1,1) for table (cm ²)

Group 10: Controls for Diagnostic Dumps

NATA contains a number of coded-in provisions for special output to facilitate tracing the operation of certain sections of the program. These diagnostic dumps are intended for use by programmers in analyzing causes of code failure. Ordinary users of NATA will rarely find occasion to invoke them. The input variables controlling these diagnostic outputs are defined below.

<u>Variable Name</u>	<u>Dimensions</u>	<u>Preset Values</u>	<u>Type</u>	<u>Definition</u>
ISW5A	1	0	I	If nonzero, the execution of subroutine RESTMP is traced by dumps.
ISW4B	1	0	I	If >0, a large dump is written each time the boundary layer routine BLAYER is called; if <0, a one-line dump is written.
ISW5B	1	0	I	If >0, large dumps are written each time the subroutines CØNM, EXACT, RNKT, PRTA are called and at a point in subroutine NØNEQ. If <0, these dumps are written

Controls for Diagnostic Dumps (Cont'd)

<u>Variable</u>		<u>Preset</u>			<u>Definition</u>
<u>Name</u>	<u>Dimensions</u>	<u>Values</u>	<u>Type</u>		
ISW5B (Cont'd)					every $ ISW5B $ th entry into CMM, and a one- or two-line dump is written by NONEQ in every step.
ISW8B	1	0	I		If nonzero, diagnostic dumps are printed in the transport property routines. For $ISW8B > 0$, PUTQIN dump is produced every $ISW8B$ times. For $ISW8B < 0$, PUTQIN dump is suppressed.

2.4 Input of Gas Species and Reactions

Elements, chemical species, and reactions other than those available in the precoded data can be defined and used in NATA flow calculations. These additional data are read in under the namelist name EINPUT. If such data are to be provided, the input variable READG in the main input must be set to .TRUE.. Then, immediately following the \$END card of the main input, there must be a card containing

\$EINPUT

in columns 2-8. This card is followed by the input data, discussed below, in the namelist format described in Section 2.1, and the input data cards must be followed by another card with \$END in columns 2-5.

The input variables for defining chemical elements are NEELS, a ten-entry array IEEP(I), and ten two-entry arrays EEP1, EEP2, ..., EEP10. These variables are defined in the following table. None of them are preset.

<u>Variable Name</u>	<u>Dimensions</u>	<u>Type</u>	<u>Definition</u>
NEELS	1	I	Number of elements being defined (≤ 10).
IEEP(I)	10	I	Indices assigned to the defined elements in the master list of elements.
EEPn(J)	2	R	Data for nth defined element J = 1 atomic number J = 2 atomic weight (g/mole)

The elements available in the precoded data and their assigned positions in the master list of elements are specified in Section 4.1.

The input variables for defining chemical species are SP1, SP2, ..., SP30, each of which is a 43-entry array. The number n in the array name SPn is the index assigned to the species in the master list. The available species, their properties, and their locations in the master list are all specified in Section 4.2. Data for any of the standard species can be changed for a particular NATA run by reading in the SPn array used to store its properties.

The data in the SPn arrays are defined and discussed in detail in Section 4.2. The definitions of the SPn array entries are summarized briefly below for convenient reference. All entries are real, but those with integer values may be punched without decimal points, as the Namelist input system will supply the decimals and NATA provides for reliable rounding down to the correct integer values in cases where this is required.

- | | |
|----------|---|
| SPn(1) | Read in 0. (Contains species name in compiled-in data; the code supplies a name for identifying the species in the output.) |
| SPn(2) | Number of chemical elements in species (≤ 3). |
| SPn(3-5) | Indices of elements in the master list of elements (as modified by input data for elements). |
| SPn(6-8) | Numbers of atoms of elements in a molecule of the species. |
| SPn(9) | Thermo-fit coefficient* n. |

*See Section 2.2 of Volume I (ref. 1).

SPn(10)	Thermo-fit coefficient b.
SPn(11)	Thermo-fit coefficient c.
SPn(12)	Thermo-fit coefficient d.
SPn(13)	Thermo-fit coefficient e.
SPn(14)	Thermo-fit coefficient k.
SPn(15)	Formation enthalpy at 0°K (cal/mole).
SPn(16)	Number of atoms per molecule*.
SPn(17)	Chemical constant,** b.
SPn(18)	Characteristic vibrational temperature (°K).
SPn(19)	Number of electronic levels (≤ 10).
SPn(20)	1 if thermo fit data are used for species, 0 if not.
SPn(21-30)	Degeneracies of the electronic levels.
SPn(31-40)	Energies of the electronic levels (cal/mole).
SPn(41-43)	Vibrational temperatures for the second, third, and fourth vibrational modes (triatomic species only) (°K).

When a new species model (as defined by an SPn array) is first set up, it is advisable to make a preliminary run with ISW6A = -1 (Section 2.3, Group 1) to print a table of species properties as calculated from the model. Errors in the species inputs can be detected more readily in such a table than in the results of flow calculations.

*Input of SPn(16) = 0 suppresses all use of the "physical model" for calculating the thermal properties of the species. In this case, the properties are calculated from the thermo fit at all temperatures, and SPn(17-19) and SPn(21-43) are not used; SPn(20) must be equal to 1 in this case.

**See Section 2.2 of Volume I (ref. 1).

The input variables for defining reactions are RP1, RP2,..., RP64, each of which is a 29-entry array. The entries are defined, and the available compiled-in reactions are specified, in Section 4.3. The definitions are repeated here for ease of reference. All of the entries are real, but those with integer values may be punched without the decimal point.

- RPn(1) Constant A in rate equation (sec^{-1} , $\text{cm}^3/\text{mole}\cdot\text{sec}$, or $\text{cm}^6/\text{mole}^2\cdot\text{sec}$).
RPn(2) Exponent η in rate constant formula.*
RPn(3) Activation energy E_a in rate constant formula.*
RPn(4) 1.0 if a list of third-body species is provided in RPn (20-29); 0.0 if not
RPn(5) Number of reactant species (≤ 3).
RPn(6) Number of product species (≤ 3).
RPn(7-9) Indices of reactant species in the master list of species, as modified by the input data for species (if any).
RPn(10-12) Indices of product species in the master list of species.
RPn(13-15) Numbers of molecules of reactants.
RPn(16-18) Numbers of molecules of products.
RPn(19) Number of third bodies (≤ 10).
RPn(20-29) Indices of third body species in master list of species.

If any transport property calculations are to be done for new species read in under EINPUT, it is also necessary to provide transport cross section data for the species. However, if only

*Equation (69) in Section 2.3 of Volume I (ref. 1); see also the definition of KTF(IR) under Group 9 in Section 2.3 above.

inviscid flow calculations are desired, the code can be run without cross section data by setting the control variable NTRAN to .TRUE. in the main input (Section 2.3, Group 1); this suppresses all transport property, boundary layer, heat flux, and wedge calculations everywhere in the code.

If transport property calculations involving a new species are required, the variable READXS in the main input must be set to .TRUE., and the cross section data for the species are then read in under the namelist name TINPUT. The input cards containing these data immediately follow the deck of cards read under the name EINPUT. They begin with a card containing

\$TINPUT

in columns 2-8. This card is followed by the cards containing the cross section input data in the namelist format described in Section 2.1. The final card of this group must contain \$END in columns 2-5.

The transport property inputs are as follows:

<u>Variable</u>			<u>Definition</u>
<u>Name</u>	<u>Dimensions</u>	<u>Type</u>	
NNKQ	1	I	Number of steps in the cross section calculation for which data are specified (including compiled-in data).
KKQ(N)	100	I	Index specifying the option to be used in the Nth step of the cross section calculations (allowed values, 2 through 14). NNKQ values are required. (The meaning of each of the allowed KKQ values is given in Section 4.6).
NNQ(N)	100	I	Number of pairs of species to which the cross sections calculated in the Nth step are to be applied. NNQ values are required. (NNQ(N) ≤ 5).

<u>Variable Name</u>	<u>Dimensions</u>	<u>Type</u>	<u>Definitions</u>
In(K)	5	I	Indices of the species to which the cross sections calculated in the Nth step are to be applied, referred to the master species list. In these variable names, n denotes an integer (equal to N) which is part of each name. There are 100 arrays of each type, namely I1(K), I2(K),..., I100(K), J1(K)..., J100(K). There are NNQ(N) pairs of indices In, Jn for each step N. Only pairs with In(K) ≤ Jn(K) are used in the transport property calculations.
Vn(K)	5	R	List of input parameters for the Nth step of the cross section calculations. There are 100 of these arrays, V1(K), V2(K),..., V100(K). The number of parameters required for each option and their definitions are discussed in Section 4.6.
ISEQ(L)	100	I	Sequencing array for specifying the order in which the defined steps will be carried out during the cross section calculations. The index N in the preceding arrays is given by N = ISEQ(L) where L = 1, 2, 3, 4,..., NNKQ is the order in which the steps are executed.*
TL	1000	R	Additional storage locations for cross
ØMEGAL	1000	R	section data. The use of these arrays
ASTAR	1000	R	is discussed in Section 4.6.
BSTAR	1000	R	

Whenever a new set of cross section data is used for the first time, it is advisable to check these inputs by making a preliminary run with ISWLB set equal to -2 in the main input to invoke the complete edit of cross sections. This edit consists of three parts.

*This input allows steps to be added to the cross section calculation (e.g., for new species) without shifting any of the compiled-in data in the Ii, Ji, and Vi arrays.

The first part lists all of the defined steps in the cross section calculation, including those compiled in for computing the transport properties of the standard species and any steps which have been added by input. The steps are listed in the order in which they would be performed if the current gas model were to include all of the standard and defined species. The second part of the edit lists the steps selected by the transport routines for the current gas model. This list omits steps which are required only for calculating the cross sections of species which are not present in the gas model, and includes steps which have been added by the default options. This second part of the edit thus shows how the transport properties will actually be calculated in the current problem. The third part of the edit is a set of tables giving the cross sections for each pair of species in the current gas model as a function of temperature up to the input reservoir temperature, CTAPI.

The simplest method for specifying the cross sections for pairs involving a new species is to rely, to the maximum extent possible, upon the default options in the NATA transport property routines. The inputs required may then be summarized briefly as follows:

- (1) If the new species is an ion, no cross section inputs for it are required, provided the species is assigned a previously unoccupied location in the master list of species.
- (2) If the new species is neutral, one step must be added to the transport cross section calculations to compute the cross sections for interaction of the species with itself. Alternatively, the like-like interaction for the new species can be added to an existing step in the cross section calculation by increasing NNQ for the step by 1 and adding the new species to the corresponding In and Jn lists. In the absence of other specifications, all of the unlike pair cross sections involving the new species will automatically be calculated using a mixing rule (option KKQ = 10).
- (3) Adding a step to the calculations requires the following changes in the transport inputs:
 - a. NNKQ must be increased by 1 (see transport block data routine for the original value).

- b. The option to be used in calculating the cross sections for the like-like interaction of the new species with itself must be specified in the form

KKQ(n) = option number

where n is the numerical index (N) of a step which is not already used by the compiled-in data.

- c. The number of pairs of species to which the new step is applied is set to unity:

NNQ(n) = 1

- d. The indices of the species are set:

In = index assigned to new species

Jn = same index

- e. The parameters for the option are set

Vn = list of values

- f. The ISEQ array must be modified to insert the new step ahead of the step in which the mixing rule (option 10) is exercised. The proper location can be determined by examining the KKQ and ISEQ arrays in transport block data. This positioning of the new step is required to allow application of the mixing rule to the unlike pairs involving the new species.
- g. If the option selected required addition of data to the TL, OMEGAI, ASTAR, and BSTAR arrays, these data must be set. This can be done most conveniently by reading in each array entry as a subscripted variable; e.g.,

TL(k) = value, TL(k + 1) = value, etc.

where k , $k + 1$, etc. are numerical index values of array elements which are not used by the compiled-in data.

If information is available concerning the cross sections for some of the unlike interactions involving the new species, the accuracy of the NATA transport property calculations can be improved by adding additional steps to calculate these cross sections. These steps, like the step for the like-like cross sections, should be inserted ahead of the step in which option 10 is applied.

2.5 Execution Time

An estimate of execution time is normally required whenever a job is submitted for running on a computer system. The per-case execution time of NATA can vary greatly depending on the types of solutions requested and the gas models used. Typical times for the various parts of the calculation are listed below for runs using the standard air models ($IGAS = 1, 2$). The times are roughly similar on the UNIVAC 1108 and the IBM 360/75.

(1) Reservoir calculations

Based on temperature and pressure: 1 sec
Based on pressure and mass flow: 30 sec
Based on enthalpy and mass flow: 60 sec

(2) Frozen or equilibrium solution: 1/3 to 1/2 min

(3) Nonequilibrium solution: 1 to 3 min

(4) Model calculations (per model point): 2 to 3 sec

The times are somewhat greater (by up to a factor of two) when the planetary atmosphere models ($IGAS = 5, 6$) are used. Non-equilibrium solutions based on the helium and argon models are in a class by themselves; experience is limited, but times of the order of an hour should be anticipated.

3. OUTPUTS

Normal outputs produced in various types of NATA runs are described and discussed in the present section. Diagnostic messages and dumps produced under abnormal circumstances are listed and explained in Appendix B.

NATA outputs are discussed in the order in which they appear in a normal run in Sections 3.1 to 3.8. The special outputs making up the transport cross section edit and the species thermal property edit are described in Sections 3.9 and 3.10.

3.1 Listings of Input Variables

The output for each NATA case begins with a complete listing of the input variables read in under namelist INPUT (Section 2.3). The names and values of the variables are printed in the namelist format, equations (1). The variables are listed in the order in which they are defined in Section 2.3. The printed arrangement of these data differs between the UNIVAC 1108 and the IBM 360. The 1108 prints each single variable on a separate line, and each array in a separate block. The 360 runs the outputs of the form (1) together to make up lines running the full width of the page. The arrangement produced by the 360 is more compact but more difficult to read.

To provide illustrations of the various types of NATA output, a job consisting of two cases dealing with air flow in an axisymmetric nozzle was run on an IBM 360/75. Figure 2 is a listing of the input cards for these cases. Figure 3 shows the listing of input variables produced by the code for the first case (to be referred to as Test Problem No. 1). Apart from the difference in arrangement described above, the output shown in figure 3 differs from that which would be produced on a UNIVAC 1108 in three additional respects:

- (1) Variables which are not referenced in the input data (figure 2), and which are not preset in the coding, contain meaningless values left in the computer core by a previous job. Since the 1108 clears core before each job, such variables would be printed as zero in the output from an 1108 run.

T PROBLEM NO. 1 - AIR FLOW IN AN AXISYMMETRIC NOZZLE WITH MODEL AND WEDGE
+INPUT
ISW4A=1, CXMAXI=50, ISW2B=-1, FLOW=.03, HSTAG=10880, NOZZLE=10,
TSDIAM=20, 25, KDIM=0, CATFAC=0, NANGLE=1, ANGLE=15, NRADLE=1, RADLE=.375,
NWX=8, WX1=2.5, 4.5, ISW9B=-2
+END
TEST PROBLEM NO. 1A - OUTPUT CONTROLS
+INPUT
ISW3A=0, ISW7B=1, ISW6B=-4, ISW1A=0, ISW3A=0
+END

ORIGINAL PAGE IS
OF POOR QUALITY

FIGURE 2 - LISTING OF INPUT CARDS FOR TEST PROBLEMS NO. 1 AND 1A

FIGURE 3 - NATA CODE OUTPUT - LISTING OF IN - VARIABLES FOR TEST PROBLEM NO. 1 (First Page)

FIGURE 3 - NATA CODE OUTPUT - LISTING OF INPUT VARIABLES FOR TEST PROBLEM NO. 1 (Second Page)

1615762224 54107384. 1610762112.-1650926647. 1610762224.-1 75424-
 1611284928. 19561208. -687841270. 1611286512.-1793796859. 161091 1. 14762.
 120695274. -721669028. -2147465232. [TR=-167730652A.-161912422A0.-170706124B. 1092374640. 109366532B. 1092634008.-1697474944.
 109335180A.-213645304C. 1085378499. 1084619700. 1172347612. 458562423. 1101048A3. 3603335216. 1698246141. 1086619988. 1095794856.
 1347435736. 1706951676. 14A. 047059. 1206954612. [FR=1736556749579296.
 0.59479598212004950D-77. -0.6522050417203651D-49. -0.3351734106639390D-59. -0.08869739393236526D-59. -0.3211530573087938D-57.
 0.3969239819119196D 0. 1664339985547326D-51. -0.4061565009453914D 24. -0.206470C690677624D-47. 4. 0.0286340735617127.
 1190649260. 4952406. -0.16663399P45437326D-51. -0.4051563757945842D 24. -0.411630551621175D-47. -0.1101970A2765391D-44.
 2.6425634640075742. 0.1613000293365167. 0.4591200311005448. -0.1555570452652230D-44. 118069412. 4962406
 7. 0.0020205407286730. 118069668R. 4962406. 0.366714702686494706D-52. 0.3029197026684821D 37. 0.374830035486916D 38.
 3.21110104766119. 41802517257. 59716. -0.16148138661956033D-57. -0.16797056560303327D-51. 1.35032167987306.
 010991. 7.17160566A65. 0.031254058479053. 0.5614065309605255D-45. 0.7532044799292914. 0.6031253916026224.
 -0.1507223867662191D-45. 12.29712296782805. -0.8669739247476316D-59. 17408817. 53131173. -0.167056071092867D-51.
 0.214520709839633D-49. -0.440257829605920D-46. 2.021591429369948. -0.2214474209781534D-44. 2.72375417911875.
 -0.1447767207375743D-45. -0.1165150077054192D-45. -0.9875506127972480D-46. 0.33977797906270175R. 36. DPAR=0. 3809521815560434D-49. TL15T=.
 -0.931808738759671567D-58. -0.48553178818072560D-58. -0.1868306548472098D-58. -0.286300883928890040-58. 252273669. 5119019.
 -0.4737793960232113C5D 19. -n. 18875192851349264D-01. 134910404. 4.662379. 1.6691944A57. 377377. 134839177. 0.938416.
 1348373591564547. 17398669. 312913576. -0.355217032690-44. 0.37585326665470573D 38. 0.4287669504361089D 38.
 0.1039795995437719A50 27. 12.05200231075661. 118061965. 4375915. 0.3735326665437049D 36. 12.9664066456174.
 0.1369028C76520A15D-77. 0.567823298312264D-78. 118061837. 4375916. 0.1365672630049463D 38. 12.76756342157422.
 0.21444236862138811D-49. 0.4830236862138811D-21. 0.797290618335659. 1.34839657. 3748173. 1.18062569. 3760387.
 252294324. 1992802. -0.46607335136909A607D 19. -0.21465512952859R5D-4A. 2.5336181951621817. -0.6805970127285425D-51.
 0.5158720016524967. 1.3.766616152939159. 0.11714555R5460707D 19. -0.60008285631235484D 20. 13.9664066456174.
 49. 6973892604116325D-44. -0.161130020575377D-48. -0.5834314125238148D-4A. -0.401665793353107D-48.
 0.20108523176807221710-49. 0.4830236862138811D-49. 0.797290618335659. 1.34839657. 3748173. 1.18062569. 3760387.
 10.03905634974666C. -0.22793399014158P6D-45. 0.2979022097853443D 29. 252294324. 10.703362. 0.266996533073430D-20.
 0.75320044799920661. 919981. 7659457326. 15.03728495413504. -0.2214481681581979D-44. -0.25011961931072270-44. ISMSA=0.
 0.1SWAB= 0.1SWB= 0.

੨੫

-48-

ORIGINAL PAGE IS
OF POOR QUALITY

- (2) NATA is run as a double-precision program on the IBM 360. Hence, the exponent in floating-point numbers is printed as D in place of E, and the values are printed to 16 digits.
- (3) Under the IBM 360 operating system used in this run, when a double precision variable is set to a single-precision value either by input or in a data statement in the program, only the first six significant figures are set correctly. The ten trailing digits are usually inaccurate or meaningless.

If data describing elements, species, or reactions are read in, the listing of the variables in namelist INPUT is followed by a listing of those in namelist EINPUT (Section 2.4). Also, if transport cross section data are read in, a listing of the variables in namelist TINPUT is produced. These listings are similar in format to the INPUT listing illustrated in figure 3.

3.2 Problem Summary

Immediately following the listings of program inputs, NATA produces a summary of the input specifications for the case. This output is headed by the title "NATA III Code Output". The problem summary for Test Problem No. 1 is shown in figure 4. In general, the summary contains the following information:

- (1) A line giving the run number (IRUN), the case number in the current job (set internally by the code), and the contents of the description card for the case.
- (2) A line stating the input specifications for the reservoir conditions.
- (3) A summary of the nozzle or channel geometry, including a table giving the parameters of the nozzle profile curvefit in centimeter units. This is omitted in subsequent cases with the same geometry.
- (4) A specification of the gas model as either a standard gas or a nonstandard gas.

FIGURE 4 - NATA CODE OUTPUT - PROBLEM SUMMARY FOR TEST PROBLEM NO. 1 (First Page)

NATA T.I. COT

RUN NO. 0 CASE 1 IN THIS JOR TEST PROBLEM NO. 1 - AIR FLOW IN AN AXISYMMETRIC NOZZLE WITH MODEL AND WEDGE

STAGNATION ENTHALPY= 10580. BTU/LB. TOTAL MASS FLOW= 0.03000 LB/SEC

STANDARD AXISYMMETRIC NOZZLE NO. 10. 1.788 INCH THROAT DIAM FOR EOS

J	I(SHAPE(J))	SHAPE	ATP(I,J)	PARAM(1,J)	PARAM(2,J)
1	1	STRAIGHT LINE	-3.5474D 00	1.9214D 00	-1.7633D-01
2	1	CIRCLE TOP	-3.4731D 00	2.2955D 00	-3.5845D 00
3	1	STRAIGHT LINE	-2.4315D 00	8.2985D-01	-4.8773D-01
4	2	CIRCLE BOTTOM	-2.3919D 00	2.2418D 00	-2.3196D 00
5	1	STRAIGHT LINE	-1.2810D 00	1.2690D 00	-3.0573D-01
6	2	CIRCLE BOTTOM	-1.2517D 00	1.9033D 00	-1.2054D 00
7	1	STRAIGHT LINE	-5.3970D-01	1.3812D 00	-2.1743D-01
8	2	CIRCLE BOTTOM	0.0	1.4072D 00	0.0
9	2	CIRCLE BOTTOM	6.5744D-03	1.4072D 00	2.5400D-02
10	1	STRAIGHT LINE	1.3809D 00	2.6795D-01	0.0

STANDARD GAS NO. 1 (AIR-1)

NO.	NAME	INDEX	MOLE FRAC.
1	N2	5	0.79823
2	O2	6	0.21177

MEAN MOLECULAR WEIGHT OF COLD GAS= 28.8581

COLD SPECIES	ATOM FRACTION	ELEMENT MOLECULAR WEIGHTS
F-	0.0	9.485970D-04
N	1.576460E-01	1.400700D 01
O	4.2354001-01	1.600000D 01

ORIGINAL PAGE IS
OF POOR QUALITY

REACTION NO.	CONSTANT FACTOR AT	TFMP. POWER DEPENDENCE	ACTIVATION ENERGY	CHI TEST	THIRD BODY MATRIX
1	1.59999990 14	-1.00000000	1.179810D 05	0.00010100000	
2	9.90000070 15	-1.00000000	1.179800D 05	0.00000000	
3	3.20000000 15	-1.00000000	1.179800D 05	0.00000000	
4	7.20000000 14	-1.00000000	1.179800D 05	0.00000000	
5	1.90000000 15	-5.00000000-01	2.250400D 05	0.00000000	
6	4.10000000 16	-1.50000000	2.250400D 05	0.00000000	
7	4.70000000 15	-5.00000000-01	2.250400D 05	0.00000000	
8	3.89999990 14	-1.50000000	1.500500D 05	0.00000000	
9	7.79999990 14	-1.50000000	1.500500D 05	0.00000000	
10	3.19999990 13	1.00000000	3.91920D 04	0.00000000	
11	7.00000000 13	0.0	7.551000D 04	0.00000000	
12	6.69999990 15	-1.50000000	0.0	0.00000000	
13	2.20000000 22	-4.50000000	0.0	0.00000000	
14	2.20000000 22	-4.50000000	0.0	0.00000000	
15	7.09999990 15	-1.50000000	0.0	0.00000000	

FIGURE 4 - NATA CODE OUTPUT - PROBLEM SUMMARY FOR TEST PROBLEM NO. 1 (Second Page)

16	7.00000D 13	5.000000D-01	0.000000
17	7.80000D 13	5.000000D-01	0.000000
18	1.5C000D 16	-1.50000D 00	0.000000
19	9.999999D 13	-2.50000D 00	0.000000
20	2.20000D 16	-2.50000D 00	0.000000
21	1.50000D 13	0.0	0.000000
22	3.40000D 11	-2.00000D 00	4.570000D 04
23	4.799999D 14	0.0	0.000000
24	1.000000D 15	5.000000D-01	0.000000
25	9.999999D 13	0.0	0.000000
26	8.799996D 16	-2.500000D 00	0.000000

SPECIES THERMAL FIT INDICATOR ALPHA MATRIX

	E-	N	O
E-	0	1	0
N2	1	0	2
O2	-1	0	0
N	0	0	1
O	0	0	0
NO	0	1	1
NDE	1	-1	1
NC	0	-1	0
OE	0	1	0
N2E	1	-1	2
O2E	1	-1	0

REACT NO. NU PRIME MATRIX

	E-	N2	O2	N	NO	NDE	NC	OE	N2E	O2E
1	0	0	0	0	0	0	0	0	0	0
2	0	0	1	0	0	0	0	0	0	0
3	0	0	0	1	0	0	0	0	0	0
4	0	0	0	0	1	0	0	0	0	0
5	0	0	0	0	0	1	0	0	0	0
6	0	0	0	0	0	0	1	0	0	0
7	0	0	0	0	0	0	0	1	0	0
8	0	0	0	0	0	0	0	0	1	0
9	0	0	0	0	0	0	0	0	0	1
10	0	0	0	0	0	0	0	0	0	0
11	0	0	0	0	0	0	0	0	0	0
12	0	0	0	0	0	0	0	0	0	0
13	0	0	0	0	0	0	0	0	0	0
14	0	0	0	0	0	0	0	0	0	0
15	0	0	0	0	0	0	0	0	0	0
16	0	0	0	0	0	0	0	0	0	0
17	0	0	0	0	0	0	0	0	0	0
18	0	0	0	0	0	0	0	0	0	0
19	0	0	0	0	0	0	0	0	0	0
20	0	0	0	0	0	0	0	0	0	0
21	0	0	0	0	0	0	0	0	0	0
22	0	0	0	0	0	0	0	0	0	0
23	0	0	0	0	0	0	0	0	0	0
24	0	0	0	0	0	0	0	0	0	0
25	0	0	0	0	0	0	0	0	0	0
26	0	0	0	0	0	0	0	0	0	0

ORIGINAL PAGE IS
OF POOR QUALITY

REACT NO. NU MATRIX

	E-	N2	O2	N	0	NO	NDE	02E	N2E	O2E
E-	0	0	0	0	0	0	0	0	0	0
N2	0	0	0	0	0	0	0	0	0	0
O2	0	0	0	0	0	0	0	0	0	0
N	0	0	0	0	0	0	0	0	0	0
0	0	0	0	0	0	0	0	0	0	0
NO	0	0	0	0	0	0	0	0	0	0
NDE	0	0	0	0	0	0	0	0	0	0
NC	0	0	0	0	0	0	0	0	0	0
OE	0	0	0	0	0	0	0	0	0	0
N2E	0	0	0	0	0	0	0	0	0	0
O2E	0	0	0	0	0	0	0	0	0	0

FIGURE 4 - NATA CODE OUTPUT - PROBLEM SUMMARY FOR TEST PROBLEM NO. 1 (Third Page)

1	0*	0*	0*	0*	0*	0*	0*	0*
2	0*	1*	0*	1*	0*	0*	0*	0*
3	0*	0*	2*	0*	0*	0*	0*	0*
4	0*	1*	1*	0*	0*	0*	0*	0*
5	0*	0*	1*	0*	0*	0*	0*	0*
6	0*	0*	0*	1*	0*	0*	0*	0*
7	0*	0*	2*	0*	0*	0*	0*	0*
8	0*	0*	0*	0*	1*	0*	0*	0*
9	0*	0*	0*	0*	0*	1*	0*	0*
10	0*	0*	0*	0*	0*	1*	0*	0*
11	0*	0*	1*	0*	0*	0*	0*	0*
12	1*	0*	0*	0*	0*	0*	0*	0*
13	2*	0*	0*	0*	0*	0*	0*	0*
14	1*	0*	0*	0*	0*	0*	0*	0*
15	1*	0*	1*	0*	0*	0*	0*	0*
16	0*	0*	0*	1*	0*	0*	0*	0*
17	0*	0*	0*	0*	1*	0*	0*	0*
18	1*	0*	0*	0*	0*	0*	0*	0*
19	1*	0*	0*	0*	0*	0*	0*	0*
20	1*	1*	0*	0*	0*	0*	0*	0*
21	0*	0*	0*	0*	0*	1*	0*	0*
22	0*	1*	0*	0*	0*	0*	1*	0*
23	0*	0*	0*	0*	0*	0*	1*	0*
24	0*	0*	0*	0*	0*	0*	0*	1*
25	0*	0*	1*	0*	0*	0*	1*	0*
26	1*	0*	1*	0*	0*	0*	1*	0*

ELECTRONIC LEVELS

SPECIES	ATOMS PER MOLECULE	CHEMICAL CONSTANT	CHAR. VIBRATIONAL TEMP.	ENTHALPY OF FORMATION	ELECTRONIC LEVELS
-152	E-	-1.492760D 01	0.0	0.0	1
	N2	-4.105990D-01	3.352000D 03	0.0	5
	O2	2.000000D 00	2.239000D 03	0.0	5
	N	1.000000D 00	0.0	1.125200D 03	5
	O	1.000000D 00	2.944000D-01	0.0	5
	NO	2.000000D 00	4.938000D-01	5.899000D 04	7
	NO2	2.000000D 00	5.455000D-01	2.146000D 04	7
	NE	1.000000D 00	3.841000D-01	2.366600D 05	4
	OC	1.000000D 00	2.943000D-01	4.476000D 05	7
	N2O	2.000000D 00	4.938000D-01	3.729400D 05	3
	O2C	2.000000D 00	-3.763000D-01	3.576800D 05	4
		2.000000D 00	-3.170000D-02	2.880000D 05	5

(DEGENERACY, ELECTRONIC ENERGY LEVEL)

SPECIES	A	B	C	D	E	F	K	HEAT OF FORMATION
E-	2.0	0*	3.0	1.435400D 05	6.0	1.704800D 05	1.0	1.715000D 05
N2	1.0	0*	2.0	2.263900D 04	1.0	3.772600D 04	3.0	1.032000D 05
O2	3.0	0*	10.0	5.496200D 04	6.0	8.245600D 04	12.0	2.362700D 05
N	4.0	0*	3.0	4.530000D 02	1.0	6.480000D 02	5.0	4.536700D 04
O	5.0	0*	2.0	3.460000D 02	2.0	1.257000D 05	4.0	1.313200D 05
NO	2.0	0*	1.0	1.060000D 05	3.0	1.600000D 05	2.0	2.000000D 05
NO2	2.0	0*	3.0	1.400000D 02	5.0	3.750000D 02	5.0	4.378900D 04
NE	1.0	0*	1.0	7.667000D 04	6.0	1.157000D 05	1.0	9.345600D 04
OC	1.0	0*	4.0	2.589000D 04	2.0	7.279700D 04	2.0	1.947600D 05
N2O	2.0	0*	2.0	5.580000D 02	8.0	9.120600D 04	4.0	1.997600D 05
O2C	2.0	0*						

ORIGINAL PAGE IS
OF POOR QUALITY

FIGURE 4 - NATA CODE OUTPUT - PROBLEM SUMMARY FOR TEST PROBLEM NO. 1 (Fourth Page)

O2	3.249473D 00	4.963449D-04	-6.70174FD-08	4.44	D-12	-1.000281D-16	5.915022D 00	0.0
NO	3.756215D 00	2.081961D-04	-2.639548D-08	1.69	/D-12	-3.611522D-17	3.611167D 00	2.146000D 04
NOC	3.397385D 00	3.749384D-04	-6.062027D-08	4.637506D-12	-1.107704D-16	4.200562D 00	2.366600D 05	
N2E	3.238063D 00	4.472570D-04	-3.958800D-08	1.529630D-12	-2.114500D-17	4.951599D 00	3.576800D 05	
O2E	3.492129D 00	3.378792D-04	-5.208410D-08	4.162070D-12	-9.727500D-17	4.667500D 00	2.866000D 05	

LEWIS NUMBER CALCULATIONS BASFD ON BINARY DIFFUSION COEFFICIENT FOR O - N2
BOUNDARY LAYER EFFECTS INCLUDED

INPUT DATA FOR MODEL PARAMETER CALCULATIONS
SPECIFIED TEST SECTION DIAMETERS IN INCHES= 20.00 25.00
MODEL TEMPERATURE= 300. DEG K FLAT PLATE TEMPERATURE= 300. DEG K
BOTH EQUILIBRIUM AND FROZEN SHOCK LAYERS ON MODEL CALCULATED
SURFACE CATALYTIC FACTOR = 0.0
TWO-DIMENSIONAL MODEL GEOMETRY

WEDGE MODEL ANGLFS OF ATTACK IN DEGREES 15.0
LEADING-EDGE RADII IN INCHES 0.3750
S DISTANCES FROM LEADING EDGE WITH A UNIFORM SEPARATION OF 1.00 INCHES STARTING AT 1.00 INCHES
SPECIFIED DISTANCES FROM LEADING EDGE IN INCHES 2.50 4.50
WEDGE SURFACE TEMPERATURE= 300. DEGREES K. NOSE DRAG COEFFICIENT=1.333

*****ELAPSED TIME= 0.03 MINUTES SINCE START OF RUN. 2. SECONDS SINCE LAST PRINTED TIME

SPECIFIC HEAT OF COLD GAS= 0.2416 BTU/LB-DEG R AT 300.00 DEG K

ORIGINAL PAGE IS
OF POOR QUALITY

- (5) A table listing the cold species with their indices in the master list of species, mole fractions in the cold gas, molecular weights and chemical formulas. The mean molecular weight of the cold gas is then given.
- (6) A table giving the elemental composition of the gas; the "atom fraction" in this table is the number of atoms of a given element per molecule of the cold gas.
- (7) A table containing the rate data for all of the chemical reactions in the current gas model. This table includes the coefficient, A , the temperature exponent η , and the activation energy E_a (in cal/mole) in the formula (69) of Volume I (ref. 1) for the forward rate constant. This table also includes the criterion value C_χ for the switch from the perturbation solution to the nonequilibrium integration. Also, for each reaction with a third-body list, the code prints a string of zeros and ones containing as many characters as there are species in the gas model. A 1 indicates that the corresponding species is a third body in the reaction, a 0 that it is not.
- (8) A table listing the chemical species in the gas model. In this table, a 1 under "thermal fit indicator" means that a thermo fit has been provided for the species, a 0 that no thermo fit has been specified. Under "alpha matrix", the number of atoms of each chemical element in a molecule of the species is given.
- (9) A table giving the matrix ν'_{ij} of the stoichiometric coefficients on the product side of the reaction. The entry under each species is the number of molecules of the species appearing as a product of the reaction.
- (10) A table giving the matrix ν_{ij} of the stoichiometric coefficients on the reactant side of the reaction.

- (11) A table containing data for the "physical model" description of the thermal properties of the species. The columns of this table contain the number of nuclei in a molecule of the species, the chemical constant b, the vibrational temperature Θ_v in degrees Kelvin, the enthalpy of formation in cal/mole, and the number of electronic energy levels. The degeneracies g and energy levels E relative to the state of formation are given in the next table, listed in pairs (g, E) across the page. The energies are again in cal/mole.
- (12) A table listing the thermo fit data for the species for which such a fit is provided. The table includes the coefficients a, b, c, d, e, and k for each species, and the enthalpy of formation in cal/mole (also given in the table (11) for the physical model in the case of species for which both methods are used). All of the tables from (5) through (12) are omitted in subsequent cases with the same standard gas model.
- (13) A statement of the species pair for which the Lewis number is calculated.
- (14) A statement of whether or not boundary layer effects are to be included in the flow solutions.
- (15) A summary of input data for calculations of conditions on models.
- (16) A summary of input data for calculations of conditions on wedge models.
- (17) A timing message giving the elapsed times since the beginning of the run and since the last time message. Such timing messages appear at several points in the output and allow the user to determine how much computer time is consumed in each major part of the calculations.
- (18) The value of the specific heat of the cold gas mixture at the nozzle wall temperature TWALL.

3.3 Definitions of Output Identifiers

In the first case of each NATA run, the code next prints a list of definitions of the alphanumeric identifiers used to label the outputs of the flow and model condition calculations. This list is shown in figure 5.

3.4 Reservoir Conditions

Next appears a page of output summarizing the calculated gas conditions in the upstream reservoir, as illustrated in figure 6. Since the same output format is also used for the throat conditions, the flow velocity and mass flux are included even though they are always zero in the reservoir. In Test Problem No. 1, the reservoir conditions were determined from mass flow and stagnation enthalpy inputs. The double iteration required in this calculation consumed over a minute of computer time, as shown by the timing message.

3.5 Flow Solutions

The nozzle flow solutions are computed and printed in the order: frozen, equilibrium, nonequilibrium. The format is the same for all three types of solution, but varies with the type of problem being run. For example, if the boundary layer on the nozzle wall is neglected, only a single area ratio is printed and the boundary layer quantities such as the displacement thickness and the Stanton number are omitted. In a channel flow problem including the boundary layer, two complete sets of boundary layer data are printed, one for each pair of channel faces. In a problem involving an electronic nonequilibrium gas model, the electron temperature, the radiative power loss, the energy transfer to the electrons, and the local stagnation enthalpy are added to the output.

The first page of output from the frozen solution for Test Problem No. 1 is shown in figure 7. The output identifiers X, T, etc., are defined in figure 5. The species mole fractions are not included in the output for the frozen solution because they are constant at their previously printed (figure 6) values in the reservoir.

DEFINITIONS SYMBOLS

FIGURE 5 - NATA CODE OUTPUT - DEFINITIONS OF OUTPUT IDENTIFIERS (First Page)

ARAT	= GEOMETRIC AREA RATIO
ARATE	= EFFECTIVE AREA RATIO
DEL_REF	= EQUILIBRIUM SHOCK STANDOFF DISTANCE ON FLAT-FACED MODEL. DIVIDED BY MODFL NOSE RADIUS
DEL_PHE	= EQUILIBRIUM SHOCK STANDOFF DISTANCE ON HEMISPHERICAL MODEL. DIVIDED BY MODEL NOSE RADIUS
DEL_RFF	= FROZEN SHOCK STANDOFF DISTANCE ON FLAT-FACED MODEL. DIVIDED BY MODEL NOSE RADIUS
DELPFH	= FROZEN SHOCK STANDOFF DISTANCE ON HEMISPHERICAL MODEL. DIVIDED BY MODEL NOSE RADIUS
DELSTR	= DISPLACEMENT THICKNESS OF BOUNDARY LAYER ON NOZZLE WALL (INCH)
DELSTW	= BOUNDARY LAYER DISPLACEMENT THICKNESS ON WEDGE (INCH)
DIAW	= NOZZLE DIAMETER (INCHES)
EPSLE	= DENSITY RATIO ACROSS EQUILIBRIUM NORMAL SHOCK
EPSLF	= DENSITY RATIO ACROSS FROZEN NORMAL SHOCK
GAMMA	= FROZEN SPECIFIC-HEA + RATIO IN FREE STREAM
H	= ENTHALPY IN FREE STREAM (BTU/LB)
HEIGHT	= SECOND TRANSVERSE DIMENSION OF CHANNEL (INCHES)
HR	= RECOVERY ENTHALPY (BTU/LB)
HRATE	= RATIO OF DISSOCIATION ENTHALPY TO (HS-HW) FOR EQUILIBRIUM SHOCK
HS	= RATIO OF DISSOCIATION ENTHALPY (BTU/LB)
K2PFE	= SHOCK-BOUNDARY LAYER INTERACTION PARAMETER PER FOOT FOR EQUILIBRIUM SHOCK
K2PFF	= SHOCK-BOUNDARY LAYER INTERACTION PARAMETER PER FOOT FOR FROZEN SHOCK
LEF	= ATOM-MOLECULE LEWIS NUMBER AT STAGNATION CONDITION FOR EQUILIBRIUM SHOCK
LEF	= ATOM-MOLECULE LEWIS NUMBER AT STAGNATION CONDITION FOR FROZEN SHOCK
M	= MACH NUMBER IN FREE STREAM
MU	= VISCOSITY IN FREE STREAM (LB/FT-SEC)
MUT2E	= VISCOSITY AT STAGNATION CONDITION FOR EQUILIBRIUM SHOCK (LB/FT-SEC)
MUT2F	= VISCOSITY AT STAGNATION CONDITION FOR FROZEN SHOCK (LB/FT-SEC)
MW	= MOLECULAR WEIGHT IN FREE STREAM (GM/MOLE)
MWT2E	= MOLECULAR WEIGHT AT STAGNATION CONDITION FOR EQUILIBRIUM SHOCK (GM/MOLE)
MWT2F	= MOLECULAR WEIGHT AT STAGNATION CONDITION FOR FROZEN SHOCK (GM/MOLE)
N	= BOUNDARY-LAYER PRESSURE-GRADIENT PARAMETER
P	= PRESSURE IN FREE STREAM (ATM)
PRE	= PRANDTL NUMBER AT STAGNATION CONDITION FOR EQUILIBRIUM SHOCK
PRF	= PRANDTL NUMBER AT STAGNATION CONDITION FOR FROZEN SHOCK
PRREF	= PRANDTL NUMBER AT REFERENCE TEMPERATURE IN BOUNDARY LAYER
PTE	= STAGNATION PRESSURE FOR EQUILIBRIUM SHOCK (ATM)
PT2F	= STAGNATION-POINT HEAT FLUX TIMES SORT(R) FOR EQUILIBRIUM SHOCK (ATM)
PW	= SURFACE PRESSURE ON A WEDGE MODEL (ATM)
QEFF	= STAGNATION-POINT HEAT FLUX TIMES SORT(R) FOR EQUILIBRIUM SHOCK ON A FLAT-FACED MODEL WITH AN EQUILIBRIUM BOUNDARY LAYER
QEF	= STAGNATION-POINT HEAT FLUX TIMES SORT(R) FOR EQUILIBRIUM SHOCK ON A FLAT-FACED MODEL WITH A FROZEN BOUNDARY LAYER
QEHF	= STAGNATION-POINT HEAT FLUX TIMES SORT(R) FOR EQUILIBRIUM SHOCK ON A HEMISPHERICAL MODEL WITH AN EQUILIBRIUM BOUNDARY LAYER
QEHF	= STAGNATION-POINT HEAT FLUX TIMES SORT(R) FOR EQUILIBRIUM SHOCK ON A HEMISPHERICAL MODEL WITH A FROZEN BOUNDARY LAYER
QELET	= NET POWER ADDED TO THE ELECTRON GAS (CAL/CU CM-SEC)
QFSRI	= STAGNATION-POINT HEAT FLUX TIMES SORT(R) FOR EQUILIBRIUM SHOCK ON A MODEL (BTU/SU FT-SEC)*0.5 SRI FORMULA
QFFE	= STAGNATION-POINT HEAT FLUX TIMES SORT(R) FOR FROZEN SHOCK ON A FLAT-FACED MODEL WITH AN EQUILIBRIUM BOUNDARY LAYER
OFFF	= STAGNATION-POINT HEAT FLUX TIMES SORT(R) FOR FROZEN SHOCK ON A FLAT-FACED MODEL WITH A FROZEN BOUNDARY LAYER
QFHF	= STAGNATION-POINT HEAT FLUX TIMES SORT(R) FOR FROZEN SHOCK ON A HEMISPHERICAL MODEL WITH AN EQUILIBRIUM BOUNDARY LAYER
QFHF	= STAGNATION-POINT HEAT FLUX TIMES SORT(R) FOR FROZEN SHOCK ON A HEMISPHERICAL MODEL WITH A FROZEN BOUNDARY LAYER
QFP	= HEAT FLUX TO A FLAT PLATE 1 FT FROM THE LEADING EDGE (BTU/SC FT-SEC)
QFRI	= STAGNATION JET HEAT FLUX TIMES SORT(R) FOR FROZEN SHOCK ON MODEL (BTU/SU FT-SEC)*0.5 SRI FORMULA
QRAD	= RADIATED FLUX (CAL/CU CM-SEC)
QW	= HEAT FLUX TO NOZZLE WALL (BTU/SU FT-SEC)
QWR	= HEAT FLUX TO SURFACE OF A WEDGE MODEL (BTU/SU FT-SEC)

FIGURE 5 - NATA CODE OUTPUT - DEFINITIONS OF OUTPUT IDENTIFIERS (Second Page)

R	= C _{TY} IN FREE STREAM (LB/CU FT)
REPF	= R ₁ - JILOS NUMBER PER FOOT IN FREE STREAM
RETH	= REYNOLDS NUMBER BASED ON MOMENTUM THICKNESS
RETHTR	= CRITICAL REYNOLDS NUMBER (BASED ON MOMENTUM THICKNESS) FOR BLUNTY LAYER TRANSITION
RT2E	= DENSITY AT STAGNATION CONDITION FOR EQUILIBRIUM SHOCK (LB/CU FT)
S	= ENTROPY IN FREE STREAM (BTU/LB-DEG R)
SIGMA	= ELECTRICAL CONDUCTIVITY IN FREE STREAM (MMHO/CM)
SIGT2E	= ELECTRICAL CONDUCTIVITY AT STAGNATION CONDITION FOR EQUILIBRIUM SHOCK (MMHO/CM)
SIST2F	= ELECTRICAL CONDUCTIVITY AT STAGNATION CONDITION FOR FROZEN SHOCK (MMHO/CM)
STANTN	= STANTON NUMBER BASED ON TOTAL ENTHALPY
SIZE	= ENTROPY AT STAGNATION CONDITION FOR EQUILIBRIUM SHOCK (BTU/LB-DEG R)
S12F	= ENTROPY AT STAGNATION CONDITION FOR FROZEN SHOCK (BTU/LB-DEG R)
T	= TEMPERATURE IN FREE STREAM (DEG K)
T2E	= TEMPERATURE AT STAGNATION CONDITION FOR EQUILIBRIUM SHOCK (DEG K)
T2F	= TEMPERATURE AT STAGNATION CONDITION FOR FROZEN SHOCK (DEG K)
TAUW	= SHEAR STRESS AT NOZZLE WALL (LBF/SQ FT)
TELEC	= ELECTRON TEMPERATURE (DEG K)
THETA	= MOMENTUM THICKNESS OF BOUNDARY LAYER ON NOZZLE WALL (INCH)
V	= VELOCITY OF FREE STREAM (FT/SEC)
WIDTH	= FIRST TRANSVERSE DIMENSION OF CHANNEL (INCHES)
X	= AXIAL DISTANCE ALONG NOZZLE. MEASURED FROM THROAT AND POSITIVE DOWNSTREAM (INCHES)
XSN	= N AVERAGED OVER SEVERAL PRECEDING POINTS OF THE SOLUTION
XW	= DISTANCE FROM LEADING EDGE OF WEDGE. MEASURED ALONG WEDGE SURFACE (INCHES)
YS	= ORDINATE OF SHOCK FROM LINE PARALLEL TO FREE STREAM LOW. PASSING THROUGH LEADING EDGE OF WEDGE (INCHES)
ZETA	= NONDIMENSIONAL STREAMWISE COORDINATE IN BLUNT WEDGE ANALYSIS

ORIGINAL PAGE IS
OF POOR QUALITY

- RESERVOIR CONDITIONS - FIGURE 6 - NATA CODE OUTPUT - REST "OIR CONDITIONS FOR TEST PROBLEM NO. 1

GAS FLOW RATE	=	0.030	LB/SEC
NOZZLE - EOS	=	1.088	"INCH THROAT DIAMETER
PRESSURE	=	0.541	ATM
TEMPERATURE	=	6735.	DEG K
ENTHALPY	=	10875.	BTU/LB
ENTROPY	=	3.35	BTU/LB-DEG R
DENSITY	=	0.00120	LB/CU FT
VELOCITY	=	0.	FT/SEC
MASS FLUX	=	0.0	LB/SQ FT-SEC
COMPUTED FLOW	=	0.030	LB/SEC
GAMMA	=	1.496	
MOLECULAR WEIGHT	=	18.23	GM/MOLE
ELECTRON DENSITY	=	3.580	14 ELECTRONS/CC

SPECIES MOLE FRACTIONS

E-	=	5.6500-04
N ₂	=	2.6070-01
O ₂	=	7.111D-05
N	=	4.712D-01
O	=	2.644D-01
NO	=	2.525D-03
NO _t	=	3.918D-04
NC	=	1.015D-04
O _b	=	5.717D-05
N ₂ _t	=	1.450D-05
O _{?C}	=	1.000D-07

*****ELAPSED TIME= 1.14 MINUTES SINCE START OF RUN. 67. SECONDS SINCE LAST PRINTED TIME

RESERVOIR TRANSPORT PROPERTIES

VISCOSITY	=	1.20D-04	LBM/FT-SEC
PRANDTL NUMBER	=	0.6701C	
SIGMA	=	3.19D 00	MHO/CM
LEWIS NUMBER	=	0.779	

FROZEN FLOW UTION

FIGURE 7 - DATA CODE OUTPUT - FOR TEST PROBLEM NO. 1

```

*****FROZEN*****
X      = 0.470      T      = 6735.      H      = 10876.      P      = 5.613D-01      R      = 1.197D-0
DIAM   = 1.202      V      = 0.0       M      = 0.0       MU     = 3.035      GAMMA = 1.406
ARATEF= 0.0       REPFF = 0.0       MW     = 18.23      S      = 1.204D-04      SIGMA = 3.193D-0
ARAT   = 0.0       DELSTR = 0.0       THETA = 0.0       QW    = 0.0       TAUW  = 0.0
HR     = 0.        PRREF = 0.0       STANTN= 0.0       RETH  = 0.        RETHTR = 200.

*****FROZEN*****
X      = -1.225     T      = 6677.      H      = 10837.      P      = 5.642D-01      R      = 1.172D-0
DIAM   = 1.849      V      = 1401.      M      = 0.206      S      = 3.35      GAMMA = 1.407
ARATEF= 2.087      REPFF = 1.372D 04    MW     = 18.23      MU     = 1.96D-04      SIGMA = 3.198D 0
ARAT   = 2.097      DELSTR = -0.008     THETA = 0.013      QW    = 4.481D 02      TAUW  = 1.625D 0
HR     = 10872.     PRREF = 0.6290    STANTN= 2.540D-02      RETH  = 15.        RETHTR = 209.

*****FROZEN*****
X      = -0.936      T      = 6619.      H      = 10798.      P      = 5.476D-01      R      = 1.147D-0
DIAM   = 1.571      V      = 1980.      M      = 0.293      S      = 3.35      GAMMA = 1.408
ARATEF= 2.086      REPFF = 1.912D C4    MW     = 18.23      MU     = 1.87D-04      SIGMA = 3.202D 0
ARAT   = 2.096      DELSTR = -0.011     THETA = 0.017      QW    = 3.450D 02      TAUW  = 1.956D 0
HR     = 10862.     PRREF = 0.6290    STANTN= 1.413D-02      RETH  = 27.        RETHTR = 214.

*****FROZEN*****
X      = -0.714      T      = 6562.      H      = 10759.      P      = 5.313D-01      R      = 1.123D-0
DIAM   = 1.436      V      = 2423.      M      = 0.360      S      = 3.35      GAMMA = 1.410
ARATEF= 1.741      REPFF = 2.308D 04    MW     = 18.23      MU     = 1.79D-04      SIGMA = 3.206D 0
ARAT   = 1.741      DELSTR = -0.012     THETA = 0.019      QW    = 3.096D 02      TAUW  = 2.223D 0
HR     = 10853.     PRREF = 0.6290    STANTN= 1.059D-02      RETH  = 36.        RETHTR = 217.

*****FROZEN*****
X      = -0.575      T      = 6504.      H      = 10720.      P      = 5.154D-01      R      = 1.099D-0
DIAM   = 1.351      V      = 2797.      M      = 0.417      S      = 3.35      GAMMA = 1.411
ARATEF= 1.542      REPFF = 2.625D 04    MW     = 18.23      MU     = 1.71D-04      SIGMA = 3.210D 0
ARAT   = 1.542      DELSTR = -0.013     THETA = 0.019      QW    = 2.935D 02      TAUW  = 2.623D 0
HR     = 10844.     PRREF = 0.6291    STANTN= 8.884D-03      RETH  = 42.        RETHTR = 220.

*****FROZEN*****
X      = -0.470      T      = 6446.      H      = 10681.      P      = 4.999D-01      R      = 1.075D-0
DIAM   = 1.202      V      = 3125.      M      = 0.468      S      = 3.35      GAMMA = 1.412
ARATEF= 1.410      REPFF = 2.891D 04    MW     = 18.23      MU     = 1.62D-04      SIGMA = 3.214D 0
ARAT   = 1.410      DELSTR = -0.014     THETA = 0.019      QW    = 2.866D 02      TAUW  = 2.942D 0
HR     = 10816.     PRREF = 0.6291    STANTN= 0.019      RETH  = 47.        RETHTR = 222.

```

Figure 8 shows the first page of output for the equilibrium solution. Here, the mole fractions are included because they vary along the flow. When the gas includes free electrons, the electron density in cm^{-3} is printed in place of the electron mole fraction.

In the nonequilibrium solution, the step size is often quite small. To avoid excessive output, the flow conditions are printed at intervals in the free stream temperature controlled by the input TPRNTI (Section 2.3, Group 2). The number of integration steps between successive printouts of the flow conditions is stated in the line of asterisks which separates the output for different flow points, as illustrated in figure 9, which shows the first page of output from the nonequilibrium solution for Test Problem No. 1. The method of calculation used in obtaining the conditions at the current flow point is also given by printing the value of the indicator, INEQ, which is 0 in the perturbation solution and 1 in the nonequilibrium integration.

When NATA is run with the preset value ISW6B=1, or with ISW6B= -1, the output includes the species mole fractions in every printed step as illustrated in figure 9. If $|ISW6B|$ is greater than 1, the mole fractions are printed only every $|ISW6B|$ th printed step. Also, if ISW6B is negative, the output of mole fractions is followed by a summary of reaction rate data as shown in figure 10. In this rate output, PI denotes the quantity P_i in equation (288) of Volume I; CHI is χ_i of equation (289); PICHI is $P_i \cdot \chi_i$; and DLG is $d \ln \gamma_j / dx$, where γ_j is the concentration of the jth species in moles/g. The quantities P_i , χ_i and $P_i \chi_i$ are listed for all of the reactions ($i = 1$ to r), together with the reaction index i. The quantity $d \ln \gamma_j / dx$ is listed for all the species together with the species names.

3.6 Model and Wedge Conditions

The conditions on models at a specified model point are printed immediately following the flow conditions at the model point, as illustrated in figure 11. If both equilibrium and frozen shock calculations have been requested ($FSTAG > 0.$), the model conditions for the case of the equilibrium shock are printed first. The species mole fractions at the stagnation point in the external flow over the model are then tabulated, and are followed by the model conditions for the case of a frozen shock. The output identifiers for the model conditions are defined in figure 5.

EQUILIBRIUM .UTION

FIGURE 8 - NATA CODE OUTPUT - EQUILIBRIUM SOLUTION FOR TEST PROBLEM NO. 1

*****EQUILIBRIUM*****

X	=	0.926	T	=	6735.	H	=	10676.	P	=	5.613D-01	R	=	1.197D-03
DIAM	=	1.566	V	=	0.	M	=	0.0	S	=	3.35	GAMMA	=	1.406
ARATEF	=	2.071	REFP	=	0.5	MW	=	1.823	MU	=	1.204D-04	SIGMA	=	3.193D 00
ARAT	=	2.071	DELSTR	=	0.0	THETA	=	0.0	OW	=	0.0	TAUW	=	0.0
HR	=	0.	PRREF	=	0.0	STANTN	=	0.0	RETH	=	0.	RETHTR	=	200.
E-	=	3.579D 14	N2	=	2.607D-01	O2	=	3.311D-05	N	=	4.712D-01	O	=	2.644D-01
NO	=	2.525D-03	NO2	=	3.916D-04	NC	=	1.0C15D-04	OC	=	5.717D-05	N2C	=	1.450D-05
O2C	=	1.0C00D-07												

*****EQUILIBRIUM*****

X	=	-1.217	T	=	6721.	H	=	10642.	P	=	5.665D-01	R	=	1.170D-03
DIAM	=	1.561	V	=	1305.	M	=	0.213	S	=	3.35	GAMMA	=	1.406
ARATEF	=	2.063	REFP	=	1.271D 04	MW	=	18.24	MU	=	1.202D-04	SIGMA	=	3.164D 00
ARAT	=	2.063	DELSTR	=	-0.008	THETA	=	0.014	OW	=	4.264D 02	TAUW	=	1.444D 00
HR	=	1.0873.	PRREF	=	0.6291	STANTN	=	2.591D-02	RETH	=	14.	RETHTR	=	210.
E-	=	3.459D 14	N2	=	2.620D-01	O2	=	3.297D-05	N	=	4.696D-01	O	=	2.647D-01
NO	=	2.511D-03	NO2	=	3.897D-04	NC	=	9.897D-05	OC	=	5.620D-05	N2C	=	1.420D-05
O2C	=	9.874D-08												

*****EQUILIBRIUM*****

X	=	-0.926	T	=	6706.	H	=	10608.	P	=	5.520D-01	R	=	1.144D-03
DIAM	=	1.566	V	=	1847.	M	=	0.302	S	=	3.35	GAMMA	=	1.406
ARATEF	=	2.071	REFP	=	1.758D 04	MW	=	18.26	MU	=	1.202D-04	SIGMA	=	3.164D 00
ARAT	=	2.071	DELSTR	=	-0.012	THETA	=	0.C18	OW	=	3.314D 02	TAUW	=	1.766D 00
HR	=	1.0865.	PRREF	=	0.6291	STANTN	=	1.460D-02	RETH	=	26.	RETHTR	=	214.
E-	=	3.342D 14	N2	=	2.633D-01	O2	=	3.284D-05	N	=	4.660D-01	O	=	2.650D-01
NO	=	2.511D-03	NO2	=	3.875D-04	NC	=	9.653D-05	OC	=	5.523D-05	N2C	=	1.390D-05
O2C	=	9.648D-08												

*****EQUILIBRIUM*****

X	=	-0.705	T	=	6692.	H	=	10774.	P	=	5.378D-01	R	=	1.118D-03
DIAM	=	1.431	V	=	2263.	M	=	0.371	S	=	3.35	GAMMA	=	1.406
ARATEF	=	1.730	REFP	=	2.105D 04	MW	=	18.28	MU	=	1.202D-04	SIGMA	=	3.164D 00
ARAT	=	1.730	DELSTR	=	-0.013	THETA	=	0.020	OW	=	2.997D 02	TAUW	=	2.013D 00
HR	=	1.0857.	PRREF	=	0.6291	STANTN	=	1.102D-02	RETH	=	35.	RETHTR	=	217.
E-	=	3.229D 14	N2	=	2.646D-01	O2	=	3.270D-05	N	=	4.664D-01	O	=	2.653D-01
NO	=	2.504D-03	NO2	=	3.854D-04	NC	=	9.414D-05	OC	=	5.426D-05	N2C	=	1.360D-05
O2C	=	9.475D-08												

*****EQUILIBRIUM*****

DRIVEN PAGE IS
DE POOR QUALITY

SOLUTION
NONEQUIILIBRIUM

FIGURE 9 - NATA CODE OUTPUT - NONEQUILIBRIUM SOLUTION FOR TEST PROBLEM NO. 1

```

DCHMIN= 1.25E0-05 DCHMAX= 6.575D-02 IMA= 5
DCHMIN= 2.619D-05 DCHMAX= 1.523D-01 IMA= 5
DCHMIN= 2.532D-05 DCHMAX= 1.401D-01 IMA= 5
DCHMIN= 1.852D-05 DCHMAX= 9.945D-02 IMA= 5
DCHMIN= 2.539D-05 DCHMAX= 1.401D-01 IMA= 5
DCHMIN= 2.184D-05 DCHMAX= 1.189D-01 IMA= 5

```

47 STEPS TO A NEW LIFE

```

X = -0.001          T = 6667.          H = 10817.          P = 5.531D-01
    1.620          V = 1715.          M = 0.271          S = 3.35
    2.216          REPF = 1.647D 04      MW = 1H.23          MU =
    2.217          DELSTR = -0.011        THETA = 0.016        OW =
    10857.          PQREF = 0.5274       STANIN = 1.574D-02      RFTH =
                                         SPECIES MOLE FRACTIONS IN THE FREEF STREAM
                                         = 2.647D-01
                                         = 1.333D-05

```

```

*****NONEQUILIBRIUM*****  

*****33 STEPS*****  

*****INEQ=1*****  

X = -0.597 T = 6600. H = 10743. P = 5.220D-01 R = 1.098D-03  

DIAM = 1.345 V = 2584. M = 0.400 S = 3.35 GAMMA = 1.406  

ARATEF = 1.541 REPF = 2.389D-04 MW = 18.26 MU = 1.18D-04 SIGMA = 3.040D-00  

ARAT = 1.573 DELSTR = -0.014 THETA = 0.020 OW = 2.85D-02 TAUN = 2.393D-01  

HR = 10850. PRREF = 0.6301 STANTN = 9.367D-03 RETH = 40. RETRTR = 219.  

SPECIES MOLE FRACTIONS IN THE FREE STREAM  

Z = 3.027D-14 N2 = 2.630D-01 O2 = 2.877D-05 N = 4.684D-01 O = 2.652D-01  

ENO = 2.299D-03 NOE = 3.711D-04 NC = 8.809D-05 N2C = 5.012D-05  

P = 1.11D-08

```

THEORY

```

K = -0.423    T = 6532.    H = 10681.    P = 4.975D-01    R = 1.059D-03
DIAM = 1.272    V = 3125.    M = 0.485    S = 3.35    GAMMA = 1.410
ARATEF = 1.322    REP = 2.809D 04    MW = 1R.27    MU = 2.951D 00
DFLSTR = -0.014    DELT = THETA = 0.020    OW = 2.015D 02    TAUW = 2.033D 00
APAT = 1.366    PAREF = 0.6301    STANTN = 7.914D-03    RETH = 223.
HR = 10836.    SPECIES MOLE FRACTIONS IN THE FREE STREAM
                N2 = 2.640D-01    O2 = 2.667D-05    N = 4.674D-01    O = 2.655D-01
                NO = 3.601D-04    NC = 8.204D-05    O2 = 4.820D-05    NC = 1.112D-05

```

CONFIDENTIAL INFORMATION

FIGURE 10 - NATA CODE OUTPUT - REACTION RATE DATA FOR TEST PROBLEM NO. 1A

X	=	-0.192	T	=	6374.	H	=	1C551.	P	=	4.488D-01	R	=	9.795D-04
DIAM	=	1.171	V	=	4036.	N	=	0.622	S	=	3.35	GAMMA	=	1.413
ARATEF	=	1.107	RPPF	=	1.420D C4	MW	=	18.028	MU	=	1.155D-04	SIGMA	=	2.761D 00
ARAT	=	1.150	DELSTR	=	-0.015	THETTA	=	0.023	OW	=	2.686D 02	TAUW	=	3.914D 00
HF	=	1C406.	DURFF	=	C.6321	STANTN	=	6.320D-03	RETH	=	57.	RETHTR	=	230.
N (1)	=	-3.650D-C1	XSN(1)	=	-7.510D-01									

***** NINE EQUILIBRIUM *****

X	=	-C.126	T	=	6285.	H	=	10484.	P	=	4.251D-01	R	=	9.412D-04
DIAM	=	1.142	V	=	4P437.	N	=	0.684	S	=	3.35	GAMMA	=	1.415
ARATEF	=	1.049	RPPF	=	3.600D C4	MW	=	18.29	MU	=	1.137D-04	SIGMA	=	2.631D 00
ARAT	=	1.103	DELSTR	=	-0.015	THETA	=	0.C23	OW	=	2.653D 02	TAUW	=	4.447D 00
HF	=	1C7G1.	DURFF	=	C.6331	STANTN	=	5.916D-03	RETH	=	61.	RETHTR	=	233.
N (1)	=	-4.577D-01	XSN(1)	=	-3.022D-C1									

***** NON EQUILIBRIUM *****

X	=	-C.C76	T	=	6192.	H	=	10469.	P	=	3.998D-01	R	=	9.001D-04
DIAM	=	1.120	V	=	4P336.	N	=	0.748	S	=	3.35	GAMMA	=	1.417
ARATEF	=	1.055	RPPF	=	3.877D C4	MW	=	18.29	MU	=	1.123D-04	SIGMA	=	2.528D 00
ARAT	=	1.050	DELSTR	=	-0.016	THETA	=	0.C23	OW	=	2.633D 02	TAUW	=	5.062D 00
HF	=	10775.	DURFF	=	C.6331	STANTN	=	5.626D-03	RETH	=	64.	RETHTR	=	236.
N (1)	=	-4. C13D-C1	XSN(1)	=	-3.612D-C1									

***** ACNE EQUILIBRIUM *****

X	=	-C.C39	T	=	6066.	H	=	1C327.	P	=	3.734D-01	R	=	8.569D-04
DIAM	=	1.104	V	=	5242.	N	=	0.615	S	=	3.35	GAMMA	=	1.420
ARATEF	=	0.974	RPPF	=	4.061D 04	MW	=	18.30	MU	=	1.106D-04	SIGMA	=	2.422D 00
ARAT	=	1.071	DELSTR	=	-C.C16	THETTA	=	0.C19	OW	=	2.621D 02	TAUW	=	5.785D 00
HF	=	1C757.	DURFF	=	C.6343	STANTN	=	5.429D-03	RETH	=	66.	RETHTR	=	240.
N (1)	=	-4.472D-C1	XSN(1)	=	-4.347D-C1									

***** MOLE FRACTIONS IN THE FREE STREAM *****

E-	=	1.771D 14	N2	=	2.650D-01	C2	=	1.540D-05	N	=	4.644D-01	D	=	2.667D-01
ND	=	1.464D-C7	N2E	=	2.876D-04	NC	=	5.5C4D-C5	DE	=	4.308D-05	N2C	=	6.166D-02
O2E	=	3.384D-C8												

REACTION RATE DATA

P1	=	1	C.1D-C8	=	2	B.4D-07	=	1.9D-11	4	7.0D-C8	=	3.5D-07	=	2.0D-05	=	8.6D-07	=	3.3D-07	
C	=	1.4D-06	1C	=	7.6D-C5	11	2.4D-C3	12	4.1D-04	13	2.7D-07	14	3.4D-07	15	5.6D-08	16	1.0D-08	17	4.5D-05
I	F	2.0Cn-C5	19	1.1D-C1	2C	4.4D-1C	21	2.6D-07	22	6.1D-C8	23	1.0D-05	24	1.8D-08	25	2.2D-08	26	1.0D-13	
CHI	I	-2.0D-CO	?	-2.2D 00	3	-2.9D CC	4	-2.9D CC	5	-3.3D 00	6	-3.3D 00	7	-3.3D 00	8	-3.3D 00	9	-3.3D 00	
C	-7.10C C	1C	-6.4D-C2	31	-4.0D-C2	12	3.6D-C2	13	8.3D-C1	14	A.0D-C1	15	1.2D-C1	16	2.2D-C1	17	-3.2D-C1	18	-3.2D-C1
I	1.11C-C1	1C	7.41C-C1	20	7.77-C1	21	2.5D-C1	22	1.5D-C1	23	1.4D-C1	24	3.0D-02	25	1.9D-01	26	7.7D-01	27	7.7D-01
PC1H	I	-1.17-C7	?	-2.5D-C6	3	-5.2D-C6	4	-2.0D-C7	5	-1.2D-C6	6	-7.1D-C5	7	-2.9D-C6	8	-1.0D-06	9	-1.0D-06	
C	-5.6D-07	1C	-4.4D-C6	11	-1.2D-C4	12	1.5D-04	13	2.2D-C7	14	2.7D-07	15	6.7D-09	16	2.4D-09	17	-1.4D-06	18	-1.4D-06

ORIGINAL PAGE IS
POOR QUALITY

1P	=	2.110-C7	19	=	4.4D-15	'C	=	3.4D-10	21	6.110-CH	=	22	9.4D-C9	=	23	1.4D-06	=	4.1D-09	=	26	7.9D-14
HC	=	-P.7D-C1	F-	=	1.3C-02	N2	=	1.3C-02	02	-1.6D OC	N	-1.7C-02	0	8.4D-03	NO	-1.3D 00	-NO	-6.6D-01			
K,	=	-1.CP CC	1F	=	-1.0D-C1	N26	=	-2.0D 00	025	-2.7D 00											

FIGURE 11 - NATA CODE OUTPUT - MODEL AND WEDGE CONDITIONS IN TEST PROBLEM NO. 1

```

X = 45.926      T = 229.          H = 6780.          P = 2.370D-05    R = 1.442D-06
DIAM = 25.000    V = 14320.        M = 10.941         S = 3.75      GAMMA = 1.1548
ARATEF = 211.874  REPF = 1.811D 03  MW = 18.32       MU = 1.140D-05   SIGMA = 9.042D-02
ARAT = 527.981   DELSTR = 4.355     THETA = 0.433       OW = 4.778D-01   TAUW = 2.146D-02
HR = 10000.      PRREF = 0.6495    STANTN = 2.153D-03  RETH = 65.      RETMTR = 2319.

E- = 3.315D 1C  N2 = 2.700D-01  O2 = 3.887D-06  N = 4.610D-01  O = 2.689D-01
NO = 3.594D-06  NOG = 3.947D-10  NG = 1.464D-05  OG = 2.903D-05  NG = 1.007D-09
O2C = 1.377D-11

T2E = 5356.      RT2E = 1.003D-05  PT2E = 4.028D-03  MUT2E = 1.017D-04  LEE = 0.737
ST2E = 3.91      MWT2E = 17.52     SIGT2E = 1.682D 00  PRF = 0.673  EPSLE = 0.156
QEFF = 9.33      QEFF = 2.67      OESRI = 28.43     DELREF = 0.566  DELRHM = 0.211

OEHE = 18.94     QEHF = 6.07      K2PFF = 3.68      HRATE = 0.713  OFP = 1.44
E- = 1.363D 12  N2 = 2.139D-01  O2 = 2.318D-06  N = 5.287D-01  O = 2.565D-01
NO = 4.097D-04  NOG = 1.873D-04  NG = 3.394D-05  OG = 2.475D-05  NG = 2.009D-06
O2C = 5.344D-05

T2F = 6956.      RT2F = 7.889D-06  PT2F = 3.936D-03  MUT2F = 1.235D-04  LEF = 0.825
ST2F = 3.89      MWT2F = 18.32     SIGT2F = 3.016D-01  PRF = 0.704  EPSLF = 0.198
OFFE = 9.53      QFFF = 3.86      OFSRI = 28.10     DELRFF = 0.572  DELRFH = 0.247
QFPC = 20.26     QFHF = 8.20      K2PFF = 4.57      HRATF = 0.619

***** CONDITIONS ON WEDGE MODELS *****
***** MODIFIED CHENG-KEMP THEORY *****

MERGING EFFECTS SIGNIFICANT FOR XW LESS THAN 1.80D 01 INCHES.
***** CONDITIONS ON WEDGE MODELS *****
UNIDENTIFIED CHENG-KEMP THEORY

MERGING EFFECTS SIGNIFICANT FOR XW LESS THAN 1.80D 01 INCHES.
STRONG-INTERACTION APPROXIMATION BREAKS DOWN FOR XW GREATER THAN 1.26D 02 INCHES.

***** LEADING-EDGE RADIUS = 0.375 INCH. ANGLE OF ATTACK = 15.0 DEGREES. CAPITAL GAMMA = 3.13D 00. OMEGA = 5.73D-01 *****
XW (INCHES) = 1.00D 00  2.00D 00  2.50D 00  3.00D 00  4.00D 00  5.00D 00  6.00D 00  7.00D 00  8.00D 00
PWN (BTU/SQ FT-SEC) = 1.42D-03 1.08D-03 9.9AD-03 9.39D-04 8.59D-04 8.05D-04 7.66D-04 7.37D-04 7.13D-04
QWN (BTU/SQ FT-SEC) = 2.21D 01* 1.48D 01 1.29D 01 1.16D 01 9.78D 00 9.14D 00 8.61D 00 7.77D 00 7.14D 00
STANTN NUMBER = 1.04D-01 6.66D-02 5.82D-02 5.22D-02 4.41D-02 4.12D-02 3.88D-02 3.50D-02 3.22D-02 2.99D-02
DELSTW (INCH) = 2.44D-01 3.80D-01 4.35D-01 4.85D-01 5.74D-01 6.14D-01 6.52D-01 7.22D-01 7.87D-01 8.46D-01
ZETA = 7.26D-03 1.45D-02 1.82D-02 2.18D-02 2.90D-02 3.27D-02 3.63D-02 4.36D-02 5.08D-02 5.81D-02

* FREE-MOLECULE LIMIT
***** CONDITIONS ON WEDGE MODELS *****
UNIDENTIFIED CHENG-KEMP THEORY

***** LEADING-EDGE RADIUS = 0.375 INCH. ANGLE OF ATTACK = 15.0 DEGREES. CAPITAL GAMMA = 3.05D 00. OMEGA = 5.73D-01 *****
XW (INCHES) = 1.00D 00  2.00D 00  2.50D 00  3.00D 00  4.00D 00  5.00D 00  6.00D 00  7.00D 00  8.00D 00
PWN (BTW) = 1.38D-03 1.03D-03 9.51D-04 8.93D-04 8.13D-04 7.59D-04 7.20D-04 6.91D-04 6.67D-04
QWN (BTW/SQ FT-SEC) = 2.24D 01 1.43D 01 1.25D 01 1.12D 01 9.40D 00 8.77D 00 8.26D 00 7.44D 00 6.82D 00
STANTN NUMBER = 1.01D-01 6.45D-02 5.62D-02 5.03D-02 4.24D-02 3.95D-02 3.72D-02 3.35D-02 3.08D-02 2.86D-02
DELSTW (INCH) = 2.51D-01 3.92D-01 4.51D-01 5.03D-01 5.97D-01 6.40D-01 6.80D-01 7.55D-01 8.23D-01 8.86D-01
ZETA = 7.26D-03 1.45D-02 1.82D-02 2.18D-02 2.90D-02 3.27D-02 3.63D-02 4.36D-02 5.08D-02 5.81D-02
FLAPSW TIME IN MODEL AND WEDGE CALCULATIONS = 30. SECONDS

```

If calculations of conditions on wedge models have been specified in the input, the wedge results follow those for the stagnation point, as shown in figure 11. The message about merging effects refers to equation (510a) in Volume I (ref. 1). The results given under "modified Cheng-Kemp theory" are based on the formulas of Section 8.2.4 in Volume I. In particular, "capital gamma" is Γ as defined by equation (501) in Volume I, and "omega" is Ω as given by (502). The output quantities X_W , P_{WW} , Q_{WW} , etc., in the table are defined in figure 5. The wedge results given under "unmodified Cheng-Kemp Theory" are based on the formulas of Section 8.2.3 in Volume I. The message referring to the strong-interaction approximation is based on equation (510b) of Volume I.

3.7 Throat Conditions

Immediately following the frozen solution is a page of output summarizing the sonic conditions in the solution. The format is similar to that used in the output of reservoir conditions, except that the transport properties are omitted. A similar page giving the sonic conditions in the equilibrium flow solution follows that solution (figure 12). Since the equilibrium sonic conditions are needed for starting the nonequilibrium solution, they are computed and printed even when the equilibrium solution is suppressed by setting ISW3A = 0, if the nonequilibrium solution has been requested ($ISW2A \neq 0$). The page containing the equilibrium sonic conditions also gives the coefficients α and C in the analytical area-density relation (equation (383) of Volume I) used in the upstream nonequilibrium solution by the inverse method.

3.8 Informative Messages

The normal forms of output, illustrated and discussed above, are sometimes interrupted with messages containing information of possible interest to the code user. For example, during the solution by the perturbation method, one line of additional output is printed for each step, giving the smallest $|\delta X_i|$ (DCHMIN), the largest (DCHMAX), and the index IMAX of the largest $|\delta X_i|$ (see Section 7.3 of Volume I (ref. 1)). This type of output is illustrated in figure 9.

When the switch from the inverse method to direct numerical integration is made (Section 7.4, Volume I (ref. 1)), subroutine

FIGURE 12 - NATA CODE OUTPUT - EQUILIBRIUM SONIC CONDITIONS FOR TEST PROBLEM NO. 1

- EO! TRITIUM THROAT CONDITIONS -

GAS FLOW RATE	=	2.030	LB/SEC
NOZZLE - EOS	=	1.088	INCH THROAT DIAMETER
PRESSURE	=	0.336	ATM
TEMPERATURE	=	6446.	DEG K
ENTHALPY	=	10175.	BTU/LB
ENTROPY	=	3.35	BTU/LB-DEG R
DENSITY	=	0.00074	LB/CU FT
VELOCITY	=	5924.	FT/SEC
MASS FLUX	=	4.375	LB/SQ FT-SEC
COMPUTED FLOW	=	0.030	LB/SEC
GAMMA	=	1.406	
MOLECULAR WEIGHT	=	18.62	GM/MOLE
ELECTRON DENSITY	=	1.74D 14	ELECTRONS/CC

SPECIES MOLE FRACTIONS

E-	4.54E0-04
N2	2.985D-01
O2	3.032D-05
N	4.377D-01
O	2.47C5D-01
NO	2.377D-03
NO2	3.467D-04
NC	5.945D-05
Oc	3.950D-05
N2O	9.132D-06
O2O	6.803D-08

*****. ***ELAPSED TIME= 2.27 MINUTES SINCE START OF RUN. 33. SECONDS SINCE LAST PRINTED TIME

DENSITY FIT-ALPHA= 1.4419063D-01 CONSTANT= 2.5604746D-02

ORIGINAL PAGE IS
OF POOR QUALITY

THRØAT is called to rescale the nozzle geometry so as to provide continuity of effective flow area between the two solutions. THRØAT prints a two-line message as illustrated in figure 13. The point at which this output is produced is neither the geometric throat nor the sonic point, but a location distinctly downstream of both. The variables given in this output are as follows:

CX Axial coordinate in nozzle (cm)

AMACH Mach number

AFNX Effective area ratio, \tilde{A}_e , based on the inverse method

DLOGA $d \ln \tilde{A}_e/dx$

S1 Effective area ratio, A_e , based on the nozzle geometry and boundary layer displacement thickness

S2 $d \ln A_e/dx$

RSA Area rescaling factor, $R_a = \tilde{A}_e/A_e$

DELBL Nondimensional displacement thickness, δ^*/R_0 (two values in the case of a channel)

During the nonequilibrium integration, under certain circumstances, the code may "freeze" a species of very low concentration which is decreasing so rapidly that it controls the step size, by switching off all of the reactions in which it appears (Section 7.5.3 of Volume I). When this occurs, a message such as the one appearing at the bottom of figure 14 is produced.

The switch from the perturbation method to the nonequilibrium integration normally occurs where the largest $|\delta\chi_i|$ is about 0.1. If one of the $|\delta\chi_i|$ is very much larger than some of the others, it can cause the integration to start at a point where some of the reactions are very close to equilibrium. Should this occur, the step size required for stability of the finite difference equations would be too small to allow significant progress in the solution. Under certain circumstances (Section 7.3.7 in Volume I), NATA prevents such a premature startup of the numerical

FIGURE 13 - NATA CODE OUTPUT - AREA RESCALING MESSAGE FROM SUBROUTINE THROAT IN TEST PROBLEM NO. 1

```

X      =  1.045          T      =  5187.          H      =  974.          P      =  2.193D-01          R      =  5.88E-
DIAM   =  1.111          V      =  7539.          M      =  1.    J2          S      =  3.35          GAMMA =  1.44E-
ARATEF =  0.996          REPF  =  4.548D 04          MW   =  18.30          MU   =  9.756D-05          SIGMA =  1.777D 00
ARAT   =  1.043          DELSTR =  -0.016          THETA =  0.020          QW   =  2.242D 02          TAUW =  7.045D 00
HR    =  10629.          PREF  =  0.6398          STANTN =  4.700D-03          RETH =  74.          RETTHR =  265.

E-    =  7.049D 13          N2   =  2.677D-01          O2   =  5.507D-06          N   =  4.634D-01          O   =  2.677D-01
NO    =  6.715D-04          NOE  =  1.708D-04          NC   =  4.057D-05          OC   =  4.224D-05          N2C  =  2.597D-06
O2C   =  8.646D-09

```

```
*****NONEQUILIBRIUM*****INEQ=1
```

```

X      =  0.059          T      =  5099.          H      =  9583.          P      =  2.072D-01          R      =  5.657D-04
DIAM   =  1.119          V      =  7730.          M      =  1.293          S      =  3.35          GAMMA =  1.447
ARATEF =  1.011          REPF  =  4.541D 04          MW   =  18.30          MU   =  9.628D-05          SIGMA =  1.689D 00
ARAT   =  1.058          DELSTR =  -0.016          THETA =  0.020          QW   =  2.173D 02          TAUW =  6.850D 00
HR    =  10616.          PREF  =  0.6408          STANTN =  4.624D-03          RETH =  75.          RETTHR =  267.

E-    =  7.146D 13          N2   =  2.679D-01          O2   =  4.603D-06          N   =  4.633D-01          O   =  2.678D-01
NO    =  5.814D-04          NOE  =  1.563D-04          NC   =  3.877D-05          OC   =  4.217D-05          N2C  =  2.352D-06
O2C   =  6.932D-09

```

```
////////// THROAT CX= 1.765D-01          AMACH= 1.322D 00          AFNX= 1.011D 00          DLOGA= 4.094D-01
S1= 1.068D 00          S2= 4.009D-01          RSA= 9.464D-01          DELBL=-2.986D-02
```

```
*****NONEQUILIBRIUM*****INEQ=1
```

```

X      =  0.075          T      =  5018.          H      =  9629.          P      =  1.960D-01          R      =  5.439D-04
DIAM   =  1.097          V      =  7921.          M      =  1.332          S      =  3.35          GAMMA =  1.450
ARATEF =  1.C18          REPF  =  4.502D 04          MW   =  18.30          MU   =  9.546D-05          SIGMA =  1.636D 00
ARAT   =  1.016          DELSTR =  -0.017          THETA =  0.021          QW   =  2.049D 02          TAUW =  6.431D 00
HR    =  10605.          PREF  =  0.6408          STANTN =  4.436D-03          RETH =  77.          RETTHR =  270.

E-    =  6.456D 13          N2   =  2.680D-01          O2   =  3.896D-06          N   =  4.632D-01          O   =  2.679D-01
NO    =  5.068D-04          NOE  =  1.438D-04          NC   =  3.715D-05          OC   =  4.210D-05          N2C  =  2.142D-06
O2C   =  5.634D-09

```

```
*****NONEQUILIBRIUM*****INEQ=1
```

```

X      =  0.092          T      =  4942.          H      =  9579.          P      =  1.863D-01          R      =  5.250D-04
DIAM   =  1.105          V      =  8057.          M      =  1.367          S      =  3.35          GAMMA =  1.452
ARATEF =  1.034          REPF  =  4.494D 04          MW   =  18.30          MU   =  9.412D-05          SIGMA =  1.551D 00
ARAT   =  1.032          DELSTR =  -0.017          THETA =  0.021          QW   =  1.995D 02          TAUW =  6.291D 00
HR    =  10595.          PREF  =  0.6417          STANTN =  4.387D-03          RETH =  78.          RETTHR =  272.

E-    =  5.870D 13          N2   =  2.681D-01          O2   =  3.325D-06          N   =  4.631D-01          O   =  2.680D-01
NO    =  4.432D-04          NOE  =  1.325D-04          NC   =  3.564D-05          OC   =  4.204D-05          N2C  =  1.961D-06
O2C   =  4.611D-C9

```

```
*****NONEQUILIBRIUM*****INEQ=1
```

```

X      =  0.111          T      =  4862.          H      =  9528.          P      =  1.766D-01          R      =  5.057D-04
DIAM   =  1.115          V      =  8216.          M      =  1.404          S      =  3.35          GAMMA =  1.455
ARATEF =  1.053          REPF  =  4.494D 04          MW   =  18.30          MU   =  9.267D-05          SIGMA =  1.471D 00

```

```
*****NONEQUILIBRIUM*****INEQ=1
```

```

X      =  0.111          T      =  4862.          H      =  9528.          P      =  1.766D-01          R      =  5.057D-04
DIAM   =  1.115          V      =  8216.          M      =  1.404          S      =  3.35          GAMMA =  1.455
ARATEF =  1.053          REPF  =  4.494D 04          MW   =  18.30          MU   =  9.267D-05          SIGMA =  1.471D 00

```

FIGURE 14 - NATA CODE OUTPUT - FREEZING & MINOR SPECIES MESSAGE IN TEST PROBLEM NO. 1

```
*****NONEQUILIBRIUM***** 4 STEPS***** .NEQ=1
X = 3.898   T = 1523.   H = 7510.   P = 5.053D-03   R =
DIAM = 3.90   V = 12981.   M = 3.876   S = 3.35   GAMMA =
ARATEF = 7.290   REPF = 1.643D 04   MW = 18.32   MU =
ARAT = A.065   DELSTR = 0.033   THETA = 0.074   QW =
HR = 10156.   PRREF = 0.6488   STANTN = 2.726D-03   RETH =
               SPECIES MOLE FRACTIONS IN THE FREE STREAM
               N2 = 2.697D-01   O2 = 1.545D-06   N =
NO = 1.501D 12   NOD = 2.192D-08   NC = 2.069D-05   O6 =
O2C = 2.506D-10   N2C = 4.093D-05   N2C = 4.013D-09

*****NONEQUILIBRIUM***** 4 STEPS***** .NEQ=1
X = 4.163   T = 1453.   H = 7470.   P = 4.397D-03   R =
DIAM = 3.238   V = 13059.   M = 3.990   S = 3.35   GAMMA =
ARATEF = 7.945   REPF = 1.564D 04   MW = 18.32   MU =
ARAT = A.859   DFLSTR = 0.040   THETA = 0.078   QW =
HR = 10147.   PRREF = 0.6488   STANTN = 2.693D-03   RETH =
               SPECIES MOLE FRACTIONS IN THE FREE STREAM
               N2 = 2.697D-01   O2 = 1.620D-06   N =
NO = 1.367D 12   NOD = 1.470D-08   NC = 2.066D-05   O6 =
O2C = 2.217D-06   N2C = 4.614D-01   N2C = 2.688D-01
               N2C = 2.708D-09

*****NONEQUILIBRIUM***** 4 STEPS***** .NEQ=1
X = 4.537   T = 1375.   H = 7424.   P = 3.735D-03   R =
DIAM = 3.423   V = 13145.   M = 4.126   S = 3.35   GAMMA =
ARATEF = 8.2   REPF = 1.474D 04   MW = 18.32   MU =
ARAT = 9.898   DELSTR = 0.051   THETA = 0.083   QW =
HR = 10137.   PRREF = 0.6488   STANTN = 2.660D-03   RETH =
               SPECIES MOLE FRACTIONS IN THE FREE STREAM
               N2 = 2.697D-01   O2 = 1.712D-06   N =
NO = 1.225D 12   NOD = 9.541D-09   NC = 2.062D-05   O6 =
O2C = 2.168D-06   N2C = 4.614D-01   N2C = 2.688D-01
               N2C = 1.665D-09

*****NONEQUILIBRIUM***** 5 STEPS***** .NEQ=1
X = 4.906   T = 1303.   H = 7383.   P = 3.18 D-03   R =
DIAM = 3.615   V = 13226.   M = 4.262   S = 3.35   GAMMA =
ARATEF = 9.711   REPF = 1.3890 04   MW = 18.32   MU =
ARAT = 11.043   DELSTR = 0.062   THETA = 0.088   QW =
HR = 10128.   PRREF = 0.6488   STANTN = 2.625D-03   RETH =
               SPECIES MOLE FRACTIONS IN THE FREE STREAM
               N2 = 2.697D-01   O2 = 1.803D-06   N =
NO = 1.101D 12   NOD = 6.591D-09   NC = 2.059D-05   O6 =
O2C = 2.125D-06   N2C = 4.613D-01   N2C = 4.075D-05
               N2C = 1.007D-09

*****NONEQUILIBRIUM***** 5 STEPS***** .NEQ=1
X = 5.222   T = 1231.   H = 7342.   P = 3.06 D-03   R =
DIAM = 3.815   V = 13306.   M = 4.422   S = 3.243D-05   GAMMA =
ARATEF = 10.911   REPF = 1.3890 04   MW = 18.32   MU =
ARAT = 12.043   DELSTR = 0.062   THETA = 0.088   QW =
HR = 10119.   PRREF = 0.6488   STANTN = 2.625D-03   RETH =
               SPECIES MOLE FRACTIONS IN THE FREE STREAM
               N2 = 2.697D-01   O2 = 1.803D-06   N =
NO = 1.010D 12   NOD = 6.591D-09   NC = 2.059D-05   O6 =
O2C = 2.145D-06   N2C = 4.613D-01   N2C = 4.075D-05
               N2C = 1.007D-09

*****CONCENTRATION OF N2C FROZEN AT 5.495D-11 MOLE/GM.
*****SUPPRESSED REACTIONS 17 18 22
*****NONEQUILIBRIUM***** 6 STEPS***** .NEQ=1
```

integration by artificially increasing the rate constant for the reaction with the largest $|\delta\chi_i|$, for the duration of the perturbation solution. When this occurs, the code prints a message such as the one illustrated in figure 15 (for a problem involving the IGAS = 5 planetary atmosphere model).

3.9 Transport Cross Section Edit

Figures 16, 17 and 18 illustrate the three parts of the transport cross section edit, which is invoked by setting ISW1E equal to -2. Figure 16 shows the edit of precoded cross section data for all species. In this table, STEP is the counter for the steps of the cross section calculation in the order in which they are carried out, while INDEX is the index of the steps in array storage. For the precoded data, these two indices are equal for all steps. However, if new steps were added by input, this equality might no longer hold. OPTION is the index of the option used to calculate the cross section generated in each step (see Section 4). The quantities VV(1) to VV(5) are parameter values for the steps. Under INTERACTION, the pairs of species to which each cross section applies are listed.

Figure 17 shows the first page of the second part of the cross section edit, which summarizes the steps of the cross section calculation for the current gas model. The edit shown in the figure is for the large standard air model (IGAS = 1). The format is similar to that in figure 16.

Figure 18 shows the first page of the third part of the cross section edit, the tabulation of averaged pair cross sections as functions of temperature. The temperature is given in degrees Kelvin at 1000 degree intervals up to CTAPI. The three tabulated cross sections are

$$Q(1) = \bar{\Omega}_{ij}^{(1,1)} \quad (2a)$$

$$Q(2) = \bar{\Omega}_{ij}^{(2,2)} \quad (2b)$$

$$Q(3) = B^* \bar{\Omega}_{ij}^{(1,1)} \quad (2c)$$

(where the notation is defined in Section 3.1 of Volume I), and are given in square Angstroms (units of 10^{-16} cm^2). The

NOVEMBER 19, 1961.

FIGURE 15 - NATIVE MODE OUTPUT - AR*
*NATURAL INCREASE OF RATE - INSTANT MESSAGE

U.S. Chemicals Inc. 5029220-C-5

124 X 344

111

DMIN = 5.297D-05 DCHMAX = 5.148D-01
 DRWINE = 1.527D-05 DCINMAX = 1.460D-01
 CCCMIN = 4.0471D-06 DCINMAX = 4.0242D-02
 CCCPMMIN = 1.0527D-05 DCINMAX = 1.0450D-01
 DCHMIN = 0.150D-06 DCHMAX = 8.725D-02
 DCHMINE = 1.0527D-05 DCINMAX = 1.0450D-01
 DCCHWINE = 1.0240D-05 DCHMAX = 1.0449D-01
 DCCHWMIN = 1.0240D-05 DCHMAX = 1.0449D-01

61 STEPS TO ACHIEVE YOUR DREAMS

NON-UNIFORMITY

X	-3.5.-2	T	=	3696.	H	=	4958.	P	=	6.1300-01	R	=	3.361D-03		
ZIAY	2.C11	V	=	1410.	M	=	0.351	S	=	2.42	GAMMA	=	1.365		
AFAGATEF	1.719	REFF	=	6.315D 04	NW	=	26.66	MU	=	7.504D-05	SIGMA	=	6.702D-03		
RAT	1.797	DFLSTR	=	-C.011	THETA	=	0.015	OW	=	1.106D 02	TAUW	=	1.275D 00		
HN	4.091e	PPREF	=	0.6604	STAIN	=	4.767D-03	RETH	=	80.	RETHTR	=	216.		
				SPECIES MOLE FRACTIONS IN THE FREE STIRFAM											
				AR	=	1.0258D-01	CC2	=	2.960D-02	N2	=	2.615D-02	O2	=	6.576D-02
				O	=	3.001D-01	NO	=	1.03.2-02	CO	=	4.420D-01	CN	=	2.967D-06
				NO	=	7.028D-07	NC	=	H.5E6D-15	OC	=	7.413D-11	N2O	=	8.806D-14
				CO	=	1.741D-14	ARC	=	5.875D-13	COC	=	1.312D-10			

CONCENTRATION OF CCE FROZEN AT 5.92°C-16 MOLE/GM.

CONCENTRATION OF NF₃ FROZEN AT 2026 AND -16 MOLE/GM.

*****ONE CUILISHIUM*****

ORIGINAL PAGE IS
OF POOR QUALITY

$\text{C}_6\text{H}_5\text{CH}_2\text{Cl} + \text{C}_6\text{H}_5\text{CH}_2\text{COCl} \rightarrow \text{C}_6\text{H}_5\text{CH}_2\text{COCH}_2\text{CH}_2\text{Cl} + \text{HCl}$

DCH₂C₆H₅ = 5.29200-05 DCH₂Cl = 1.04940-03 IMAX=44

TOTAL CONCENTRATION OF REACTANT = 30.670-03 MOLE/LITER

CONCENTRATION OF C₆H₅CH₂Cl IN REACTION NO. 44 IS 2.360-14 MOLE/GM.

CONCENTRATION OF C₆H₅CH₂COCl IN REACTION NO. 44 IS 2.360-14 MOLE/GM.

PERCENTAGE CONCENTRATION OF C₆H₅CH₂COCl IN REACTION NO. 44 IS 8.0840-03 FOR PERTURBATION SOLUTION.

DCHMAX = 5.148D-01 **I MAX = 19**
DCHMIN = 1.460D-01 **I MAX = 15**
DCHMAX = 4.024D-02 **I MAX = 19**
DCHMIN = 1.040D-01 **I MAX = 19**
DCHMAX = 5.725D-02 **I MAX = 19**
DCHMIN = 1.046D-01 **I MAX = 15**
DCHMAX = 1.049D-01 **I MAX = 19**

61 STEPS TO ACHIEVE YOUR DREAMS

*** NON CUILIER

X	-3.5.-2	T	=	3696.	H	=	4958.	P	=	6.1300-01	R	=	3.361D-03		
ZIAY	2.C11	V	=	1410.	M	=	0.351	S	=	2.42	GAMMA	=	1.365		
AFAGATEF	1.719	REFF	=	6.315D 04	NW	=	26.66	MU	=	7.504D-05	SIGMA	=	6.702D-03		
RAT	1.797	DFLSTR	=	-C.011	THETA	=	0.015	OW	=	1.106D 02	TAUW	=	1.275D 00		
HN	4.091e	PPREF	=	0.6604	STAIN	=	4.767D-03	RETH	=	80.	RETHTR	=	216.		
				SPECIES MOLE FRACTIONS IN THE FREE STIRFAM											
				AR	=	1.0258D-01	CC2	=	2.960D-02	N2	=	2.615D-02	O2	=	6.576D-02
				O	=	3.001D-01	NO	=	1.03.2-02	CO	=	4.420D-01	CN	=	2.967D-06
				NO	=	7.028D-07	NC	=	H.5E6D-15	OC	=	7.413D-11	N2O	=	8.806D-14
				CO	=	1.741D-14	ARC	=	5.875D-13	COC	=	1.312D-10			

..... CONCENTRATION OF C6 FROZEN AT 5.92°C-16 MOLE/GM.
SUPPRESSO REACTIONS 34 15 16 38 40

CONCENTRATION OF NF
SUBOCCESSED REACTIONS FROZEN AT 2426AD-16 MOLE/G MO.

FIGURE 16 - NATA CODE OUTPUT - TRANSPORT CROSS SECTION EDIT (INPUT) (First Page)
 TRANS.ORT CROSS SECT. N DATA
 {INPUT}

STEP	INDEX	OPTION	VV(1)	VV(2)	VV(3)	VV(4)	VV(5)	INTERACTION
1	1	3	2.553D-37	2.970D-01	1.000D-00	0.0	0.0	AR = AR
2	2	3	6.244D-10	1.969D-01	1.000D-00	0.0	0.0	ARM = ARM
3	3	3	1.477D-07	3.21D-01	1.000D-00	0.0	0.0	AR* = AR*
4	4	3	2.414D-06	3.64D-01	1.000D-00	0.0	0.0	AR = ARC
5	5	6	9.990D-02	6.89D-00	0.0	0.0	0.0	AR = N2
6	6	14	1.733D-02	1.116D-00	1.000D-00	0.0	0.0	N = AR
7	7	14	1.656D-02	1.114D-00	1.000D-00	0.0	0.0	C = C
8	8	14	1.420D-02	1.141D-00	1.000D-00	0.0	0.0	C = C
9	9	5	1.000D-00	5.100D-01	2.000D-00	0.0	0.0	C = C
10	10	6	9.989D-12	4.824D-00	0.0	0.0	0.0	NC = NC
11	11	6	9.970D-02	4.722D-00	0.0	0.0	0.0	OC = OC
12	12	5	1.000D-23	8.100D-01	2.000D-01	0.0	0.0	N = N
13	13	5	1.000D-00	1.010D-02	2.000D-01	0.0	0.0	CN = CN
14	14	5	1.000D-00	1.210D-02	2.000D-01	0.0	0.0	N = N2
15	15	5	1.000D-00	1.410D-02	2.000D-01	0.0	0.0	CO = CO
16	16	5	1.000D-00	1.410D-02	2.000D-01	0.0	0.0	CO = CO
17	17	5	1.000D-00	1.410D-02	2.000D-01	0.0	0.0	CO2 = CO2
18	18	5	1.000D-00	1.610D-02	2.000D-01	0.0	0.0	N2 = N2
19	19	5	1.000D-00	1.810D-02	2.000D-01	0.0	0.0	O = O
20	20	5	1.000D-00	1.810D-02	2.000D-01	0.0	0.0	N2 = NO
21	21	5	1.000D-00	2.010D-02	2.000D-01	0.0	0.0	N2 = O2
22	22	5	1.000D-00	2.210D-02	2.000D-01	0.0	0.0	O = CN
23	23	5	1.000D-00	2.410D-02	2.000D-01	0.0	0.0	O = O2
24	24	9	2.000D-20	6.000D-00	5.000D-01	1.000D-00	1.000D-00	O2 = O2
25	25	14	5.000D-01	1.000D-00	1.000D-00	0.0	0.0	NO = NO
								NN = NN

FIGURE 16 - NATA CODE OUTPUT - TRANSPORT CROSS SECTION EDIT (INPUT) (Second Page)

26	14	1.0000 00	1.0000 00	1.	00	0.0	0.0	N	- N2	
27	14	9.1390-01	1.01170 00	1.00000 00	0.0	0.0	0.0	CO	- CO	
28	14	9.5400-01	1.1950 00	1.00000 00	0.0	0.0	0.0	CO	- CO	
29	14	9.5100-01	1.1240 00	1.00000 00	0.0	0.0	0.0	N2	- CO	
30	14	8.9100-01	1.1190 00	1.00000 00	0.0	0.0	0.0	CO	- CO	
31	14	9.2300-01	1.0620 00	1.00000 00	0.0	0.0	0.0	CO	- CO	
32	14	9.6400-01	1.0820 00	1.00000 00	0.0	0.0	0.0	CO	- CO	
33	14	1.0000 00	1.2740 00	1.00000 00	0.0	0.0	0.0	CO	- CO	
34	14	9.8200-01	1.1170 00	1.00000 00	0.0	0.0	0.0	N2	- CO	
35	14	9.4100-01	1.1150 00	1.00000 00	0.0	0.0	0.0	CO	- CO	
36	14	2.5000-01	1.0000 00	1.00000 00	0.0	0.0	0.0	NO	- NO	
37	14	5.3000-91	1.0000 00	1.00000 00	0.0	0.0	0.0	N2	- CN	
38	14	1.0000 00	1.0000 00	1.00000 00	0.0	0.0	0.0	N2	- N2	
39	14	5.0000-01	1.0000 00	1.00000 00	0.0	0.0	0.0	O	- N2	
					0	0	0	O	- CN	
					N	0	0	O	- NO	
					02	CN	02	O2	- NO	
					02	CN	02	O2	- CN	
40	40	<	7.0000 00	7.0000 00	1.00000 00	1.00000 00	1.00000 00	NO	- CO	
41	41	<	1.0000 00	2.6110 02	2.0000 01	0.0	0.0	E-	- E-	
42	42	5	1.0000 00	2.8100 02	2.0000 01	0.0	0.0	E-	- E-	
43	43	5	1.0000 00	7.1000 01	2.0000 00	0.0	0.0	E-	- N	
44	44	5	1.0000 00	3.0110 02	2.0000 01	0.0	0.0	E-	- CN	
45	45	5	1.0000 00	3.2100 02	2.0000 01	0.0	0.0	E-	- NO	
46	46	5	1.0000 00	3.4100 02	2.0000 01	0.0	0.0	E-	- N2	
47	47	5	1.0000 00	3.6100 02	2.0000 01	0.0	0.0	E-	- O	
48	48	5	1.0000 00	3.8100 02	2.0000 01	0.0	0.0	E-	- O2	
49	49	13	2.0000 00	1.0000 00	1.00000 00	0.0	0.0	E-	- AR	
					CO	- CO	E-	- CN		
					CO	- CN2	E-	- N		
					02	CN	02	- NO		
50	50	13	2.0000 00	1.0000 00	1.00000 00	0.0	0.0	E-	- N2	
					02	CN	02	- O		
51	51	3	2.6450 06	2.3530-01	1.00000 00	0.0	0.0	E-	- O2	
					HE	- HE	HE	- HE3S		
					HE	- HE1S	HE	- HF1S		
					HF3S	- HF3S	HF3S	- HE3S		
52	52	3	2.6450 06	2.3530-01	1.00000 00	0.0	0.0	HF1S	- HE1S	
53	53	3	5.1530 05	4.6360-01	1.00000 00	0.0	0.0	HE2	- HE2	
					HE	- HE	HE	- HF2C		
					HF	- HF	HF	- HF2C		
54	54	3	5.1530 05	4.6360-01	1.00000 00	0.0	0.0	HF3S	- HF2C	
55	55	5	1.0000 00	4.7100 02	2.00000 01	0.0	0.0	HF1S	- HE2	
					F-	- F	F-	- HE1S		
					E-	- E	E-	- HE2		

FIGURE 15 - NATA CODE OUTPUT - TRANSPORT CROSS SECTION EDIT (INPUT) (Third Page)

56	56	1.0	0.0	0.0	C	0.0	0.0	0.0	YY.- = Y
57	57	4	1.345D 01	1.413D 00	4	30 00	1.0000D 00	0.0	HE = HE
									HEG = HEG
									HF3S = HF3S
									HE = HE
									HE1S = HE1S
									HF3S = HF3S
									HF1S = HF1S
									HE3S = HE3S
									HEJS = HEJS
									HE1S = HE1S
									CC = CC
									NO = NO
									CO = CO
									CC = CC
									N = N
									NC = NC
									AR = AR
									ARC = ARC
									ARH = ARH
									ARR = ARR
									NO = NO
58	58	4	1.346D 01	1.413D 00	4.003D 00	1.0000D 00	0.0		
59	59	6	9.960D 02	5.000D 00	0.0	0.0	0.0		
60	60	4	1.530D 01	1.600D 00	1.401D 01	1.0000D 00	0.0		
61	61	4	1.490D 01	1.570D 00	1.6000 01	1.0000D 00	0.0		
62	62	4	1.593D 01	1.700D 00	3.994D 01	1.0000D 00	0.0		
63	63	4	1.470D 01	1.670D 00	3.001D 01	1.0000D 00	0.0		

ORIGINAL PAGE IS
OF POOR QUALITY

FIGURE 17 - NATA CODE OUTPUT - TRANSPORT CROSS SECTION EDIT (EDITED)
TRANSPORT CROSS SECTION DATA
(EDITED)

STEP	INDEX	OPTION	VV(1)	VV(2)	VV(3)	VV(4)	VV(5)	INTERACTION
1	6	9.98200 02	4.82400 00					N - NC
2	6	9.97000 02	4.72200 00					O - O2
3	5	1.00000 00	8.10000 01	2.00000 01				N - N
4	5	1.00000 00	1.01000 02	2.00000 01				N2 - NO
5	5	1.00000 00	1.21000 02	2.00000 01				N2 - N
6	5	1.00000 00	1.41000 02	2.00000 01				N - O
								NO - NO
								N2 - NO
								N2 - N2
7	5	1.00000 00	1.61000 02	2.00000 01				N2 - O
8	5	1.00000 00	1.81000 02	2.00000 01				O2 - NO
9	5	1.00000 00	1.81000 02	2.00000 01				O2 - NO
10	5	1.00000 00	2.01000 02	2.00000 01				N2 - O2
11	5	1.00000 00	2.21000 02	2.00000 01				O - O
12	5	1.00000 00	2.41000 02	2.00000 01				O - NO
								O2 - O
13	9	3.00000 00	4.00000 00	5.00000-01	1.00000 00	1.00000 00		NO - NO
14	14	5.00000-01	1.00000 00	1.00000 00				N - NO
15	14	1.00000 00	1.00000 00	1.00000 00				N2 - N
16	14	2.50000-01	1.00000 00	1.00000 00				O - NO
17	14	5.00000-01	1.00000 00	1.00000 00				N2 - NO
18	14	1.00000 00	1.00000 00	1.00000 00				N2 - N2
19	14	5.00000-01	1.00000 00	1.00000 00				O - NO
								O2 - NO
20	5	1.00000 00	7.10000 01	2.00000 00				O2 - NO
21	5	1.00000 00	3.01000 02	2.00000 01				E - N
22	5	1.00000 00	3.21000 02	2.00000 01				E - NO

FIGURE 18 - NATA CODE OUTPUT - TRANSPORT CROSS SECTION EDIT (AVERAGED PAIR CROSS SECTIONS)
AVERAGED PAIR CROSS-SECTIONS / JUNCTIONS OF TEMPERATURE

TEMP.	Q(1)	Q(2)	Q(3)	INDICES	SPECIES	COUNT
1000.	6.5470 04	1.0610 05	1.0230 05	1- 1	E- -E-	1
2000.	2.2120 04	3.5830 04	3.4560 04	1- 1	F- -E-	2
3000.	1.1430 04	1.8510 04	1.7850 04	1- 1	F- -E-	3
4000.	7.0940 03	1.0140 04	1.0100 04	1- 1	F- -E-	4
5000.	4.5320 03	7.9490 03	7.6260 03	1- 1	F- -E-	5
6000.	3.5910 03	5.8150 03	5.6080 03	1- 1	E- -E-	6

TEMP.	Q(1)	Q(2)	Q(3)	INDICES	SPECIES	COUNT
1000.	5.3000 00	5.3000 00	5.3000 00	1- 2	E- -N2	7
2000.	7.7000 00	7.7000 00	7.7000 00	1- 2	F- -N2	8
3000.	8.8000 00	8.8000 00	8.8000 00	1- 2	E- -N2	9
4000.	9.5200 00	9.5000 00	9.5000 00	1- 2	E- -N2	10
5000.	9.9000 00	9.9000 00	9.9000 00	1- 2	E- -N2	11
6000.	1.0300 01	1.0330 01	1.0300 01	1- 2	F- -N2	12

TEMP.	Q(1)	Q(2)	Q(3)	INDICES	SPECIES	COUNT
1000.	2.7000 00	2.7000 00	2.7000 00	1- 3	E- -O2	13
2000.	3.0000 00	3.0000 00	3.0000 00	1- 3	E- -O2	14
3000.	3.5000 00	3.5000 00	3.5000 00	1- 3	F- -O2	15
4000.	4.1000 00	4.1000 00	4.1000 00	1- 3	F- -O2	16
5000.	4.8000 00	4.8000 00	4.8000 00	1- 3	E- -C2	17
6000.	5.7000 00	5.7000 00	5.7000 00	1- 3	F- -O2	18

TEMP.	Q(1)	Q(2)	Q(3)	INDICES	SPECIES	COUNT
1000.	5.0000 00	5.0000 00	5.0000 00	1- 4	E- -N	19
2000.	5.0000 00	5.0000 00	5.0000 00	1- 4	E- -N	20
3000.	5.0000 00	5.0000 00	5.0000 00	1- 4	E- -N	21
4000.	5.0000 00	5.0000 00	5.0000 00	1- 4	E- -N	22
5000.	5.0000 00	5.0000 00	5.0000 00	1- 4	E- -N	23
6000.	5.0000 00	5.0000 00	5.0000 00	1- 4	E- -N	24

TEMP.	Q(1)	Q(2)	Q(3)	INDICES	SPECIES	COUNT
1000.	1.0100 00	1.0100 00	1.0100 00	1- 5	E- -O	25
2000.	1.1430 00	1.1400 00	1.1400 00	1- 5	E- -O	26
3000.	1.3200 00	1.3200 00	1.3200 00	1- 5	E- -O	27
4000.	1.4000 00	1.5000 00	1.5000 00	1- 5	E- -O	28
5000.	1.6700 00	1.6700 00	1.6700 00	1- 5	E- -O	29
6000.	1.8500 00	1.8500 00	1.8500 00	1- 5	F- -O	30

TEMP.	Q(1)	Q(2)	Q(3)	INDICES	SPECIES	COUNT
1000.	3.6000 00	3.6000 00	3.6000 00	1- 6	E- -NO	31
2000.	5.0000 00	5.0000 00	5.0000 00	1- 6	F- -NO	32
3000.	6.6000 00	6.6000 00	6.6000 00	1- 6	E- -NO	33
4000.	8.4000 00	8.4000 00	8.4000 00	1- 6	F- -NO	34
5000.	1.0200 01	1.0200 01	1.0200 01	1- 6	E- -NO	35
6000.	1.1900 01	1.1900 01	1.1900 01	1- 6	F- -NO	36

indices printed refer to the list of species for the current gas model, as given in the problem summary (Section 3.2 above).

3.10 Species Thermal Properties

Output from the edit of species thermal properties (invoked by input of a negative value for ISW6A) is illustrated by figures in Section 4 below. In these figures H00 denotes the species formation enthalpy, MU0 the chemical potential at standard pressure (1 atm), H the enthalpy, CP the specific heat, and S0 the entropy at standard pressure. The left half of the output gives the properties as calculated from the physical model, and the right half gives values based on the thermo fit (see Section 2.2 of Volume I). The right half is left blank for species for which no thermo fit has been supplied. In the case of a nonstandard species for which no physical model data are provided, the left half of the table is filled with zeros.

4. PRECODED DATA

To reduce the quantity of input data required for use of the code, NATA contains precoded data on the properties of elements and chemical species, on reaction rates and electronic nonequilibrium processes, on standard gas models, and on the geometries of nozzles and channels in use at the NASA/Johnson Space Center Arc Tunnel Facility. This information is compiled into the code by means of data statements. In the present section, these precoded data are both summarized and, where applicable, documented as to source. Section 4.1 deals with the data for elements, Section 4.2 with the thermochemical properties of species, Section 4.3 with reaction rates, and Section 4.4 with electronic nonequilibrium processes. Section 4.5 summarizes the six standard gas models available in NATA. Section 4.6 reviews the transport cross section data for all of the standard species. Finally, Section 4.7 discusses the standard nozzle and channel geometries.

4.1 Elements

The only data required for the chemical elements are the atomic weights (in normal units of g/mole) and the chemical symbols. These data are compiled into the present version of the code for six elements, as follows:

<u>Index (IE)</u>	<u>Element</u>
1	e ⁻
3	He
4	C
5	N
6	O
7	Ar

This list will be referred to as the "master list of elements".

The data for elements are stored in an array EPRP(I, IE), contained in common block /ELEM/. This array is dimensioned (2,10). The entries in this array are defined as follows, for

the element with index IE in the master list:

EPRP(I,IE) I = 1 Name of element
 I = 2 Atomic weight

For convenience in adding to or altering the compiled-in data, EPRP is equivalence to ten singly dimensioned arrays of dimension (2), as follows:

EPL(I)	Equivalent to EPRP(I,1)
.	.
.	.
.	.
.	.
EP10(I)	Equivalent to EPRP(I,10)

The data provided for elements in the current code version are summarized in Table I.

TABLE I
DATA FOR ELEMENTS

IE	Name	Atomic Weight
1	E-	5.48597×10^{-4}
3	HE	4.0026
4	C	12.0111
5	N	14.007
6	Ø	16.000
7	AR	39.948

4.2 Thermochemical Data for Species

Data for the following chemical species are compiled into the current version of NATA:

<u>Index (IS)</u>	<u>Species</u>
1	e ⁻
2	N
3	O
4	Ar (ground state)
5	N ₂
6	O ₂
7	NO
8	NO ⁺
9	N ⁺
10	O ⁺
11	N ₂ ⁺
12	O ₂ ⁺
13	CO ₂
14	CO
15	CN
16	He (ground state)
17	C
18	C ⁺
19	He ⁺ (ground state)
20	Ar ⁺

<u>Index (IS)</u>	<u>Species</u>
21	He (³ S metastable state)
22	He (¹ S metastable state)
23	He_2^+
24	He_2
25	CO^+
26	Ar (³ P ₂ and ³ P ₀ metastable states)
27	Ar (³ P ₁ and ¹ P ₁ resonant states)
28	$\text{Ar}_2^+ ({}^2\Sigma_u^+ \text{ molecular ion})$

This is the "master list of species". The helium and argon species in specified electronic states are used in the electronic nonequilibrium models.

The thermochemical data for the above species are stored in an array SPRP(I,IS), contained in common block /SPEC/. This array is dimensioned (43,30). The entries in this array are defined as follows, for the species with index IS in the master list of species:

SPRP(I,IS)	I = 1	Name of species
	*I = 2	Number of elements in species (≤ 3)
	*I = 3-5	Indices of elements in master list of elements
	I = 6-8	Numbers of atoms of elements

*All values in the array are real. The values indicated by asterisks are converted by the program into integers. To ensure rounding down to the correct value, the stored values have been increased by 0.1.

SPRP(I,IS)	I = 9	a	Thermo-fit parameters*
	I = 10	b	
	I = 11	c	
	I = 12	d	
	I = 13	e	
	I = 14	k	
	I = 15	Formation enthalpy (cal/mole)	
	I = 16	r, number of atoms in a molecule of the species	
	I = 17	b, chemical constant**	
	I = 18	Θ_v , vibrational temperature (°K)	
***I = 19	IGM, number of electronic levels (≤ 10)		
***I = 20	IGJ, 1 if thermo fit is used 0 if not		
I = 21-30	g_m , degeneracies of electronic levels		
I = 31-40	E_m , energies of electronic levels (cal/mole above ground state)		
I = 41-43	Second, third, and fourth vibrational temperatures for triatomic species		

*See equations (33), (34) in Volume I (ref. 1).

**See equation (51) in Volume I.

***All values in the array are real. The values indicated by asterisks are converted by the program into integers. To ensure rounding down to the correct value, the stored values have been increased by 0.1.

For convenience in adding to or altering the compiled-in data, SPRP is equivalenced to 30 singly dimensioned arrays of dimension (43), as follows:

SP1(I)	Equivalent to SPRP(I,1)
.	.
.	.
SP30(I)	Equivalent to SPRP(I,30)

The species thermochemical data compiled into the current version of NATA are summarized in Tables II through VI. The data are listed, in this series of tables, in the order in which they appear in the SPRP array, except that the species name is repeated in each table. Table II shows how positively charged ionic species are represented as containing a negative number of electrons. The thermo fits given in Table III are from reference 4, p. 131-132, except those for N_2^+ , O_2^+ , CO, CN, and CO^+ , which are based upon unpublished Avco calculations. The formation enthalpy values H_f° in Table IV are based on data in the JANAF tables (ref. 5), NBS Circular 467 (ref. 6), the Handbook of Chemistry and Physics (N_2^+ and O_2^+) (ref. 7), Herzberg (ref. 8) and a paper by Ginter and Brown (ref. 9). The electronic states for monatomic species in Tables V and VI are from NBS Circular 467. Some of the states listed are combinations of two or more actual states with nearly the same energy. The degeneracies g for the atoms and atomic ions were calculated from the total angular momentum quantum number J, which is also given in Circular 467, using the relation

$$g = 2J + 1 \quad (s)$$

The electronic energy states, degeneracies, vibrational temperatures Θ_v , and rotational temperatures Θ_r for the diatomic species were obtained from the spectroscopic data summarized in Table VII. The sources of the data are indicated in the last column of this table. The states of NO^+ do not appear to be very well known. Rotational and vibrational constants are given in Table VII only for the ground state of each molecule, because the physical model in NATA assumes (as an approximation) that these constants are the same for all of the electronic states of each molecule. The chemical constants b and vibrational temperatures Θ_v in Table IV were calculated from the data of Table VII using

TABLE II
COMPOSITION DATA FOR SPECIES

IS	Name	No. Of Elements	Indices IE of Elements			Nos. Of Atoms Of Elements		
1	E-	1	1	0	0	1.	0.	0.
2	N	1	5	0	0	1.	0.	0.
3	Ø	1	6	0	0	1.	0.	0.
4	AR	1	7	0	0	1.	0.	0.
5	N ₂	1	5	0	0	2.	0.	
6	Ø ₂	1	6	0	0	2.	0.	0.
7	NØ	2	5	6	0	1.	1.	0.
8	NØ+	3	1	5	6	-1.	1.	1.
9	N+	2	1	5	0	-1.		
10	Ø+	2	1	6	0	-1.	1.	0.
11	N ₂ +	2	1	5	0	-1.	2.	0.
12	Ø ₂ +	2	1	6	0	-1.	2.	0.
13	CØ ₂	2	4	6	0	1.	2.	0.
14	CØ	2	4	6	0	1.	1.	0.
15	CN	2	4	5	0	1.	1.	0.
16	HE	1	3	0	0	1.	0.	0.
17	C	1	4	0	0	1.	0.	0.
18	C+	2	1	4	0	-1.	1.	0.
19	HE+	2	1	3	0	-1.	1.	0.
20	AR+	2	1	;	0	-1.	1.	0.
21	HE ₃ S	1	3	0	0	1.	0.	0.
22	HE ₁ S	1	3	0	0	1.	0.	0.
23	HE ₂ +	2	1	3	0	-1.	2.	0.
24	HE ₂	1	3	0	0	2.	0.	0.
25	CØ+	3	1	4	6	-1.	1.	1.
26	AR*M	1	7	0	0	1.	0.	0.
27	AR*R	1	,	0	0	1.	0.	0.
28	AR ₂ +	2	1	7	0	-1.	2.	0.

TABLE III
THERMO FIT DATA*

IS	Name	TFA	10^4	TFB	$10^8 \times TFC$	$10^{12} \times TFD$	$10^{16} \times TFE$	TFK
5	N2	3.451483	3.088332		-4.251428	2.729295	-0.546832	3.071269
6	$\emptyset 2$	3.249473	4.963449		-6.701753	4.443339	-1.000281	5.915022
7	$N\emptyset$	3.756216	2.083961		-2.639548	1.690332	-0.361152	3.611167
8	$N\emptyset +$	3.397385	3.749384		-6.062030	4.637506	-1.107704	4.200563
11	N2+	~.23806	4.47257		-3.95880	1.52963	-0.21145	4.95160
12	$\emptyset 2 +$	3.49213	3.37873		-5.20841	4.16207	-0.97275	4.66750
14	C \emptyset	3.39468	3.22824		-3.94364	2.17519	-0.42966	4.20400
15	CN	3.25545	4.33773		-3.93346	1.59712	-0.23789	5.63340
25	C $\emptyset +$	3.49411	2.10083		-1.11714	0.58582	-0.13605	4.2967

*The thermo-fit technique is not used for monatomic species, for the helium and argon molecular species, or for carbon dioxide.

TABLE IV
DATA FOR PHYSICAL MODEL

IS	Name	H_0° cal/mole	n	b	θ_v $^\circ K$	IGM	IGJ
1	E-	0.	1.	-14.9276	0.	1	0
2	N	112520.	1.	0.2944	0.	5	0
3	\emptyset	58989.	1.	0.4938	0.	7	0
4	AR	0.	1.	1.8664	0.	1	0
5	N2	0.	2.	- 0.4106	3352.	5	1
6	$\emptyset 2$	0.	2.	0.1140	2239.	5	1
7	N \emptyset	21456.	2.	0.5455	2699.	7	1
8	N \emptyset +	236660.	2.	0.3841	3373.	4	1
9	N+	447600.	1.	0.2943	0.	7	0
10	$\emptyset +$	372940.	1.	0.4938	0.	3	0
11	N2+	357680.	2.	- 0.3763	3114.	4	1
12	$\emptyset 2 +$	288800.	2.	- 0.0317	2628.	5	1
13	C $\emptyset 2$	0.*	3.	1.8958	1977.**	1	0
14	C \emptyset	66770.*	2.	0.3169	3083.	5	1
15	CN	197170.*	2.	0.2226	2939.	3	1
16	HE	0.	1.	- 1.5846	0.	1	0
17	C	263550.*	1.	0.0637	0.	10	0
18	C+	523310.*	1.	0.0636	0.	4	0
19	HE+	566840.	1.	- 1.5846	0.	1	0
20	AR+	363318.	1.	1.8663	0.	2	0
21	HE3S	456910.	1.	- 1.5846	0.	1	0
22	HE1S	475260.	1.	- 1.5846	0.	1	0
23	HE2+	511490.	1.	- 3.5619	2343.	1	0
24	HE2	406170.	1.	- 3.6287	2492.	1	0
25	C \emptyset +	389950.*	2.	0.2931	3142.	3	1
26	AR*M	266350.	1.	1.8663	0.	1	0
27	AR*R	267970.	1.	1.8663	0.	1	0
28	AR2+	337040.	2.	3.597	115.	1	0

*These formation enthalpies for the carbon-containing species are based on CO_2 as the reference state for carbon. They are 93970 cal/mole higher than the JANAF values, which are based on graphite as the reference state.

**The other three vibrational temperatures for CO_2 are 960, 960, and $3380^\circ K$.

TABLE V
DEGENERACIES OF ELECTRONIC STATES

IS	Name	1	2	3	4	5	6	7	8	9	10
1	E-	2.									
2	N	4.	10.	6.	12.	18.					
3	Ø	5.	3.	1.	5.	1.	8.	24.			
4	AR	1.									
5	N2	1.	3.	6.	1.	2.					
6	Ø2	3.	2.	1.	3.	3.					
7	NØ	2.	2.	2.	4.	2.	2.	2.			
8	NØ+	1.	6.	3.	2.						
9	N+	1.	3.	5.	5.	1.	5.	15.			
10	Ø+	4.	10.	6.							
11	N2+	2.	4.	2.	2.	4.					
12	Ø2+	2.	2.	8.	4.	4.					
13	CØ2	1.									
14	CØ	1.	6.	3.	6.	2.					
15	CN	2.	4.	2.	4.	2.	4.	4.	4.		
16	HE	1.									
17	C	9.	5.	1.	5.	9.	3.	15.	34.	99.	401.
18	C+	2.	4.	12.	10.						
19	HE+	2.									
20	AR+	4.	2.								
21	HE3S	3.									
22	HE1S	1.									
23	HE2+	2.									
24	HE2	3.									
25	CØ+	2.	4.	2.							
26	AR*M	6.									
27	AR*R	6.									
28	AR2+	2.									

TABLE VI

ENERGIES OF ELECTRONIC STATES
(CAL/MOLE)

IS	Name	1	2	3	4	5	6	7	8	9	10
1	E-	0.									
2	N	0.	54962.	82456.	238270.	250140.					
3	Ø	0.	453.	648.	45367.	96616.	213990.	249820.			
4	AR	0.									
5	N2	0.	143540.	170480.	171500.	198110.					
6	Ø2	0.	22639.	37726.	103200.	142390.					
7	NØ	0.	346.	125700.	131320.	149100.	151770.	173340.			
8	NØ+	0.	106000.	160000.	200000.						
9	N+	0.	140.	375.	43789.	93456.	134860.	263740.			
10	Ø+	0.	76670.	115700.							
11	N2+	0.	25890.	72797.	184760.						
12	Ø2+	0.	558.	91206.	109760.	138860.					
13	CØ2	0.									
14	CØ	0.	139200.	159830.	178120.	186055.					
15	CN	0.	26069.	73759.	154263.	168570.	170640.	174230.	185220.		
16	HE	0.									
17	C	85.	29146.	61894.	96452.	172580.	177213.	183240.	200100.	214400.	243000.
18	C+	0.	183.	123040.	214240.						
19	HE+	0.									
20	AR+	0.	4094.								
21	HE3S	0.									
22	HE1S	0.									
23	HE2+	0.									
24	HE2	0.									
25	CØ+	0.	59278.	131166.							
26	AR*M	0.									
27	AR*R	0.									
28	AR2+	0.									

equations (38), (40b), (51b), and (45) of Volume I, i.e.,

$$b = -3.66505 + \frac{3}{2} \ln W - (n - 1) \ln [1.43879 \sigma (B_e - \frac{1}{2} \alpha_e)] \quad (4)$$

$$\theta_v = 1.43879 (\omega_e - 2 \omega_e x_e + \frac{13}{4} \omega_e y_e) \quad (5)$$

in which W denotes the molecular weight and n the number of atoms per molecule (for monatomic and diatomic species). The degeneracies g for the molecular states in Table V were obtained from the state symbols using the following rule, based on Herzberg (ref. 8):

$$\begin{aligned} {}^n \Sigma \text{ states} \quad g &= n \\ {}^n\Pi, {}^n\Delta, \text{ etc.} \quad g &= 2n \end{aligned} \quad (6)$$

Figures 19 through 46* are tables of thermal properties for the compiled-in species, computed by NATA from the precoded data, under the option ISW6A = -1. For each species, the properties calculated from the physical model are given for temperatures up to 30,000°K. For the molecular species for which the thermo fit is used, corresponding results based on the thermo fit are given for comparison. At the normal switchover temperature, CTMX = 5000°K, the results from the two techniques are seen to be in reasonably good agreement. Above about 15,000°K, the properties calculated from the thermo fits become very inaccurate in all cases. This behavior results from the inability of the polynomial form used in the thermo fit to represent the actual property variations over excessively wide temperature ranges. This is not considered to be a serious problem because, at temperatures of 15000°K and higher, the mole fractions of the molecular species (for which the thermo fit is used) are quite small, so that errors in the thermal properties of these species have only very minor effects upon the properties of the gas mixture. However, at temperatures above about 20,000°K, the properties computed from the thermo fit show wild variations which could lead

*The equipment used to produce these figures printed the BCD "+" sign appearing in some of the species names as an ampersand.

***** PHYSICAL MODEL *****

THERMAL PROPERTIES OF E- 0= 0.0 KCAL/MOLE)

FIGURE 19

*ORIGINAL PAGE IS
OF POOR QUALITY*

T	(MUO-MOO)/RT	H-HCO KCAL/MOLE	CAL/MOLE	CP CAL/MOLE-DEG	SO CAL/MOLE-DEG
100.	2.722	0.497	4.968	-0.440	
200.	0.989	0.994	4.968	3.003	
300.	-0.025	1.490	4.968	5.018	
400.	-0.744	1.987	4.968	6.447	
500.	-1.302	2.484	4.968	7.555	
600.	-1.758	2.981	4.968	8.461	
700.	-2.143	3.478	4.968	9.227	
800.	-2.477	3.974	4.968	9.890	
900.	-2.772	4.471	4.968	10.476	
1000.	-3.035	4.968	4.968	10.999	
1200.	-3.491	5.962	4.968	11.905	
1400.	-3.876	6.955	4.968	12.671	
1600.	-4.210	7.949	4.968	13.334	
1800.	-4.504	8.942	4.968	13.919	
2000.	-4.768	9.936	4.968	14.443	
2200.	-5.006	10.930	4.968	14.916	
2400.	-5.224	11.923	4.968	15.348	
2600.	-5.424	12.917	4.968	15.746	
2800.	-5.609	13.910	4.968	16.114	
3000.	-5.781	14.904	4.968	16.457	
3500.	-6.167	17.388	4.968	17.223	
4000.	-6.501	19.872	4.968	17.886	
4500.	-6.795	22.356	4.968	18.471	
5000.	-7.059	24.840	4.968	18.995	
5500.	-7.297	27.324	4.968	19.468	
6000.	-7.514	29.808	4.968	19.900	
6500.	-7.714	32.292	4.968	20.298	
7000.	-7.900	34.776	4.968	20.666	
7500.	-8.072	37.260	4.968	21.009	
8000.	-8.234	39.744	4.968	21.330	
8500.	-8.385	42.228	4.968	21.631	
9000.	-8.529	44.712	4.968	21.915	
9500.	-8.663	47.196	4.968	22.183	
10000.	-8.791	49.680	4.968	22.438	
11000.	-9.030	54.648	4.968	22.912	
12000.	-9.247	59.616	4.968	23.344	
130.	-9.447	64.584	4.968	23.742	
140.	-9.633	69.552	4.968	24.110	
15000.	-9.805	74.520	4.968	24.453	
16000.	-9.966	79.488	4.968	24.773	
17000.	-10.118	84.456	4.968	25.074	
18000.	-10.261	89.424	4.968	25.358	
19000.	-10.396	94.392	4.968	25.627	
20000.	-10.524	99.360	4.968	25.862	
22000.	-10.763	109.296	4.968	26.355	
24000.	-10.980	119.232	4.968	26.788	
26000.	-11.180	129.168	4.968	27.185	
28000.	-11.365	139.104	4.968	27.553	
30000.	-11.538	149.040	4.968	27.896	

*****PHYSICAL MODEL*****

T	(MUO-HOO)/RT	H-HOO KCAL/MOLE	CP CAL/MOLE-DEG	SC CAL/MOLE-DEG
10.0	-13.194	0.497	4.968	31.186
20.0	-14.946	0.994	4.968	34.630
30.0	-15.940	1.490	4.968	36.644
40.0	-16.659	1.987	4.968	38.073
50.0	-17.217	2.484	4.968	39.182
60.0	-17.673	2.981	4.968	40.088
70.0	-18.056	3.478	4.968	40.854
80.0	-18.392	3.974	4.968	41.517
90.0	-18.687	4.471	4.968	42.102
100.0	-18.950	4.968	4.968	42.626
120.0	-19.406	5.962	4.968	43.531
140.0	-19.791	6.955	4.968	44.297
160.0	-20.125	7.949	4.968	44.961
180.0	-20.420	8.942	4.968	45.546
200.0	-20.683	9.936	4.968	46.069
220.0	-20.921	10.930	4.971	46.547
240.0	-21.139	11.925	4.975	46.976
260.0	-21.339	12.920	4.982	47.374
280.0	-21.524	13.917	4.993	47.744
300.0	-21.697	14.918	5.010	48.089
350.0	-22.063	17.440	5.086	48.866
400.0	-22.418	20.012	5.213	49.553
450.0	-22.716	22.661	5.390	50.176
500.0	-22.984	25.409	5.608	50.755
550.0	-23.229	28.273	5.850	51.301
600.0	-23.456	31.260	6.100	51.821
650.0	-23.667	34.372	6.344	52.319
700.0	-23.866	37.601	6.569	52.797
750.0	-24.054	40.937	6.768	53.258
800.0	-23.232	44.364	6.935	53.700
850.0	-24.403	47.866	7.068	54.124
900.0	-24.566	51.426	7.169	54.531
950.0	-24.722	55.029	7.239	54.921
1000.0	-24.873	58.660	7.281	55.293
1100.0	-25.157	65.957	7.300	55.989
1200.0	-25.422	73.240	7.257	56.623
1300.0	-25.670	80.461	7.180	57.201
1400.0	-25.902	87.595	7.089	57.729
1500.0	-26.120	94.638	6.997	58.215
1600.0	-26.326	101.593	6.914	58.664
1700.0	-26.520	108.471	6.843	59.081
1800.0	-26.704	115.284	6.786	59.471
1900.0	-26.878	122.047	6.742	59.836
2000.0	-27.044	128.772	6.710	60.181
2200.0	-27.354	142.151	6.674	60.819
2400.0	-27.637	155.484	6.663	61.399
2600.0	-27.809	168.808	6.663	61.932
2800.0	-28.141	182.136	6.665	62.426
3000.0	-28.367	195.464	6.663	62.886

ORIGINAL PAGE IS
OF POOR QUALITY

FIGURE 21
THERMAL PROPERTIES OF O₂
100 = 58.990 KCAL/MOLE)

*****PHYSICAL MODEL*****

T (MUO-HCO) / RT	H-HOO KCAL/MOLE	CP CAL/MOLE-DEG	SO CAL/MOLE-DEG
100.	-13.683	0.527	5.665
200.	-15.557	1.085	5.0434
300.	-16.661	1.617	5.235
400.	-17.438	2.135	5.135
500.	-18.035	2.646	5.081
600.	-18.519	3.152	5.049
700.	-18.925	3.656	5.029
800.	-19.275	4.158	5.015
900.	-19.582	4.659	5.006
1000.	-19.856	5.159	4.999
1200.	-20.328	6.158	4.990
1400.	-20.726	7.155	4.984
1600.	-21.068	8.152	4.981
1800.	-21.370	9.147	4.978
2000.	-21.639	10.143	4.978
2200.	-21.882	11.139	4.978
2400.	-22.104	12.135	4.981
2600.	-22.307	13.131	4.986
2800.	-22.496	14.129	4.994
3000.	-22.671	15.129	5.004
3500.	-23.062	17.640	5.041
4000.	-23.401	20.172	5.091
4500.	-23.700	22.732	5.149
5000.	-23.968	25.322	5.210
5500.	-24.211	27.942	5.269
6000.	-24.434	30.590	5.323
6500.	-24.640	33.264	5.371
7000.	-24.831	35.961	5.413
7500.	-25.010	38.676	5.447
8000.	-25.177	41.427	5.475
8500.	-25.325	44.150	5.497
9000.	-25.485	46.903	5.514
9500.	-25.627	49.663	5.527
10000.	-25.762	52.429	5.537
11000.	-26.014	57.973	5.550
12000.	-26.246	63.528	5.560
13000.	-26.459	69.093	5.571
14000.	-26.658	74.672	5.588
15000.	-26.843	80.271	5.612
16000.	-27.017	85.899	5.645
17000.	-27.182	91.565	5.688
18000.	-27.337	97.277	5.738
19000.	-27.484	103.044	5.797
20000.	-27.621	108.873	5.861
22000.	-27.886	120.735	6.002
24000.	-28.128	132.886	6.149
26000.	-28.352	145.326	6.289
28000.	-28.561	158.035	6.416
30000.	-28.758	170.978	6.524

FIGURE 22
THERMAL PROPERTIES OF AR

*****PHYSICAL MODEL*****

100= 0.0 KCAL/MOLE

T	(MUO-HOO)/RT	H-HOO KCAL/MOLE	CAL/MOLE	CP CAL/MOLE-DEG	S0 CAL/MOLE-DEG
100.	-13.379	0.497	4.968	31.555	
200.	-15.112	0.994	4.968	34.999	
300.	-16.126	1.490	4.968	37.013	
400.	-16.845	1.987	4.968	38.442	
500.	-17.403	2.484	4.968	39.551	
600.	-17.859	2.981	4.968	40.457	
700.	-18.244	3.478	4.968	41.222	
800.	-18.573	3.974	4.968	41.886	
900.	-18.872	4.471	4.968	42.471	
1000.	-19.136	4.968	4.968	42.994	
1200.	-19.591	5.962	4.968	43.900	
1400.	-19.977	6.955	4.968	44.666	
1600.	-20.311	7.949	4.968	45.329	
1800.	-20.605	8.942	4.968	45.915	
2000.	-20.869	9.936	4.968	46.438	
2200.	-21.107	10.930	4.968	46.911	
2400.	-21.324	11.923	4.968	47.344	
2600.	-21.524	12.917	4.968	47.741	
2800.	-21.710	13.910	4.968	48.110	
3000.	-21.882	14.924	4.968	48.452	
3500.	-22.263	17.388	4.968	49.18	
4000.	-22.601	19.872	4.968	49.982	
4500.	-22.896	22.356	4.968	50.467	
5000.	-23.159	24.840	4.968	50.990	
5500.	-23.398	27.324	4.968	51.464	
6000.	-23.615	29.808	4.968	51.296	
6500.	-23.815	32.292	4.968	52.294	
7000.	-24.000	34.776	4.968	52.662	
7500.	-24.173	37.260	4.968	53.004	
8000.	-24.334	39.744	4.968	53.325	
8500.	-24.486	42.228	4.968	53.626	
9000.	-24.629	44.712	4.968	53.710	
9500.	-24.764	47.196	4.968	54.179	
10000.	-24.892	49.650	4.968	54.434	
11000.	-25.130	54.648	4.968	54.907	
12000.	-25.348	59.616	4.968	55.339	
13000.	-25.548	64.584	4.968	55.737	
14000.	-25.733	69.552	4.968	56.105	
15000.	-25.906	74.520	4.968	56.448	
16000.	-26.067	79.488	4.968	56.877	
17000.	-26.219	84.456	4.968	57.769	
18000.	-26.362	89.424	4.968	58.351	
19000.	-26.497	94.392	4.968	58.783	
20000.	-26.625	99.360	4.968	59.181	
22000.	-26.863	109.296	4.968	59.549	
24000.	-27.081	119.232	4.968	59.892	
26000.	-27.281	129.168	4.968		
28000.	-27.466	139.104	4.968		
30000.	-27.639	149.040	4.968		

**ORIGINAL PAGE IS
OF POOR QUALITY**

FIRE 23
THERMAL PROPERTIES OF N2
100= 0.0 KCAL/MOLE)

T	(MUO-HCO)/RT	H-HOO KCAL/MOLE	CP CAL/MOLE-DEG	SO CAL/MOLE-DEG	(MUO-HOO)/RT	KCAL/MOLE	H-HOO KCAL/MOLE	CP CAL/MOLE-DEG	SO CAL/MOLE-DEG
100.	-15.707	0.696	6.955	38.169	-15.545	0.692	6.979	37.811	
200.	-18.134	1.391	6.955	42.990	-17.968	1.396	7.094	42.684	
300.	-19.553	2.087	6.959	45.811	-19.397	2.111	7.205	45.581	
400.	-20.560	2.784	6.987	47.815	-20.419	2.836	7.311	47.669	
500.	-21.342	3.486	7.065	49.382	-21.219	3.573	7.412	49.311	
600.	-21.982	4.198	7.189	50.680	-21.877	4.319	7.509	50.671	
700.	-22.527	4.925	7.341	51.800	-22.437	5.074	7.601	51.835	
800.	-23.001	5.667	7.500	52.790	-22.926	5.839	7.689	52.856	
900.	-23.422	6.424	7.654	53.683	-23.360	6.612	7.774	53.767	
1000.	-23.802	7.197	7.795	54.497	-23.750	7.393	7.854	54.590	
1200.	-24.468	8.781	8.032	55.940	-24.433	8.979	8.003	56.035	
1400.	-25.040	10.406	8.214	57.112	-25.016	10.594	8.138	57.279	
1600.	-25.543	12.063	8.351	58.298	-25.527	12.234	8.259	58.374	
1800.	-25.993	13.744	8.455	59.288	-25.983	13.897	8.368	59.353	
2000.	-26.400	15.444	8.536	60.183	-26.394	15.580	8.465	60.240	
2200.	-26.772	17.157	8.599	61.132	-26.769	17.282	8.552	61.051	
2400.	-27.115	18.882	8.649	61.750	-27.114	19.000	8.628	61.798	
2600.	-27.433	20.616	8.689	62.444	-27.434	20.732	8.695	62.492	
2800.	-27.730	22.357	8.721	63.089	-27.733	22.477	8.753	63.138	
3000.	-28.008	24.104	8.748	63.692	-28.012	24.233	8.804	63.744	
3500.	-28.635	28.492	8.797	65.045	-28.643	28.661	8.902	65.109	
4000.	-29.185	32.899	8.830	66.222	-29.197	33.130	8.968	66.302	
4500.	-29.675	37.320	8.853	67.263	-29.690	37.625	9.011	67.361	
5000.	-30.116	41.751	8.870	68.197	-30.135	42.139	9.042	68.312	
5500.	-30.518	46.190	8.885	69.043	-30.541	46.666	9.068	69.175	
6000.	-30.866	50.636	8.898	69.817	-30.913	51.208	9.098	69.965	
6500.	-31.227	55.089	8.915	70.529	-31.258	55.766	9.138	70.695	
7000.	-31.544	59.551	8.936	71.191	-31.579	60.349	9.196	71.374	
7500.	-31.839	64.026	8.967	71.808	-31.879	64.965	9.275	72.011	
8000.	-32.117	68.520	9.009	72.388	-32.161	69.628	9.380	72.613	
8500.	-32.379	73.038	9.057	72.936	-32.427	74.350	9.516	73.186	
9000.	-32.626	77.590	9.143	73.456	-32.679	79.140	9.684	73.734	
9500.	-32.861	82.184	9.239	73.953	-32.919	84.041	9.888	74.263	
10000.	-33.085	86.833	9.358	74.430	-33.148	89.043	10.129	74.776	
11000.	-33.503	96.335	9.661	75.335	-33.578	99.455	10.719	75.769	
12000.	-33.889	106.183	10.049	76.192	-33.978	110.528	11.450	76.731	
13000.	-34.247	116.455	10.504	77.014	-34.353	122.395	12.301	77.681	
14000.	-34.584	127.294	11.000	77.810	-34.708	135.161	13.241	78.626	
15000.	-34.901	138.460	11.510	78.587	-35.048	148.892	14.225	79.573	
16000.	-35.204	150.218	12.002	79.345	-35.375	163.605	15.193	80.522	
17000.	-35.493	162.449	12.451	80.087	-35.692	179.249	16.074	81.471	
18000.	-35.770	175.099	12.837	80.810	-36.000	195.695	16.783	82.410	
19000.	-36.037	188.098	13.148	81.513	-36.300	212.726	17.224	83.331	
20000.	-36.295	201.367	13.378	82.193	-36.593	230.018	17.296	84.218	
22000.	-36.785	226.398	13.604	83.481	-37.157	263.493	15.763	85.814	
24000.	-37.246	255.606	13.567	84.665	-37.686	290.959	11.069	87.012	
26000.	-37.679	282.547	13.350	85.743	-38.168	304.756	1.650	87.569	
28000.	-38.088	308.937	13.028	86.721	-38.586	294.303	-13.458	87.189	
30000.	-38.473	334.630	12.661	87.608	-38.915	245.690	-36.624	85.521	

FIGURE 24
THERMAL PROPERTIES OF 02
00= 0.0 KCAL/MOL/F)

*****PHYSICAL MODEL*****									
T	(MUO-HOO)/RT	H-HOO KCAL/MOLE	CAL/MOLE	CP CAL/MOLE-DEG	SC CAL/MOLE-DEG	H-HOO KCAL/MOLE	CAL/MOLE	CP CAL/MOLE-DEG	SC CAL/MOLE-DEG
100.	-17.331	0.696	6.955	41.395	-17.679	0.655	6.651	41.667	41.667
200.	-19.757	1.391	6.959	46.216	-19.980	1.330	6.836	46.354	46.354
300.	-21.176	2.089	49.C46	49.C46	-21.346	2.022	7.014	49.167	49.167
400.	-22.186	2.799	7.188	51.086	-22.328	2.732	7.185	51.201	51.201
500.	-22.975	3.529	7.418	52.714	-23.100	3.459	7.348	52.822	52.822
600.	-23.626	4.282	7.651	54.087	-23.738	4.202	7.505	54.176	54.176
700.	-24.183	5.058	7.857	55.282	-24.285	4.960	7.654	55.344	55.344
800.	-24.672	5.853	8.030	56.343	-24.763	5.733	7.797	56.375	56.375
900.	-25.108	6.663	8.171	57.297	-25.190	6.519	7.934	57.302	57.302
1000.	-25.502	7.496	8.287	58.165	-25.576	7.319	8.065	58.145	58.145
1200.	-26.196	9.162	8.463	59.692	-26.254	8.957	8.308	59.637	59.637
1400.	-26.793	10.868	8.594	61.007	-26.839	10.641	8.529	60.934	60.934
1600.	-27.319	12.598	8.702	62.161	-27.354	12.367	8.729	62.087	62.087
1800.	-27.788	14.349	8.301	63.192	-27.815	14.131	8.999	63.125	63.125
2000.	-28.213	16.118	8.895	64.124	-28.235	15.930	9.071	64.073	64.073
2200.	-28.602	17.907	8.987	64.977	-28.619	17.759	9.216	64.944	64.944
2400.	-29.960	19.713	9.075	65.762	-29.975	19.615	9.346	65.752	65.752
2600.	-29.222	21.537	9.160	66.492	-29.306	21.496	9.461	66.504	66.504
2800.	-29.502	23.377	9.240	67.174	-29.616	23.398	9.563	67.209	67.209
3000.	-29.893	25.232	9.314	67.814	-29.907	25.320	9.653	67.872	67.872
3500.	-30.551	29.930	9.471	69.262	-30.569	30.194	9.833	69.374	69.374
4000.	-31.130	34.696	9.586	70.535	-31.154	35.144	9.962	70.696	70.696
4500.	-31.647	39.510	9.664	71.669	-31.679	40.150	10.055	71.875	71.875
5000.	-32.115	44.355	9.712	72.690	-32.155	45.195	10.126	72.938	72.938
5500.	-32.542	49.218	9.738	73.617	-32.591	50.274	10.188	73.906	73.906
6000.	-32.935	54.090	9.749	74.464	-32.994	55.384	10.251	74.796	74.796
6500.	-33.300	58.966	9.752	75.245	-33.367	60.527	10.325	75.619	75.619
7000.	-33.639	63.842	9.751	75.968	-33.716	65.712	10.417	76.387	76.387
7500.	-33.956	68.717	9.750	76.640	-34.043	70.948	10.534	77.110	77.110
8000.	-34.255	73.592	9.750	77.270	-34.351	76.251	10.681	77.794	77.794
8500.	-34.536	78.467	9.752	77.861	-34.643	81.635	10.861	78.447	78.447
9000.	-34.802	83.344	9.757	78.418	-34.920	87.118	11.076	79.074	79.074
9500.	-35.054	88.224	9.764	78.946	-35.185	92.717	11.327	79.679	79.679
10000.	-35.294	93.109	9.775	79.447	-35.443	98.450	11.611	80.267	80.267
11000.	-35.742	102.897	9.803	80.380	-35.914	110.383	12.272	81.404	81.404
12000.	-36.152	112.716	9.836	81.234	-36.358	123.024	13.019	82.503	82.503
13000.	-36.531	122.569	9.870	82.023	-36.776	136.430	13.791	83.576	83.576
14000.	-36.883	132.455	9.903	82.756	-37.172	150.586	14.502	84.625	84.625
15000.	-37.212	142.373	9.932	83.440	-37.550	165.377	15.040	85.645	85.645
16000.	-37.521	152.317	9.955	84.082	-37.913	180.565	15.273	86.625	86.625
17000.	-37.812	162.282	9.973	84.686	-38.260	195.768	15.042	87.547	87.547
18000.	-38.087	172.261	9.985	85.256	-38.594	210.433	14.165	88.385	88.385
19000.	-38.347	182.250	9.991	85.796	-38.914	223.815	12.438	89.109	89.109
20000.	-38.595	192.242	9.992	86.309	-39.218	234.950	9.631	99.681	99.681
22000.	-39.057	212.215	9.979	87.260	-39.771	245.395	-0.260	90.186	90.186
24000.	-39.480	232.147	9.951	88.128	-40.229	228.805	-17.821	89.476	89.476
26000.	-39.870	252.013	9.914	88.923	-40.557	167.211	-45.745	87.025	87.025
23000.	-40.232	271.799	9.871	89.656	-40.709	36.875	-87.107	82.215	82.215
29000.	-40.569	291.495	9.824	90.335	-40.631	-192.471	-145.364	74.326	74.326

FIGURE 25

THERMAL PROPERTIES OF NO
30= 21.460 KCAL/MOLE)

*****PHYSICAL MODEL*****

T	(MUC-HOO)/RT	H-HOO KCAL/MOLE	CP CAL/MOLE-DEG	S0 CAL/MOLE-DEG	(MUO-HOO)/RT	H-HOO KCAL/MOLE	CP CAL/MOLE-DEG	S0 CAL/MOLE-DEG
10.0	-17.518	0.747	7.720	4.2•284	-17.174	0.751	7.546	41.633
20.0	-20.133	1.493	7.269	4.7•473	-19.798	1.509	7.624	46.887
30.0	-21.646	2.211	7.129	5.0•387	-21.341	2.275	7.699	49.993
40.0	-22.709	2.924	7.151	5.2•438	-22.441	3.049	7.771	52.217
50.0	-23.528	3.645	7.278	5.4•046	-23.299	3.829	7.841	53.959
60.0	-24.198	4.382	7.454	5.5•388	-24.004	4.617	7.908	55.395
70.0	-24.765	5.136	7.638	5.6•551	-24.602	5.411	7.972	56.618
80.0	-25.260	5.909	7.809	5.7•582	-25.122	6.211	8.033	57.687
90.0	-25.699	6.697	7.960	5.8•511	-25.583	7.017	8.092	58.636
100.0	-26.095	7.500	8.090	5.9•357	-25.998	7.829	8.148	59.492
120.0	-26.789	9.139	8.291	6.0•850	-26.719	9.470	8.254	60.987
140.0	-27.384	10.812	8.434	6.2•140	-27.333	11.130	8.351	62.267
160.0	-27.906	12.510	8.537	6.3•273	-27.869	12.810	8.439	63.388
180.0	-28.372	14.226	8.613	6.4•283	-28.345	14.506	8.520	64.387
200.0	-28.793	15.954	8.670	6.5•194	-28.774	16.217	8.593	65.288
220.0	-29.177	17.693	8.714	6.6•022	-29.164	17.942	8.660	66.110
240.0	-29.530	19.439	8.748	6.6•782	-29.522	19.680	8.720	66.866
260.0	-29.857	21.192	8.775	6.7•483	-29.853	21.430	8.774	67.556
280.0	-30.162	22.949	8.797	6.8•135	-30.161	23.190	8.823	68.219
300.0	-30.448	24.710	8.815	6.8•742	-30.449	24.959	8.867	68.829
350.0	-31.090	29.127	8.848	7.0•104	-31.098	29.416	8.958	70.203
400.0	-31.651	33.555	8.870	7.1•287	-31.665	33.913	9.028	71.404
450.0	-32.150	37.995	8.885	7.2•332	-32.170	38.441	9.082	72.470
500.0	-32.599	42.441	8.897	7.3•269	-32.624	42.993	9.127	73.429
550.0	-33.007	46.892	8.907	7.4•117	-33.038	47.567	9.167	74.301
600.0	-33.381	51.348	8.918	7.4•893	-33.417	52.160	9.206	75.100
650.0	-33.726	55.810	8.931	7.5•607	-33.768	56.773	9.249	75.939
700.0	-34.047	60.279	8.948	7.6•270	-34.095	61.410	9.298	76.526
750.0	-34.346	64.758	8.970	7.6•888	-34.400	66.074	9.358	77.170
800.0	-34.627	69.250	8.998	7.7•467	-34.687	70.770	9.429	77.776
850.0	-34.892	73.758	9.034	7.8•014	-34.957	75.505	9.514	78.350
900.0	-35.141	78.296	9.078	7.8•532	-35.213	80.286	9.615	78.896
950.0	-35.378	82.838	9.130	7.9•024	-35.457	85.120	9.728	79.419
1000.0	-35.604	87.417	9.190	7.9•494	-35.688	90.016	9.859	79.921
1100.0	-36.024	96.676	9.331	8.0•376	-36.122	100.023	10.164	80.875
1200.0	-36.410	106.086	9.494	8.1•195	-36.522	110.362	10.520	81.774
1300.0	-36.767	115.668	9.672	8.1•962	-36.895	121.074	10.998	82.632
1400.0	-38.250	166.229	1.0•506	85.245	-38.472	179.635	12.075	86.431
1500.0	-38.502	125.432	9.855	82.626	-38.816	191.593	11.788	87.078
2000.0	-38.743	135.378	1.0•037	83.364	-39.006	203.098	11.301	87.668
2200.0	-39.196	145.502	1.0•209	84.024	-37.888	155.480	11.663	88.625
2400.0	-39.985	155.791	1.0•366	84.648	-38.187	167.523	12.199	89.169
2600.0	-40.004	252.733	1.0•930	89.216	-40.314	234.396	-5.205	89.127
2800.0	-40.368	273.562	1.0•893	90.025	-40.626	211.715	-16.329	88.292
3000.0	-40.710	296.285	1.0•826	90.774	-40.851	235.550	-37.198	86.421

ORIGINAL PAGE IS
OF POOR QUALITY

*****THERMO MODEL*****
THERMAL PROPERTIES OF NOE 00= 236.660 KCAL/MOLE)

*****PHYSICAL MODEL*****									
T	(MUO-HOO)/RT	H-HOO KCAL/MOLE	CP CAL/MOLE-DEG	SC CAL/MOLE-DEG	(MUO-HOO)/RT	H-HOO KCAL/MOLE	CP CAL/MOLE-DEG	SC CAL/MOLE-DEG	(MUO-HOO)/RT
100.	-16.502	0.696	6.955	39.748	-16.486	0.682	6.897	39.585	
200.	-18.928	1.391	6.955	44.569	-10.877	1.379	7.035	44.400	
300.	-20.347	2.087	6.958	47.390	-20.291	2.089	7.167	47.286	
400.	-21.354	2.784	6.986	49.394	-21.304	2.812	7.292	49.365	
500.	-22.136	3.485	7.062	50.960	-22.097	3.547	7.411	51.005	
600.	-22.777	4.197	7.184	52.258	-22.750	4.294	7.523	52.366	
700.	-23.321	4.923	7.354	53.377	-23.308	5.052	7.630	53.574	
800.	-23.795	5.665	7.492	54.366	-23.795	5.820	7.731	54.560	
900.	-24.216	6.421	7.645	55.258	-24.228	6.598	7.826	55.476	
1000.	-24.596	7.193	7.786	56.071	-24.618	7.385	7.916	56.305	
1250.	-25.261	8.775	8.024	57.512	-25.300	8.985	8.080	57.763	
1400.	-25.833	10.399	8.207	58.763	-25.884	10.616	8.226	59.020	
1600.	-26.336	12.055	8.345	59.869	-26.397	12.274	8.354	60.127	
1800.	-23.785	13.735	8.450	60.858	-26.854	13.956	8.466	61.117	
2000.	-27.192	15.434	8.531	61.753	-27.267	15.660	8.563	62.015	
2200.	-27.564	17.146	8.595	62.569	-27.644	17.381	8.647	62.835	
2400.	-27.907	18.871	8.671	63.319	-27.992	19.118	8.719	63.599	
2600.	-28.225	20.604	8.686	64.013	-28.314	20.868	8.780	64.291	
2800.	-28.521	22.344	8.719	64.658	-28.614	22.629	8.832	64.943	
3000.	-28.799	24.91	8.746	65.260	-28.805	24.400	8.875	65.554	
3500.	-29.426	28.477	8.796	66.612	-29.531	28.859	8.955	66.929	
4000.	-29.976	32.885	8.832	67.789	-30.088	33.850	9.007	68.128	
4500.	-30.465	37.309	8.864	68.831	-30.584	37.864	9.047	69.191	
5000.	-30.966	41.749	8.900	69.767	-31.032	42.397	9.087	70.147	
5500.	-31.308	46.211	8.951	70.618	-31.440	46.953	9.141	71.015	
6000.	-31.677	50.734	9.022	71.399	-31.815	51.542	9.218	71.814	
6500.	-32.018	55.238	9.121	72.125	-32.162	56.177	9.327	72.555	
7000.	-32.336	59.830	9.250	72.806	-32.486	60.876	9.475	73.252	
7500.	-32.634	64.494	9.412	73.473	-32.789	65.659	9.668	73.912	
8000.	-32.914	69.247	9.604	74.063	-33.074	70.552	9.909	74.543	
8500.	-33.179	74.103	9.824	74.651	-33.344	75.577	10.200	75.152	
9000.	-33.431	79.075	10.067	75.220	-33.601	80.760	10.541	75.745	
9500.	-33.671	84.173	10.328	75.771	-33.846	86.126	10.932	76.325	
10000.	-33.901	89.404	10.473	76.308	-34.082	91.790	11.370	76.897	
11000.	-34.313	100.279	11.148	77.344	-34.527	103.555	12.374	78.026	
12000.	-34.737	111.620	11.666	78.336	-34.945	116.466	13.469	79.143	
13000.	-35.115	123.587	12.114	79.288	-35.343	130.502	14.600	80.272	
14000.	-35.474	135.887	12.470	80.200	-35.724	145.630	15.650	81.393	
15000.	-35.814	148.424	12.725	81.069	-36.091	161.730	16.483	82.503	
16000.	-36.139	161.395	12.881	81.896	-36.448	178.479	16.936	83.583	
17000.	-36.449	174.226	12.947	82.679	-36.793	195.414	16.823	84.610	
18000.	-36.746	187.175	12.940	93.419	-37.128	211.864	15.927	85.551	
19000.	-37.035	200.085	12.83	84.118	-37.451	226.927	14.098	86.366	
20000.	-37.304	212.006	12.763	84.775	-37.760	239.451	15.799	87.029	
22000.	-37.819	238.142	12.460	85.978	-38.324	250.828	16.692	87.559	
24000.	-38.296	262.717	12.112	87.07	-38.790	230.669	15.217	86.695	
25000.	-38.738	286.590	11.763	88.003	-39.114	157.888	15.864	83.893	
29000.	-39.1	309.747	11.439	88.63	-39.240	4.707	-102.149	78.149	
30000.	-39.5	332.369	11.148	89.642	-39.102	-263.745	-170.006	68.912	

FIGURE 27
THERMAL PROPERTIES OF NI⁺ HOO⁻ 447.600 KCAL/MOLE)

T	(M _O O-M _O C)/RT	H-HO KCAL/MOLE	CP CAL/MOLE-DEG	SC CAL/MOLE-DEG
100.	-12.983	0.649	5.915	32.285
200.	-15.161	1.196	5.235	36.109
300.	-16.352	1.711	5.096	16.197
400.	-17.165	2.217	5.034	39.652
500.	-17.782	2.719	5.010	40.773
600.	-18.277	3.219	4.797	41.645
700.	-18.691	3.718	4.989	42.455
800.	-19.047	4.217	4.954	43.120
900.	-19.358	4.715	4.981	43.707
1000.	-19.635	5.213	4.978	44.232
1200.	-20.112	6.206	4.975	45.139
1400.	-20.512	7.203	4.973	45.906
1600.	-20.857	8.198	4.972	46.570
1800.	-21.160	9.192	4.972	47.156
2000.	-21.430	10.186	4.973	47.679
2200.	-21.674	11.181	4.975	48.153
2400.	-21.897	12.177	4.980	48.517
2600.	-22.101	13.173	4.987	48.985
2800.	-22.290	14.172	4.996	49.355
3000.	-22.465	15.172	5.009	49.700
3500.	-22.857	17.686	5.051	50.476
4000.	-23.197	20.226	5.107	51.154
4500.	-23.497	22.794	5.169	51.759
5000.	-23.766	25.394	5.232	52.306
5500.	-24.010	28.025	5.292	52.808
6000.	-24.233	30.605	5.347	53.271
6500.	-24.440	33.371	5.395	53.701
7000.	-24.632	36.079	5.437	54.102
7500.	-24.811	38.807	5.472	54.478
8000.	-24.979	41.551	5.503	54.833
8500.	-25.138	44.309	5.528	55.167
9000.	-25.288	47.078	5.550	55.484
9500.	-25.431	49.858	5.569	55.784
10000.	-25.566	52.647	5.585	56.070
11000.	-25.820	58.247	5.613	56.604
12000.	-26.052	63.871	5.636	57.093
13000.	-26.267	69.517	5.656	57.545
14000.	-26.467	75.184	5.676	57.965
15000.	-26.654	80.870	5.696	58.357
16000.	-26.829	86.576	5.717	58.726
17000.	-26.994	92.394	5.739	59.073
18000.	-27.151	98.055	5.762	59.402
19000.	-27.299	103.829	5.796	59.714
20000.	-27.441	109.627	5.811	60.011
22000.	-27.704	121.300	5.862	60.567
24000.	-27.946	133.075	5.913	61.080
26000.	-28.170	144.951	5.961	61.555
28000.	-28.379	156.918	6.004	61.998
30000.	-28.574	168.963	6.040	62.414

ORIGINAL PAGE IS
OF POOR QUALITY

THERMAL PROPERTIES OF OC 100% 372.940 KCAL/MOLE)

*****PHYSICAL MODELS*****

T	(MUO-HOO)/RT	H-HOO KCAL/MOLE	CAL/MOLE	CP CAL/MOLE-DEG	CAL/MOLE-DEG	SO
100.	-13.393	0.937	4.968	31.583	31.583	
200.	-15.126	0.994	4.968	35.926	35.926	
300.	-16.140	1.490	4.968	37.041	37.041	
400.	-16.859	1.987	4.968	38.470	38.470	
500.	-17.417	2.484	4.968	39.578	39.578	
600.	-17.872	2.981	4.968	40.484	40.484	
700.	-18.258	3.478	4.968	41.250	41.250	
800.	-18.592	3.974	4.968	41.913	41.913	
900.	-18.886	4.471	4.968	42.498	42.498	
1000.	-19.149	4.968	4.968	43.022	43.022	
1200.	-19.605	5.962	4.968	43.928	43.928	
1400.	-19.91	6.955	4.968	44.693	44.693	
1600.	-20.324	7.949	4.968	45.357	45.357	
1800.	-20.619	8.942	4.968	45.942	45.942	
2000.	-20.882	9.936	4.968	46.465	46.465	
2200.	-21.121	12.930	4.968	46.939	46.939	
2400.	-21.338	11.923	4.968	47.371	47.371	
2600.	-21.539	12.917	4.968	47.769	47.769	
2800.	-21.724	13.911	4.968	48.137	48.137	
3000.	-21.896	14.904	4.970	48.480	48.480	
3500.	-22.281	17.391	4.978	49.247	49.247	
4000.	-22.615	19.884	4.998	49.912	49.912	
4500.	-22.910	22.393	5.038	50.503	50.503	
5000.	-23.174	24.927	5.103	51.037	51.037	
5500.	-23.414	27.500	5.1528			
6000.	-23.633	30.126	5.313	51.945	51.945	
6500.	-23.836	32.817	5.455	52.415	52.415	
7000.	-24.025	35.584	5.614	52.825	52.825	
7500.	-24.202	38.434	5.786	53.218	53.218	
8000.	-24.369	41.371	5.954	53.598	53.598	
8500.	-24.528	44.98	6.143	53.964	53.964	
9000.	-24.679	47.13	6.317	54.321	54.321	
9500.	-24.823	50.713	6.481	54.667	54.667	
10000.	-24.962	53.993	6.634	55.003	55.003	
11000.	-25.223	60.761	6.893	55.648	55.648	
12000.	-25.468	67.755	7.084	56.256	56.256	
13000.	-25.698	74.906	7.207	56.829	56.829	
14000.	-25.915	82.149	7.270	57.365	57.365	
15000.	-26.120	89.429	7.283	57.868	57.868	
16000.	-26.315	96.702	7.257	58.337	58.337	
17000.	-26.500	103.933	7.201	58.775	58.775	
18000.	-26.677	111.098	7.126	59.185	59.185	
19000.	-26.846	118.160	7.037	59.568	59.568	
20000.	-27.007	125.169	6.940	59.926	59.926	
22000.	-27.308	138.850	6.740	60.576	60.576	
24000.	-27.595	152.135	6.546	61.157	61.157	
26000.	-27.841	165.046	6.369	61.673	61.673	
29000.	-28.078	177.622	6.210	62.139	62.139	
30000.	-28.298	189.930	6.071	62.563	62.563	

THERMAL PROPERTIES OF N₂I
-100- F[°]URE 29

357.680 KCAL/MOLE)

*****PHYSICAL MODEL*****

T	(H ₂ O-H ₂ O)/RT	H-H ₂ O	CP	SO	H-H ₂ O	CP	SO
		KCAL/MOLE	CAL/MOLE-DEG	CAL/MOLE-DEG	KCAL/MOLE	CAL/MOLE-DEG	CAL/MOLE-DEG
100.	-16.435	0.696	6.955	39.615	-16.670	0.652	6.610
200.	-18.861	1.391	6.955	44.435	-18.956	1.322	6.781
300.	-20.280	2.087	6.962	47.256	-20.315	2.056	6.947
400.	-21.287	2.785	7.004	49.264	-21.290	2.711	7.109
500.	-22.070	3.490	7.106	50.837	-22.056	3.430	7.266
600.	-22.712	4.207	7.254	52.445	-22.689	4.164	7.419
700.	-23.257	4.941	7.422	53.230	-23.230	4.914	7.567
800.	-23.733	5.692	7.591	54.278	-23.704	5.678	7.712
900.	-24.157	6.459	7.748	55.181	-24.127	6.456	7.852
1000.	-24.539	7.241	7.890	56.005	-24.509	7.248	7.986
1200.	-25.209	8.844	8.127	57.465	-25.181	8.872	8.248
1400.	-25.785	10.489	8.320	58.733	-25.720	10.546	8.493
1600.	-26.293	12.170	8.492	59.855	-26.270	12.264	8.723
1800.	-26.747	13.885	8.660	60.865	-26.728	12.404	8.938
2000.	-27.158	15.634	8.832	61.786	-27.145	12.542	9.140
2200.	-27.536	17.416	9.009	62.636	-27.526	12.689	9.326
2400.	-27.884	19.239	9.187	63.428	-27.862	12.853	9.503
2600.	-28.229	21.094	9.368	64.170	-28.213	12.940	9.665
2800.	-28.514	22.985	9.539	64.871	-28.523	13.034	9.816
3000.	-28.800	24.900	9.699	65.535	-28.816	13.182	9.945
3500.	-29.453	29.846	10.033	67.056	-29.482	13.470	10.255
4000.	-30.033	34.924	10.259	68.412	-30.074	13.660	10.493
4500.	-30.555	40.089	10.390	69.629	-30.608	14.054	10.676
5000.	-31.032	45.301	10.447	70.727	-31.095	14.328	10.811
5500.	-31.470	50.528	10.454	71.723	-31.542	15.156	10.903
6000.	-31.874	55.749	10.429	72.632	-31.957	15.725	11.292
6500.	-32.250	60.954	10.387	73.465	-32.344	16.211	11.662
7000.	-32.601	66.115	10.335	74.213	-32.705	16.602	11.979
7500.	-32.930	71.288	10.279	74.944	-33.045	17.366	12.355
8000.	-33.240	76.414	10.223	75.606	-33.365	17.915	12.716
8500.	-33.532	81.511	10.168	76.224	-33.668	18.460	13.163
9000.	-33.808	86.582	10.116	76.803	-33.955	19.016	13.602
9500.	-34.070	91.628	10.066	77.349	-34.226	19.540	13.735
10000.	-34.319	96.649	10.020	77.864	-34.487	20.071	14.667
11000.	-34.724	106.627	9.938	78.815	-34.972	21.153	15.916
12000.	-35.208	116.529	9.868	79.677	-35.416	21.836	16.434
13000.	-35.600	126.366	9.808	80.464	-35.825	22.235	17.370
14000.	-35.962	136.148	9.758	81.189	-36.205	22.593	18.131
15000.	-36.4300	145.885	9.716	81.861	-36.559	23.294	18.847
16000.	-36.616	155.561	9.681	82.487	-36.890	23.840	19.355
17000.	-36.912	165.249	9.651	83.073	-37.202	24.363	20.023
18000.	-37.192	174.897	9.626	83.624	-37.497	24.848	20.773
19000.	-37.456	184.502	9.604	84.144	-37.776	25.369	21.406
20000.	-37.707	194.095	9.584	84.636	-38.042	26.742	22.237
22000.	-38.172	213.230	9.552	85.548	-38.540	27.577	23.563
24000.	-38.595	232.307	9.525	86.378	-39.000	28.259	24.533
26000.	-38.986	251.333	9.502	87.139	-39.425	28.945	25.603
28000.	-39.346	270.315	9.480	87.842	-39.819	29.523	26.948
30000.	-39.681	289.255	9.460	AB.496	-40.182	309.951	27.462

THERMAL PROPERTIES OF O2

FIGURE 30 HOO= 288.000 KCAL/MOLE)

*****PHYSICAL MODEL*****

T	(MUO-HOO)/RT	H-HOO KCAL/MOLE	CP CAL/MOLE-DEG	50 KCAL/MOLE	CP CAL/MOLE-DEG	50 KCAL/MOLE	CP CAL/MOLE-DEG
100.	-16.838	0.727	7.796	40.733	-17.291	0.701	7.071
200.	-19.425	1.501	7.576	46.107	-19.744	1.414	7.196
300.	-20.956	2.245	7.331	49.125	-21.193	2.140	7.315
400.	-22.036	2.974	7.293	51.225	-22.229	2.077	7.429
500.	-22.869	3.708	7.390	52.861	-23.040	2.025	7.537
600.	-23.550	4.454	7.548	54.221	-23.708	2.084	7.641
700.	-24.126	5.218	7.720	55.398	-24.277	2.153	7.739
800.	-24.629	5.998	7.881	56.439	-24.773	2.232	7.832
900.	-25.075	6.793	8.023	57.376	-25.214	2.319	7.920
1000.	-25.476	7.602	8.145	58.228	-25.611	2.416	8.004
1200.	-26.178	9.251	8.334	59.731	-26.305	2.512	8.159
1400.	-26.780	10.932	8.469	61.026	-26.899	2.676	8.298
1600.	-27.308	12.636	8.565	62.164	-27.419	2.845	8.422
1800.	-27.778	14.356	8.636	63.177	-27.882	3.016	8.533
2000.	-28.203	16.089	8.680	64.090	-28.301	3.183	8.632
2200.	-28.590	17.831	8.730	64.920	-28.683	3.356	8.721
2400.	-28.946	19.581	8.762	65.681	-29.035	3.511	8.799
2600.	-29.276	21.336	8.787	66.383	-29.361	3.661	8.869
2800.	-29.583	23.095	8.808	67.035	-29.665	3.822	8.932
3000.	-29.870	24.858	8.825	67.643	-29.949	4.000	8.989
3500.	-30.516	29.279	8.856	69.006	-30.592	4.215	9.109
4000.	-31.080	33.714	8.881	70.190	-31.157	4.421	9.233
4500.	-31.581	38.160	8.906	71.238	-31.660	4.629	9.313
5000.	-32.032	42.621	8.933	72.179	-32.115	4.811	9.423
5500.	-32.442	47.101	8.983	73.032	-32.530	5.003	9.552
6000.	-32.817	51.607	9.044	73.816	-32.913	5.269	9.712
6500.	-33.165	56.148	9.123	74.543	-33.268	5.517	9.909
7000.	-33.487	60.733	9.220	75.222	-33.600	5.855	10.152
7500.	-33.789	65.371	9.335	75.862	-33.912	6.200	10.444
8000.	-34.073	70.070	9.464	76.469	-34.207	6.553	10.790
8500.	-34.341	74.837	9.606	77.047	-34.487	6.913	11.192
9000.	-34.595	79.677	9.755	77.600	-34.754	7.219	11.651
9500.	-34.836	84.593	9.909	78.132	-35.011	7.511	12.166
10000.	-35.067	89.587	10.065	78.644	-35.256	7.811	12.736
11000.	-35.499	99.864	10.366	79.617	-35.728	8.116	14.023
12000.	-35.899	110.309	10.537	80.531	-36.173	8.477	14.771
13000.	-36.272	121.036	10.865	81.392	-36.600	8.843	15.467
14000.	-36.621	132.023	11.043	82.204	-37.013	9.191	16.531
15000.	-36.951	143.134	11.171	82.971	-37.415	9.445	17.767
16000.	-37.262	154.348	11.250	83.694	-37.808	9.718	18.945
17000.	-37.558	165.621	11.288	84.378	-38.195	10.013	20.104
18000.	-37.839	176.913	11.291	85.023	-38.574	10.319	21.846
19000.	-38.108	188.194	11.266	85.633	-38.946	10.610	22.932
20000.	-38.365	199.438	11.219	86.210	-39.308	10.886	24.023
22000.	-38.845	221.746	11.082	87.273	-39.997	11.632	25.884
24000.	-39.289	243.744	10.914	88.230	-40.615	12.056	27.350
26000.	-39.699	265.397	10.739	89.097	-41.127	12.507	28.190
28000.	-40.080	286.703	10.524	89.886	-41.486	12.728	29.781
30000.	-40.436	307.678	10.409	90.610	-41.634	13.061	31.433

ORIGINAL PAGE IS
OF POOR QUALITY

FIGURE 31

THERMAL PROPERTIES OF CO₂————— 0.0 KCAL/MOLE)

*****PHYSICAL MODEL*****

T	(MUO-HOO)/RT	H-HOO KCAL/MOLE	H-HOO CAL/MOLE	CP KCAL/MOLE-DEG	CP CAL/MOLE-DEG	S0
150.	-18.014	0.696	6.980	42.755	42.755	
200.	-20.456	1.493	7.731	47.766	47.766	
300.	-21.944	2.254	8.360	51.120	51.120	
400.	-23.067	3.192	9.349	53.613	53.613	
500.	-23.985	4.218	10.629	56.097	56.097	
600.	-24.777	5.314	11.279	58.001	58.001	
700.	-25.479	6.468	11.801	59.872	59.872	
800.	-26.112	7.671	12.243	61.478	61.478	
900.	-26.689	8.914	12.610	62.942	62.942	
1000.	-27.227	10.191	12.916	64.286	64.286	
1200.	-28.180	12.323	13.384	66.685	66.685	
1400.	-29.025	15.527	13.714	68.775	68.775	
1600.	-29.782	18.307	13.953	70.622	70.622	
1800.	-30.469	21.112	14.129	72.276	72.276	
2000.	-31.097	23.952	14.262	77.772	77.772	
2200.	-31.677	26.815	14.364	75.136	75.136	
2400.	-32.214	29.696	14.444	76.390	76.390	
2600.	-32.716	32.592	14.508	77.549	77.549	
2800.	-33.186	35.499	14.560	78.626	78.626	
3000.	-33.629	38.415	14.602	79.632	79.632	
3500.	-34.632	45.737	14.680	81.889	81.889	
4000.	-35.517	53.090	14.731	83.853	83.853	
4500.	-36.309	60.465	14.766	85.590	85.590	
5000.	-37.025	67.855	14.792	87.147	87.147	
5500.	-37.679	75.256	14.811	88.558	88.558	
6000.	-38.280	82.666	14.826	89.847	89.847	
6500.	-38.837	90.082	14.837	91.035	91.035	
7000.	-39.355	97.503	14.846	92.135	92.135	
7500.	-39.839	104.928	14.854	93.159	93.159	
8000.	-40.295	112.356	14.860	94.118	94.118	
8500.	-40.724	119.798	14.865	95.019	95.019	
9000.	-41.130	127.221	14.869	95.869	95.869	
9500.	-41.515	134.656	14.873	96.673	96.673	
10000.	-41.881	142.094	14.876	97.436	97.436	
11000.	-42.564	156.972	14.881	98.854	98.854	
12000.	-43.190	171.854	14.884	100.149	100.149	
13000.	-43.768	186.740	14.887	101.340	101.340	
14000.	-44.304	201.629	14.890	102.444	102.444	
15000.	-44.805	216.519	14.891	103.471	103.471	
16000.	-45.274	231.411	14.893	104.432	104.432	
17000.	-45.716	246.305	14.894	105.335	105.335	
18000.	-46.133	261.199	14.895	106.186	106.186	
19000.	-46.528	276.095	14.896	106.992	106.992	
20000.	-46.903	290.992	14.897	107.756	107.756	
22000.	-47.602	320.787	14.899	109.176	109.176	
24000.	-48.241	350.584	14.899	110.472	110.472	
26000.	-48.830	380.383	14.900	111.665	111.665	
28000.	-49.376	410.183	14.900	112.769	112.769	
30000.	-49.885	439.984	14.901	113.797	113.797	

FIGURE 32 THERMAL PROPERTIES OF CO MOO= 66.770 KCAL/MOLE)

*****#PHYSICAL MODULUS*****

*****#THERMO FIT*****

T	(MUO-MOO)/RT	H-HOO KCAL/MOLE	CP CAL/MOLE-DEG	SO CAL/MOLE-DEG	H-HOO KCAL/MOLE	CP CAL/MOLE-DEG	SO CAL/MOLE-DEG
100.	-16.435	0.696	6.955	39.615	-16.474	0.681	39.547
200.	-18.861	1.391	6.955	44.436	-18.859	1.374	44.348
300.	-20.280	2.087	6.962	47.257	-20.267	2.079	47.206
400.	-21.287	2.785	7.008	49.265	-21.274	2.796	49.267
500.	-22.070	3.490	7.114	50.839	-22.062	3.524	50.890
600.	-22.712	4.209	7.267	52.149	-22.712	4.262	52.236
700.	-23.258	4.944	7.438	53.282	-23.265	5.011	53.390
800.	-23.734	5.697	7.608	54.286	-23.747	5.769	54.402
900.	-24.158	6.466	7.766	55.192	-24.176	6.537	55.306
1000.	-24.541	7.249	7.906	56.017	-24.563	7.313	56.124
1200.	-25.212	8.854	8.134	57.480	-25.238	8.892	57.563
1400.	-25.789	10.499	8.302	58.747	-25.816	10.503	58.804
1600.	-26.296	12.172	8.427	59.864	-26.323	12.142	59.890
1800.	-26.750	13.868	8.520	60.862	-26.776	13.808	60.879
2000.	-27.161	15.579	8.592	61.764	-27.184	15.497	61.769
2200.	-27.536	17.303	8.647	62.585	-27.558	17.208	62.585
2400.	-27.882	19.037	8.690	63.340	-27.902	18.939	63.337
2600.	-28.203	20.779	8.725	64.037	-28.221	20.676	64.037
2800.	-28.502	22.527	8.753	64.684	-28.519	22.449	64.690
3000.	-28.782	24.260	8.776	65.289	-28.798	24.225	65.292
3500.	-29.414	28.679	8.819	66.645	-29.429	28.713	66.686
4000.	-29.967	33.096	8.847	67.825	-29.984	33.251	67.898
4500.	-30.460	37.525	8.867	68.868	-30.480	37.621	68.974
5000.	-30.903	41.962	8.893	69.803	-30.921	42.406	69.940
5500.	-31.307	46.407	8.928	70.653	-31.336	46.996	9.017
6000.	-31.677	50.861	8.916	71.425	-31.711	51.581	9.162
6500.	-32.019	55.324	8.941	72.140	-32.058	56.156	9.139
7000.	-32.337	59.804	8.979	72.804	-32.381	60.719	9.113
7500.	-32.634	64.306	9.034	73.425	-32.683	65.269	9.068
8000.	-32.913	68.842	9.112	74.011	-32.966	69.807	9.067
8500.	-33.176	73.423	9.217	74.566	-33.232	74.377	74.785
9000.	-33.425	78.064	9.353	75.997	-33.484	78.864	9.053
9500.	-33.662	82.781	9.521	75.607	-33.723	83.393	9.063
10000.	-33.887	87.591	9.722	76.100	-33.950	87.930	9.087
11000.	-34.310	97.552	10.221	77.049	-34.372	97.056	9.174
12000.	-34.701	108.069	10.826	77.964	-34.759	106.296	9.312
13000.	-35.067	119.228	11.498	78.856	-35.117	115.693	9.446
14000.	-35.412	131.070	12.185	79.734	-35.449	125.272	9.672
15000.	-35.741	143.585	12.816	80.597	-35.761	135.029	9.835
16000.	-36.055	156.714	13.407	81.444	-36.054	144.919	9.930
17000.	-36.358	170.362	13.868	82.271	-36.331	154.849	9.903
18000.	-36.649	184.407	14.202	83.074	-36.594	164.663	9.666
19000.	-36.931	198.722	14.407	83.848	-36.843	174.136	9.209
20000.	-37.203	213.162	14.493	84.590	-37.080	182.964	8.380
22000.	-37.723	242.101	14.371	85.968	-37.515	195.994	5.281
24000.	-38.211	270.491	13.988	87.203	-37.897	202.304	-0.501
26000.	-38.669	297.972	13.482	88.303	-38.218	192.502	-10.222
28000.	-39.099	324.399	12.946	89.283	-38.465	158.916	-24.590
30000.	-39.502	349.773	12.435	90.158	-38.619	90.277	-45.320

***** THERMAL PROPERTIES OF CN *****

F° *RE 33 100= 197.170 KCAL/MOLE)

*****PHYSICAL MODEL*****

T	(MUO-HOO)/RT	H-HOO KCAL/MOLE	CP CAL/MOLE-DEG	SO CAL/MOLE-DEG	CP CAL/MOLE-DEG	SO CAL/MOLE-DEG	CP CAL/MOLE-DEG	SO CAL/MOLE-DEG	CP CAL/MOLE-DEG	SO CAL/MOLE-DEG
100.	-17.034	0.696	6.955	40.805	-17.413	0.655	6.639	41.158	-	-
200.	-19.460	1.391	6.955	45.626	-19.712	1.326	6.805	45.811	-	-
300.	-20.879	2.087	6.966	48.447	-21.075	2.016	6.966	48.601	-	-
400.	-21.887	2.786	7.024	50.457	-22.053	2.721	7.122	50.626	-	-
500.	-22.670	3.494	7.149	52.037	-22.821	3.441	7.274	52.232	-	-
600.	-23.312	4.217	7.316	53.355	-23.456	4.175	7.422	53.571	-	-
700.	-23.860	4.958	7.497	54.496	-23.999	4.925	7.565	54.726	-	-
800.	-24.338	5.716	7.672	55.509	-24.474	5.688	7.705	55.745	-	-
900.	-24.763	6.492	7.830	56.422	-24.898	6.466	7.840	56.661	-	-
1000.	-25.147	7.262	7.969	57.254	-25.280	7.256	7.971	57.493	-	-
1200.	-25.821	8.899	8.197	58.728	-25.952	8.876	8.222	58.969	-	-
1400.	-26.401	10.557	8.379	60.006	-26.531	10.544	8.457	60.254	-	-
1600.	-26.912	12.249	8.540	61.135	-27.042	12.258	8.676	61.398	-	-
1800.	-27.369	13.973	8.638	62.150	-27.499	14.014	8.884	62.432	-	-
2000.	-27.783	15.729	8.861	63.075	-27.915	15.810	9.077	63.379	-	-
2200.	-28.163	17.518	9.031	63.928	-28.297	17.644	9.257	64.252	-	-
2400.	-28.513	19.342	9.205	64.721	-28.651	19.512	9.424	65.065	-	-
2600.	-28.840	21.200	9.379	65.465	-28.980	21.413	9.579	65.825	-	-
2800.	-29.146	23.093	9.547	66.166	-29.289	23.343	9.722	66.541	-	-
3000.	-29.434	24.918	9.704	66.830	-29.580	25.301	9.854	67.216	-	-
3500.	-30.089	29.957	10.035	68.352	-30.243	30.302	10.139	68.757	-	-
4000.	-30.671	35.035	10.261	69.708	-30.832	35.430	10.365	70.126	-	-
4500.	-31.195	40.202	10.393	70.925	-31.362	40.658	10.539	71.358	-	-
5000.	-31.673	45.416	10.451	72.023	-31.845	45.961	10.666	72.475	-	-
5500.	-32.112	50.645	10.460	73.020	-32.289	51.318	10.753	73.496	-	-
6000.	-32.517	55.870	10.437	73.930	-32.701	56.709	10.807	74.434	-	-
6500.	-32.894	61.080	10.398	74.763	-33.084	62.120	10.832	75.300	-	-
7000.	-33.246	66.267	10.351	75.532	-33.442	67.537	10.834	76.103	-	-
7500.	-33.575	71.431	10.304	76.245	-33.778	72.950	10.817	76.859	-	-
8000.	-33.805	76.572	10.261	76.908	-34.095	78.351	10.785	77.548	-	-
8500.	-34.178	81.692	10.224	77.529	-34.395	83.734	10.743	78.208	-	-
9000.	-34.455	86.797	10.195	78.113	-34.679	89.094	10.695	78.813	-	-
9500.	-34.718	91.889	10.175	78.664	-34.949	94.428	10.643	79.390	-	-
10000.	-34.968	96.973	10.165	79.185	-35.206	99.736	10.591	79.930	-	-
11000.	-35.434	107.139	10.173	80.154	-35.685	110.278	10.496	80.939	-	-
12000.	-35.861	117.331	10.214	81.041	-36.125	120.736	10.425	81.849	-	-
13000.	-36.256	127.577	10.282	81.861	-36.531	131.141	10.391	82.682	-	-
14000.	-36.522	137.902	10.369	82.626	-36.908	141.533	10.399	83.452	-	-
15000.	-36.965	148.318	10.465	83.345	-37.259	151.953	10.447	84.171	-	-
16000.	-37.287	158.833	10.565	84.023	-37.588	162.439	10.511	84.848	-	-
17000.	-37.590	169.446	10.661	84.667	-37.898	173.022	10.637	85.489	-	-
18000.	-37.877	180.152	10.749	85.278	-38.191	183.715	10.749	86.100	-	-
19000.	-38.150	190.941	10.827	85.862	-38.470	194.515	10.844	86.684	-	-
20000.	-38.410	201.802	10.892	86.419	-38.734	205.388	10.893	87.242	-	-
22000.	-38.896	223.682	10.979	87.462	-39.228	227.070	10.708	88.275	-	-
24000.	-39.343	245.683	11.013	88.419	-39.680	247.775	9.852	89.177	-	-
26000.	-39.756	267.705	11.002	89.300	-40.095	265.741	7.899	89.897	-	-
28000.	-40.141	289.667	10.955	90.114	-40.471	278.245	4.295	90.362	-	-
30000.	-40.501	311.510	10.884	90.867	-40.808	281.425	-1.546	90.474	-	-

**ORIGINAL PAGE IS
OF POOR QUALITY**

THERMAL PROPERTIES OF HE 100% 0.0 KCAL/MOLE)

*****PHYSICAL MODEL*****

FIGURE 34

T	(HOO-HOO)/RT	KCAL/MOLE	C/I MOLE-DEG	CP CAL/MOLE-DEG	SO
100.	-9.928	0.497	4.968	24.698	
200.	-11.661	0.994	4.968	28.141	
300.	-12.675	1.490	4.968	30.155	
400.	-13.394	1.987	4.968	31.585	
500.	-13.952	2.484	4.968	32.693	
600.	-14.408	2.981	4.968	33.599	
700.	-14.793	3.478	4.968	34.365	
800.	-15.127	3.974	4.968	35.028	
900.	-15.421	4.471	4.968	35.613	
1000.	-15.685	4.968	4.968	36.137	
1100.	-16.141	5.932	4.968	37.043	
1200.	-16.526	6.955	4.968	37.808	
1300.	-16.860	7.949	4.968	38.472	
1400.	-17.154	8.942	4.968	39.057	
1500.	-17.418	9.936	4.968	39.580	
1600.	-17.656	10.930	4.968	40.054	
1700.	-17.873	11.923	4.968	40.486	
1800.	-18.074	12.917	4.968	40.884	
1900.	-18.259	13.910	4.968	41.252	
2000.	-18.431	14.904	4.968	41.595	
2100.	-18.617	17.388	4.968	42.361	
2200.	-19.151	19.872	4.968	43.024	
2300.	-19.445	22.356	4.968	43.609	
2400.	-19.708	24.840	4.968	44.132	
2500.	-19.947	27.324	4.968	44.606	
2600.	-20.164	29.808	4.968	45.038	
2700.	-20.364	32.292	4.968	45.436	
2800.	-20.550	34.776	4.968	45.804	
2900.	-20.722	37.260	4.968	46.147	
3000.	-20.833	39.744	4.968	46.467	
3100.	-21.035	42.228	4.968	46.769	
3200.	-21.178	44.712	4.968	47.053	
3300.	-21.313	47.196	4.968	47.321	
3400.	-21.441	49.690	4.968	47.576	
3500.	-21.680	54.648	4.968	48.050	
3600.	-21.897	59.616	4.968	48.482	
3700.	-22.097	64.584	4.968	48.879	
3800.	-22.282	69.552	4.968	49.248	
3900.	-22.455	74.520	4.968	49.590	
4000.	-22.616	79.488	4.968	49.911	
4100.	-22.768	84.456	4.968	50.212	
4200.	-22.911	89.424	4.968	50.496	
4300.	-23.046	94.392	4.968	50.765	
4400.	-23.174	99.360	4.968	51.020	
4500.	-23.412	109.296	4.968	51.493	
4600.	-23.630	119.232	4.968	51.925	
4700.	-23.830	129.168	4.968	52.323	
4800.	-24.015	139.104	4.968	52.691	
4900.	-24.188	149.040	4.968	53.034	
5000.					

FIGURE 35
THERMAL PROPERTIES OF C -100 = 263.550 KCAL/MOLE)

*****PHYSICAL MODEL*****

T	(MUO-HOO)/RT	H-HOO KCAL/MOLE	CAL/MOLE-DEG	CP CAL/MOLE-DEG	S0
100.	-13.346	0.582	4.968	32.339	
200.	-15.293	1.079	4.968	35.783	
300.	-16.376	1.575	4.968	37.797	
400.	-17.133	2.072	4.968	39.227	
500.	-17.712	2.569	4.968	40.335	
600.	-18.182	3.066	4.968	41.241	
700.	-18.578	3.563	4.968	42.007	
800.	-18.919	4.059	4.968	42.670	
900.	-19.210	4.556	4.968	43.255	
1000.	-19.488	5.053	4.968	43.779	
1200.	-19.950	6.047	4.968	44.684	
1400.	-20.341	7.041	4.972	45.451	
1600.	-20.679	8.036	4.978	46.115	
1800.	-20.976	9.032	4.990	46.702	
2000.	-21.242	10.032	5.007	47.228	
2200.	-21.483	11.036	5.031	47.707	
2400.	-21.702	12.045	5.060	48.146	
2600.	-21.945	13.060	5.094	48.552	
2800.	-22.092	14.082	5.130	48.931	
3000.	-22.267	15.112	5.167	49.286	
3500.	-22.658	17.719	5.261	50.090	
4000.	-23.000	20.371	5.345	50.798	
4500.	-23.302	23.062	5.414	51.431	
5000.	-23.575	25.783	5.468	52.005	
5500.	-23.823	28.528	5.509	52.528	
6000.	-24.051	31.290	5.541	53.009	
6500.	-24.261	34.067	5.565	53.453	
7000.	-24.457	36.855	5.586	53.856	
7500.	-24.640	39.652	5.605	54.252	
8000.	-24.812	42.461	5.628	54.615	
8500.	-24.975	45.281	5.655	54.957	
9000.	-25.128	48.117	5.692	55.281	
9500.	-25.274	50.976	5.743	55.590	
10000.	-25.413	53.863	5.811	55.886	
11000.	-25.672	59.768	6.016	56.449	
12000.	-25.911	65.633	6.336	56.985	
13000.	-26.134	72.485	6.792	57.509	
14000.	-26.344	79.563	7.386	58.034	
15000.	-26.543	87.297	8.101	58.567	
16000.	-26.735	95.795	8.905	59.115	
17000.	-26.921	105.122	9.751	59.680	
18000.	-27.102	115.293	10.584	60.261	
19000.	-27.279	126.268	11.351	60.855	
20000.	-27.454	137.957	12.007	61.454	
22000.	-27.797	162.945	12.874	62.644	
24000.	-28.131	189.031	13.112	63.779	
26000.	-28.457	215.045	12.831	64.620	
28000.	-28.771	240.134	12.218	65.750	
30000.	-29.073	263.815	11.449	66.567	

THERMAL PROPERTIES OF CC F₁-TRE 36 100= 523•310 KCAL/MOLE)

*****+PHYSICAL MODEL*****

T	(MUO-HOO)/RT	H-HOO KCAL/MOLE	H-HOO CAL/MOLE-DEG	CP CAL/MOLE-DEG
100.	-12•855	0•578	5•384	50 31•326
200.	-14•819	1•096	5•072	34•926
300.	-15•921	1•599	5•013	36•969
400.	-16•687	2•100	4•993	38•408
500.	-17•273	2•598	4•984	39•521
600.	-17•748	3•096	4•979	40•430
700.	-18•147	3•594	4•976	41•197
800.	-18•492	4•092	4•974	41•861
900.	-18•794	4•589	4•973	42•447
1000.	-19•064	5•096	4•972	42•971
1200.	-19•530	6•080	4•971	43•877
1400.	-19•923	7•074	4•970	44•643
1600.	-20•262	8•068	4•969	45•307
1800.	-20•560	9•062	4•969	45•892
2000.	-20•827	10•056	4•969	46•416
2200.	-21•068	11•050	4•969	46•889
2400.	-21•288	12•044	4•969	47•322
2600.	-21•490	13•037	4•969	47•719
2800.	-21•677	14•031	4•968	48•088
3000.	-21•851	15•025	4•968	48•430
3500.	-22•239	17•509	4•968	49•196
4200.	-22•575	19•993	4•968	49•860
4500.	-22•871	22•477	4•969	50•445
5000.	-23•136	24•962	4•971	50•969
5500.	-23•376	27•449	4•975	51•442
6000.	-23•594	29•938	4•982	51•876
6500.	-23•795	32•432	4•995	52•275
7000.	-23•981	34•933	5•013	52•646
7500.	-24•154	37•446	5•039	52•992
8000.	-24•317	39•974	5•073	53•319
8500.	-24•469	42•520	5•115	53•627
9000.	-24•613	45•090	5•165	53•921
9500.	-24•750	47•686	5•222	54•202
10000.	-24•879	50•313	5•287	54•471
11000.	-25•121	55•671	5•433	54•982
12000.	-25•344	61•185	5•596	55•462
13000.	-25•550	66•867	5•769	55•916
14000.	-25•743	72•724	5•944	56•350
15000.	-25•924	78•753	6•114	56•766
16000.	-26•095	84•949	6•275	57•166
17000.	-26•258	91•299	6•423	57•551
18000.	-26•414	97•789	6•555	57•922
19000.	-26•562	104•403	6•670	58•279
20000.	-26•705	111•124	6•768	58•624
22000.	-26•974	124•816	6•912	59•276
24000.	-27•225	138•731	6•994	59•882
26000.	-27•460	152•755	7•022	60•443
28000.	-27•680	166•793	7•010	60•963
30000.	-27•888	180•775	6•967	61•446

*****PHYSICAL MODEL*****

T	(MUO-HOO)/RT	H-HOO KCAL/MOLE	CAL/MOLE-DEG	CP CAL/MOLE-DEG
100.	-10.621	C.497	4.968	26.075
200.	-12.354	0.994	4.968	29.519
300.	-13.368	1.493	4.968	31.533
400.	-14.087	1.987	4.968	32.962
500.	-14.645	2.484	4.968	34.071
600.	-15.101	2.981	4.968	34.976
700.	-15.486	3.478	4.958	35.742
800.	-15.820	3.974	4.968	36.406
900.	-16.115	4.471	4.968	36.991
1000.	-16.378	4.968	4.968	37.514
1100.	-16.834	5.962	4.968	38.420
1200.	-17.219	6.955	4.968	39.186
1300.	-17.553	7.949	4.968	39.849
1400.	-17.847	8.942	4.968	40.434
1500.	-18.111	9.936	4.968	40.958
1600.	-18.349	10.930	4.968	41.431
1700.	-18.567	11.923	4.968	41.864
1800.	-18.767	12.917	4.968	42.261
1900.	-18.952	13.910	4.968	42.629
2000.	-19.124	14.904	4.968	42.972
2100.	-19.510	17.388	4.968	43.738
2200.	-19.844	19.872	4.968	44.491
2300.	-20.138	22.356	4.968	44.986
2400.	-20.402	24.840	4.968	45.510
2500.	-20.640	27.324	4.968	45.983
2600.	-20.857	29.808	4.968	46.416
2700.	-21.057	32.292	4.968	46.813
2800.	-21.243	34.776	4.968	47.182
2900.	-21.415	37.260	4.968	47.524
3000.	-21.577	39.744	4.968	47.845
3100.	-21.728	42.228	4.968	48.146
3200.	-21.871	44.712	4.968	48.430
3300.	-22.006	47.196	4.968	48.699
3400.	-22.134	49.680	4.968	48.953
3500.	-22.373	54.642	4.968	49.427
3600.	-22.590	59.616	4.968	49.859
3700.	-22.790	64.584	4.968	50.257
3800.	-22.976	69.552	4.968	50.625
3900.	-23.148	74.520	4.968	50.968
4000.	-23.309	79.488	4.968	51.286
4100.	-23.461	84.456	4.968	51.590
4200.	-23.604	89.424	4.968	51.874
4300.	-23.739	94.392	4.968	52.142
4400.	-23.867	99.360	4.968	52.397
4500.	-23.999	109.296	4.968	52.871
4600.	-24.106	119.232	4.968	53.303
4700.	-24.323	129.168	4.968	53.700
4800.	-24.523	139.104	4.968	54.069
4900.	-24.76	149.040	4.968	54.411

ORIGINAL PAGE IS
OF POOR QUALITY

FIGURE 38
THERMAL PROPERTIES OF ARE
00 = 363.330 KCAL/MOLE)

*****PHYSICAL MODEL*****

T	(MU0-H00)/RT	H-H00 KCAL/MOLE	CP CAL/MOLE-DEG	SO CAL/MOLE-DEG
100.	-14.766	0.497	4.968	34.310
200.	-16.448	0.994	4.972	37.754
300.	-17.513	1.493	5.017	39.776
400.	-18.234	1.999	5.120	41.232
500.	-18.797	2.517	5.238	42.388
600.	-19.261	3.046	5.334	43.352
700.	-19.656	3.583	5.399	44.179
800.	-20.001	4.125	5.434	44.903
900.	-20.368	4.669	5.446	45.544
1000.	-20.584	5.213	5.443	46.117
1200.	-21.064	6.299	5.411	47.107
1400.	-21.472	7.377	5.365	47.938
1600.	-21.826	8.445	5.319	48.651
1800.	-22.139	9.525	5.276	49.275
2000.	-22.419	10.556	5.239	49.829
2200.	-22.672	11.621	5.207	50.327
2400.	-22.903	12.639	5.179	50.779
2600.	-23.115	13.673	5.156	51.192
2800.	-23.311	14.702	5.136	51.574
3000.	-23.493	15.727	5.119	51.928
3500.	-23.899	18.277	5.085	52.714
4000.	-24.249	20.814	5.061	53.391
4500.	-24.557	23.340	5.044	53.986
5000.	-24.832	25.858	5.031	54.517
5500.	-25.079	28.371	5.021	54.996
6000.	-25.305	30.880	5.013	55.433
6500.	-25.512	33.385	5.007	55.834
7000.	-25.703	35.887	5.002	56.205
7500.	-25.881	38.387	4.998	56.550
8000.	-26.047	40.885	4.994	56.872
8500.	-26.203	43.382	4.992	57.175
9000.	-26.350	45.877	4.989	57.460
9500.	-26.488	48.371	4.987	57.730
10000.	-26.620	50.864	4.985	57.985
11000.	-26.864	55.848	4.982	58.460
12000.	-27.086	60.629	4.980	58.894
13000.	-27.290	65.808	4.978	59.292
14000.	-27.478	70.786	4.977	59.661
15000.	-27.654	75.763	4.976	60.005
16000.	-27.813	80.738	4.975	60.326
17000.	-27.972	85.713	4.974	60.627
18000.	-28.117	90.687	4.974	60.912
19000.	-28.254	95.660	4.973	61.180
20000.	-28.384	100.633	4.973	61.436
22000.	-28.625	110.577	4.972	61.909
24000.	-28.845	120.520	4.971	62.342
26000.	-29.047	130.462	4.971	62.740
28000.	-29.234	140.403	4.970	63.108
30000.	-29.408	150.343	4.970	63.451

FIGURE 39
THERMAL PROPERTIES OF HE₃ 0= 456.910 KCAL/MOLE)

*****PHYSICAL MODE*****

T	(HOO-HOO)/RT	H-HOO KCAL/MOLE	CP CAL/MOLE-DEG	S0 CAL/MOLE-MOLE
100.	-11.027	0.497	4.968	26.881
200.	-12.760	0.994	4.968	30.324
300.	-1.773	1.490	4.968	32.359
400.	-14.493	1.987	4.968	33.768
500.	-15.051	2.484	4.968	34.876
600.	-15.506	2.981	4.968	35.782
700.	-15.892	3.478	4.968	36.548
800.	-16.226	3.974	4.968	37.211
900.	-16.520	4.471	4.968	37.797
1000.	-16.783	4.968	4.968	38.320
1200.	-17.239	5.962	4.968	39.226
1400.	-17.625	6.955	4.968	39.992
1600.	-17.958	7.949	4.968	40.655
1800.	-18.253	8.942	4.968	41.240
2000.	-18.516	9.936	4.968	41.764
2200.	-18.755	10.930	4.968	42.237
2400.	-18.972	11.923	4.968	42.669
2600.	-19.172	12.917	4.968	43.067
2800.	-19.357	13.910	4.968	43.435
3000.	-19.530	14.904	4.968	43.778
3500.	-19.915	17.388	4.968	44.544
4000.	-20.249	19.872	4.968	45.207
4500.	-20.544	22.356	4.968	45.792
5000.	-20.807	24.840	4.968	46.316
5500.	-21.045	27.324	4.968	46.789
6000.	-21.263	29.808	4.968	47.221
6500.	-21.463	32.292	4.968	47.619
7000.	-21.648	34.776	4.968	47.987
7500.	-21.821	37.260	4.968	48.339
8000.	-21.982	39.744	4.968	48.651
8500.	-22.134	42.228	4.968	48.952
9000.	-22.276	44.712	4.968	49.236
9500.	-22.412	47.196	4.968	49.504
10000.	-22.540	49.680	4.968	49.759
11000.	-22.778	54.648	4.968	50.233
12000.	-22.996	59.616	4.968	50.663
13000.	-23.196	64.584	4.968	51.063
14000.	-23.381	69.552	4.968	51.431
15000.	-23.554	74.520	4.968	51.774
16000.	-23.715	79.498	4.968	52.094
17000.	-23.866	84.456	4.968	52.395
18000.	-24.009	89.424	4.968	52.679
19000.	-24.144	94.392	4.968	52.948
20000.	-24.273	9.360	4.968	53.203
22000.	-24.511	109.296	4.968	53.676
24000.	-24.729	119.232	4.968	54.109
25000.	-24.929	129.168	4.968	54.506
29000.	-25.114	139.104	4.968	54.874
30000.	-25.286	149.040	4.968	55.217

*****PHYSICAL MODEL*****

T	(MUO-HOO)/RT	H-HCO KCAL/MOLE	H-HCO CAL./MOLE-DEG	CP CAL./MOLE-DEG	50 CAL./MOLE-DEG
100.	-9.928	C.497	4.968	24.698	24.698
200.	-11.661	0.994	4.968	28.141	28.141
300.	-12.675	1.490	4.968	30.155	30.155
400.	-13.394	1.987	4.968	31.585	31.585
500.	-13.952	2.484	4.968	32.693	32.693
600.	-14.458	2.981	4.968	33.509	33.509
700.	-14.793	3.478	4.968	34.365	34.365
800.	-15.127	3.974	4.968	35.028	35.028
900.	-15.421	4.471	4.968	35.613	35.613
1000.	-15.685	4.968	4.968	36.137	36.137
1100.	-16.141	5.962	4.968	37.043	37.043
1200.	-16.526	6.955	4.968	37.808	37.808
1300.	-16.860	7.949	4.968	38.472	38.472
1400.	-17.154	8.942	4.968	39.057	39.057
1500.	-17.418	9.936	4.968	39.580	39.580
1600.	-17.656	10.939	4.968	40.054	40.054
1700.	-17.873	11.923	4.968	40.486	40.486
1800.	-18.074	12.917	4.968	40.884	40.884
1900.	-18.259	13.910	4.968	41.252	41.252
2000.	-18.431	14.904	4.968	41.595	41.595
2100.	-18.817	17.388	4.968	42.361	42.361
2200.	-19.151	19.872	4.968	43.024	43.024
2300.	-19.445	22.356	4.968	43.609	43.609
2400.	-19.708	24.840	4.968	44.132	44.132
2500.	-19.947	27.324	4.968	44.606	44.606
2600.	-20.164	29.808	4.968	45.038	45.038
2700.	-20.364	32.292	4.968	45.436	45.436
2800.	-20.550	34.776	4.968	45.804	45.804
2900.	-20.722	37.260	4.968	46.147	46.147
3000.	-20.883	39.744	4.968	46.467	46.467
3100.	-21.035	42.228	4.968	46.769	46.769
3200.	-21.178	44.712	4.968	47.053	47.053
3300.	-21.313	47.196	4.968	47.321	47.321
3400.	-21.441	49.680	4.968	47.576	47.576
3500.	-21.583	54.648	4.968	48.053	48.053
3600.	-21.689	59.616	4.968	48.482	48.482
3700.	-21.897	64.584	4.968	48.879	48.879
3800.	-22.097	69.552	4.968	49.248	49.248
3900.	-22.282	74.520	4.968	49.590	49.590
4000.	-22.441	79.488	4.968	49.911	49.911
4100.	-22.689	84.456	4.968	50.212	50.212
4200.	-22.768	89.424	4.968	51.925	51.925
4300.	-22.911	119.232	4.968	50.496	50.496
4400.	-23.839	129.168	4.968	52.323	52.323
4500.	-23.046	94.392	4.968	50.765	50.765
4600.	-24.015	132.104	4.968	52.691	52.691
4700.	-24.188	149.040	4.968	53.034	53.034

ORIGINAL PAGE IS
OF POOR QUALITY

FIGURE 41
THERMAL PROPERTIES OF H₂O (H₂O = 511.720 KCAL/MOLE)

T	(MHO-HOO)/RT	H-HOO KCAL/MOLE	CAL/MOLE-DEG	CF CAL/MOLE-DEG	SO
100.	-13.249	0.696	6.955	33.284	
200.	-15.675	1.391	6.957	38.125	
300.	-17.095	2.088	7.004	40.932	
400.	-18.104	2.775	7.151	42.765	
500.	-18.892	3.521	7.365	44.583	
600.	-19.541	4.269	7.591	45.946	
700.	-20.096	5.039	7.797	47.132	
800.	-20.582	5.827	7.972	48.165	
900.	-21.017	6.632	8.118	49.133	
1000.	-21.470	7.450	8.237	49.995	
1200.	-22.100	9.116	8.415	51.513	
1400.	-22.694	10.812	8.537	52.820	
1600.	-23.216	12.529	8.622	53.966	
1800.	-23.683	14.260	8.684	54.985	
2000.	-24.105	16.001	8.730	55.907	
2200.	-24.491	17.751	8.765	56.736	
2400.	-24.845	19.507	8.792	57.500	
2600.	-25.174	21.267	8.813	58.205	
2800.	-25.480	23.032	8.830	58.859	
3000.	-25.766	24.799	8.844	59.468	
3500.	-26.411	29.228	8.870	60.834	
4000.	-26.974	33.668	8.897	62.019	
4500.	-27.474	38.114	8.898	63.067	
5000.	-27.925	42.565	8.906	64.005	
5500.	-28.334	47.020	8.913	64.854	
6000.	-28.709	51.478	8.917	65.630	
6500.	-29.055	55.937	8.921	66.344	
7000.	-29.376	60.398	8.924	67.005	
7500.	-29.676	64.861	8.926	67.621	
8000.	-29.957	69.325	8.928	68.197	
8500.	-30.222	73.789	8.930	68.738	
9000.	-30.472	78.254	8.931	69.249	
9500.	-30.709	82.720	8.932	69.731	
10000.	-30.933	87.187	8.933	70.190	
11000.	-31.352	96.121	8.935	71.041	
12000.	-31.735	105.056	8.936	71.819	
13000.	-32.088	113.993	8.937	72.534	
14000.	-32.415	122.950	8.932	73.196	
15000.	-32.720	131.869	8.938	73.813	
16000.	-33.006	140.807	8.939	74.390	
17000.	-33.275	149.746	8.939	74.832	
18000.	-33.528	158.686	8.940	75.443	
19000.	-33.769	167.625	8.940	75.926	
20000.	-33.996	176.565	8.941	76.385	
22000.	-34.419	184.446	8.941	77.237	
24000.	-34.807	212.327	8.941	78.015	
26000.	-35.163	230.209	8.941	78.730	
28000.	-35.493	248.092	8.941	79.393	
30000.	-35.801	265.974	8.941	80.010	

THERMAL PROPERTIES OF HE2 00* 413.650 KCAL/MOLE)

FIGURE 42

T	(MUG-HOO)/RT	H-HOO KCAL/MOLE	CAL/MOLE	CP CAL/MOLE-DEG	CAL/MOLE-DEG	SO
100.	-13.508	0.696	6.955	33.957	33.957	
200.	-16.014	1.391	6.956	38.778	38.778	
300.	-17.433	2.088	6.989	41.603	41.603	
400.	-19.442	2.792	7.108	43.628	43.628	
500.	-19.228	3.512	7.298	45.233	45.233	
600.	-19.875	4.252	7.511	46.583	46.583	
700.	-20.428	5.014	7.714	47.756	47.756	
800.	-20.911	5.794	7.892	48.798	48.798	
900.	-21.343	6.591	8.043	49.736	49.736	
1000.	-21.733	7.402	8.169	50.591	50.591	
1200.	-22.419	9.056	8.359	52.098	52.098	
1400.	-23.009	10.742	8.491	53.397	53.397	
1500.	-23.527	12.450	8.585	54.537	54.537	
1800.	-23.993	14.174	8.653	55.553	55.553	
2000.	-24.412	15.910	8.704	56.467	56.467	
2200.	-24.795	17.655	8.743	57.299	57.299	
2400.	-25.148	19.407	8.773	58.061	58.061	
2600.	-25.475	21.164	8.797	58.764	58.764	
2800.	-25.779	22.925	8.816	59.417	59.417	
3000.	-26.064	24.690	8.832	60.025	60.025	
3500.	-26.705	29.114	8.861	61.389	61.389	
4000.	-27.268	33.549	8.879	62.574	62.574	
4500.	-27.766	37.992	8.892	63.620	63.620	
5000.	-28.215	42.441	8.902	64.558	64.558	
5500.	-28.623	46.893	8.909	65.406	65.406	
6000.	-28.997	51.349	8.914	66.182	66.182	
6500.	-29.343	55.807	8.918	66.895	66.895	
7000.	-29.663	60.267	8.922	67.557	67.557	
7500.	-29.963	64.729	8.924	68.172	68.172	
8000.	-30.243	69.191	8.926	68.748	68.748	
8500.	-30.507	73.655	8.928	69.289	69.289	
9000.	-30.757	78.120	8.930	69.800	69.800	
9500.	-30.991	82.585	8.931	70.283	70.283	
10000.	-31.219	87.051	8.932	70.741	70.741	
11000.	-31.636	95.994	8.934	71.592	71.592	
12000.	-32.018	104.918	8.935	72.370	72.370	
13000.	-32.371	113.854	8.936	73.085	73.085	
14000.	-32.697	122.791	8.937	73.747	73.747	
15000.	-33.002	131.728	8.938	74.364	74.364	
16000.	-33.287	140.667	8.938	74.941	74.941	
17000.	-33.556	149.605	8.939	75.482	75.482	
18000.	-33.809	158.544	8.939	75.993	75.993	
19000.	-34.049	167.484	8.940	76.477	76.477	
20000.	-34.276	176.423	8.940	76.935	76.935	
22000.	-34.700	194.303	8.940	77.787	77.787	
24000.	-35.087	212.184	8.941	78.565	78.565	
26000.	-35.443	230.066	8.941	79.281	79.281	
28000.	-35.773	247.949	8.941	79.943	79.943	
30000.	-36.081	265.830	8.941	80.560	80.560	

ORIGINAL PAGE IS
OF POOR QUALITY

FIGURE 43
THERMAL PROPERTIES OF COC (HOO = 389.950 KCAL/MOLE)

*****PHYSICAL MODEL*****

FIGURE 43
389.950 KCAL/MOLE)

T	(MUO-HOO)/RT	H-HOO KCAL/MOLE	CP CAL/MOLE-DEG	CP CAL/MOLE-DEG	CP CAL/MOLE-DEG	CP CAL/MOLE-DEG
100.	-17.104	0.696	6.955	40.945	-16.915	0.599
200.	-19.539	1.391	6.955	45.066	-19.357	1.405
300.	-20.950	2.087	6.961	46.587	-20.795	2.120
400.	-21.957	2.785	7.003	50.594	-21.821	2.843
500.	-22.739	3.489	7.102	52.066	-22.621	3.573
600.	-23.381	4.207	7.248	53.473	-23.278	4.312
700.	-23.926	4.940	7.415	54.603	-23.837	4.422
800.	-24.402	5.690	7.583	55.604	-24.324	5.611
900.	-24.826	6.456	7.740	56.507	-24.756	6.572
1000.	-25.209	7.237	7.881	57.330	-25.144	7.340
1200.	-25.877	8.837	8.111	58.768	-25.820	8.637
1400.	-26.453	10.478	8.283	60.052	-26.398	10.483
1600.	-26.960	12.148	8.410	61.166	-26.904	12.095
1800.	-27.411	13.840	8.506	62.163	-27.354	13.734
2000.	-27.822	15.549	8.580	63.063	-27.760	15.399
2200.	-28.197	17.271	8.637	63.884	-28.131	17.099
2400.	-28.542	19.003	8.684	64.637	-28.473	18.803
2600.	-28.862	20.744	8.723	65.334	-28.790	20.541
2800.	-29.161	22.492	9.757	65.981	-29.086	22.304
3000.	-29.441	24.246	9.739	66.587	-29.363	24.089
3500.	-30.072	28.651	8.872	67.948	-29.992	28.653
4000.	-30.625	33.121	8.971	69.130	-30.547	33.359
4500.	-31.118	37.636	9.093	70.202	-31.046	38.204
5000.	-31.564	42.218	0.238	71.167	-31.500	43.191
5500.	-31.971	46.876	9.398	72.055	-31.918	48.326
6000.	-32.346	51.616	9.564	72.880	-32.306	53.614
6500.	-32.694	56.440	9.729	73.652	-32.669	59.066
7000.	-33.019	61.344	9.885	74.379	-33.010	64.696
7500.	-33.325	66.323	10.029	75.066	-33.334	70.519
8000.	-33.613	71.371	10.158	75.717	-33.642	76.554
8500.	-33.886	76.478	10.269	76.337	-33.936	82.825
9000.	-34.146	81.636	10.362	76.926	-34.219	89.356
9500.	-34.394	86.837	10.438	77.489	-34.492	96.181
10000.	-34.631	92.072	10.499	78.026	-34.756	103.326
11000.	-35.075	102.615	10.579	79.030	-35.262	118.744
12000.	-35.481	113.213	10.611	79.953	-35.746	135.944
13000.	-35.868	123.826	10.611	80.802	-36.215	155.373
14000.	-36.225	134.427	10.586	81.588	-36.673	177.380
15000.	-36.559	144.993	10.545	82.317	-37.127	202.625
16000.	-36.874	155.513	10.493	82.996	-37.561	231.682
17000.	-37.171	165.977	10.435	83.610	-38.039	265.240
18000.	-37.453	176.382	10.373	84.225	-38.506	304.069
19000.	-37.720	186.724	10.310	84.784	-38.985	349.023
20000.	-37.974	197.003	10.248	85.311	-39.480	401.040
22000.	-38.447	217.377	10.127	85.202	-40.534	530.472
24000.	-38.890	237.519	10.016	87.159	-41.696	701.731
25000.	-39.279	257.448	9.915	87.956	-42.996	925.769
28000.	-39.648	277.187	9.825	88.698	-44.463	1215.233
30000.	-39.999	296.756	9.745	89.363	-46.126	1584.565

THERMAL PROPERTIES OF AR#1 FILE 44
3= 266.350 KCAL/MOLE)

*****PHYSICAL MODEL*****

T	(MUO-HOO)/RT	H-HOO KCAL/MOLE	CAL/MOLE	CP CAL/MOLE-DEG	SO CAL/MOLE-DFC
100.	-15.171	0.497	4.968	35.116	
200.	-16.904	0.994	4.968	38.559	
300.	-17.918	1.490	4.968	40.574	
400.	-18.637	1.987	4.968	42.003	
500.	-19.195	2.484	4.968	43.111	
600.	-19.650	2.981	4.968	44.017	
700.	-20.036	3.478	4.968	44.783	
800.	-20.370	3.974	4.968	45.446	
900.	-20.664	4.471	4.968	46.032	
1000.	-20.927	4.965	4.968	46.555	
1200.	-21.383	5.962	4.968	47.461	
1400.	-21.769	6.955	4.968	48.227	
1600.	-22.102	7.949	4.968	48.890	
1800.	-22.397	8.942	4.968	49.475	
2000.	-22.660	9.936	4.968	49.999	
2200.	-22.899	10.930	4.968	50.472	
2400.	-23.116	11.923	4.968	50.904	
2600.	-23.316	12.917	4.968	51.302	
2800.	-23.501	13.910	4.968	51.670	
3000.	-23.674	14.904	4.968	52.013	
3500.	-24.059	17.388	4.968	52.779	
4000.	-24.393	19.872	4.968	53.442	
4500.	-24.688	22.356	4.968	54.027	
5000.	-24.951	24.840	4.968	54.551	
5500.	-25.189	27.324	4.968	55.024	
6000.	-25.407	29.808	4.968	55.456	
6500.	-25.607	32.292	4.968	55.854	
7000.	-25.792	34.776	4.968	56.222	
7500.	-25.965	37.260	4.968	56.565	
8000.	-26.126	39.744	4.968	56.886	
8500.	-26.278	42.228	4.968	57.187	
9000.	-26.421	44.712	4.968	57.471	
9500.	-26.556	47.196	4.968	57.739	
10000.	-26.684	49.680	4.968	57.994	
11000.	-26.922	54.648	4.968	58.468	
12000.	-27.140	59.616	4.968	58.900	
13000.	-27.340	64.584	4.968	59.298	
14000.	-27.525	69.552	4.968	59.666	
15000.	-27.698	74.520	4.968	60.009	
16000.	-27.859	79.488	4.968	60.329	
17000.	-28.010	84.456	4.968	61.911	
18000.	-28.153	89.424	4.968	62.344	
19000.	-28.289	94.392	4.968	62.741	
20000.	-28.417	99.360	4.968	63.109	
22000.	-28.655	109.296	4.968	63.452	
24000.	-28.873	119.232	4.968		
26000.	-29.073	129.168	4.968		
28000.	-29.258	139.104	4.968		
30000.	-29.430	149.040	4.968		

FIGURE 45 THERMAL PROPERTIES OF AR_n 00 = 267.970 KCAL/MOLE)

*****PHYSICAL MODEL*****

T	(MUG-MOO)/RT	H-HOO KCAL/MOLE	CAL/MOLE-DEG CAL/MOLE- η E _G	CP CAL/MOLE-DEG	CP CAL/MOLE- η E _G
100.	-15.171	4.97	4.968	4.968	35.116
200.	-16.904	0.994	4.968	4.968	36.559
300.	-17.918	1.490	4.968	4.968	40.574
400.	-18.637	1.987	4.968	4.968	42.003
500.	-19.195	2.484	4.968	4.968	43.111
600.	-19.650	2.981	4.968	4.968	44.017
700.	-20.036	3.478	4.968	4.968	44.793
800.	-20.370	3.974	4.968	4.968	45.016
900.	-20.664	4.471	4.968	4.968	46.032
1000.	-20.927	4.968	4.968	4.968	46.555
1200.	-21.383	5.962	4.968	4.968	47.461
1400.	-21.769	6.955	4.968	4.968	48.227
1600.	-22.102	7.949	4.968	4.968	49.090
1800.	-22.397	8.942	4.968	4.968	49.475
2000.	-22.660	9.936	4.968	4.968	49.999
2200.	-22.899	10.930	4.968	4.968	50.472
2400.	-23.116	11.923	4.968	4.968	50.904
2600.	-23.316	12.917	4.968	4.968	51.302
2800.	-23.501	13.910	4.968	4.968	51.670
3000.	-23.674	14.904	4.968	4.968	52.013
3500.	-24.059	17.388	4.968	4.968	52.779
4000.	-24.393	19.872	4.968	4.968	53.442
4500.	-24.688	22.356	4.968	4.968	54.027
5000.	-24.951	24.840	4.968	4.968	54.551
5500.	-25.189	27.324	4.968	4.968	55.024
6000.	-25.407	29.808	4.968	4.968	55.456
6500.	-25.607	32.292	4.968	4.968	55.854
7000.	-25.792	34.776	4.968	4.968	56.222
7500.	-25.905	37.260	4.968	4.968	56.565
8000.	-26.126	39.744	4.968	4.968	56.886
8500.	-26.278	42.228	4.968	4.968	57.187
9000.	-26.421	44.712	4.968	4.968	57.471
9500.	-26.556	47.196	4.968	4.968	57.739
10000.	-26.684	49.680	4.968	4.968	57.994
11000.	-26.922	54.648	4.968	4.968	58.468
12000.	-27.140	59.616	4.968	4.968	58.900
13000.	-27.340	64.584	4.968	4.968	59.298
14000.	-27.525	69.552	4.968	4.968	59.666
15000.	-27.698	74.520	4.968	4.968	60.009
16000.	-28.417	79.488	4.968	4.968	61.438
22000.	-28.655	109.296	4.968	4.968	61.911
24000.	-28.873	119.232	4.968	4.968	62.344
26000.	-29.073	129.168	4.968	4.968	62.741
28000.	-29.258	139.104	4.968	4.968	63.109
30000.	-29.430	149.040	4.968	4.968	63.452

ORIGINAL PAGE IS
OF POOR QUALITY

FIGURE 46 THERMAL PROPERTIES OF AR2C (HOO) 337.040 KCAL/MOLE)

*****PHYSICAL MODEL*****

T (MUO-HOO)/RT	H-HOO KCAL/MOLE	H-HOO CAL/MOLE	CP KCAL/MOLE-DEG	CP CAL/MOLE-DEG
100.	-20.789	C.801	8.737	49.326
200.	-23.661	1.685	8.889	55.445
300.	-25.398	2.576	8.918	59.056
400.	-26.647	3.468	8.929	61.624
500.	-27.624	4.361	8.934	63.617
600.	-28.426	5.255	8.936	65.246
700.	-29.106	6.149	8.938	66.623
800.	-29.697	7.042	8.939	67.817
900.	-30.219	7.936	8.940	68.870
1000.	-30.687	8.830	8.940	69.812
1200.	-31.498	10.618	8.941	71.442
1400.	-32.185	12.407	8.941	72.820
1600.	-32.781	14.195	8.942	74.014
1800.	-33.307	15.983	8.942	75.067
2000.	-33.778	17.772	8.942	76.009
2200.	-34.204	19.560	8.942	76.861
2400.	-34.594	21.348	8.942	77.640
2600.	-34.952	23.137	8.942	78.355
2800.	-35.254	24.925	8.942	79.018
3000.	-35.593	26.714	8.942	79.635
3500.	-36.284	31.185	8.942	81.013
4000.	-36.823	35.656	8.942	82.207
4500.	-37.411	40.127	8.942	83.261
5000.	-37.884	44.598	8.942	84.203
5500.	-38.312	49.069	8.942	85.055
6000.	-38.703	53.540	8.942	85.833
6500.	-39.062	58.012	8.942	86.549
7000.	-39.395	62.483	8.942	87.212
7500.	-39.705	66.954	8.942	87.829
8000.	-39.995	71.425	8.942	88.406
8500.	-40.267	75.896	8.942	88.948
9000.	-40.524	80.368	8.942	89.459
9500.	-40.767	84.839	8.942	89.943
10000.	-40.957	89.310	8.942	90.401
11000.	-41.426	98.252	8.942	91.253
12000.	-41.817	107.195	8.942	92.032
13000.	-42.177	116.137	8.942	92.747
14000.	-42.510	125.079	8.942	93.410
15000.	-42.820	134.022	8.942	94.027
16000.	-43.110	142.964	8.942	94.700
17000.	-43.393	151.907	8.942	95.452
18000.	-43.640	160.849	8.942	96.230
19000.	-43.883	169.791	8.942	96.141
22000.	-44.114	178.734	8.942	96.670
22000.	-44.542	196.619	8.942	97.452
24000.	-44.934	214.503	8.942	98.230
26000.	-45.294	232.378	8.942	98.946
28000.	-45.627	250.273	8.942	99.608
30000.	-45.937	268.158	8.942	100.225

ORIGINAL PAGE IS
OF POOR QUALITY

TABLE VII

Species	State	SPECTROSCOPIC DATA FOR MOLECULES						Source
		E_1 kcal/mole	σ	B_e cm^{-1}	α_e^{∞} cm^{-1}	ω_{∞}^e cm^{-1}	ω_{∞}^g cm^{-1}	
N_2	X $'\Sigma^+_g$	0.	2	1.99825	0.01791	2357.55	14.059	JANAF (ref. 5) Herzberg (ref. 8) Reference 8 Reference 8 Reference 8
	A $'\Sigma^+_g$	143.54						
	B $'\Pi_g^+$	170.48						
	C $'\Sigma^+_g$	171.55						
O_2	A $'\Pi_g$	198.11						Reference 5 Reference 8 Reference 8 Reference 8 Reference 8
	X $'\Sigma^-$	0.	2	1.445	0.0158	1580.246	12.071	
	A $'\Delta_u$	22.639						
	B $'\Sigma^+_u$	37.726						
NO	A $'\Sigma^+_u$	103.20						Reference 5 Reference 8 Reference 8 Reference 8 Reference 8
	B $'\Sigma^+_u$	142.39						
	C $'\Sigma^+_u$							
	D $'\Sigma^+_u$							
NO^+	X $'\Pi_g$	0	1	1.7042	0.0178	1903.60	13.97	Reference 5 Reference 8 Reference 8 Reference 8 Reference 8 Reference 8
	X $'\Pi_g$	0.346						
	A $'\Sigma^+_g$	125.70						
	B $'\Sigma^+_g$	131.32						
	C $'\Sigma^+_g$	149.10						
	D $'\Sigma^+_g$	151.77						
N_2^+	E $'\Sigma^+_g$	173.34						Reference 5 Predvoditelev (ref. 10) Reference 10 Reference 10
	X $'\Sigma^+_g$	0.	1	2.002	0.0202	2377.1	16.35	
	A $'\Pi_g$	106.						
	B $'\Sigma^+_g$	160.						
O_2^+	C $'\Pi_g$	200.						Reference 5 Reference 10 Reference 8 Reference 8
	X $'\Sigma^+_g$	0.	2	1.932	0.02	2191.02	13.19	
	A $'\Pi_g$	25.89						
	B $'\Sigma^+_g$	72.797						
CO_2	C $'\Sigma^+_g$	184.76						Reference 8 Reference 10 Reference 10 Reference 10
	X $'\Sigma^+_g$	{ 0. 558.	2	1.6722	0.01984	1859.87	16.53	
	A $'\Pi_u$	91206.						
	B $'\Sigma^+_g$	109760. 138860.						
CO_2	X $'\Sigma^+_g$	0.	2	0.39021	---	1388.17	---	Herzberg (ref. 11)
						667.40		
						667.40		
						2349.16		

**ORIGINAL PAGE IS
OF POOR QUALITY**

TABLE VII (CONCL'D)
SPECTROSCOPIC DATA FOR MOLECULES

Species	State	E^1 /mole kcal/mole	σ	B_e cm^{-1}	α_e cm^{-1}	ω_e cm^{-1}	$\omega_e \gamma_e$ cm^{-1}	Source
CO	X $^1\Sigma^+$	0.	1	1.930*	0.01746	2169.52	13.453	-----
	$\alpha' ^3\Pi_g$	139.20						Reference 5
	$\alpha' ^3\Sigma^+$	159.83						Reference 8
	$\alpha' ^3\pi_u$	178.12						Reference 8
CN	A $^1\pi_u$	186.055						Reference 8
	X $^1\Sigma^+$	0.	1	1.8989	0.0172	2068.61	13.114	-----
	A $^3\Pi_g$	26.069						Reference 5
	$\beta ^3\Sigma^+$	73.759						Reference 5
He ₂	X $^1\Sigma^+$	154.263						Reference 5
	$\alpha ^3\Sigma^+$	168.57						Reference 5
	$\alpha ^3\pi_u$	170.64						Reference 5
	$\beta ^3\pi_u$	174.23						Reference 5
He ₂ ⁺	X $^1\Sigma^+$	185.22						Reference 5
	$\alpha ^3\Sigma^+$	0.	2	7.211	0.224	1698.5	35	-----
	$\alpha ^3\pi_u$	0.*	2	7.710	0.243	1809.9	38.8	-----
	$\beta ^3\pi_u$	0.	2	7.211	0.224	1698.5	35	Ginter (ref. 9, 12)
He ₂ ⁺	X $^1\Sigma^+$	0.	2	7.211	0.224	1698.5	35	-----
	$\alpha ^3\Sigma^+$	0.*	2	7.710	0.243	1809.9	38.8	-----
	$\beta ^3\pi_u$	0.	2	7.211	0.224	1698.5	35	-----
CO ⁺	X $^1\Sigma^+$	0.	1	1.9772	0.01896	2214.24	15.164	-----
	A $^3\Pi_g$	59.278						Reference 8
	$\beta ^3\Sigma^+$	131.166						Reference 8
Ar ₂ ⁺	X $^1\Sigma^+$	0.	2	0.174	---	80.	---	Teng and Conway (ref. 13)
	$\alpha ^3\Sigma^+$	0.	2	0.174	---	80.	---	Teng and Conway (ref. 13)

*The excitation energy of the a state of He₂⁺ is included in the formation enthalpy.

to code failure or grossly inaccurate results. Since the thermo fit is not used in the helium and argon models, these models can be used at higher temperatures, up to the onset of significant second ionization.

4.3 Data for Reactions

Tables VIII, IX, X, and XI list the chemical reactions for which data have been compiled into the current version of NATA. These tables define the "master list of reactions". They also give the parameters A , η , and E_a in the curvefit*

$$k_f = A \left(\frac{T}{10,000^{\circ}\text{K}} \right)^\eta e^{-E_a/R_0 T} \quad (7)$$

to the forward rate constant k_f for each reaction. The reaction system for air (Table VIII) is one recommended recently by Cornell Aeronautical Laboratory (ref. 14). Those for argon and helium (Tables IX, X) are documented in Appendix A of the present report. The reactions for the carbon-containing species (Table XI) are from Dunn (ref. 15), except the CN reactions which are from McKenzie and Arnold (ref. 16).

The rate constants of interest in NATA applications are not accurately known. Experimental determinations of the rate for a given reaction at a given temperature typically differ by factors ranging from 2 up to an order of magnitude or more. In many cases, the temperature range over which the rate has been measured is considerably smaller than the range over which it is used in NATA. The extrapolation which is thus required is a further source of error. However, in spite of these uncertainties, calculations based on the reaction system for air (Table VIII) have given results in reasonable agreement with experimental data (ref. 14).

The main sources for the data in Table VIII are cited in reference 14. The reactions for the neutral species in high temperature air have been reviewed by Wray (ref. 17), those for the charged species by Dunn and Treanor (ref. 18).

*Equation (69) of Volume I.

ORIGINAL PAGE IS
OF POOR QUALITY

TABLE VIII
REACTION SYSTEM FOR AIR

Index (IR)	Reaction	A cm ³ /mole sec or cm ⁶ /mole ² -sec	γ	E_a cal/mole	Third Bodies (M)
1	$O_2 + N \rightleftharpoons 2 O + M$	3.6×10^{14}	-1	117980	$N, NO, Ar, C, CO, CN, CO_2$
2	$O_2 + O \rightleftharpoons 2 O + O$	9.0×10^{15}	-1	117980	
3	$O_2 + O_2 \rightleftharpoons 2 O + O_2$	3.2×10^{15}	-1	117980	
4	$O_2 + N_2 \rightleftharpoons 2 O + N_2$	7.2×10^{14}	-1	117980	
5	$N_2 + M \rightleftharpoons 2 N + M$	1.9×10^{15}	-0.5	225040	
6	$N_2 + N \rightleftharpoons 2 N + N$	4.1×10^{16}	-1.5	225040	
7	$N_2 + N_2 \rightleftharpoons 2 N + N_2$	4.7×10^{15}	-0.5	225040	
8	$NO + M \rightleftharpoons N + O + M$	3.9×10^{14}	-1.5	150050	O_2, N_2, Ar, CO, CO_2
9	$NO + M \rightleftharpoons N + O + M$	7.8×10^{14}	-1.5	150050	O, N, NO, C
10	$O + NO \rightleftharpoons N + O_2$	3.2×10^{13}	-1.	39150	
11	$O + N_2 \rightleftharpoons N + NO$	7×10^{13}	0.	75510	
12	$NO + e^- \rightleftharpoons N + O$	6.7×10^{15}	-1.5	0	
13	$O^+ + e^- \rightleftharpoons O + e^-$	2.2×10^{22}	-4.5	0	
14	$N^+ + e^- \rightleftharpoons N + e^-$	2.2×10^{22}	-4.5	0	
15	$O^+ + e^- \rightleftharpoons O + O$	8×10^{15}	-1.5	0	
16	$O_2 + O^+ \rightleftharpoons O + O_2^+$	7.8×10^{13}	0.5	0	
17	$N^+ + N_2^+ \rightleftharpoons N_2 + N^+$	7.8×10^{13}	0.5	0	
18	$N_2^+ + e^- \rightleftharpoons N + N$	1.5×10^{16}	-1.5	0	
19	$NO^+ + NO^+ + e^- \rightleftharpoons O_2 + N_2$	1×10^{14}	-2.5	0	
20	$NO^+ + e^- + N_2 \rightleftharpoons NO + N_2$	2.2×10^{16}	-2.5	0	
21	$NO + O^+ \rightleftharpoons O + NO^+$	1.5×10^{13}	0.	0	
22	$N_2^+ + O^+ \rightleftharpoons O + N_2^+$	3.4×10^{11}	-2.	45700	
23	$NO^+ + N^+ \rightleftharpoons N + NO^+$	4.8×10^{14}	0.	0	
24	$NO + O_2^+ \rightleftharpoons O_2 + NO^+$	1.8×10^{15}	0.5	0	
25	$O_2^+ + N^+ \rightleftharpoons O + NO^+$	1×10^{14}	0.	0	
26	$NO^+ + e^- + O_2 \rightleftharpoons NO + O_2$	8.8×10^{16}	-2.5	0	

ORIGINAL PAGE IS
OF POOR QUALITY

TABLE IX
REACTION SYSTEM FOR ARGON

Index (IR)	Reaction	A $\text{sec}^{-1}, \text{cm}^3/\text{mole}\cdot\text{sec}$, or $\text{cm}^6/\text{mole}^2\cdot\text{sec}^2$	η	E_a cal/mole	KTF*	BPAR*
76	$\text{Ar}^+ + 2e^- \rightleftharpoons \text{Ar}^*(m) + e^-$	3.64×10^{21}	-4.3	0.	2	
77	$\text{Ar}^+ + 2e^- \rightleftharpoons \text{Ar}^*(r) + e^-$	3.64×10^{21}	-4.3	0.	2	
78	$\text{Ar}^+ + e^- \rightleftharpoons \text{Ar}^*(m)$	8.22×10^{10}	-0.81	0.	2	
79	$\text{Ar}^+ + e^- \rightleftharpoons \text{Ar}^*(r)$	8.22×10^{10}	-0.81	0.	2	
80	$\text{Ar}^+ + e^- \rightleftharpoons \text{Ar}$	8.22×10^{10}	-0.81	0.	2	2×10^7
81	$\text{Ar}^{2+}(m) + e^- \rightleftharpoons \text{Ar} + e^-$	6.	-0.5	0.	4	
82	$\text{Ar}^{2+}(r) + e^- \rightleftharpoons \text{Ar} + e^-$	5.	0.5	0.	2	
83	$\text{Ar}^*(r) \rightleftharpoons \text{Ar} + h\nu$	7.2	0.	0.	2	
84	$\text{Ar}^*(r) + e^- \rightleftharpoons \text{Ar}^*(m) + e^-$	8.	0.	0.	5	
85	$\text{Ar}^*(m) + \text{Ar} \rightleftharpoons 2\text{Ar}$	1.	0.	0.	2	
86	$\text{Ar}^*(m) + 2\text{Ar} \rightleftharpoons 3\text{Ar}$	1.	0.	0.	1	
87	$\text{Ar}^*(r) + \text{Ar} \rightleftharpoons 2\text{Ar}$	8.7	0.	0.	1	
88	$\text{Ar}^*(r) + 2\text{Ar} \rightleftharpoons 3\text{Ar}$	3.5	0.	0.	1	
B9	$\text{Ar}^+ + 2\text{Ar} \rightleftharpoons \text{Ar}^2+ + \text{Ar}$	8.7	0.	0.	1	
90	$\text{Ar}^2+ + e^- \rightleftharpoons \text{Ar}^*(m) + \text{Ar}$	5.2	0.	-0.75	1	
91	$\text{Ar}^2+ + e^- \rightleftharpoons \text{Ar}^*(r) + \text{Ar}$	2.8	0.	-0.67	3	
92	$\text{Ar}^2+ + 2e^- \rightleftharpoons 2\text{Ar} + e^-$	2.8	0.	-0.67	3	
		2.	0.	-4.3	0.	2

*The various forward reaction rate constant formulas indexed by KTF are explained in Section 2.3 under Group 9.

TABLE X
REACTION SYSTEM FOR HELIUM

Index (IR)	Reaction	A $\text{cm}^3/\text{mole sec}$ or $\text{cm}^6/\text{mole}^2\text{sec}$	γ	E_a cal/mole	Third Bodies (M)
35	$e^- + He^+ + M \rightleftharpoons He(^3S) + M$	5.46×10^{21}	-4.3	0	e^-
36	$e^- + He^+ + M \rightleftharpoons He(^1S) + M$	1.82×10^{21}	-4.3	0	e^-
37	$e^- + He^+ \rightleftharpoons He(^3S)$	1.27×10^{11}	-0.81	0	
38	$e^- + He^+ \rightleftharpoons He(^1S)$	3.8×10^{10}	-0.85	0	
39	$He + He^+ \rightleftharpoons He_2^+ + N$	3.92×10^{16}	0.	0	He
40	$e^- + He_2^+ + M \rightleftharpoons He_2 + M$	1.54×10^{21}	-4.3	0	e^-
41	$e^- + He_2^+ + M \rightleftharpoons 2 He + M$	5.13×10^{20}	-4.3	0	e^-
42	$e^- + He_2^+ \rightleftharpoons He + He(^3S)$	2.26×10^{14}	0.	0	
43	$e^- + He_2^+ \rightleftharpoons He + (^1S)$	7.5×10^{13}	0.	0	
44	$He(^1S) + M \rightleftharpoons He(^3S) + M$	3.65×10^{16}	-0.5	0	e^-
45	$He(^3S) + M \rightleftharpoons He + M$	8×10^{14}	-0.25	1272	e^-
46	$He(^1S) + M \rightleftharpoons He + M$	8×10^{14}	-0.25	1272	e^-
47	$He(^1S) + M \rightleftharpoons He + M$	5.2×10^{10}	0.	1590	He
48	$He(^3S) + He(^3S) \rightleftharpoons e^- + He + He^+$	1.87×10^{15}	0.167	0	
49	$He(^3S) + He(^1S) \rightleftharpoons e^- + He + He^+$	5.05×10^{15}	0.167	0	
50	$He(^1S) + He(^1S) \rightleftharpoons e^- + He + He^+$	6.28×10^{15}	0.167	0	
51	$He + He(^3S) + M \rightleftharpoons He_2 + M$	5.2×10^{14}	0.5	0	He
52	$He_2 + He_2 \rightleftharpoons e^- + 3 He + He^+$	1.87×10^{15}	0.167	0	
53	$He_2 + M \rightleftharpoons 2 He + M$	8×10^{14}	-0.25	1272	e^-

**ORIGINAL PAGE IS
OF POOR QUALITY**

TABLE XI.
REACTION SYSTEM FOR CARBON AND ARGON SPECIES IN THE PLANETARY ATMOSPHERE MODELS

Index (IR)	Reaction	A cm ³ /mole sec or cm ⁶ /mole ² sec	η	E _a cal/mole	Third Bodies
54	CO + M \rightleftharpoons C + O + M	4.48 \times 10 ¹⁵	-1.0	256000	N, O, Ar, N ₂ , O ₂ , CO, CN, C
55	CO ₂ + M \rightleftharpoons O + CO + M	8.81 \times 10 ¹⁴	-2.0	125600	N, O, Ar, N ₂ , O ₂ , CO, CN, C
56	CO + CO \rightleftharpoons C + CO ₂	2.33 \times 10 ¹¹	0.5	130500	
57	O + CO \rightleftharpoons C + O ₂	2.73 \times 10 ¹³	0.5	138100	
58	CO + N \rightleftharpoons NO + C	2.86 \times 10 ¹³	0.5	106500	
59	NO + CO \rightleftharpoons CO ₂ + N	4.59 \times 10 ¹⁰	0.5	23970	
60	CO ₂ + O \rightleftharpoons O ₂ + CO	2.55 \times 10 ¹¹	0.5	7606	
61	CO + CO ⁺ \rightleftharpoons CO ₂ + C ⁺	1.07 \times 10 ¹⁴	0.5	67050	
62	CO + C ⁺ \rightleftharpoons C + CO ⁺	6.03 \times 10 ¹³	0.5	63360	
63	O + C ⁺ \rightleftharpoons C + O ⁺	6.66 \times 10 ¹⁴	0.5	54160	
64	CO + O ⁺ \rightleftharpoons O + CO ⁺	1.09 \times 10 ¹⁴	0.5	9222	
65	O + CO ⁺ \rightleftharpoons O ₂ + C ⁺	5.47 \times 10 ¹⁴	0.5	74700	
65	CO ⁺ + e ⁻ \rightleftharpoons C + O	1.5 \times 10 ¹⁶	-1.5		
67	C ⁺ + 2e ⁻ \rightleftharpoons C + e ⁻	2.2 \times 10 ²²	-4.5	0	
68	CO + NO ⁺ \rightleftharpoons CO ⁺ + NO	4.59 \times 10 ¹⁴	0.5	109600	
69	CO + O ² \rightleftharpoons CO ⁺ + O ₂	4.53 \times 10 ¹⁴	0.5	44490	
70	C + NO ₂ \rightleftharpoons CO ⁺ + N	5.96 \times 10 ¹⁴	0.5	3227	
71	Ar ⁺ + 2e ⁻ \rightleftharpoons Ar + e ⁻	2.2 \times 10 ²²	-4.5	0	
72	CN + M \rightleftharpoons C + N + M	3.6 \times 10 ¹⁵	-1.0	131160	
73	CO + N \rightleftharpoons CN + O	4.3 \times 10 ¹⁴	0.5	69670	
74	N ₂ + C \rightleftharpoons CN + N	1.5 \times 10 ¹³	0.5	57670	
75	CN + O \rightleftharpoons C + NO	2 \times 10 ¹⁴	1.0	55640	

In Table VIII, the reactions given in reference 14 have been rearranged to place the reactions having the same effect (e.g., dissociation of O_2) together, and to place the reactions involving only neutral species ahead of those involving charged species. Reference 14 gives both forward and backward rates for each reaction. In each case, the rate coefficient in one direction is based directly on chemical kinetic data, while that in the other direction is a curvefit to the results of calculations based on equation (62) of Volume I. In Table VIII, the reactions have been written in such a form that the rate based on experimental data is in the forward direction. In NATA, the backward rate is computed internally using equation (62) of Volume I.

The reaction rate data summarized in Tables VIII to XI are stored in an array RPRP(I,IR), contained in common block /REAC/. This array is dimensioned (29,92). The entries in this array are defined as follows, for the reaction with index IR in the master list of reactions:

RPRP(I,IR)	I = 1	Coefficient A in eq. (7) (cm^3 mole sec or $cm^6/mole^2$ sec)
	I = 2	Exponent η in eq. (7)
	I = 3	Activation energy E_a in eq. (7), cal/mole
	I = 4	QQ: 1.0 if a third-body list is provided in I = 20-29 0.0 if not
	*I = 5	Number of reactant species (≤ 3)
	*I = 6	Number of product species (≤ 3)
	*I = 7-9	Indices of reactant species in master list of species
	*I = 10-12	Indices of product species in master list of species

*All values in the array are real. The values indicated by asterisks are converted by the program into integers. To ensure rounding down to the correct value, the stored values have been increased by 0.1

$I = 13-15$	Numbers of molecules of reactants
$I = 16-18$	Numbers of molecules of products
$*I = 19$	Number of third bodies (≤ 10)
$*I = 20-29$	Indices of third body species in master list of species

For convenience in adding to or altering the compiled-in data, RPRP is equivalence to 92 singly dimensioned arrays of dimension (29), as follows:

RPl(I)	Equivalent to RPRP (I,1)
.	.
.	.
.	.
RP92(I)	Equivalent to RPRP(I,92)

4.4 Electronic Nonequilibrium Data

When an ionized gas expands to low density, as in the diverging nozzle section of an arc-heated wind tunnel, a condition of nonequilibrium between the electron temperature and the heavy-particle temperature develops. This phenomenon is a result of the smallness of the cross section for elastic energy transfer between electrons and heavy particles. At high gas densities, there are enough collisions to keep the two temperatures approximately in equilibrium in spite of the small cross section; but at low densities this is no longer true. In an expanding plasma flow, electron-ion recombination processes supply energy to the electron gas, so that the electron temperature normally falls more slowly than the gas temperature.

The forward rate for a reaction which includes the electron, as either a reactant or a third body, usually depends upon the electron temperature rather than the gas temperature. Thus, thermal nonequilibrium between the electrons and the heavy particles can affect the rates of production and destruction of species. This phenomenon is not considered in the current NATA models for air. It has been studied, for the case of an atomic

nitrogen plasma, by Bowen and Park (ref. 19). Nonequilibrium between the electron and gas temperatures is included explicitly in the NATA models for helium and argon (Volume I, Sec. 7.1.2). These noble gas models require additional data for each reaction to specify the dependence of the forward and backward rate constants upon the electron and gas temperatures and to specify the partition of the energy of reaction between electron kinetic energy and radiative losses. Data are also required to provide the elastic collision cross section between the electrons and the neutral heavy particles (assumed to be the same for all neutral species). These extra data for the thermal nonequilibrium models are stored in an array TNEP(I,INT), contained in common block /TNE/. This array is dimensioned (186,2). The index INT specifies the gas model in which the data are to be used. For helium, INT = 1, and for argon, INT = 2. The entries in TNEP(I,INT) are defined below in terms of the reaction index JR for whichever gas model is being used. The index JR runs from 1 up to ISR. The dimensioning of TNEP allows the number of reactions ISR to be as high as 25 for gas models involving electronic nonequilibrium. For conventional gas models, ISR can be as high as 64.

The entries in TNEP(I,INT) are defined as follows:

*I = JR KTF(JR), indicator of type of formula for forward rate constant for the JRth reaction:

KTF = 1 k_f given by (7) as a function of gas temperature T

KTF = 2 k_f given by (7) as a function of electron temperature T_e

KTF = 3 $k_f = A (T_e/10^4)^{\eta} (1 - e^{-E_a/R_0 T})$

KTF = 4 $k_f = A (T_e/10^4)^{\eta} / \max(1, \tau)$
 where $\tau = b n_p R/N_0$

KTF = 5 $k_f = A/\sqrt{R}$

Note: R denotes the local nozzle radius (or a corresponding effective value in the case of a channel). Also, n_p is the number density of the atomic species appearing on the product side of the reaction, and b is a coefficient stored as BPAR (below). The types KTF = 3, 4, and 5 are used only in the model for argon (IGAS = 3); see Appendix A.

*All values in the array are real. The values indicated by asterisks are converted by the program into integers. To ensure rounding down to the correct value, the stored values have been increased by 0.1.

*I = JR + 25	KTR(JR), equal to 0 if the backward rate constant $k_r = 0$ for the JRth reaction; equal to 1 if $k_r = k_r(T)$; equal to 2 if $k_r = k_r(T_e)$, where the functional dependence is given by equations (277-278) of Vol. I (ref. 1).
*I = JR + 50	ITR(JR), indicator of rule for partitioning the reaction energy for the JRth reaction. In the definitions below, ϵ_f and $-\epsilon_r$ denote the energies gained by the electron gas in N_0 reactions in the forward and reverse directions, respectively, and q_f , $-q_r$ denote the corresponding energies lost by radiation. Also N_0 = Avogadro's number.
ITR = 1	$\epsilon_f = -a R_0 T_e$ $q_f = \epsilon_0 - \epsilon_f$ $\epsilon_r = q_r = 0$
ITR = 2	$\epsilon_f = -\frac{3}{2} R_0 T_e$ $q_f = \epsilon_0 - \epsilon_f$ $\epsilon_r = q_r = 0$
ITR = 3	$\epsilon_f = q_f = \epsilon_r = q_r = 0$
ITR = 4	$\epsilon_f = \epsilon_r = -\frac{3}{2} R_0 T_e$ $q_f = q_r = 0$
ITR = 5	$\epsilon_f = \epsilon_r = \epsilon_0$ $q_f = q_r = 0$
ITR = 6	$q_f = \epsilon_0$ $\epsilon_f = \epsilon_r = q_r = 0$

*All values in the array are real. The values indicated by asterisks are converted by the program into integers. To ensure rounding down to the correct value, the stored values have been increased by 0.1.

I = JR + 75 EPAR(1,JR), parameter ϵ_0 for the JRth reaction
 (cal per N_0 reactions)

 I = JR + 100 EPAR(2,JR), parameter "a" for the JRth reaction
 if ITR(IR) = 1

 I = 126-155 TLIST(J), temperature values for table of elastic
 collision cross section, $\bar{Q}^{(1,1)}$ (see Appendix A)

 I = 156-185 PØM(J), $\bar{Q}^{(1,1)}$ values for table

 I = 186 BPAR, parameter b for all reactions with KTF = 4

For convenience in adding to or altering the compiled-in data for reactions involving electronic nonequilibrium, TNEP is equivalenced to two singly dimensioned arrays of dimension (186), as follows:

TN1(K) Equivalent to TNEP(K,1)
 TN2(K) Equivalent to TNEP(K,2)

Tables XII through XV summarize the precoded electronic non-equilibrium data for the helium and argon models (IGAS = 4 and 3). The data in these tables are documented in Appendix A.

TABLE XII
ELECTRONIC NONEQUILIBRIUM DATA FOR HELIUM MODEL

JR	IR	KTF(JR)	KTR(JR)	ITR(JR)	EPAR(1,JR) cal/mole
1	35	2	2	5	109890
2	36	2	2	5	91540
3	37	2	0	2	109890
4	38	2	0	2	91540
5	39	1	1	3	0
6	40	2	2	5	98040
7	41	2	2	5	458270
8	42	2	1	4	0
9	43	2	1	4	0
10	44	2	2	5	18350
11	45	2	2	5	456730
12	46	2	2	5	475080
13	47	1	0	6	475080
14	48	1	2	5	346840
15	49	1	2	5	365190
16	50	1	2	5	383540
17	51	1	1	3	0
18	52	1	2	5	260350
19	53	2	2	5	413480

TABLE XIII
ELECTRONIC NONEQUILIBRIUM DATA FOR ARGON MODEL

JR	IR	KTF (JR)	KTR (JR)	ITR (JR)	EPAR(1,JR) cal/mole	EPAR(2,JR)	BPAR
1	76	2	2	5	96970	0	-
2	77	2	2	5	95360	0	-
3	78	2	0	1	96970	0.7	-
4	79	2	0	1	95360	0.7	-
5	80	4	0	1	363330	1.0	2×10^7
6	81	2	2	5	266350	0	-
7	82	2	2	5	267970	0	-
8	83	5	0	6	267970	0	-
9	84	2	2	5	1600	0	-
10	85	1	1	3	0	0	-
11	86	1	0	6	226000	0	-
12	87	1	1	3	0	0	-
13	88	1	0	6	226000	0	-
14	89	1	1	3	0	0	-
15	90	3	2	5	70680	0	-
16	91	3	2	5	69070	0	-
17	92	2	2	5	337040	0	-

TABLE XIV
 e^- - He MOMENTUM TRANSFER CROSS SECTION

T_e °K	$\frac{\bar{\sigma}}{A^2}$ $(1,1)$	T_e °K	$\frac{\bar{\sigma}}{A^2}$ $(1,1)$
0	0.00	9000	6.80
100	5.00	10000	6.77
200	5.59	12000	6.57
400	5.83	14000	6.55
600	5.99	16000	6.42
800	6.11	18000	6.29
1000	6.21	20000	6.15
1500	6.39	25000	5.80
2000	6.51	30000	5.46
3000	6.67	35000	5.14
4000	6.76	40000	4.85
5000	6.81	45000	4.60
6000	6.84	50000	4.32
7000	6.84	70000	3.4
8000	6.83	100000	2.4

TABLE XV
 e^- -Ar MOMENTUM TRANSFER CROSS SECTION

T_e $^{\circ}\text{K}$	$\bar{Q}^{(1,1)}$ A^2	T_e $^{\circ}\text{K}$	$\bar{Q}^{(1,1)}$ A^2
0	10.	2500	0.51
25	10.	4000	0.98
50	6.	6000	1.69
100	3.57	8000	2.40
200	2.12	10000	3.08
300	1.39	12000	3.73
400	0.97	15000	4.65
600	0.57	20000	6.02
800	0.40	25000	7.19
900	0.35	30000	8.11
1000	0.32	35000	8.81
1200	0.29	40000	9.30
1400	0.29	45000	9.63
1600	0.31	50000	9.82
2000	0.38	100000	10.

4.5 Standard Gas Models

A "gas model" is the specification of a set of species with their thermochemical properties, a system of reactions among these species with their rate constants, and other data. The NATA code contains provisions for invoking certain standard gas models by input of a single index value, IGAS. The standard gas models available are summarized in Table XVI. The third and fourth columns in this table specify the pair of species whose binary diffusion coefficient is used in computing the Lewis number. The variable INT pertains to the treatment of electronic nonequilibrium in the model. For INT = 0, electronic nonequilibrium is neglected. For INT > 0, electronic nonequilibrium is taken into account, and INT is the index for selecting the reaction parameters from TNEP(I,INT). If the indicator LEWIS is equal to 1, the Fay-Riddell Lewis number factor is used in calculating the stagnation point heat flux. For LEWIS = 2, it is not. The reaction indices in Table XVI refer to the master list of reactions.

AIR-1 is the general model for argon-free air, suitable for use in cases with reservoir temperatures up to about 15,000-20,000°K. Temperatures above 15000°K are beyond the range of validity of the thermo fits for the diatomic molecules. Above 20,000°K, the specific heats for some of these species (as computed from the thermo fit) go negative, and the chemical potentials begin to decrease with increasing temperature. However, the temperature capability of the AIR-1 model appears more than adequate for describing the flow in state-of-the-art arc heated wind tunnels.

AIR-2 is a truncated air model obtained from AIR-1 by deleting all of the ion species except NO⁺. It is suitable for use in cases with reservoir temperatures up to about 6000°K. The ion NO⁺ is retained because the ionization potential of NO (9.5 ev) is much lower than those of the other neutral species in high temperature air (12.5-15.5 ev). In problems with reservoir temperatures below 6000°K, use of the AIR-2 model in place of AIR-1 economizes on computer time without significantly affecting the results.

HELIUM and ARGON are the electronic nonequilibrium models for helium and argon. Since the thermo fit is not used in these models, they are suitable for use up to temperatures at which the doubly ionized species He⁺⁺ and Ar⁺⁺ become important.

ORIGINAL PAGE IS
OF POOR QUALITY

TABLE XVI.
STANDARD GAS MODELS

IGAS	Model Name	Atom for Le	Molecule for Le	INT	LEWIS	Cold Species (Mole Fractions)	Species	Reactions
1	AIR-1	O	N ₂	0	1	N ₂ (0.78823)	O ₂ (0.21177)	e ⁻ , N ₂ , O ₂ , N, O, NO, NO ⁺ , N ⁺ O ⁺ , N ₂ ⁺ , O ₂ ⁺
2	AIR-2	O	N ₂	0	1	N ₂ (0.78823)	O ₂ (0.21177)	e ⁻ , N ₂ , O ₂ , N, O, NO, NO ⁺
3	ARGON	Ar ⁺	Ar	2	2	Ar (1.0000)	e ⁻ , Ar, Ar ⁺ , Ar ⁴ , Ar ^{*(r)} , Ar ₂	76-92
4	HELIUM	He ⁺	He	1	2	He (1.0000)	e ⁻ , He, He(¹ S), He ⁽² S), He ₂ , He ₂ ⁺	35-53
5	CONAR	O	CO	0	2	CO ₂ (0.75)	Ar (0.20) (0.05)	e ⁻ , Ar, CO ₂ , N ₂ , O ₂ , N, O, NO, CO, CN, C, NO ⁺ , N ⁺ , O ⁺ , N ₂ ⁺ , O ₂ ⁺ , C ⁺ , Ar ⁺ , CO ⁺
6	CONAR2	O	CO	0	2	CO ₂ (0.75)	Ar (0.20) (0.05)	e ⁻ , Ar, CO ₂ , N ₂ , O ₂ , N, O, NO, CO, CN, C, NO ⁺ , C ⁺ , CO ⁺
								1-12, 19-20 26, 54-62, 65-68, 70, 72-75

CONAR* is a model for a planetary atmosphere containing 75 mole percent CO₂, 20 mole percent argon, and 5 mole percent N₂. These mole fractions can be adjusted easily in the code input, so that CONAR is usable as a general CO₂-Ar-N₂ model for the atmospheres of Venus and Mars.

CONAR2 is a smaller version of CONAR with some of the ion species omitted, designed for use at temperatures up to 7000°K. In this temperature range, it gives practically the same results as CONAR with less expenditure of computer time.

The data required for generating these standard gas models are stored in an array GPRP(I,IGAS), which is contained in common block /MIXT/. This array is dimensioned (124,6). Its entries are defined as follows, for the model with index IGAS:

I = 1	Mixture name
**I = 2	Number of elements in mixture (ISC)
**I = 3	Number of species in mixture (ISS)
**I = 4	Number of reactions included (ISR)
**I = 5	Number of ion species (IC)
**I = 6-15	Indices (IE) of elements in master list of elements
I = 16-25	Mole fractions of cold species (QPJ)
**I = 26-45	Indices (IS) of species in master list of species
**I = 46-109	Indices (IR) of reactions in master list of reactions
**I = 110-119	Indices (JCS) of cold species in master list of species
**I = 120	Number of cold species (NCS)

*Acronym for Carbon-Oxygen-Nitrogen-Argon.

**All values in the array are real. The values indicated by asterisks are converted by the program into integers. To ensure rounding down to the correct value, the stored values have been increased by 0.1.

- *I = 121 Atom index (ISATØM) for Lewis number in master list of species
- *I = 122 Molecule index (ISMØL) for Lewis number in master list of species
- *I = 123 INT. If INT = 0, electron temperature equals gas temperature. If INT > 0, the model includes electronic nonequilibrium, and INT is the index of extra reaction properties required in TNEP(I,INT)
- *I = 124 Indicator (LEWIS) for inclusion (1) or exclusion (2) of Fay-Riddell Lewis number factor in stagnation point heat flux.

Most of these definitions are self explanatory. However, the reference to "cold species" requires some discussion. In NATA, the overall composition of the gas in terms of the chemical elements is specified by giving the composition of the cold gas mixture which is fed into the arc heater. The chemical species in this cold gas are called cold species. For example, the cold species in argon-free air are N₂ and O₂, and their mole fractions are assumed to be 0.78823 and 0.21177, respectively. The weight fractions of the elements nitrogen and oxygen, which are determined by these data, are invariant under all chemical changes in the system.

For convenience in adding to or altering the compiled-in gas models, GPRP is equivalenced to 6 singly dimensioned arrays of dimension (124) as follows:

GP1(I)	Equivalent to GPRP(I,1)
.	.
.	.
.	.
GP6(I)	Equivalent to GPRP(I,6)

4.6 Transport Cross Section Data

The cross section data required for calculating the transport properties of arbitrary mixtures of the standard species (listed in Section 4.2) are compiled into NATA. The methods used in the transport property calculations have been explained in Section 3 of Volume I (ref. 1). Briefly, the transport coefficients are computed from formulas involving the cross sections

$\bar{\Omega}_{ij}^{(1,1)}$, $\bar{\Omega}_{ij}^{(2,2)}$, and $B^* \bar{\Omega}_{ij}^{(1,1)}$ for collisions between pairs of species (i,j) . These cross sections are calculated in a series of steps. First, the cross sections for all pairs are set to zero. Then, in each step, the values of $\bar{\Omega}_{ij}^{(1,1)}$, $\bar{\Omega}_{ij}^{(2,2)}$, and $B^* \bar{\Omega}_{ij}^{(1,1)}$ are computed by a particular method (or "option") with a particular set of parameter values, and these values are added to the corresponding cross sections for each pair of species to which the step is applicable. The information concerning the applicability of steps to species pairs is stored in index arrays KKQ(M), NNQ(M), as explained below. If only one step of the cross section calculation is applicable to a particular species pair, then the cross sections for the pair are the values computed during that step. If two or more steps are applicable to the pair, the cross sections for the pair are built up by adding contributions from the different steps. If the cross sections are poorly known for several minor pairs of species, but are considered likely to be roughly the same for all pairs, then the cross sections for all of these pairs can be set in a single step.

In the present section, the twelve options for calculating cross sections are defined, and the default methods used by the code to determine unspecified cross sections are explained. The variables and arrays used to store the precoded transport cross section data are then defined. Finally, the precoded data for the standard species are tabulated and documented as to source.

The options for calculating cross sections are selected by an index KKQ. For each option, there is an associated list of input parameters, VV(J). Array dimensions limit the number of these parameters to five. Other numerical data required by some of the options are stored at specified locations in four arrays (TL, ØMEGAL, ASTAR, BSTAR), as explained below. Each of these arrays is dimensioned (1000). The cross section options available in NATA are as follows:

KKQ = 2 Coulomb Cross Sections

Here

$$\begin{aligned}\bar{\Omega}_{ij}^{(1,1)} &= 0.8 VV(1) Q_C \\ \bar{\Omega}_{ij}^{(2,2)} &= VV(2) \bar{\Omega}_{ij}^{(1,1)} \\ B^* &= 1.5625\end{aligned}\tag{8}$$

where Q_C is defined by

$$Q_C = \left(\frac{e^2}{kT}\right)^2 \ln (\gamma \Lambda) \quad (9a)$$

$$\Lambda = \frac{3}{2} \frac{(kT)^{3/2}}{e^3 (\pi n_e)^{1/2}} \quad (9b)$$

$$\gamma = \left[1 + \frac{64\pi}{9} \frac{e^2}{kT} n_e^{1/3} \right]^{\frac{1}{2}} \quad (9c)$$

(Section 3.2 of Volume I). In equations (9), e denotes the electron charge, k Boltzmann's constant, T the absolute temperature and n_e the electron density.

KKO = 3 Exponential Potential

In this option, the cross sections are obtained from Manchick's (ref. 20) tabulated collision integrals for the exponential potential

$$\phi = Ae^{-r/\rho} \quad (10)$$

which are compiled into NATA in the TL, ØMEGAL, ASTAR, and BSTAR arrays starting at location 1 in each array. The parameters are

$$\begin{aligned} VV(1) &= A/k \text{ in } {}^\circ\text{K} \\ VV(2) &= \rho \text{ in } \text{\AA} \end{aligned} \quad (11)$$

VV(3) = 1.0 = position of first entry in tabulated collision integrals

KKO = 4 Charge Exchange Cross Section

In this option, $\bar{\Omega}^{(1,1)}$ and B^* are calculated for a resonant charge exchange cross section of the form

$$Q_{ex} = (A - B \log_{10} v)^2$$

where v is the relative velocity in cm/sec. $\bar{\Omega}^{(2,2)}$ is not calculated in this option. The required input parameters are

VV(1) = A in Å^0
VV(2) = B in Å^0
VV(3) = molecular weight of atom
VV(4) = control parameter

(12)

For $VV(4) > 0.$, the computed cross sections $\bar{\Omega}^{(1,1)}$ and B^* replace those computed in earlier steps of the calculations, while for $VV(4) \leq 0.$, they are added to the earlier values.

KKO = 5 Tabulated Cross Section

In this option, the cross section data are given in tabular form as a function of temperature. The input parameters are

VV(1) = A = factor by which the tabulated values must be multiplied to give the collision integrals in Å^2
VV(2) = I = position of first entry in tabulated cross section data
VV(3) = N = number of entries in cross section table

The cross section data themselves are stored in the TL, OMEGAI, ASTAR, and BSTAR arrays, starting at element I, as follows:

TL(I) to TL(I - 1 + N) = temperatures at which cross section data are tabulated in $^\circ\text{K}$. Values must be in order of increasing temperature.
OMEGAI(I to I - 1 + N) = values of $\bar{\Omega}^{(1,1)}$ at the tabulated temperatures
ASTAR(I to I - 1 + N) = values of $\bar{\Omega}^{(2,2)}$ at the tabulated temperatures

BSTAR(I to I - 1 + N) = values of E* at the tabulated temperatures

KKQ = 6 Power Law Potential

This option calculates cross sections for an inverse power potential,

$$\phi = Ar^{-\eta} \quad (13)$$

based on the analysis of Kihara, Taylor, and Hirschfelder (ref. 21). The parameters are

VV(1) = ITL = index in ØMEGAL, ASTAR, BSTAR arrays where data are stored

VV(2) = η

For each value of η used, the following additional data are stored:

$$\phi_{MEGAL}(ITL) = \pi \Gamma(3 - \frac{2}{\eta}) \eta^{2/\eta} A^{(1)}(\eta) \left| \frac{A}{k} \right|^{2/\eta} \quad (14a)$$

$$ASTAR(ITL) = (\frac{3}{2} - \frac{1}{\eta}) A^{(2)}(\eta) / A^{(1)}(\eta) \quad (14b)$$

$$BSTAR(ITL) = (1 - \frac{2}{3\eta}) (1 + \frac{2}{\eta}) \quad (14c)$$

where A/k is in °K, $A^{(1)}(\eta)$ and $A^{(2)}(\eta)$ are tabulated functions which are given for both attractive and repulsive potentials in reference 21, and Γ denotes the gamma function.

KKQ = 8 Lennard-Jones (6-12) Potential

This option calculates cross sections for the Lennard-Jones (6-12) potential,

$$\phi(r) = 4 \epsilon \left[\left(\frac{\sigma}{r} \right)^{12} - \left(\frac{\sigma}{r} \right)^6 \right] \quad (15)$$

The parameters are

$$VV(1) = \epsilon/k \text{ in } {}^\circ\text{K}$$

$$VV(2) = \sigma \text{ in } \text{\AA}$$

$$VV(3) = 501.$$

Tabulated collision integrals for the Lennard-Jones potential are compiled into the code in the TL, ØMEGAL, ASTAR, and BSTAR arrays, starting at location 501.

KKQ = 9 Scaling of Previously Computed Cross Sections for Other Species

This option allows cross sections calculated for one pair of species to be used also for other species, possibly with a constant multiplying factor. The cross sections are calculated from the formulas

$$\begin{aligned}\bar{\Omega}^{(1,1)} &= c_1 \bar{\Omega}_{ij}^{(1,1)} \\ \bar{\Omega}^{(2,2)} &= c_1 c_2 \bar{\Omega}_{ij}^{(2,2)} \\ B^* &= c_3 B_{ij}^*\end{aligned}\tag{16}$$

where the c_k are constant factors and the subscript ij indicates cross sections calculated previously for the pair (i,j) . The parameters for the option are

VV(1) = i = first index of previously calculated cross section

VV(2) = j = second index of previously calculated cross section

VV(3) = c_1

VV(4) = c_2

VV(5) = c_3

KKQ = 10 Empirical Mixing Rule

This option calculates the cross sections for a pair of unlike species i, j ($i \neq j$) from the empirical mixing rule

$$\bar{\Omega}_{ij}^{(l,s)} = \frac{1}{4} \left[\sqrt{\bar{\Omega}_{ii}^{(l,s)}} + \sqrt{\bar{\Omega}_{jj}^{(l,s)}} \right]^2 \quad (17)$$

The values calculated from (17) are then added to the previously calculated cross sections for the pair. This option uses no VV parameters.

KKQ = 11 Fairing Option

This option modifies the previously calculated cross value for a species pair according to the formula

$$\bar{\Omega}_{\text{new}}^{(l,s)} = f(T) \bar{\Omega}_{\text{old}}^{(l,s)} \quad (18a)$$

where $f(T)$ is a linear fairing factor given by

$$f(T) = \max \left[0, \min \left(1, \frac{T-T_0}{T_1-T_0} \right) \right] \quad (18b)$$

Use of this option thus permits different forms to be used for the cross section in different parts of the temperature range, with a smooth transition between them. The parameters are

VV(1) = T_0 = temperature at which the $\bar{\Omega}$ are to be set to zero

VV(2) = T_1 = temperature at which the $\bar{\Omega}$ are to remain unchanged

KKQ = 12 Generalized Mixing Rule

This option is a generalization of the empirical mixing rule KKQ = 10 in which the cross sections are calculated from

the formula

$$\bar{\Omega}^{(l,s)}_{ij} = \sqrt{\bar{\Omega}_{ij}^{(l,s)} + \bar{\Omega}_{mn}^{(l,s)}}^2 \quad (19)$$

where i , j , and m , n are any specified molecular pairs. The parameters are

$$VV(1) = i$$

$$VV(2) = j$$

$$VV(3) = m$$

$$VV(4) = n$$

KKQ = 13 Scaling of Previously Computed Cross Section for
the Same Species Pair

This option calculates one of the averaged collision cross sections $\bar{\Omega}^{(l,s)}$ for a pair of species from previously calculated values of a different $\bar{\Omega}^{(l,s)}$ for the pair. In terms of the notation

$$\begin{aligned}\bar{\Omega}_{ij}^{(1)} &\equiv \bar{\Omega}_{ij}^{(1,1)} \\ \bar{\Omega}_{ij}^{(2)} &\equiv \bar{\Omega}_{ij}^{(2,2)} \\ \bar{\Omega}_{ij}^{(3)} &\equiv B^* \bar{\Omega}_{ij}^{(1,1)}\end{aligned} \quad (20)$$

the option calculates a new value of the cross section $\bar{\Omega}_{ij}^{(m)}$ from the formula

$$\bar{\Omega}_{ij}^{(m)} = C \bar{\Omega}_{ij}^{(n)} \quad (21)$$

where m and n are two specified integers in the range $1 \leq m \leq 3$, $1 \leq n \leq 3$ and C is a constant. The newly calculated value of

$\bar{\Omega}_{ij}^{(m)}$ then replaces the previous value of this cross section.
The parameters are

$$VV(1) = m$$

$$VV(2) = n$$

$$VV(3) = c$$

KKQ = 14 Multiplication by a Constant

This option multiplies previously calculated values of the collision cross sections for a pair of species by a constant factor, according to the formulas

$$\begin{aligned}\bar{\Omega}_{ij}^{(1,1)} &= c_1 \bar{\Omega}_{ij}^{(1,1)}_{\text{(old)}} \\ \bar{\Omega}_{ij}^{(2,2)} &= c_1 c_2 \bar{\Omega}_{ij}^{(2,2)}_{\text{(old)}} \\ B_{ij}^* &= c_3 B_{ij}^*_{\text{(old)}}\end{aligned}\tag{22}$$

The option is the same as KKQ = 9, except that here the cross sections for a species pair are obtained from previously calculated values for the same pair, instead of from values for a different pair as in KKQ = 9. Parameters for the option are

$$VV(1) = c_1$$

$$VV(2) = c_2$$

$$VV(3) = c_3$$

NATA contains default provisions for estimating some cross sections if they are not specified explicitly in the precoded data or the input. If none of the specified steps in the cross section calculation is applicable to a particular pair, and if both of the species are ions, then the effective Coulomb cross sections(8) are used. If one species is neutral and the other ionized, the formulas

$$\begin{aligned}
 \bar{\Omega}^{(1,1)} &= A^{(1)} T^{-0.4} \\
 \bar{\Omega}^{(2,2)} &= A^{(2)} T^{-0.4} \\
 B^* \bar{\Omega}^{(1,1)} &= A^{(3)} T^{-0.4}
 \end{aligned} \tag{23}$$

give the default option. The constants $A^{(m)}$ are compiled into the program in the locations ØMEGAL (996), ASTAR(996), and BSTAR(996) for $m = 1, 2, 3$, respectively. If both species are neutral and unlike (not the same species), the cross sections are estimated using the mixing rule (17). However, if cross section data are not specified for like-like collisions of a neutral species, the code does not attempt to provide estimates of the cross sections, but returns an error message and terminates the care.

The variables and arrays used to store the precoded cross section data are as follows:

<u>Variable</u>		<u>Definition</u>
<u>Name</u>	<u>Dimension</u>	
NNQ	1	Number of steps in the cross section calculation for which data are specified.
NNQ(M)	100	Index specifying the option to be used in the Mth step of the cross section calculation (see above).
NNQ(M)	100	Number of species pairs to which the cross sections calculated in the Mth step are to be applied ($NNQ(M) \leq 5$).
II _m (K) JJ _m (K)	5 5	Indices of the species to which the cross sections calculated in the mth step are to be applied, referred to the master list of species (Section 4.2). In these variable names, m denotes an integer which is part of each name. Thus, for example, II23(2) and JJ23(2) are the indices defining the second pair of species to which the cross sections calculated in the 23rd step are applied. There are 100 arrays of each type, e.g., II1(K), II2(K), ... ,

$II100(K)$. There are $NNQ(m)$ pairs of indices set for each step m . Only pairs with $IIm(K) \leq JJm(K)$ are used in the calculations.*

$VVm(K)$	5	Parameter values for the m th step of the cross section calculation (see discussion of KKQ options above). There are 100 of these arrays, $VV1(K), \dots, VV100(K)$.*
$ISEQ(L)$	100	Sequencing array for specifying the order in which the defined steps are carried out during the cross section calculation. The index M or m in the preceding arrays is given by $M = ISEQ(L)$, where $L = 1, 2, 3, \dots, NNQ$.
TL	1000	Additional array storage for cross sec-
$\emptyset MEGAL$	1000	tion data. The data compiled into these
ASTAR	1000	arrays are discussed below.
BSTAR	1000	

To prevent the data statements used in setting the TL, $\emptyset MEGAL$, ASTAR and BSTAR arrays from exceeding the 20-card limit in Fortran IV, these arrays are equivalenced to 40 arrays each of dimension (100), as follows:

TL1(1)	equivalent to TL(1)
TL2(1)	equivalent to TL(101)
.	.
.	.
.	.
TL10(1)	equivalent to TL(901)
TL11(1)	equivalent to $\emptyset MEGAL(1)$
.	.
.	.
.	.
TL20(1)	equivalent to $\emptyset MEGAL(901)$

*The arrays $IIm(K)$, $JJm(K)$, $VVm(K)$ are the same as the input arrays $Im(K)$, $Jm(K)$, $Vm(K)$ discussed in Section 2.4. The shorter names are used for input to keep the defining statement for name-list TINPUT within the 20-card limit allowed by Fortran IV.

TL21(1)	equivalent to ASTAR(1)
.	.
.	.
.	.
TL30(1)	equivalent to ASTAR(901)
TL31(1)	equivalent to BSTAR(1)
.	.
.	.
.	.
TL40(1)	equivalent to BSTAR(901)

The precoded data for cross section calculations will now be tabulated and documented. These data have been taken from previous transport property studies at Avco Systems Division and have not been revised during the present program. Thus, in some cases the values used in NATA may not represent the latest available data. Nevertheless, the data in the code should be generally satisfactory for most engineering applications.

For most of the important cross sections, with the exceptions of those involving carbon-containing species, the precoded cross section data should be accurate to within 20 to 40 percent. For the carbon-containing species, very few data are currently available on the collision cross sections at high temperatures, and the values used in NATA are based for the most part on rough estimates. In general, it is believed that these estimates should be accurate to within about a factor of two. For some interactions involving minor species such as the metastable states of He and Ar, nominal cross sections are used which may be in error by large factors. However, because of the low concentrations of the species in question, the effects of these cross section errors upon the calculated gas transport properties are small.

The sources of the cross section data used in NATA are indicated, for each pair of species in the master list, in Table XVII. In this table, the numbers preceded by A in the third column refer to the notes at the end of the table, while the numbers in the final column indicate the steps in the cross section calculation where computations for the given species pair are specified. The steps defined in the compiled-in data for the standard species are summarized in the cross section edit, figure 16. In the many cases where the final column contains no entry for a species pair, one of the default options is used as indicated in the Notes.

TABLE XVII
SOURCES OF CROSS SECTION DATA

Species Indices	Species Names	Notes	Computation Steps
1-1	e ⁻ - e ⁻	A1	
1-2	e ⁻ - N	A2	43,50
1-3	e ⁻ - O	A2	46,50
1-4	e ⁻ - Ar	A5,A6,A7,A8	48
1-5	e ⁻ - N ₂	A2	45,50
1-6	e ⁻ - O ₂	A2	47,50
1-7	e ⁻ - NO	A2	44,50
1-8	e ⁻ - NO ⁺	A1	
1-9	e ⁻ - N ⁺	A1	
1-10	e ⁻ - O ⁺	A1	
1-11	e ⁻ - N ₂ ⁺	A1	
1-12	e ⁻ - O ₂ ⁺	A1	
1-13	e ⁻ - CO ₂	A5,A6,A9	42,49
1-14	e ⁻ - CO	A5,A6,A9	41,49
1-15	e ⁻ - CN	A11	44,49
1-16	e ⁻ - He	A8	55
1-17	e ⁻ - C	A10	43,49
1-18	e ⁻ - C ⁺	A1	
1-19	e ⁻ - He ⁺	A1	
1-20	e ⁻ - Ar ⁺	A1	
1-21	e ⁻ - He(³ S)	A33	55
1-22	e ⁻ - He(¹ S)	A33	55
1-23	e ⁻ - He ₂ ⁺	A1	
1-24	e ⁻ - He ₂ ⁺	A33	55
1-25	e ⁻ - CO ⁺	A1	
1-26	e ⁻ - Ar*(m)	A14	
1-27	e ⁻ - Ar*(r)	A14	
1-28	e ⁻ - Ar ₂ ⁺	A1	
2-2	N - N	A2,A4	12,60
2-3	N - O	A2	14,26
2-4	N - Ar	A12	4
2-5	N - N ₂	A2	13,26
2-6	N - O ₂	A2	18,22,39
2-7	N - NO	A2	13,24,25
2-8	N - NO ⁺	A14	
2-9	N - N ⁺	A2,A3	10,60
2-10	N - O ⁺	A2	
2-11	N - N ₂ ⁺	A14	
2-12	N - O ₂ ⁺	A14	

TABLE XVII (Cont'd)

Species Indices	Species Names	Notes	Computation Steps
2-13	N - CO ₂	A13	
2-14	N - CO	A13	
2-15	N - CN	A11	13, 24, 25
2-16	N - He	A13	
2-17	N - C	A18, A19	5, 7
2-18	N - C ⁺	A14	
2-19	N - He ⁺	A14	
2-20	N - Ar ⁺	A14	
2-21	N - He(³ S)	A13	
2-22	N - He(¹ S)	A13	
2-23	N - He ₂ ⁺	A14	
2-24	N - He ₂	A13	
2-25	N - CO [†]	A14	
2-26	N - Ar*(m)	A13	
2-27	N - Ar*(r)	A13	
2-28	N - Ar ₂ ⁺	A14	
3-3	O - O	A2, A4	21, 61
3-4	O - Ar	A13	
3-5	O - N ₂	A2	18, 38
3-6	O - O ₂	A2	22
3-7	O - NO	A2	18, 22, 39
3-8	O - NO ⁺	A14	
3-9	O - N ⁺	A2	
3-10	O - O ⁺	A2, A3	11, 61
3-11	O - N ₂ ⁺	A14	
3-12	O - O ₂ ⁺	A14	
3-13	O - CO ₂	A13	
3-14	O - CO	A13	
3-15	O - CN	A11	18, 22, 39
3-16	O - He	A13	
3-17	O - C	A18, A20	5, 8, 9
3-18	O - C ⁺	A14	
3-19	O - He ⁺	A14	
3-20	O - Ar ⁺	A14	
3-21	O - He(³ S)	A13	
3-22	O - He(¹ S)	A13	
3-23	O - He ₂ ⁺	A14	
3-24	O - He ₂	A13	
3-25	O - CO [†]	A14	
3-26	O - Ar*(m)	A13	

TABLE XVII (Cont'd)

Species Indices	Species Names	Notes	Computation Steps
3-27	O - Ar*(r)	A13	
3-28	O - Ar ₂ ⁺	A14	
4-4	Ar - Ar	A17, A4	1, 62
4-5	Ar - N ₂	A12	3
4-6	Ar - O ₂	A13	
4-7	Ar - NO	A13	
4-8	Ar - NO ⁺	A14	
4-9	Ar - N ⁺	A14	
4-10	Ar - O ⁺	A14	
4-11	Ar - N ₂ ⁺	A14	
4-12	Ar - O ₂ ⁺	A14	
4-13	Ar - CO ₂	A13	
4-14	Ar - CO	A13	
4-15	Ar - CN	A13	
4-16	Ar - He	A13	
4-17	Ar - C	A13	
4-18	Ar - C ⁺	A14	
4-19	Ar - He ⁺	A14	
4-20	Ar - Ar ⁺	A17	2, 62
4-21	Ar - He(³ S)	A13	
4-22	Ar - He(¹ S)	A13	
4-23	Ar - He ₂ ⁺	A14	
4-24	Ar - He ₂ ²	A13	
4-25	Ar - CO ⁺	A14	
4-26	Ar - Ar*(m)	A13	
4-27	Ar - Ar*(r)	A13	
4-28	Ar - Ar ₂ ⁺	A14	
5-5	N ₂ - N ₂	A2	17, 38
5-6	N ₂ - O ₂	A2	20
5-7	N ₂ - NO	A2	17, 19, 37
5-8	N ₂ - NO ⁺	A14	
5-9	N ₂ - N ⁺	A14	
5-10	N ₂ - O ⁺	A14	
5-11	N ₂ - N ₂ ⁺	A14	
5-12	N ₂ - O ₂ ⁺	A14	
5-13	N ₂ - CO ₂	A22, A24, A26	16, 34
5-14	N ₂ - CO	A22, A23	15, 29
5-15	N ₂ - CN	A11	17, 19, 37
5-16	N ₂ - He	A13	
5-17	N ₂ - C	A13	
5-18	N ₂ - C ⁺	A14	

TABLE XVII (Cont'd)

Species Indices	Species Names	Notes	Computation Steps
5-19	N ₂ - He ⁺	A14	
5-20	N ₂ - Ar ⁺	A14	
5-21	N ₂ - He(³ S)	A13	
5-22	N ₂ - He(¹ S)	A13	
5-23	N ₂ ⁺ - He ₂	A14	
5-24	N ₂ - He ₂	A13	
5-25	N ₂ - CO ⁺	A14	
5-26	N ₂ - Ar*(m)	A13	
5-27	N ₂ - Ar*(r)	A13	
5-28	N ₂ - Ar ₂	A14	
6-6	O ₂ - O ₂	A2	23
6-7	O ₂ - NO	A2	19, 23, 39
6-8	O ₂ - NO ⁺	A14	
6-9	O ₂ - N ⁺	A14	
6-10	O ₂ - O ⁺	A14	
6-11	O ₂ - N ₂ ⁺	A14	
6-12	O ₂ - O ₂ ⁺	A14	
6-13	O ₂ - CO ₂	A22, A24	17, 35
6-14	O ₂ - CO	A22, A24	15, 30
6-15	O ₂ - CN	A11	19, 23, 39
6-16	O ₂ - He	A13	
6-17	O ₂ - C	A13	
6-18	O ₂ - C ⁺	A14	
6-19	O ₂ - He ⁺	A14	
6-20	O ₂ - Ar ⁺	A14	
6-21	O ₂ - He(³ S)	A13	
6-22	O ₂ - He(¹ S)	A13	
6-23	O ₂ ⁺ - He ₂	A14	
6-24	O ₂ - He ₂	A13	
6-25	O ₂ - CO ⁺	A14	
6-26	O ₂ - Ar*(m)	A13	
6-27	O ₂ - Ar*(r)	A13	
6-28	O ₂ - Ar ₂ ⁺	A14	
7-7	NO - NO	A2	17, 19, 20, 23, 36
7-8	NO - NO ⁺	A2	59, 63
7-9	NO - N ⁺	A14	
7-10	NO - O ⁺	A14	
7-11	NO - N ₂ ⁺	A14	
7-12	NO - O ₂ ⁺	A14	
7-13	NO - CO ₂	A30	16, 32

TABLE XVII (Cont'd)

Species Indices	Species Names	Notes	Computation Steps
7-14	NO - CO	A29	15,31
7-15	NO - CN	A11	40
7-16	NO - He	A13	
7-17	NO - C	A13	
7-18	NO - C ⁺	A14	
7-19	NO - He ⁺	A14	
7-20	NO - Ar ⁺	A14	
7-21	NO - He(³ S)	A13	
7-22	NO - He(¹ S)	A13	
7-23	NO - He ₂ ⁺	A14	
7-24	NO - He ₂	A13	
7-25	NO - CO ⁺	A14	
7-26	NO - Ar*(m)	A13	
7-27	NO - Ar*(r)	A13	
7-28	NO - Ar ₂ ⁺	A14	
8-8	NO ⁺ - NO ⁺	A1	
8-9	NO ⁺ - N ⁺	A1	
8-10	NO ⁺ - O ⁺	A1	
8-11	NO ⁺ - N ₂ ⁺	A1	
8-12	NO ⁺ - O ₂ ⁺	A1	
8-13	NO ⁺ - CO	A14	
8-14	NO ⁺ - CO ₂	A14	
8-15	NO ⁺ - CN	A14	
8-16	NO ⁺ - He	A14	
8-17	NO ⁺ - C	A14	
8-18	NO ⁺ - C ⁺	A1	
8-19	NO ⁺ - He ⁺	A1	
8-20	NO ⁺ - Ar ⁺	A1	
8-21	NO ⁺ - He(³ S)	A14	
8-22	NO ⁺ - He(¹ S)	A14	
8-23	NO ⁺ - He ₂ ⁺	A1	
8-24	NO ⁺ - He ₂	A14	
8-25	NO ⁺ - CO ⁺	A1	
8-26	NO ⁺ - Ar*(m)	A14	
8-27	NO ⁺ - Ar*(r)	A14	
8-28	NO ⁺ - Ar ₂ ⁺	A1	
9-9	N ⁺ - N ⁺	A1	
9-10	N ⁺ - O ⁺	A1	
9-11	N ⁺ - N ₂ ⁺	A1	
9-12	N ⁺ - O ₂ ⁺	A1	

TABLE XVII (Cont'd)

Species Indices	Species Names	Notes	Computation Steps
9-13	N ⁺ - CO ₂	A14	
9-14	N ⁺ - CO	A14	
9-15	N ⁺ - CN	A14	
9-16	N ⁺ - He	A14	
9-17	N ⁺ - C	A14	
9-18	N ⁺ - C ⁺	A1	
9-19	N ⁺ - He ⁺	A1	
9-20	N ⁺ - Ar ⁺	A1	
9-21	N ⁺ - He(³ S)	A14	
9-22	N ⁺ - He(¹ S)	A14	
9-23	N ⁺ - He ₂ ⁺	A1	
9-24	N ⁺ - He ₂	A14	
9-25	N ⁺ - CO ⁺	A1	
9-26	N ⁺ - Ar*(m)	A14	
9-27	N ⁺ - Ar*(r)	A14	
9-28	N ⁺ - Ar ₂ ⁺	A1	
10-10	O ⁺ - O ⁺	A1	
10-11	O ⁺ - N ⁺	A1	
10-12	O ⁺ - O ₂ ⁺	A1	
10-13	O ⁺ - CO ₂	A14	
10-14	O ⁺ - CO	A14	
10-15	O ⁺ - CN	A14	
10-16	O ⁺ - He	A14	
10-17	O ⁺ - C	A14	
10-18	O ⁺ - C ⁺	A1	
10-19	O ⁺ - He ⁺	A1	
10-20	O ⁺ - Ar ⁺	A1	
10-21	O ⁺ - He(³ S)	A14	
10-22	O ⁺ - He(¹ S)	A14	
10-23	O ⁺ - He ₂ ⁺	A1	
10-24	O ⁺ - He ₂	A14	
10-25	O ⁺ - CO ⁺	A1	
10-26	O ⁺ - Ar*(m)	A14	
10-27	O ⁺ - Ar*(r)	A14	
10-28	O ⁺ - Ar ₂ ⁺	A1	
11-11	N ₂ ⁺ - N ⁺	A1	
11-12	N ₂ ⁺ - O ₂ ⁺	A1	
11-13	N ₂ ⁺ - CO ₂	A14	
11-14	N ₂ ⁺ - CO	A14	
11-15	N ₂ ⁺ - CN	A14	
11-16	N ₂ ⁺ - He	A14	

TABLE XVII (Cont'd)

Species Indices	Species Names	Notes	Computation Steps
11-17	$N_2^+ - C$	A14	
11-18	$N_2^+ - C^+$	A1	
11-19	$N_2^+ - He^+$	A1	
11-20	$N_2^+ - Ar^+$	A1	
11-21	$N_2^+ - He(^3S)$	A14	
11-22	$N_2^+ - He(^1S)$	A14	
11-23	$N_2^+ - He_2^+$	A1	
11-24	$N_2^+ - He_2$	A14	
11-25	$N_2^+ - CO^+$	A1	
11-26	$N_2^+ - Ar^*(m)$	A14	
11-27	$N_2^+ - Ar^*(r)$	A14	
11-28	$N_2^+ - Ar_2^+$	A1	
12-12	$O_2^+ - O_2$	A1	
12-13	$O_2^+ - CO_2$	A14	
12-14	$O_2^+ - CO$	A14	
12-15	$O_2^+ - CN$	A14	
12-16	$O_2^+ - He$	A14	
12-17	$O_2^+ - C$	A14	
12-18	$O_2^+ - C^+$	A1	
12-19	$O_2^+ - He^+$	A1	
12-20	$O_2^+ - Ar^+$	A1	
12-21	$O_2^+ - He(^3S)$	A14	
12-22	$O_2^+ - He(^1S)$	A14	
12-23	$O_2^+ - He_2^+$	A1	
12-24	$O_2^+ - He_2$	A14	
12-25	$O_2^+ - CO^+$	A1	
12-26	$O_2^+ - Ar^*(m)$	A14	
12-27	$O_2^+ - Ar^*(r)$	A14	
12-28	$O_2^+ - Ar_2^+$	A1	
13-13	$CO_2 - CO_2$	A22, A25, A27	16, 33
13-14	$CO_2 - CO$	A31	15, 28
13-15	$CO_2 - CN$	A11	16, 32
13-16	$CO_2 - He$	A13	
13-17	$CO_2 - C$	A13	
13-18	$CO_2 - C^+$	A14	
13-19	$CO_2 - He^+$	4	
13-20	$CO_2 - Ar^+$		
13-21	$CO_2 - He(^3S)$	A13	
13-22	$CO_2 - He(^1S)$	A13	
13-23	$CO_2 - He_2^+$	A14	

TABLE XVII (Cont'd)

Species Indices	Species Names	Notes	Computation Steps
13-24	$\text{CO}_2 - \text{He}_2$	A13	
13-25	$\text{CO}_2 - \text{CO}^f$	A14	
13-26	$\text{CO}_2 - \text{Ar}^*(m)$	A13	
13-27	$\text{CO}_2 - \text{Ar}^*(r)$	A13	
13-28	$\text{CO}_2 - \text{Ar}_2^+$	A14	
14-4	$\text{CO} - \text{CO}$	A22, A23, A28	15, 27
14-15	$\text{CO} - \text{CN}$	A11	16, 31
14-16	$\text{CO} - \text{He}$	A13	
14-17	$\text{CO} - \text{C}$	A13	
14-18	$\text{CO} - \text{C}^+$	A14	
14-19	$\text{CO} - \text{He}^+$	A14	
14-20	$\text{CO} - \text{Ar}^+$	A14	
14-21	$\text{CO} - \text{He}(^3\text{S})$	A13	
14-22	$\text{CO} - \text{He}(^1\text{S})$	A13	
14-23	$\text{CO} - \text{He}_2^+$	A14	
14-24	$\text{CO} - \text{He}_2$	A13	
14-25	$\text{CO} - \text{CO}^f$	A14	
14-26	$\text{CO} - \text{Ar}^*(m)$	A13	
14-27	$\text{CO} - \text{Ar}^*(r)$	A13	
14-28	$\text{CO} - \text{Ar}_2^+$	A14	
15-15	$\text{CN} - \text{CN}$	A11	40
15-16	$\text{CN} - \text{He}$	A13	
15-17	$\text{CN} - \text{C}$	A13	
15-18	$\text{CN} - \text{C}^+$	A14	
15-19	$\text{CN} - \text{He}^+$	A14	
15-20	$\text{CN} - \text{Ar}^+$	A14	
15-21	$\text{CN} - \text{He}(^3\text{S})$	A13	
15-22	$\text{CN} - \text{He}(^1\text{S})$	A13	
15-23	$\text{CN} - \text{He}_2^+$	A14	
15-24	$\text{CN} - \text{He}_2$	A13	
15-25	$\text{CN} - \text{CO}^f$	A14	
15-26	$\text{CN} - \text{Ar}^*(m)$	A13	
15-27	$\text{CN} - \text{Ar}^*(r)$	A13	
15-28	$\text{CN} - \text{Ar}_2^+$	A14	
16-16	$\text{He} - \text{He}$	A34, A4	51, 57
16-17	$\text{He} - \text{C}$	A13	
16-18	$\text{He} - \text{C}^+$	A14	
16-19	$\text{He} - \text{He}^+$	A35	53, 57
16-20	$\text{He} - \text{Ar}^+$	A14	
16-21	$\text{He} - \text{He}(^3\text{S})$	A33	51, 57

TABLE XVII (Cont'd)

Species Indices	Species Names	Notes	Computation Steps
16-22	He - He (¹ S)	A33	51, 57
16-23	He - He ₂ ⁺	A33	53
16-24	He - He ₂	A13	
16-25	He - CO ⁺	A14	
16-26	He - Ar* (m)	A13	
16-27	He - Ar* (r)	A13	
16-28	He - Ar ₂ ⁺	A14	
17-17	C - C	A18, A21, A4	5, 6, 60
17-18	C - C ⁺	A32	59, 60
17-19	C - He ⁺	A14	
17-20	C - Ar ⁺	A14	
17-21	C - He(³ S)	A13	
17-22	C - He(¹ S)	A13	
17-23	C - He ₂ ⁺	A14	
17-24	C - He ₂	A13	
17-25	C - CO ²	A14	
17-26	C - Ar* (m)	A13	
17-27	C - Ar* (r)	A13	
17-28	C - Ar ₂ ⁺	A14	
18-18	C ⁺ - C ²	A1	
18-19	C ⁺ - He ⁺	A1	
18-20	C ⁺ - Ar ⁺	A1	
18-21	C ⁺ - He(³ S)	A14	
18-22	C ⁺ - He(¹ S)	A14	
18-23	C ⁺ - He ₂ ⁺	A1	
18-24	C ⁺ - He ₂	A14	
18-25	C ⁺ - CO ²	A1	
18-26	C ⁺ - Ar* (m)	A14	
18-27	C ⁺ - Ar* (r)	A14	
18-28	C ⁺ - Ar ₂ ⁺	A1	
19-19	He ⁺ - He ⁺	A1	
19-20	He ⁺ - Ar ⁺	A1	
19-21	He ⁺ - He(³ S)	A33	53, 57
19-22	He ⁺ - He(¹ S)	A33	53, 58
19-23	He ⁺ - He ₂ ⁺	A1	
19-24	He ⁺ - He ₂	A33	53
19-25	He ⁺ - CO ²	A1	
19-26	He ⁺ - Ar* (m)	A14	
19-27	He ⁺ - Ar* (r)	A14	
19-28	He ⁺ - Ar ₂ ⁺	A1	

TABLE XVII (Cont'd)

Species Indices	Species Names	Notes	Computation Steps
20-20	$\text{Ar}^+ - \text{Ar}^+$	A1	
20-21	$\text{Ar}^+ - \text{He}(^3\text{S})$	A14	
20-22	$\text{Ar}^+ - \text{He}(^1\text{S})$	A14	
20-23	$\text{Ar}^+ - \text{He}_2^+$	A1	
20-24	$\text{Ar}^+ - \text{He}_2$	A14	
20-25	$\text{Ar}^+ - \text{CO}^+$	A1	
20-26	$\text{Ar}^+ - \text{Ar}^*(m)$	A14	
20-27	$\text{Ar}^+ - \text{Ar}^*(r)$	A14	
20-28	$\text{Ar}^+ - \text{Ar}_2^+$	A1	
21-21	$\text{He}(^3\text{S}) - \text{He}(^3\text{S})$	A33	51, 58
21-22	$\text{He}(^3\text{S}) - \text{He}(^1\text{S})$	A33	51, 58
21-23	$\text{He}(^3\text{S}) - \text{He}_2^+$	A33	54
21-24	$\text{He}(^3\text{S}) - \text{He}_2$	A13	
21-25	$\text{He}(^3\text{S}) - \text{CO}^+$	A14	
21-26	$\text{He}(^3\text{S}) - \text{Ar}^*(m)$	A13	
21-27	$\text{He}(^3\text{S}) - \text{Ar}^*(r)$	A13	
21-28	$\text{He}(^3\text{S}) - \text{Ar}_2^+$	A14	
22-22	$\text{He}(^1\text{S}) - \text{He}(^1\text{S})$	A33	52, 58
22-23	$\text{He}(^1\text{S}) - \text{He}_2^+$	A33	54
22-24	$\text{He}(^1\text{S}) - \text{He}_2$	A13	
22-25	$\text{He}(^1\text{S}) - \text{CO}^+$	A14	
22-26	$\text{He}(^1\text{S}) - \text{Ar}^*(m)$	A13	
22-27	$\text{He}(^1\text{S}) - \text{Ar}^*(r)$	A13	
22-28	$\text{He}(^1\text{S}) - \text{Ar}_2^+$	A14	
23-23	$\text{He}_2^+ - \text{He}_2^+$	A1	
23-24	$\text{He}_2^+ - \text{He}_2$	A33	54
23-25	$\text{He}_2^+ - \text{CO}^+$	A1	
23-26	$\text{He}_2^+ - \text{Ar}^*(m)$	A14	
23-27	$\text{He}_2^+ - \text{Ar}^*(r)$	A14	
23-28	$\text{He}_2^+ - \text{Ar}_2^+$	A1	
24-24	$\text{He}_2 - \text{He}_2$	A33	52
24-25	$\text{He}_2 - \text{CO}^+$	A14	
24-26	$\text{He}_2 - \text{Ar}^*(m)$	A13	
24-27	$\text{He}_2 - \text{Ar}^*(r)$	A13	
24-28	$\text{He}_2 - \text{Ar}_2^+$	A14	
25-25	$\text{CO}^+ - \text{CO}^+$	A1	
25-26	$\text{CO}^+ - \text{Ar}^*(m)$	A14	
25-27	$\text{CO}^+ - \text{Ar}^*(r)$	A14	
25-28	$\text{CO}^+ - \text{Ar}_2^+$	A1	
26-26	$\text{Ar}^*(m) - \text{Ar}^*(m)$	A15	1, 62

TABLE XVII (Cont'd)

Species Indices	Species Names	Notes	Computation Steps
26-27	Ar*(m) - Ar*(r)	A13	
26-28	Ar*(m) - Ar ₂ ⁺	A14	
27-27	Ar*(r) - Ar*(r)	A15	1,62
27-28	Ar*(r) - Ar ₂ ⁺	A14	
28-28	Ar ₂ ⁺ - Ar ₂ ⁺	A1	

Notes to Table XVII

- A1. Default option; uses effective Coulomb cross sections calculated from equations (100) of Volume I (ref. 1).
- A2. Reference 22.
- A3. Reference 23.
- A4. The self-diffusion coefficient for atoms is set equal to the atom-ion charge exchange cross section in calculating the internal thermal conductivity, in order to account approximately for the effects of resonant excitation energy exchange (see ref. 22).
- A5. Effective cross sections are used, based on curvefit to mobility data.
- A6. Reference 24.
- A7. References 25, 26, 27.
- A8. Reference 28.
- A9. Reference 29.
- A10. For electron-carbon atom collisions, we assume a constant collision cross section $\pi \bar{\Omega}(1,1) = \pi \bar{\Omega}(2,2) = 5 \times 10^{-16} \text{ cm}^2$, in analogy to the case of e-N. This value appears to be consistent with available theoretical estimates (see ref. 30).

- A11. The collision cross sections for CN have arbitrarily been set equal to the corresponding cross sections for NO.
- A12. Curvefit to data of reference 31.
- A13. Default option; cross sections calculated from the empirical mixing rule, equation (17).
- A14. Default option; cross sections arbitrarily set equal to the estimated values for N - O⁺ collisions. See equation (23).
- A15. Cross sections of excited argon arbitrarily assumed equal to those for the ground state atoms.
- A16. Curvefit to data of reference 32.
- A17. Reference 33.
- A18. Cross sections estimated from an approximate perfect pairing calculation, with the parameters determined from available spectroscopic data and by analogy with the oxygen and nitrogen results (refs. 34-37).
- A19. Reference 38.
- A20. Reference 39.
- A21. References 40, 41.
- A22. Cross sections obtained by fitting experimental transport property data below about 1000°K and extrapolating to higher temperatures assuming the same temperature dependence as for N₂-N₂ collisions.
- A23. Reference 42.
- A24. References 43, 44.
- A25. Reference 45.
- A26. Reference 46.
- A27. Reference 47.

- A28. Reference 48.
- A29. Mean of CO-N₂ and CO-O₂ cross sections.
- A30. Mean of CO₂-N₂ and CO₂-O₂ cross sections.
- A31. Mean of CO-CO and CO₂-CO₂ cross sections.
- A32. For C-C⁺ collisions, the charge exchange cross section is arbitrarily set equal to the N-N⁺ cross section, while the gas kinetic cross section is set equal to the N-O⁺ value.
- A33. Cross sections of excited He arbitrarily assumed equal to those for ground-state He.
- A34. Reference 49.
- A35. Reference 50.

The precoded data for NNKQ, NNQ, IIM, JJM, VVm, and ISEQ can all be read or inferred from the cross section edit, figure 16. The steps are performed in the order listed. The first column in figure 16 is a counter for the steps in this order. The second column gives the values of the sequencing array, ISEQ. For the precoded data, ISEQ(L)=L. The third column gives the values of the option index, KKQ. The columns headed V(1),...,VV(5) list the parameter values for each step. Finally, the last column gives the pairs of species to which the step is applied. In some cases (e.g., steps 51 and 52), a step is repeated to circumvent the limit of five species pairs per step.

Table XVIII summarizes the precoded contents of the TL, ØMEGAL, ASTAR, and BSTAR arrays. In the many cases in which "cross section table" is entered under "Remarks" the data are tabulated cross sections for use with the option KKQ=5. In these cases, the TL, ØMEGAL, ASTAR, and BSTAR arrays contain data as specified above in the discussion of this option. For the indices 996-999 containing data for the power law interaction (KKQ=6), no data are stored in TL, and the data in the other arrays are as specified in equations (14).

TABLE XVIII
PRECODED DATA IN THE TL, ØMEGAL, ASTAR, AND BSTAR ARRAYS

Index	Description	Step	Remarks
1-50	Exponential potential (KKQ=3)	-	TL contains values of $\alpha = \ln(A/kT) / \sum_{i=1}^n (1, 1) / (\rho_1 \rho_2)$ ØMEGAL contains corresponding $\bar{\Omega}(1, 1)$ (4 π α² ρ²) ASTAR contains corresponding $\bar{\Omega}(2, 2) / \bar{\Omega}(1, 1)$ BSTAR contains corresponding B*
51-52	O-C interaction	9	Cross section table
71-72	e--N interaction	43	Cross section table
81-100	N-N interaction	12	Cross section table
101-120	N-N₂ interaction	13	Cross section table
121-140	N-O interaction	14	Cross section table
141-160	N₂-N₂ interaction	15	Cross section table
161-180	O-N₂ interaction	18	Cross section table
181-200	N₂-O₂ interaction	19	Cross section table

TABLE XVIII (cont'd)

Index	Description	Step	Remarks
201-220	O-O interaction	21	Cross section table
221-240	O-O ₂ interaction	22	Cross section table
241-260	O ₂ -O ₂ interaction	23	Cross section table
261-280	e ⁻ -CO interaction	41	Cross section table
281-300	e ⁻ -CO ₂ interaction	42	Cross section table
301-320	e ⁻ -NO interaction	44	Cross section table
321-340	e ⁻ -N ₂ interaction	45	Cross section table
341-360	e ⁻ -O interaction	46	Cross section table
361-380	e ⁻ -O ₂ interaction	47	Cross section table
381-400	e ⁻ -Ar interaction	48	Cross section table
471-490	e ⁻ -He interaction	55	Cross section table

TABLE XVIII (Concl'd)

Index	Description	Step	Remarks
501-537	Lennard-Jones (6-12) potential	--	TL contains values of $T^* = \frac{\Psi(\epsilon/k)}{\sigma^2}$ \emptyset MEGAL contains corresponding $\frac{\Omega(1,1)}{\Omega(2,2)}$ ASTAR contains corresponding $\frac{\Omega(1,1)}{\Omega(2,2)}$ BSTAR contains corresponding B^*
996	N-O ⁺ interaction	--	Default for neutral-ion interaction; see eq. (23).
997	O-O ⁺ interaction	11	Power law interaction, KKQ = 6
998	N-N ⁺ interaction	10	Power law interaction, KKQ = 6
999	C-C, N-C, and O-C interactions	5	Power law interaction, KKQ = 6

4.7 Nozzle and Channel Geometries

The geometric profiles for ten standard NASA Johnson Space Center nozzles and two rectangular channels are compiled into NATA. These data are indexed as explained in the definitions of NOZZLE and NPRØFL in Section 2.3 (Group 4). NATA users at other laboratories can advantageously replace these data with geometric descriptions applicable to their own facilities.

The geometry of an axisymmetric nozzle is defined by a single profile. That of a rectangular channel requires two profiles for its description. As explained in Section 4.3 of Volume I (ref. 1), each profile is represented by an analytical curvefit containing up to 12 sections. The sections are joined end to end with value and slope continuity. At least two sections must be upstream of the throat, and at least two must lie downstream. The throat must be a section boundary. Each section in a profile fit may have one of three forms:

- (1) Straight Line (ISHAPE = 1)

$$y(x) = P_1 + P_2 x \quad (24a)$$

- (2) Circular Arc Convex Downward (ISHAPE = 2)

$$y(x) = P_1 - \sqrt{P_3^2 - (x-P_2)^2} \quad (24b)$$

- (3) Circular Arc Convex Upward (ISHAPE = 3)

$$y(x) = P_1 + \sqrt{P_3^2 - (x-P_2)^2} \quad (24c)$$

In the second and third forms, P_3 is the radius of the circular arc and (P_2, P_1) are the x and y coordinates, respectively, of the circle center. The geometric summary in figure 4 gives an illustration of a NATA profile curvefit. The inlet position listed is the starting point for boundary layer calculations. The column headed "ATPI(J)" contains the downstream boundaries of the sections. The parameters P_1 , P_2 , P_3 are listed as PARAM(1,J), PARAM(2,J), PARAM(3,J), respectively

The precoded profile data are stored in an array ZPRP(I,NOZZLE), dimensioned (64,20). The dimensions allow as many as 20 compiled-in profiles. For convenience in adding to or altering the precoded data, ZPRP is equivalenced to 20 singly dimensioned arrays (ZP1(I), ZP2(I), etc., as follows:

ZP1(1)	equivalent to ZPRP(1,1)
.	.
.	.
.	.
.	.
ZP20(1)	equivalent to ZPRP(1,20)

Thus, ZP1 contains the precoded data for NOZZLE = 1, ZP2 those for NOZZLE = 2, and so forth. The data in each ZPn array are as follows:

<u>Array Element</u>	<u>Definition</u>
ZPn(1)	Throat radius (cm)
ZPn(2)	Starting point for boundary layer calculations (negative value in cm upstream of the throat).
ZPn(3)	Number of profile sections upstream of the throat.*
ZPn(4)	Number of profile sections downstream of the throat.*
ZPn(4+I)	For I = 1 to 12, ISHAPE value for the Ith profile section.*
SPn(16+I)	For I = 1 to 11, the downstream boundary of the Ith profile section in centimeters from the throat (negative upstream).

*These integer data are stored as real values, increased by 0.1 in each case to ensure reliable rounding down to the original integer values when the data are used.

<u>Array Element</u>	<u>Definition</u>
ZPn(24+3I+K)	For K = 1 to 3 and I = 1 to 12, the Kth parameter value P_K (see eqs. 24) for the Ith profile section. The parameters having length dimension are given in centimeters.
ZPn(64)	Facility name (Hollerith data)

The precoded data for standard channels are stored in an array CP(I,ICHAN), dimensioned (5,5). CP is equivalenced to five singly dimensioned arrays, CP1(I), CP2(I),..., CP5(I). each of which contains or can contain the data for a channel. For example, CP1(I) contains the data for ICHAN = 1. The contents of these arrays are defined as follows:

<u>Array Element</u>	<u>Definition</u>
CPn(1)	NPRØFL(1), the index specifying the precoded data for the first profile of the channel; these data are stored in ZPRP(I,NPRØFL(1)) for I = 1 to 64.
CPn(2)	NPRØFL(2), the index specifying the precoded data for the second profile of the channel.
CPn(3)	Channel name (Hollerith data).
CPn(4)	Index (1 or 2) specifying the profile which diverges from the axis least rapidly downstream of the throat (corresponds to NBL in Section 2.3, Group 4).
CPn(5)	Facility name (Hollerith data).

NATA includes precoded data for two channels, as indicated in the definition of ICHAN in Section 2.3 (Group 4).

Figures 47 to 59 are plots showing the throat regions of all of the precoded profiles. Each of these figures shows a 15.24-cm (6-inch) long portion of a profile. The profile actually continues indefinitely far to the right and left of the figure boundaries;

FIGURE 47 - PROFILE FOR DCA 1.90-cm THROAT (N₀ZZLE=1)

DCA 0.75-INCH THROAT

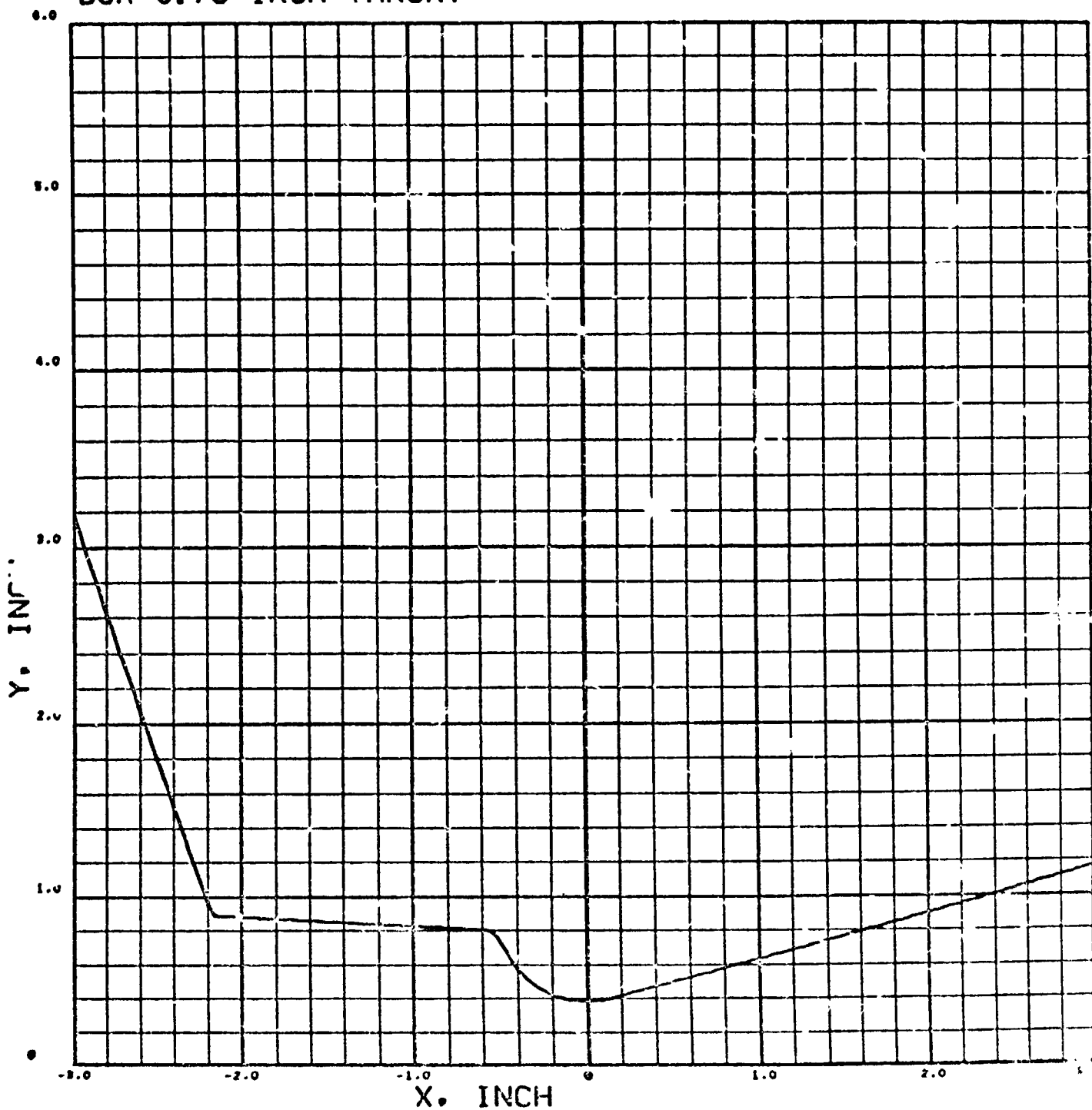


FIGURE 48 - PROFILE FOR DCA 3.81-cm THROAT (NOZZLE=2)

DCA 1.5-INCH THROAT

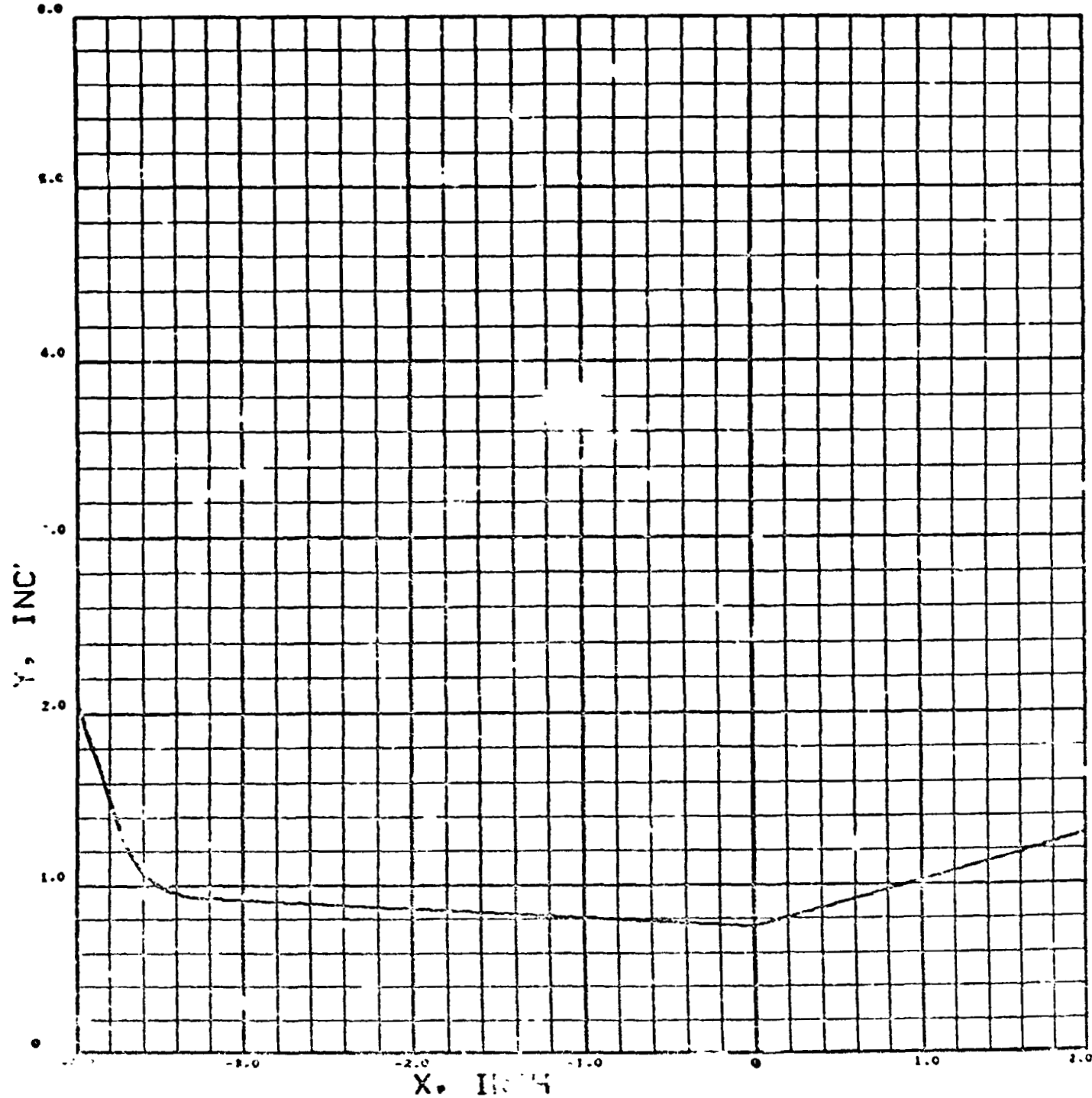


FIGURE 49 - PROFILE FOR MRA 5.72-cm THROAT (NOZZLE=3)

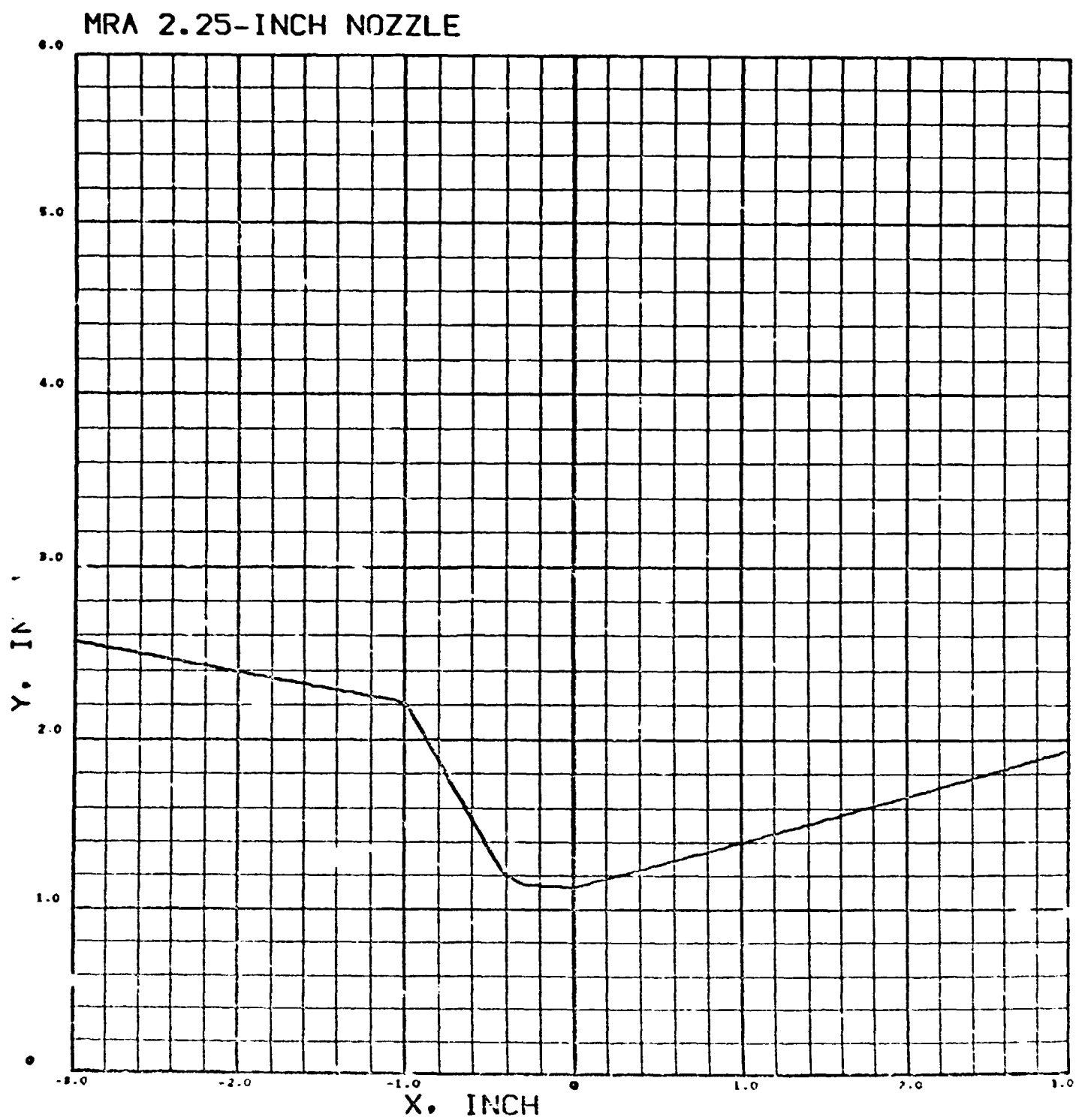


FIGURE 50 - PROFILE FOR MRA 2.54-cm THROAT (N₀ZZLE=4)

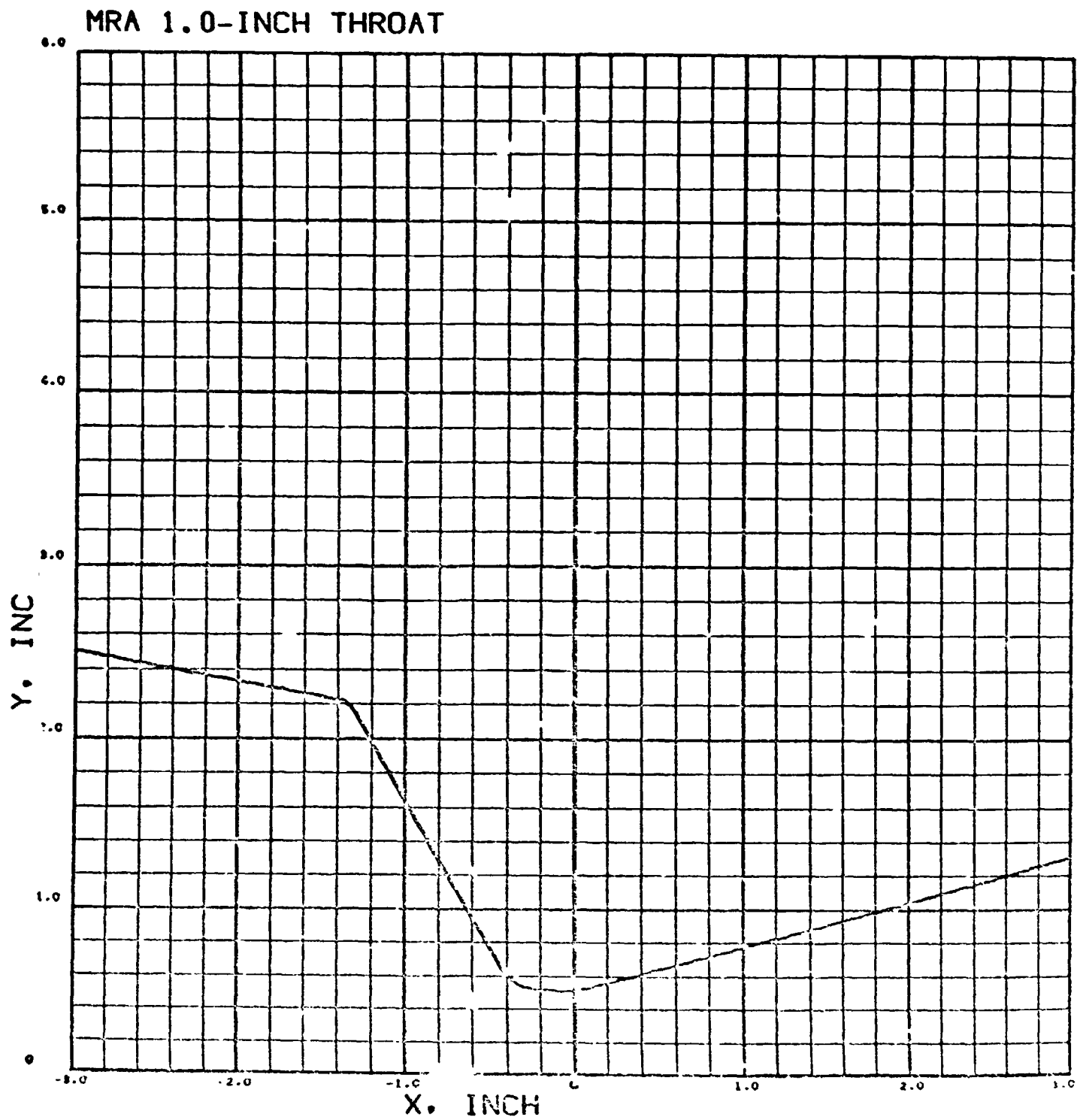


FIGURE 51 - PROFILE FOR EOS 0.81-cm THROAT (NOZZLE=5)

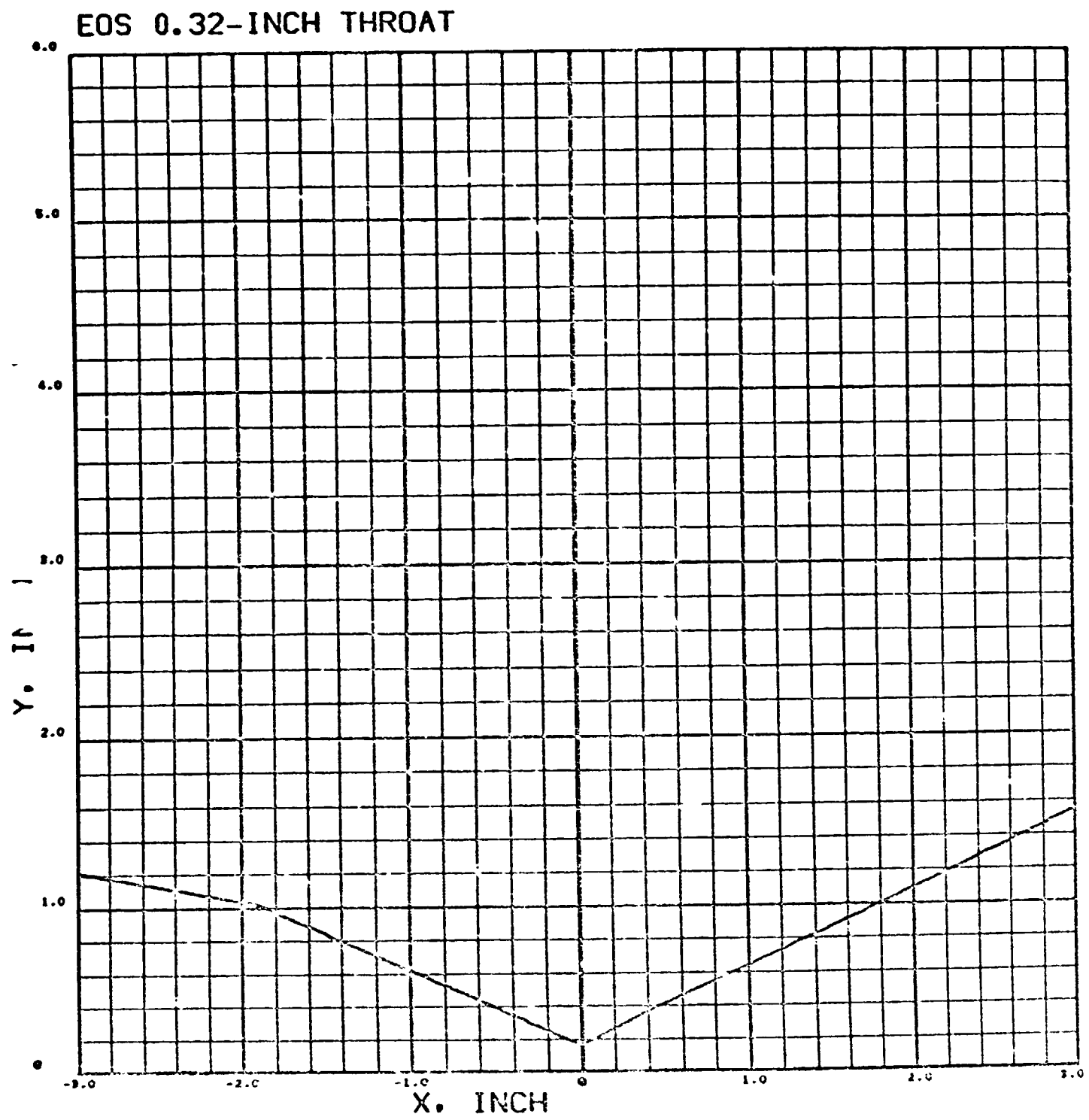


FIGURE 52 - PROFILE FOR EOS 1.97-cm THROAT (NOZZLE=6)

EOS 0.775-INCH THROAT

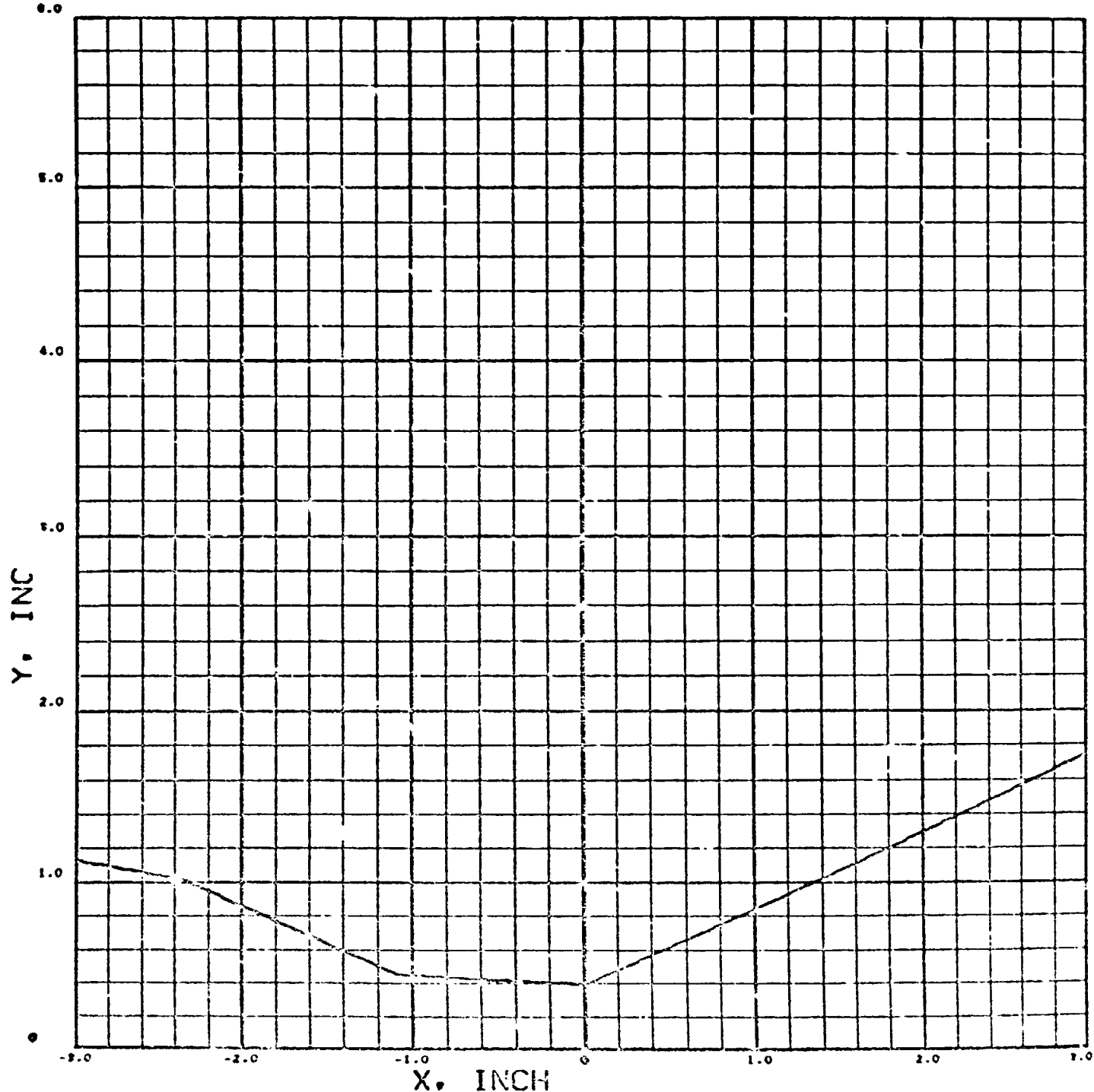


FIGURE 53 - PROFILE FOR MRA 1.90-cm THROAT (N₀ZZLE=7)

MRA 0.75-INCH THROAT

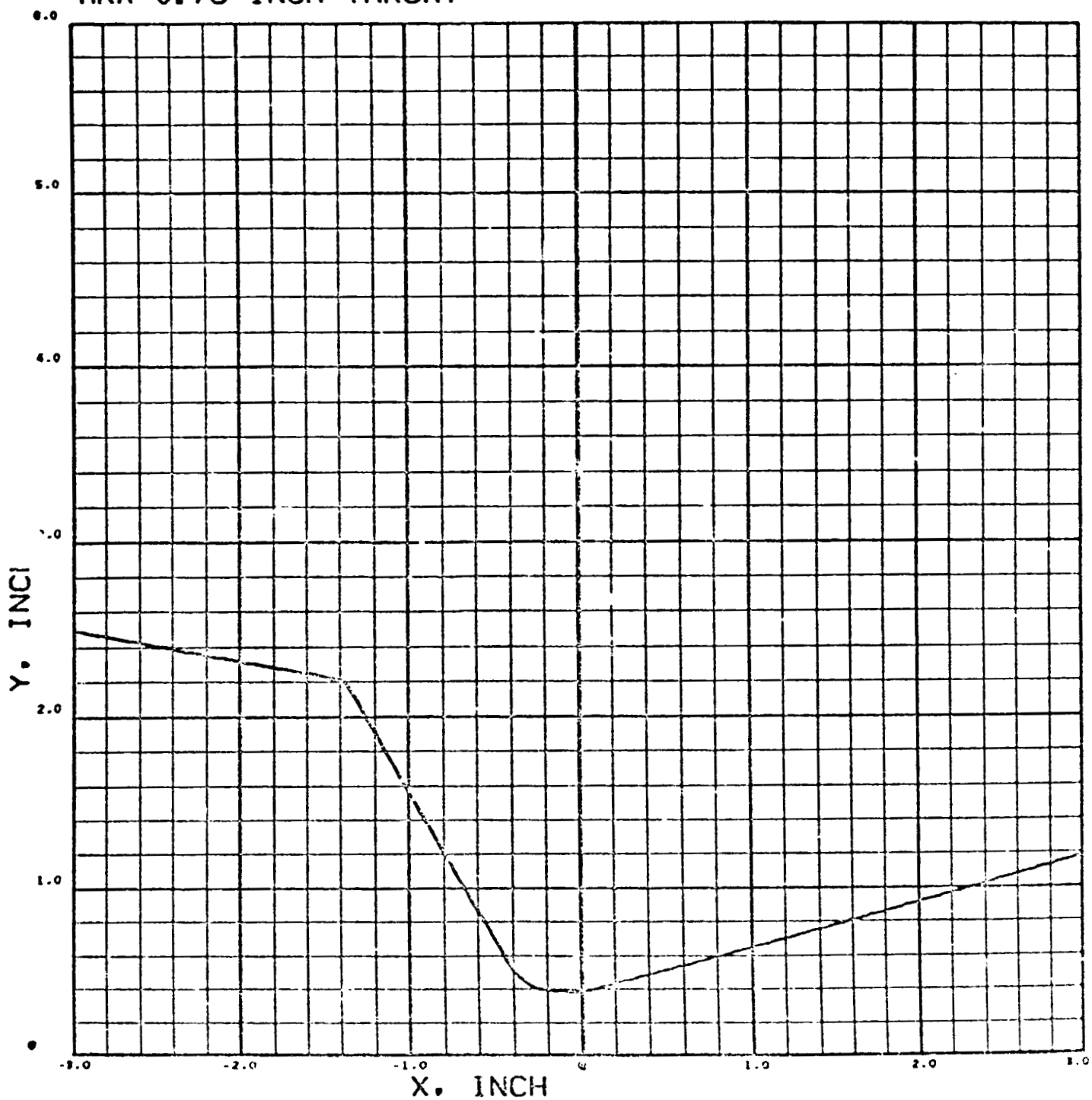


FIGURE 54 - PROFILE FOR MRA 3.81-cm THROAT (NOZZLE=8)

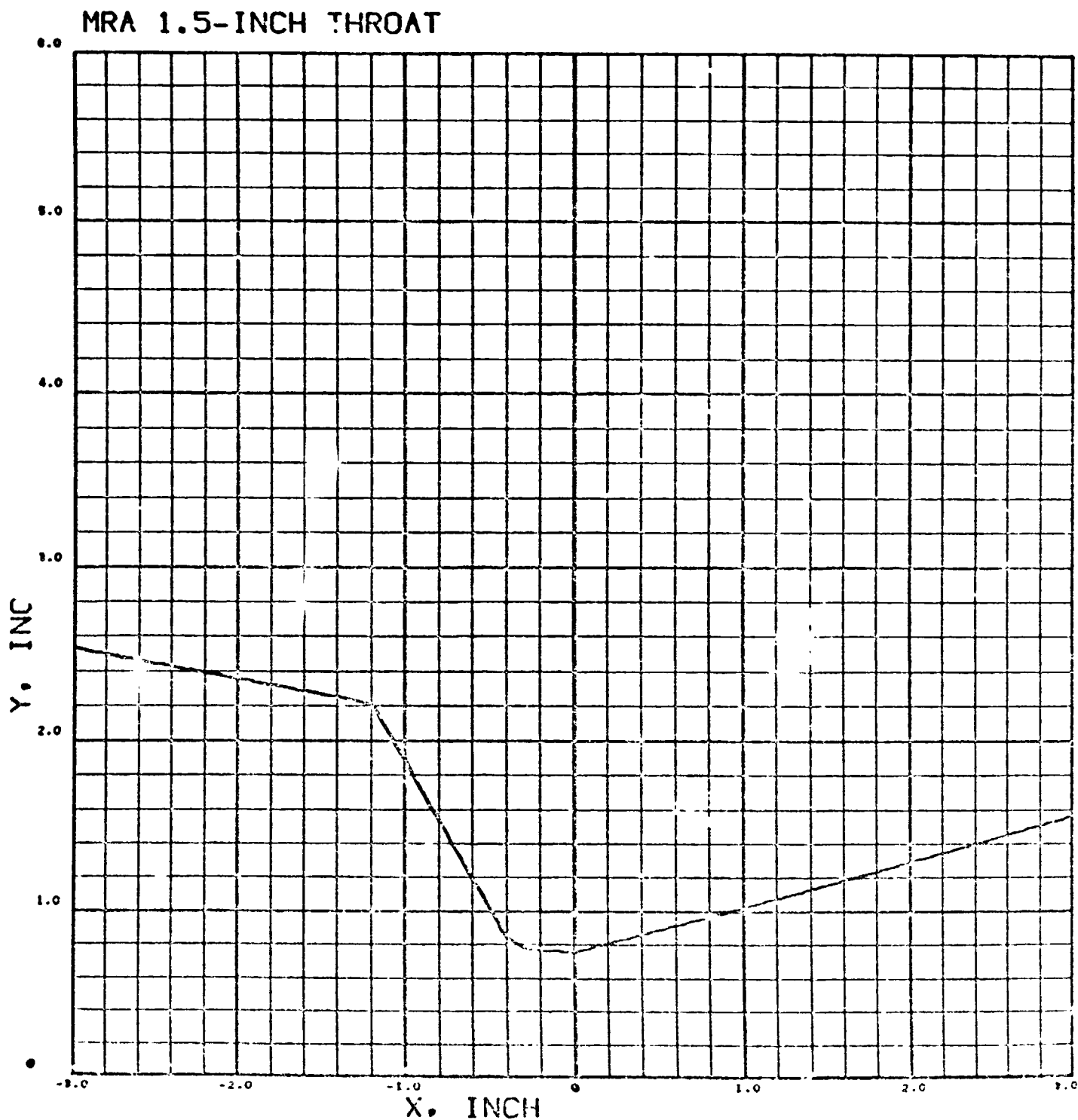


FIGURE 55 - PROFILE FOR 10 MW 5.72-cm THROAT (NOZZLE=9)

10MW 2.25-INCH NOZZLE

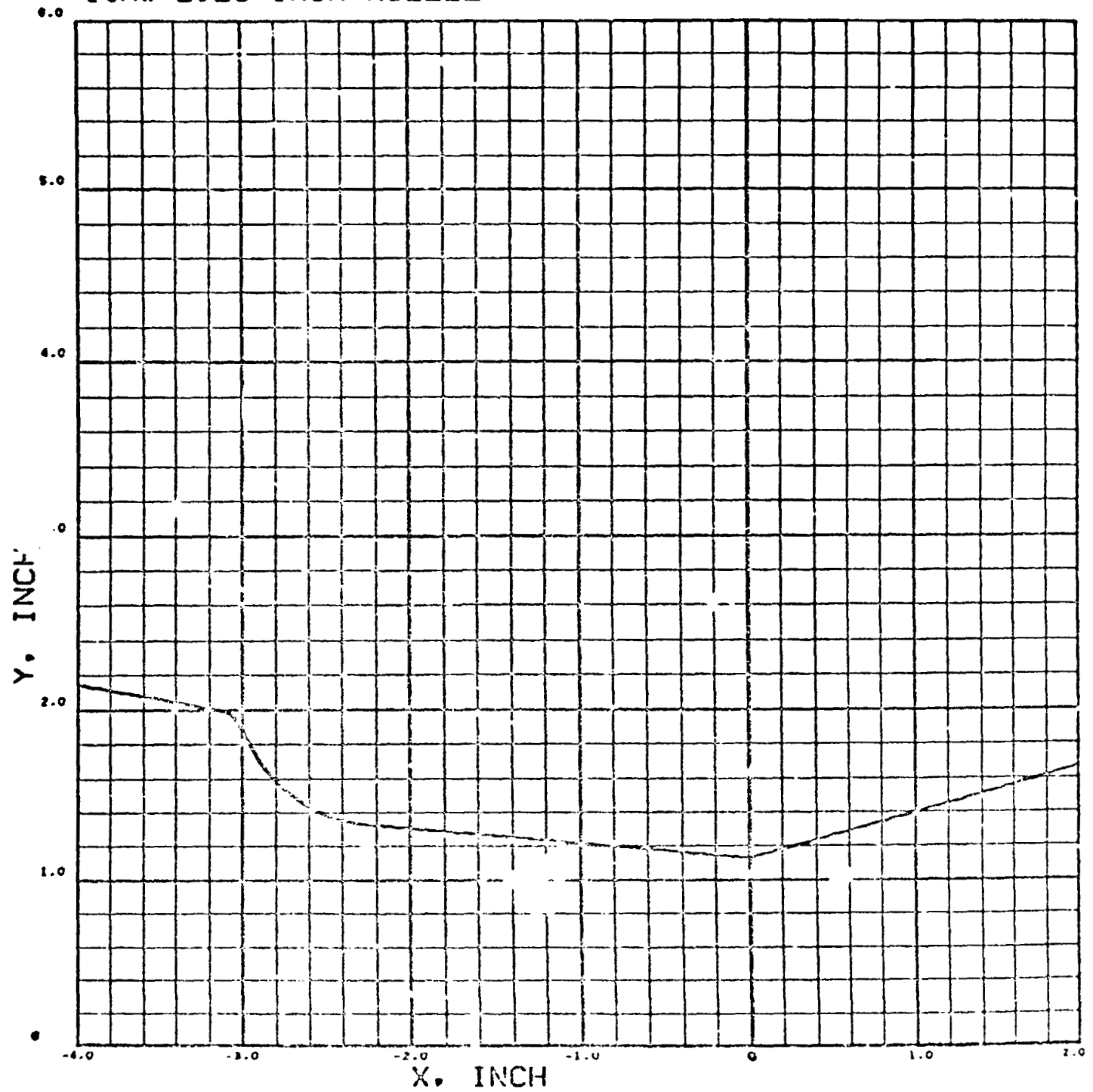


FIGURE 56 - PROFILE FOR EOS 2.77-cm THROAT (N₀/ZZLE=10)

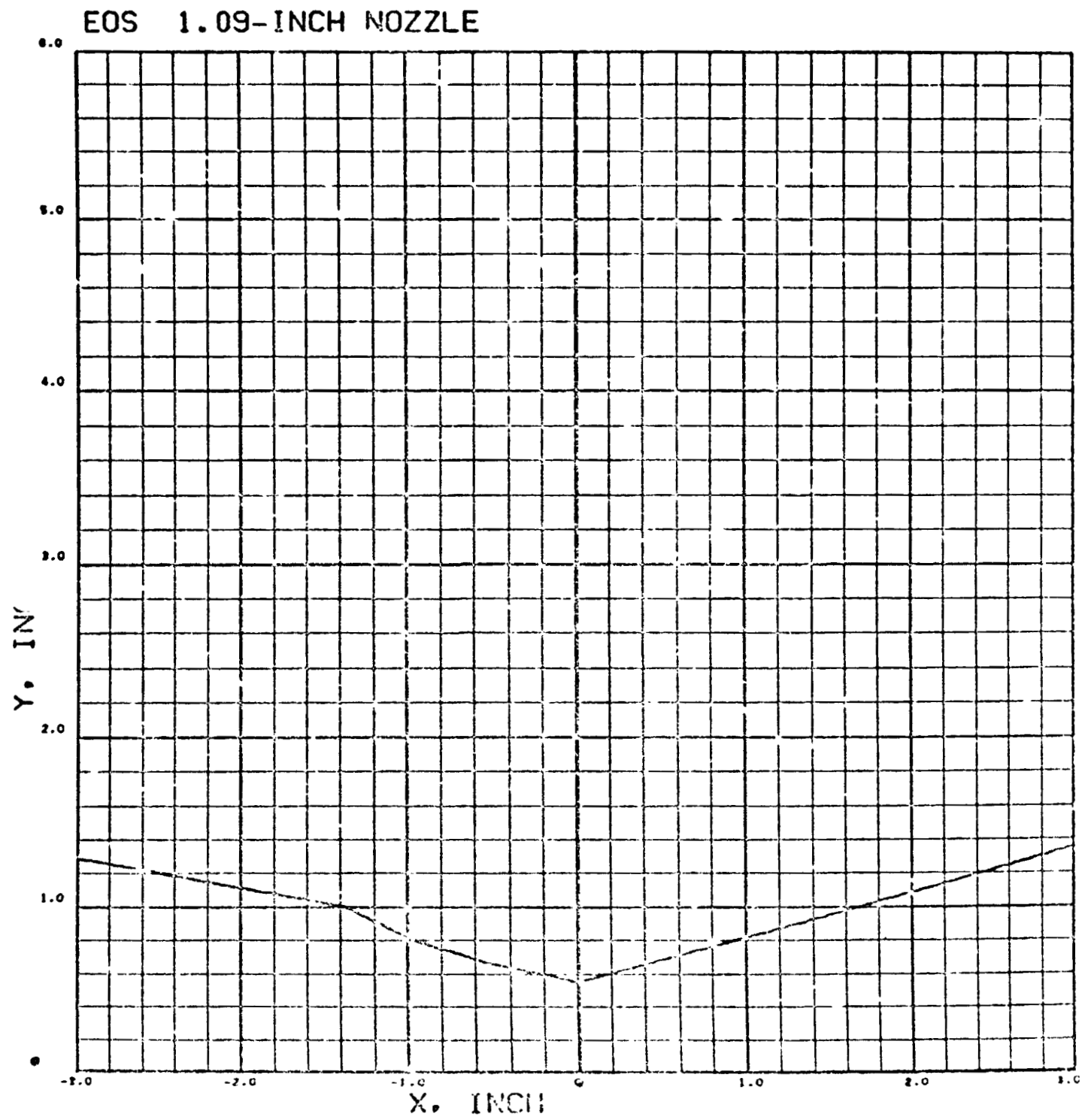


FIGURE 57 - FIRST PROFILE FOR T12 AND T22 CHANNELS (NPRØFL=11)

DCA T12 CHANNEL, PROFILE 1

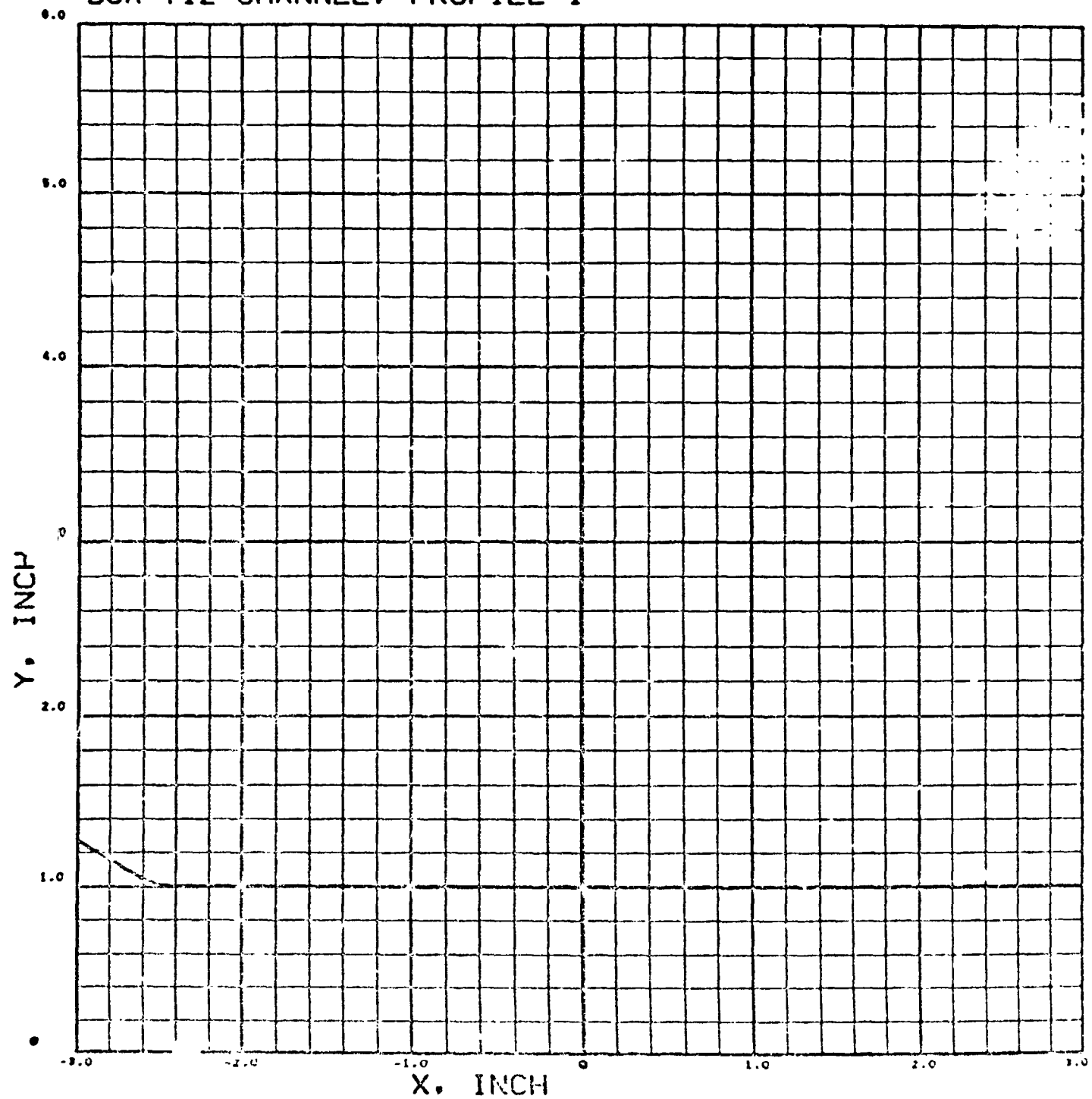


FIGURE 58 - SECOND PROFILE FOR T12 CHANNEL (NPR \varnothing FL=12)

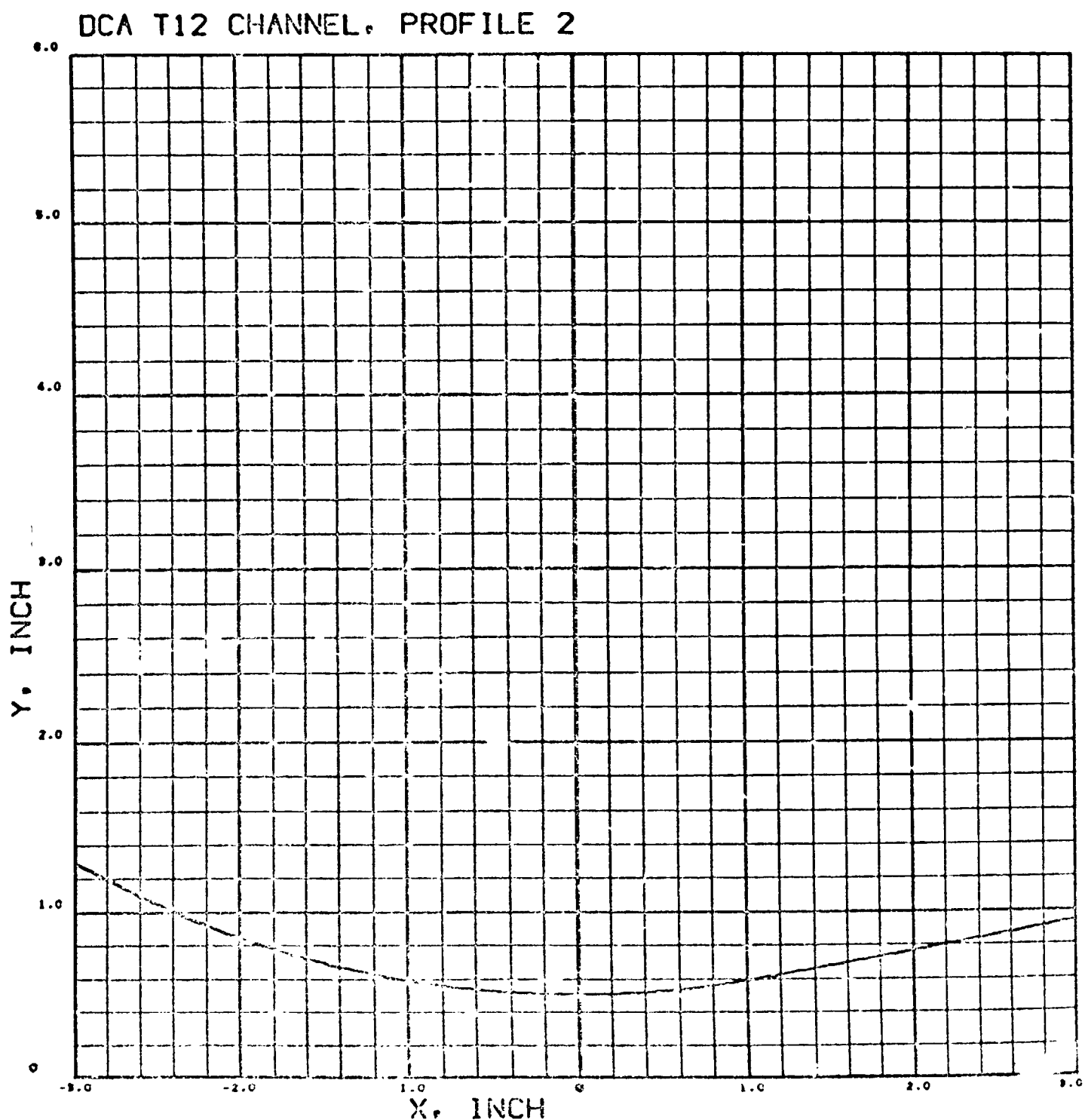
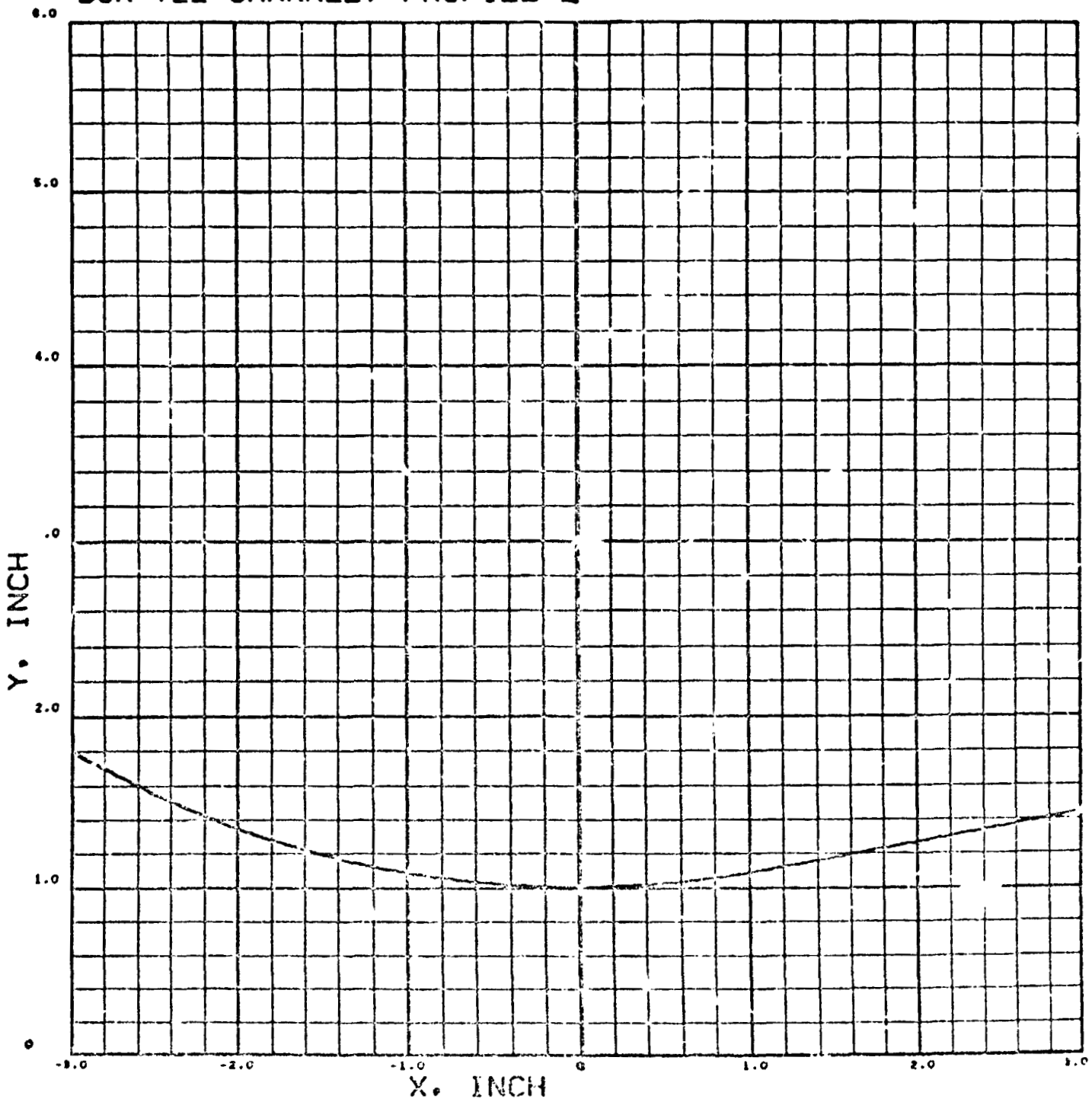


FIGURE 59 - SECOND PROFILE FOR T22 CHANNEL (NPR₀FL=13)

DCA T22 CHANNEL, PROFILE 2



the program uses as much of the mathematically defined profile as it needs in each problem. The plots shown in figures 47-59 were produced by the NOZFIT code, an auxiliary computer program for setting up NATA-type profile curvefits from data provided by nozzle design drawings. A user's manual for NOZFIT is included in the present report (Appendix D).

The profiles as used in NATA, and as shown in the figures, differ in several respects from the profiles of the actual nozzle hardware:

- (1) The NATA profiles expand conically to the left (in the upstream direction), while the actual nozzles have finite-diameter plenum or arc-chamber radii.
- (2) Sharp corners in the actual nozzle profiles are rounded in the NATA fits, to provide continuity of the profile slope (dy/dx) as required by the code. A standard 0.127 cm (50-mil) rounding radius is used, except in cases where a larger radius has proved necessary for code reliability.
- (3) In the fits for many of the nozzles, sections of constant radius near the throat are represented as conical, usually with a 3° convergence half angle. This is done to avoid instabilities in the nonequilibrium solution (Section 4.3, Volume I).

APPENDIX A

REACTION DATA FOR THE HELIUM AND ARGON MODELS

This appendix documents the reaction system and the electronic nonequilibrium parameters assumed in the standard gas models for helium (IGAS = 4) and argon (IGAR = 3). In addition to chemical nonequilibrium these models include effects of non-equilibrium excitation of the gases by treating each of the important excited states as a separate species. Approximate reaction parameters for the important reactions among these states are then obtained from a survey of the available literature.

The species and parameter values used in the models are given in Tables XIX, XX, XXI, and XXII. The reasons for choice of the tabulated values are discussed below.

A.1 Helium Model.

Elastic collisions -- The simplest type of collision process occurring in a gas is the elastic collision in which kinetic energy is transferred from one particle to another without any change in the internal structure or excitation of the particles. Although such collisions obviously do not contribute to the species production term r_j in equation (321a) of Volume I, the kinetic energy transferred between electrons and heavy particles in elastic collisions can be important in determining the net energy gain term \dot{q}_e for the electron gas. Under the assumption that the electrons and heavy particles have Maxwellian velocity distributions corresponding to the temperatures T_e and T , respectively, it can be shown (ref. 51) that the contribution to the electron energy gain term \dot{q}_e in equation (321c) (Volume I) due to elastic collisions is given to a very good approximation by the formula*

$$\dot{q}_{elas} = \sum_{j=2}^n \epsilon_{j,clas} \frac{N_{ej,clas}}{N_0} \quad (25)$$

*It is assumed in equation (25) and throughout this Appendix that the species $j = 1$ represents the electrons.

ORIGINAL PAGE IS
OF POOR QUALITY

TABLE XXX
THERMOCHEMICAL DATA FOR HELIUM SPECIES

No.	Symbol	Species Identification	Ground-State Energy* (ev)	Statistical Weight	ω_{e^-} (cm $^{-1}$)	$\omega_{e^-X^+}$ (cm $^{-1}$)	B_{e^-1} (cm $^{-1}$)	v' (cm $^{-1}$)	r_e (Å)	Reference
1	e^-	Electron	0.0	2						Ref. 6
2	He	Ground-state helium atom	0.0	1						Ref. 6
3	He (3S)	Metastable helium atom $1s2s3S$	19.813	3						Ref. 6
4	He (1S)	Metastable helium atom $1s2s1S$	20.609	1						Ref. 6
5	He $^+$	Ground-state atomic ion He $^+$ (1s2S)	24.580	2						Ref. 6
6	He $_2$	Metastable helium molecule He $_2$ (${}^3\Sigma_u^+$)	17.937	3	1809.9	38.8	7.710	.243	1.045	Refs. 9, 12, 70
7	He $_2$ $^+$	Ground-state helium molecular ion He $_2$ $^+$ (${}^1\Sigma_u^+$)	22.190	2	1698.5	35	7.211	.224	1.08	Refs. 9, 12, 70

*For molecular species, the tabulated ground-state energy is the energy of the lowest vibrational level, $v = 0$.

ORIGINAL PAGE IS
OF POOR QUALITY

TABLE XX
REACTION RATE PARAMETERS FOR HELIUM

Reaction No.	Reaction	Forward Reaction Rate				Reverse Reaction Rate				Energy Transfer Terms (kcal/mole)			
		A ^a	η	E/R (OK)	j ^b	ϵ_4	ϵ_r	\dot{q}_r	\dot{q}_x				
1	$\text{He}^+ + e^- \rightarrow \text{He}(^3S) + e^-$	5.46×10^{21}	-4.3	0.0	e	2	109.89	109.89	0.	0.	0.	0.	0.
2	$\text{He}^+ + e^- \rightarrow \text{He}(^1S) + e^-$	1.92×10^{21}	-4.3	0.0	e	2	91.54	91.54	0.	0.	0.	0.	0.
3	$\text{He}^+ + e^- \rightarrow \text{He}(^3\sigma)$	1.27×10^{11}	-0.81	0.0	e	0	-3/2 R ₀ T _e	—	109.89 + 3/2 R ₀ T _e	—	—	—	—
4	$\text{He}^+ + e^- \rightarrow \text{He}(^1S)$	3.30×10^{10}	-0.85	0.0	e	0	-3/2 R ₀ T _e	—	91.54 + 3/2 R ₀ T _e	—	—	—	—
5	$\text{He}^+ + e^- \rightarrow \text{He}$	0	-0.47	0.0	e	0	-3/2 R ₀ T _e	—	566.6 + 3/2 R ₀ T _e	—	—	—	—
6	$\text{He}(^3S) + e^- \rightarrow \text{He} + e^-$	8.0×10^{14}	-0.25	640.	e	2	456.73	456.73	0.	0.	0.	0.	0.
7	$\text{He}(^1S) + e^- \rightarrow \text{He} + e^-$	8.0×10^{14}	-0.25	640.	e	2	475.04	475.04	0.	0.	0.	0.	0.
8	$\text{He}(^1S) + e^- \rightarrow \text{He}(^3S) + e^-$	3.65×10^{16}	-0.5	0.	e	2	18.35	18.35	0.	0.	0.	0.	0.
9	$\text{He}(^3S) + \text{He}(^3S) \rightarrow \text{He} + \text{He}^+ + e^-$	1.87×10^{15}	0.167	0.	g	2	346.84	346.84	0.	0.	0.	0.	0.
10	$\text{He}(^3S) + \text{He}(^1S) \rightarrow \text{He} + \text{He}^+ + e^-$	5.05×10^{15}	0.167	0.	g	2	365.19	365.19	0.	0.	0.	0.	0.
11	$\text{He}(^1S) + \text{He}(^1S) \rightarrow \text{He} + \text{He}^+ + e^-$	6.28×10^{15}	0.167	0.	g	2	383.54	383.54	0.	0.	0.	0.	0.
12	$\text{He}(^1S) + \text{He} \rightarrow 2\text{He}$	5.2×10^{10}	0.0	800.	g	0	0.	—	475.08	—	—	—	—
13	$\text{He}(^3S) + 2\text{He} \rightarrow \text{He}_2 + \text{He}$	5.2×10^{14}	0.5	0.0	g	1	0.	0.	0.	0.	0.	0.	0.
14	$\text{He}^+ + \text{He} \rightarrow \text{He}_2^+ + \text{He}$	3.92×10^{16}	0.	0.0	g	1	0.	0.	0.	0.	0.	0.	0.
15	$\text{He}_2^+ + e^- \rightarrow \text{He}_2 + e^-$	1.54×10^{21}	-4.3	0.0	e	2	98.04	98.04	0.	0.	0.	0.	0.
16	$\text{He}_2^+ + e^- \rightarrow \text{He} + \text{He} + e^-$	5.13×10^{20}	-4.3	0.0	e	2	458.27	458.27	c.	c.	0.	0.	0.
17	$\text{He}_2^+ + e^- \rightarrow \text{He}(^3S) + \text{He}$	2.26×10^{14}	0.0	0.0	e	1	-3/2 R ₀ T _e	-3/2 R ₀ T _e	0.	0.	0.	0.	0.
18	$\text{He}_2^+ + e^- \rightarrow \text{He}(^1S) + \text{He}$	7.5×10^{13}	0.0	0.0	e	1	-3/2 R ₀ T _e	-3/2 R ₀ T _e	0.	0.	0.	0.	0.
19	$\text{He}_2 + e^- \rightarrow 2\text{He} + e^-$	8.0×10^{14}	-0.25	640.	e	2	413.48	413.48	0.	0.	0.	0.	0.
20	$\text{He}_2 + \text{He} \rightarrow 3\text{He} + \text{He}^+ + e^-$	1.87×10^{15}	0.167	0.	g	2	260.35	260.35	0.	0.	0.	0.	0.

a Units are cm³/mole-sec for two-body reactions and cm⁶/mole²-sec for three body reactions.

b c indicates reaction rate calculated using the electron temperature. g indicates reaction rate calculated using the gas temperature.

c 1 indicates reverse reaction calculated from detailed balance using the gas temperature

2 indicates reverse reaction calculated from detailed balance using the electron temperature

0 indicates no reverse reaction or reverse reaction neglected.

TABLE XXI
THERMOCHEMICAL DATA FOR ARGON SPECIES

No.	Symbol	Species Identification	Ground-State Energy* (ev)	Statistical Weight	ω_{e^-} (cm ⁻¹)	B_{e^-} (cm ⁻¹)	r_{e^-} (Å)	Reference
1	e^-	Electron	0.0	2				
2	Ar	Ground-state argon atom	0.0	1				Moore ⁶
3	Ar*(m)	Metastable argon atom ($4s^3P_2$ and $4s^3P_0$)	11.55	6				Moore ⁶
4	Ar*(r)	Resonant state argon atom ($4s^3P_1$ and $4s^1P_1$)	11.62	6				Moore ⁶
5	Ar ⁺	Ground-state argon atomic ion ($3p^5^2P_{3/2}$ and $3p^5^2P_{1/2}$)	15.755	6				Moore ⁶
6	Ar ₂ ⁺	Ground-state argon molecular ion ($X^2\Sigma_u^+$)	14.615	2	80	0.174	2.2	Teng and Conway ¹³

*For molecular species, the tabulated ground-state energy is taken to be the energy of the lowest vibrational level, $v = 0$.

ORIGINAL PAGE IS
OF POOR QUALITY

TABLE XII
REACTION RATE PARAMETERS FOR ARGON

Reaction No.	Reaction	Forward Reaction Rate				Reverse Reaction Rate				Energy Transfer Terms (kcal/mole)			
		A ^a	η	E/R ₀ (°K) ^b	j ^b	Rate _c , k _r	ϵ_f	ϵ_x	\dot{q}_f	\dot{q}_x	\dot{q}_r		
1	Ar ⁺ + e ⁻ ⇌ Ar ^{+(m)} + e ⁻	3.6 × 10 ⁻²¹	-4.3	0.0	e	2	96.97	96.97	0.	0.	0.		
2	Ar ⁺ + e ⁻ ⇌ Ar ^{+(x)} + e ⁻	3.6 × 10 ⁻²¹	-4.3	0.0	e	2	95.36	95.36	0.	0.	0.		
3	Ar ⁺ + e ⁻ → Ar ^{+(m)}	8.2 × 10 ⁻¹⁰	-0.81	0.0	e	0	-0.7 R ₀ T _e	—	96.97 + 0.7 R ₀ T _e	—	—		
4	Ar ⁺ + e ⁻ → Ar ^{+(x)}	8.2 × 10 ⁻¹⁰	-0.81	0.0	e	0	-0.7 R ₀ T _e	—	95.36 + 0.7 R ₀ T _e	—	—		
5	Ar ⁺ + e ⁻ ⇌ Ar ⁺	6.0 × 10 ⁻¹⁰	-0.5	0.0	ed	0	-R ₀ T _e	—	363.33 + R ₀ T _e	363.33 + R ₀ T _e	363.33 + R ₀ T _e		
6	Ar ^{+(m)} + e ⁻ ⇌ Ar ⁺ + e ⁻	5.0 × 10 ⁻¹⁴	0.5	0.0	e	2	266.35	266.35	0.	0.	0.		
7	Ar ^{+(x)} + e ⁻ ⇌ Ar ⁺ + e ⁻	7.2 × 10 ⁻¹³	0.5	0.0	e	2	267.97	267.97	0.	0.	0.		
8	Ar ^{+(x)} + e ⁻ ⇌ Ar ^{+(m)} + e ⁻	1.0 × 10 ⁻¹⁷	-0.5	0.0	e	2	1.60	1.60	0.	0.	0.		
9	Ar ^{+(x)} → Ar	k _f = 8.0 × 10 ⁴ / \sqrt{R} sec ⁻¹	0	0.	—	—	267.97	267.97	—	—	—		
10	Ar ^{+(m)} + Ar ⇌ Ar ⁺ + Ar	3.5 × 10 ⁻⁹	0.5	0.0	g	1	0.	0.	0.	0.	0.		
11	Ar ^{+(m)} + 2Ar → 3Ar	8.7 × 10 ⁻¹⁴	-0.56	0.0	g	0	0.	0.	226.0	0.	226.0		
12	Ar ^{+(x)} + Ar ⇌ 2Ar	3.5 × 10 ⁻⁹	0.5	0.0	g	1	0.	0.	0.	0.	0.		
13	Ar ^{+(x)} + 2Ar → 3Ar	8.7 × 10 ⁻¹⁴	-0.56	0.0	g	0	0.	0.	226.0	0.	226.0		
14	Ar ⁺ + 2Ar ⇌ Ar ₂ ⁺ + Ar	5.2 × 10 ⁻¹⁵	0.75	0.0	g	1	0.	0.	0.	0.	0.		
15	Ar ₂ ⁺ + e ⁻ ⇌ Ar ^{+(m)} + Ar	$\left\{ \begin{array}{l} k_f = 2.8 \times 10^{16} (\tau_g / 10^4 \text{ °K})^{-0.67} \\ \times [1 - \exp(-630^\circ \text{K} / \tau_g)] \end{array} \right.$	2	70.68	70.68	0.							
16	Ar ₂ ⁺ + e ⁻ ⇌ Ar ^{+(x)} + Ar		2	69.07	69.07	0.							
17	Ar ₂ ⁺ + 2e ⁻ ⇌ 2Ar + e ⁻	2.0 × 10 ⁻²¹	-4.3	0.0	e	2	337.0	337.0	0.	0.	0.		

a Units are cm³/mole-sec for two-body reactions and cm⁶/mole²-sec for three body reactions.

b e indicates reaction rate calculated using the electron temperature. g indicates reaction rate calculated using the gas temperature.

c 1 indicates reverse reaction calculated from detailed balance using the gas temperature.

2 indicates reverse reaction calculated from detailed balance using the electron temperature.

0 indicates no reverse reaction or reverse reaction neglected.

d The forward rate constant for reaction 5 is reduced by a factor of 1/τ whenever τ = 3.4 × 10⁻¹⁷ n_{Ar} R is greater than 1, R is the nozzle radius in cm and n_{Ar} the ground state Ar number density in cm⁻³.

where the sum extends over all heavy particles j present in the gas,

$$\epsilon_{j,\text{elas}} \equiv (2w_e/w_j) \frac{3}{2} R_0 (T - T_e) \quad (26)$$

represents the mean energy gained by the electrons in N_0 elastic collisions with particles of the j th species and

$$N_{ej,\text{elas}} \equiv n_e \nu_{ej} \equiv N_0 k_{ej,\text{elas}} (\rho \gamma_e) (\rho \gamma_j) \quad (27)$$

represents the number of elastic collisions occurring between electrons and particles of the j th species per unit volume per unit time. Here

$$n_j = N_0 \rho \gamma_j \quad (28)$$

is the number of particles of the j th species per unit volume, $\nu_{ej} \equiv n_j k_{ej,\text{elas}} / N_0$ is the momentum transfer collision frequency for elastic collisions between electrons and particles of the j th species, and the reaction rate $k_{ej,\text{elas}}$ is given by

$$k_{ej,\text{elas}} / N_0 \equiv \frac{4}{3} \sqrt{\frac{8 R_0 T_e}{\pi w_e}} \bar{\sigma}_{ej}^{(1,1)} \quad (29)$$

where

$$\bar{\sigma}_{ej}^{(1,1)} \equiv \frac{1}{2(kT_e)^3} \int_0^\infty w^2 e^{-w/kT_e} \sigma_{ej}^m(w) dw \quad (30)$$

is the Maxwell-averaged momentum transfer cross section for elastic collisions between electrons and particles of species j at the temperature T_e and $\sigma_{ej}^m(w)$ is the actual momentum transfer cross section as a function of electron energy w .

The integral in equation (30) has been evaluated approximately for electron-ion collisions in reference 51 to obtain

$$\begin{aligned}\bar{\Omega}_{ej}^{(1,1)} &= \frac{\pi}{4} \frac{e^4}{(kT_e)^2} \ln \left[\frac{(kT_e)^3}{\pi n_e e^6} \right] \\ &= \frac{2.193 \times 10^{-6}}{T_e^2} \ln \left(\frac{6.821 \times 10^7 T_e^3}{n_e} \right) \text{ cm}^2 \text{ for ions}\end{aligned}\quad (31)$$

in the limit when the logarithm in (31) is much greater than 1, where T_e is in $^{\circ}\text{K}$ and n_e in cm^{-3} . This approximation should be adequate for most cases of interest in the present study.

To obtain the cross section $\bar{\Omega}_{ej}^{(1,1)}$ for ground-state helium atoms, we have evaluated the integral in (30) numerically using literature data on the electron-helium momentum transfer cross section $\sigma_{e-\text{He}}^m(w)$ as a function of electron energy. Below an electron energy of 5 ev, we have used the recent experimental measurements of Crompton, Elford, and Robertson (ref. 52), who give values of the electron-helium momentum transfer cross section

$\sigma_{e-\text{He}}^m$ in the energy range from 0.008 ev to 6 ev with an estimated experimental error of about 2 percent. Since accurate experimental data on the momentum transfer cross section are not presently available for electron energies above 6 ev, we have obtained the cross sections in this range by integrating the theoretical differential scattering cross sections of LaBahn and Callaway (ref. 53) over the scattering angle. On the basis of comparisons with experimental data at both low and high ($\gtrsim 100$ ev) energies, LaBahn and Callaway estimate that their cross sections should be accurate to within about 5% in this energy range.

Figure 60 shows the electron-helium momentum transfer cross sections obtained from the data of Crompton, Elford, and Robertson (ref. 52) and from LaBahn and Callaway (ref. 53) as a function of electron energy. The results of these two studies are in good agreement for electron energies near the upper limit of Crompton's measurements at 5 ev. For the present calculations, we have adopted the cross section values of Crompton, Elford, and Robertson below 5 ev and those of LaBahn and Callaway above 5 ev, as shown by the solid curve in figure 60. Using this adopted cross section, the integral in equation (30) was evaluated numerically to obtain the Maxwell-averaged electron-helium cross section $\bar{\Omega}_{e-\text{He}}^{(1,1)}$ shown in figure 61 as a function of electron temperature. Since numerical errors in the integration process should be negligible, the accuracy of the averaged cross section shown in figure 61 is

FIGURE 60 - MOMENTUM TRANSFER CROSS SECTION FOR ELECTRON-HELIUM COLLISIONS

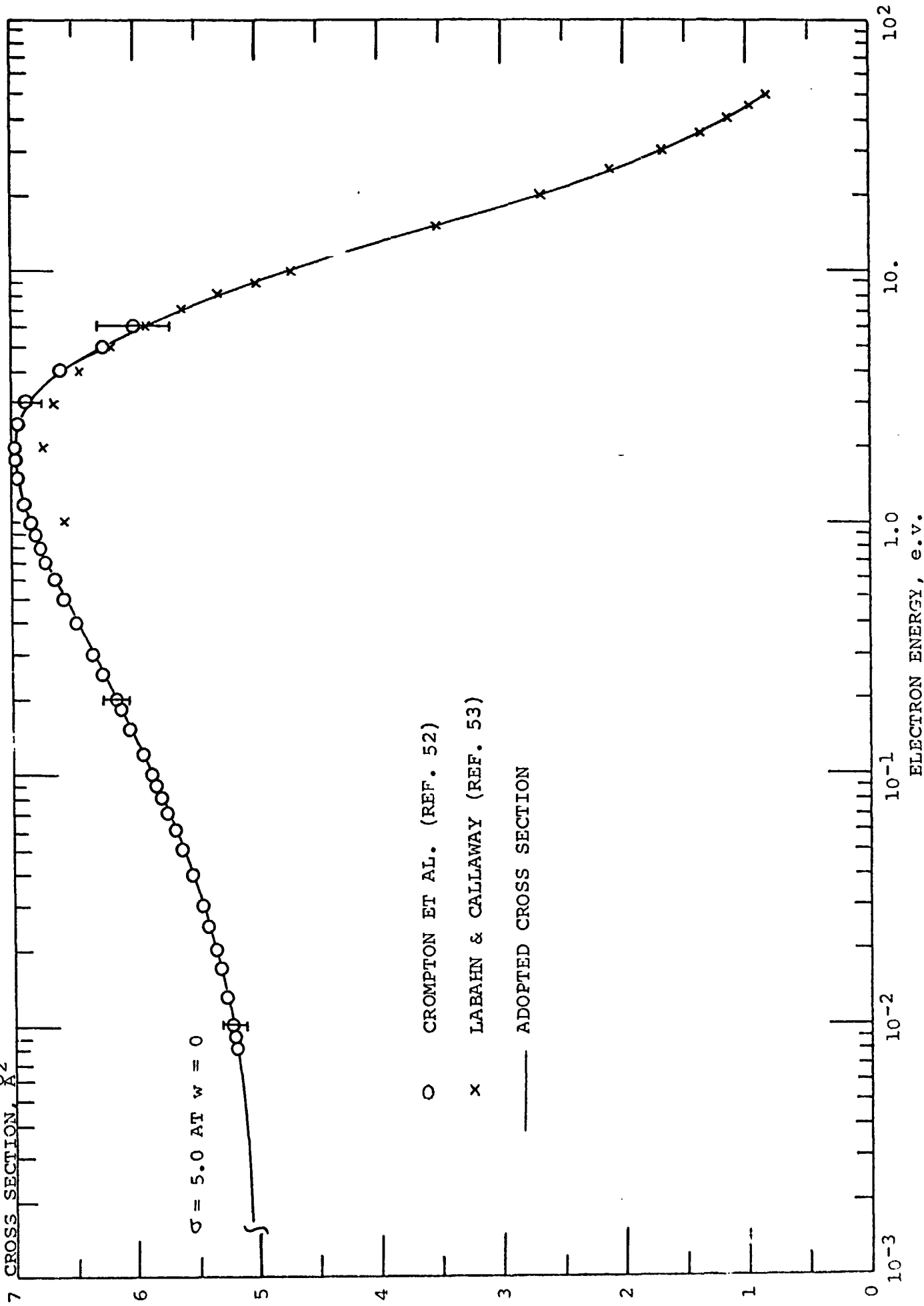
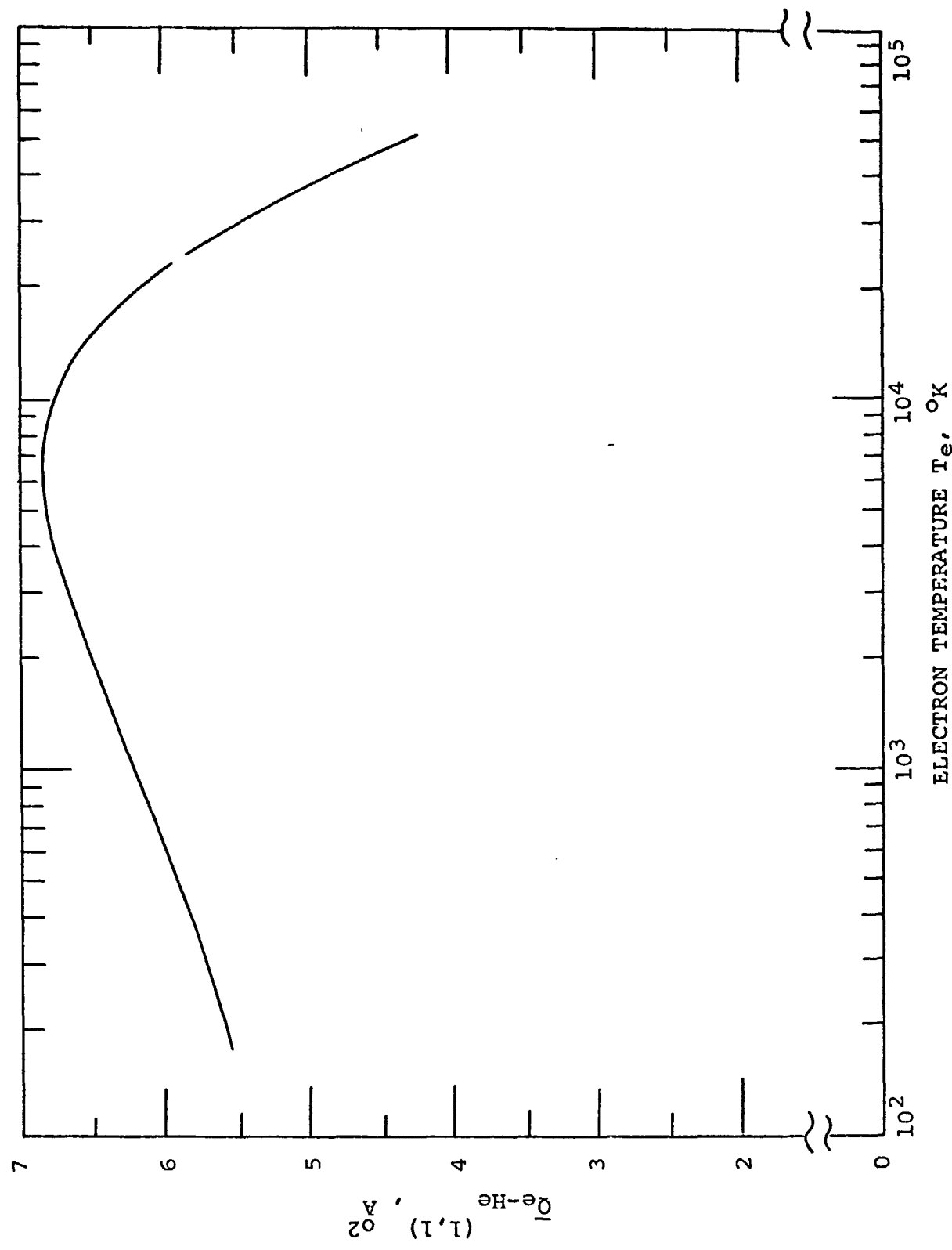


FIGURE 61 - MAXWELL AVERAGED ELECTRON-HELIUM MOMENTUM TRANSFER CROSS SECTION,
 $\bar{Q}_{e-\text{He}}^{(1,1)}$



determined by the accuracy of the original cross section data used in the computations, and should be within the 2 percent experimental error of Crompton's measurements over most of the temperature range from 200 to 50,000°K shown in the figure.

Sufficient data to determine accurate elastic collision cross sections for other neutral helium species (i.e., molecules or excited atoms) do not appear to be available at present, and in our calculations we have simply taken the elastic cross sections for such species equal to the cross section for ground-state helium atoms shown in figure 61. Although not accurate in detail, this approximation should have a negligible effect on the final results of the calculations, since, for excited species, the energy transfer due to inelastic processes should almost always be much greater than the elastic losses. Thus whenever the concentration of excited species in the gas becomes large enough to significantly affect the average collision cross section for the gas in equations (25) to (30), the elastic energy loss term (25) will itself become negligible compared to inelastic loss processes in determining the overall energy balance for the electron gas.

In addition to the energy transferred to the heavy particles, elastic collisions also result in some energy loss from the electrons due to free-free radiative processes (bremsstrahlung). In the present model these losses are included as part of the general collisional-radiative mechanism discussed below, so that a separate radiative loss term to account for them is not required in our treatment of elastic collisions. For the usual experimental situation in which the electron thermal energy is small compared to the recombination energy, free-free radiation processes account for only a small part of the total radiative loss from the gas (ref. 54).

Collisional-radiative recombination.— It now appears to be well established that the recombination of atomic ions in a helium plasma occurs primarily by the collisional-radiative process suggested by Bates, Kingston, and McWhirter (ref. 55), in which electrons recombine first into highly excited atomic states and are then stabilized by collisional and radiative transitions to lower states. Detailed calculations of the electronic recombination rates for this mechanism were carried out by Bates, Kingston, and McWhirter under the assumption that atomic excitation accounts for a negligible fraction of the total gas energy, and using approximate theoretical values for the required collisional excitation and de-excitation cross sections between excited atoms and electrons.

This calculation was later extended by Bates and Khare (ref. 56) to account for the stabilization of excited atoms by collisions with ground state neutral atoms, and by Bates, Bell, and Kingston (ref. 57) to obtain a more accurate determination of the population of atoms in metastable excited states. More recently, the original calculations of Bates, Kingston, and McWhirter have been repeated by Johnson and Hinnov (ref. 58) over a limited range of gas conditions using excitation cross sections adjusted to fit their experimental spectroscopic data on the population of excited state atoms in helium. The results of these calculations have been found to be in reasonably satisfactory agreement with available experimental data on the recombination of electrons in helium (refs. 58-60), within the accuracy of the rather large uncertainties presently existing both in the experimental data and in the cross sections assumed in the theoretical calculations. Although these uncertainties have as yet precluded a detailed quantitative test of the accuracy of the theoretical predictions, the basic correctness of the collisional-radiative model appears to be well substantiated by the general agreement between theory and experiment which has been obtained.

Although the collisional-radiative model of Bates, Kingston and McWhirter appears to be the most accurate theory presently available for treating the recombination of atomic ions in helium, there are several disadvantages to the direct use of this model in the NATA code. First, of course, the model requires rather lengthy numerical calculations to determine the electron recombination rate for any given set of gas conditions, so that direct use of this model in a nonequilibrium flow program such as the NATA code, in which reaction rates must be determined at many points, would lead to excessively long execution times for the code. Further, the collisional radiative model requires input data on a large number of excited state excitation and de-excitation cross sections which appear to be known less accurately at present (ref. 58) than are the overall electronic recombination rates (ref. 59). Thus, to obtain accurate results for the recombination rate from the model, it would probably be necessary to carry out a parametric study similar to that of Johnson and Hinnov (ref. 59) in which the excited state cross sections were adjusted to obtain the best fit between the theoretical predictions and available experimental data, and these adjusted cross sections were then used in the theoretical model to predict the electronic recombination rate as a function of gas conditions. Such a study would go beyond the scope of the present effort; and furthermore, since sufficient data are

not presently available to uniquely determine the large number of adjustable cross sections in the model, the final accuracy which could be obtained in the recombination rates by this approach is somewhat uncertain. For the present study we have, therefore, adopted a simpler and less ambitious approach in which the electronic recombination rates calculated by Bates, Kingston, and McWhirter are curvefitted as a function of electron temperature and number density by a simple analytic formula and the parameters in this curvefit are then adjusted to give recombination rates in agreement with experiment. Following Bowen and Park (ref. 19), we have taken this curvefit to be of the form

$$k_f = a_1 T_e^{-\alpha_1} n_e + a_2 T_e^{-\alpha_2} \quad (32)$$

where the a_i and α_i are adjustable constants. This form has the correct theoretical dependence on electron density in the limits of high and low electron densities and, with the proper choice of constants, can be made to fit the calculations of Bates, Kingston, and McWhirter (ref. 55) at intermediate electron densities within about a factor of three over the entire range of conditions covered in their calculations (i.e., for electron temperatures from 250 to 64000°K and electron number densities from 10^8 to $10^{18}/\text{cm}^3$). Although a more accurate approximation could no doubt be obtained, we feel that the accuracy of equation (32) is probably consistent with the accuracy of the other approximations made in the model, and should be adequate to give a good prediction of the overall heat balance and flow parameters for the arc tunnel. Details of the electron number and excited state distributions in the flow may be less accurately given, however.*

The recombination of electrons in helium plasmas has been extensively studied experimentally (ref. 60). The status of these experimental studies has been summarized recently by Collins, et.al. (ref. 60). Initially, many of the experiments appeared to give discordant results, apparently because of uncertainties as to the exact ion involved in the recombination process

*Note, however, that because of the steep dependence of the recombination coefficient on electron number density and temperature, the error in these parameters at any point in the flow resulting from the curvefit (32) will be much less than the error in the curvefit itself (ref. 61).

and in the electron temperature. However, in the more recent experiments, in which care has been taken to identify the experimental parameters more exactly, a more consistent picture of the recombination process has begun to emerge, although some points still remain unclear. For the present study, we have adopted the recombination coefficient for electrons and atomic helium ions at high electron densities which has been recommended by Collins, et. al. (ref. 60) on the basis of a fit to their own experimental data and earlier data in which the ions involved appeared to be clearly identified (ref. 59). This yields for the high density portion of the curvefit (32),

$$k_{f1} = 7.1 \times 10^{-20} (T_e/300^\circ K)^{-4.3} n_e \text{ cm}^3/\text{sec} \quad (33)$$

for the recombination of electrons and atomic He^+ ions.

In the low electron density region, electronic recombination rates are controlled by the direct radiative recombination of electrons and positive ions, as discussed in detail, for example, by Bates & Dalgarno (ref. 62). A fit to the theoretical calculations of Burgess and Seaton (ref. 63) gives the recombination rates for He^+ ions in this region as follows:

$$k_f = 6.3 \times 10^{-14} (T_e/10^4 \text{ }^\circ\text{K})^{-0.85} \text{ cm}^3/\text{sec} \quad (34a)$$

for recombination into excited singlet states of the He atom,

$$k_f = 2.10 \times 10^{-13} (T_e/10^4 \text{ }^\circ\text{K})^{-0.81} \text{ cm}^3/\text{sec} \quad (34b)$$

for recombination into excited triplet states of the He atom, and

$$k_f = 1.59 \times 10^{-13} (T_e/10^4 \text{ }^\circ\text{K})^{-0.47} \text{ cm}^3/\text{sec} \quad (34c)$$

for direct radiative recombination into the ground state He atom.

To determine the remaining parameters required for the recombination of electrons and He^+ ions in our reaction rate model (equations (320) and (321) in Vol. I), it is necessary to specify the species formed in the recombination reaction and the fraction of the recombination energy going into the electron gas and into

radiation. Although recombination occurs initially into highly excited atomic states, Bates et. al (ref. 55) have shown that the net change in population of these states is negligible under conditions for which the collisional-radiative model is applicable, so that the state of the plasma can be described completely over times of interest for macroscopic flow problems by giving simply the net rates of recombination into the ground state helium atom and the two metastable excited states He ($1s2s\ 3S$) and He ($1s2s\ 1S$). Further, it has been pointed out by Bates, Bell, and Kingston (ref. 57) that, under optically thick conditions, practically all recombining electrons in a helium plasma will pass through one of the metastable excited states before reaching the ground state, so that it is not necessary to consider recombination directly into the ground state. This follows because the cross sections for collisional de-excitation directly into the ground-state are much smaller than those for de-excitation into one of the metastable states when the electron energy is of the order of a few electron volts or less, while direct radiative transitions to the ground state are not effective in de-exciting the gas when the plasma is optically thick, since the emitted radiation is re-absorbed by ground state atoms to produce new excitation before it can leave the plasma.

For helium plasmas at temperatures of the order of a few ev or less, the mean free path for the line radiation emitted by radiative transitions to the ground state is of the order of $10^{14}/n_0$ cm at the line center*, where n_0 is the number of ground state atoms per cm^3 . Thus, for the conditions of interest in the NATA code, essentially all of this radiation will be re-absorbed before it can escape from the plasma. Accordingly, the gas will be optically thick to this radiation and direct radiative transitions from excited atoms to the ground state may be neglected to a good approximation in the code.

The situation is less clear for the continuum radiation which results from direct radiative recombination of free electrons into the ground state according to the process indicated in equation (34c). For this radiation the mean free path is about $1.6 \times 10^{17}/n_0$ cm**, so that, for example for helium at 20,000°K and atmospheric pressure the mean free path would be about 0.5 cm. This is somewhat smaller than typical nozzle dimensions, so that under these

*This estimate assumes Doppler broadening of the line profiles; this should be valid under the conditions of interest except for very high excited states.

**Calculated from (34c), using detailed balance.

conditions one might expect that the larger part of the continuum radiation (34c) would be re-absorbed and re-ionize the gas, but a significant fraction, especially near the edges of the nozzle, would escape. As the gas expanded down the nozzle, the ratio of the radiative mean free path to the nozzle dimensions would increase, so that eventually a point would be reached at which most of the continuum radiation (34c) escaped. For higher initial pressures or lower initial temperatures, on the other hand, the mean free path of the radiation would be decreased, so that under some conditions it might be a good approximation to treat the flow as optically thick to the continuum radiation (34c) over the major portion of its expansion.

Although the helium kinetic model developed in this appendix does not contain any provisions for treating radiative re-absorption in the gas explicitly, one can allow approximately for this effect by adjusting the radiative recombination rate for the process (34c) so as to match the net radiative recombination expected in the flow as well as possible. For this purpose it is probably most important to match the net recombination rate in the high temperature region near the nozzle entrance, since the importance of radiative recombination is expected to decrease as the flow expands (see equations (33) and (34)), and to become negligible far downstream. In many cases it should be an adequate approximation to assume that the flow is optically thick to the recombination radiation (34c) in the nozzle entrance region, so that direct radiative recombination to the ground state according to the process (34c) may be neglected in the calculations; however, if this approximation is not adequate for a particular case a better estimate may be made on the basis of eq. (34c) and the particular nozzle geometry.

The reaction rate parameters given in Table XX for the recombination of electrons and atomic He^+ ions are derived from equations (32) through (34) on the assumption that the gas is optically thick to all radiation arising from transitions to the He atom ground state, so that essentially all recombinations will produce a metastable helium atom in either the $2s^1S$ or $2s^3S$ state. Since direct information as to the relative numbers of electrons recombining into each of the two metastable states does not appear to be available at present for the higher electron densities, we have assumed that the two states will be populated in proportion to their statistical weights (ref. 59), i.e., $3/4$ of the recombinations (33) will lead to atoms in the 3S metastable state and $1/4$ to atoms in the 1S state. For the lower electron densities, the number of electrons recombining into either of the two

metastable states is, of course, given directly by (34a) and (34b). For non-optically-thick conditions, a term based on equation (34c) may also be included in the model, as discussed above, to account for radiative recombinations directly into the ground state.

In addition to the rates for collisional-radiative recombination discussed above, Bates, Kingston, and McWhirter (ref. 55) have also calculated rates for the reverse process of "collisional-radiative ionization" from their model. At the higher electron densities, their results show that the collisional-radiative ionization rate is given to a good approximation by applying detailed balance arguments based on the electron temperature to the calculated overall collisional-radiative recombination rate, as indicated in Table XX; however, at the lower electron densities the ionization rates calculated from the collisional-radiative model may fall significantly below the values predicted from these simple detailed balance arguments. We have not attempted to fit the calculated ionization rate data in the present model, however, since for an ionized gas flow expanding through a nozzle, ionization will generally be negligible compared to recombination in the region where the detailed balance estimates of the ionization rate become inadequate. This would not be true, however, for cases such as the ionization of a gas behind a shock wave in which additional ionization is being produced in an initially cold gas, so that the reaction parameters given in Table XX would need to be revised to treat such cases.

According to the collisional-radiative model, all of the recombination energy of an electron-ion pair is transferred either into kinetic energy of the electrons or into radiation. For the lower electron densities, collisional processes are unimportant so that the entire recombination energy of the atom, together with the initial kinetic energy of the electron, will be emitted as radiation, as indicated for reactions 3 to 5 in Table XX. For higher electron densities there is a close coupling between collisional and radiative de-excitation processes so that the exact fraction of the recombination energy which will be emitted as radiation can only be determined from a complete solution of the collisional-radiative equations as formulated by Bates, Kingston, and McWhirter. However, as a rough approximation, experimental data indicate that the total radiant emission from a helium plasma at high electron densities does not differ from the predictions of the low density formula by more than about a factor of two over the range of conditions for which radiant emission makes a significant contribution to the overall energy balance of the system.

In the present model we have, therefore, used the low electron density formula to calculate the radiation due to recombination under all conditions and have assumed that the rest of the recombination energy goes into the kinetic energy of the electron gas, as indicated for reactions 1 and 2 in Table XX.

In addition to reactions 1 and 2 of Table XX in which the collisional processes contributing to recombination are assumed to be with an electron as the third body, Bates and Khare (ref. 56) have also predicted recombination rates for processes stabilized by collisions with a ground-state helium atom. We have not included such processes in the present model, however, since their existence does not appear to be verified by the experimental data (ref. 60).

De-excitation of metastable atoms.— Bates and Kingston (ref. 61) have pointed out the importance of the metastable atom population in determining the overall electronic recombination rate in a decaying helium plasma. This effect arises because, as we have seen above, the net collisional-radiative recombination rate is a strong function of electron temperature (see equation 33), and the metastables serve as an energy source for the electrons, raising the electron temperature and thus impeding the recombination process. A proper treatment of the processes determining the metastable population in the flow is thus important if one wishes to obtain an accurate prediction of electronic recombination rates in an expanding gas.

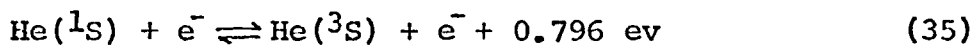
The processes which may lead to the destruction of metastable atoms in a decaying helium plasma have been surveyed by Bates, Bell, and Kingston (ref. 57). For the present one-dimensional flow model we shall neglect the loss of metastables from the flow due to diffusion and de-excitation at the walls. This should be a good approximation in the region outside the boundary layer, where the one-dimensional model is expected to be applicable. Further, the de-excitation of metastables by direct radiative transitions to the ground-state (two photon emission) is completely negligible in helium for gas densities of interest in laboratory applications (ref. 57). Thus, the rate at which metastable atoms are removed from the flow will be determined entirely by collisional processes in the present model.

Approximate rate constants for several of the processes leading to the destruction of metastable atoms in a helium plasma have

been given by Bates, Bell, and Kingston (ref. 57) in their study of metastable atom populations in a decaying plasma. For the conditions of interest in the present study, it appears that the most important metastable destruction process will ordinarily be the de-excitation of metastable atoms by collisions with slow electrons, the excitation energy being transferred to the kinetic energy of the electron. Bates, Bell, and Kingston have calculated the reaction rate for the de-excitation of a He(³S) metastable atom by this process in the electron temperature range from 250 to 4000°K, using a cross section obtained by detailed balance from the measured He(³S) excitation cross section of Schulz and Fox (ref. 64) and averaging over a Maxwellian distribution of electron energies. The parameters given for this reaction in Table XX (reaction no. 6) were obtained from a curvefit to their calculations. Figure 62 compares this curvefit for the reaction rate with the original calculations of Bates, Bell, and Kingston (ref. 57).

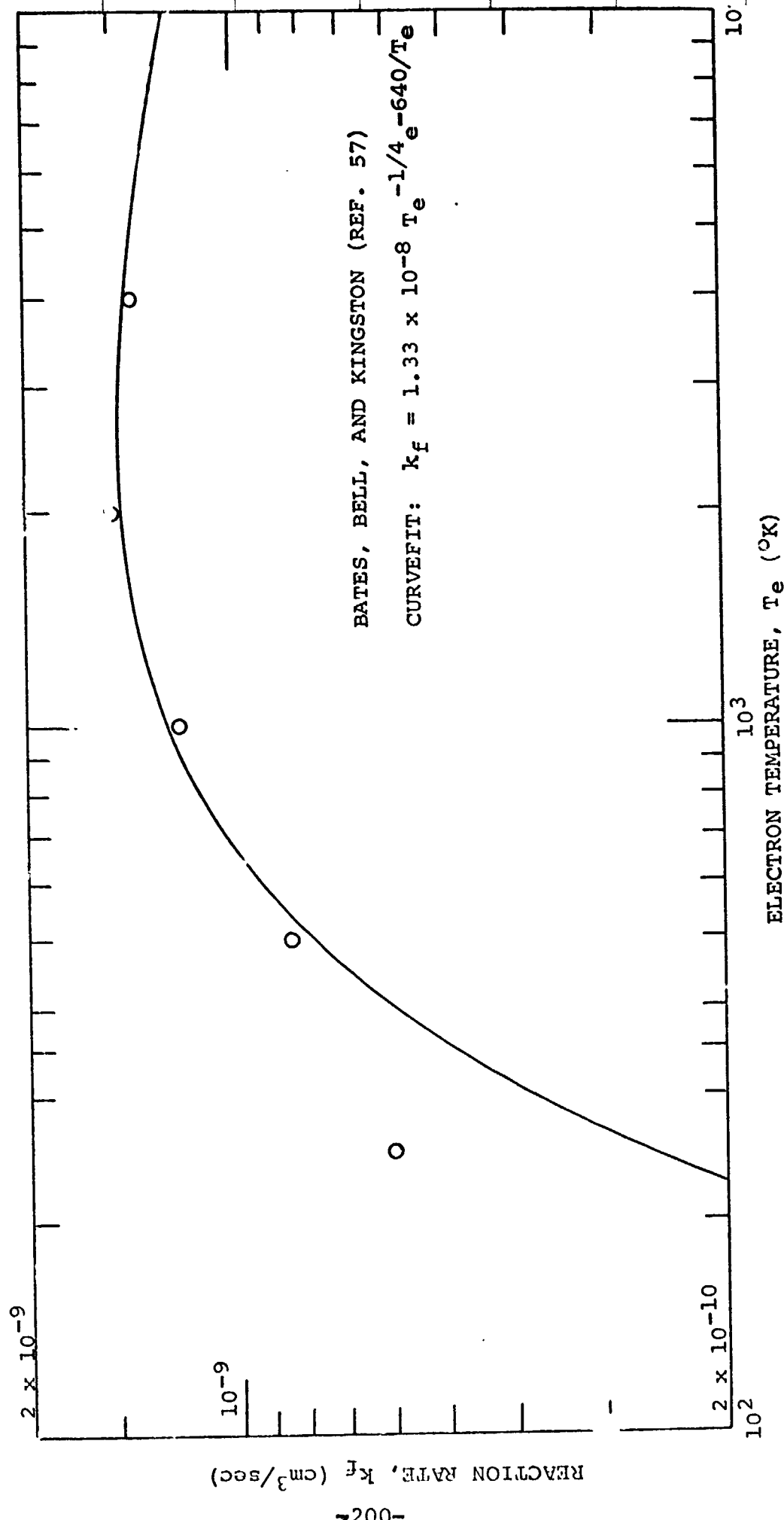
Bates, Bell, and Kingston do not give the rate for de-excitation of He(¹S) metastable atoms to the ground-state; however, since the excitation cross section for the He(¹S) metastable state is about 1/3 that for the He(³S) state (refs. 65, 66), it appears, taking account of the differing multiplicities of the two states, that the calculated rates given by Bates et. al., (ref. 57) for He(³S) de-excitation should also be approximately applicable to He(¹S), as we have assumed for reaction 7 in Table XX.

In addition to de-excitation to the ground state, electron collisions with metastables can also produce transitions between the He(¹S) and He(³S) metastable states according to the reaction scheme



Phelps (ref. 67) has measured a reaction rate for this process of $3.5 \times 10^{-7} \text{ cm}^3/\text{sec}$ at 300°K, corresponding to a reaction cross section of $3 \times 10^{-14} \text{ cm}^2$. To estimate the temperature dependence of the reaction rate, we make use of the work of Johnson and Hinnov (ref. 58), who have estimated a reaction cross section of about 10^{-15} cm^2 for the process (35) at electron temperatures of the order of 10,000°K, based on their spectroscopic studies of the population distribution of the helium excited states. Thus

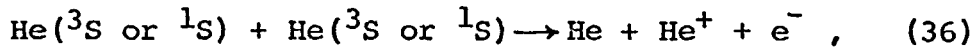
FIGURE 6.2 - REACTION RATE FOR THE COLLISIONAL DE-EXCITATION PROCESS
 $\text{He}(2^3\text{S}) + \text{e}^- \rightleftharpoons \text{He}(1\text{s}^2) + \text{e}^-$



the reaction cross section is approximately proportional to $1/T_e$ and the reaction rate to $T_e^{-\frac{1}{2}}$, as shown in Table XX.

It may be noted that the reaction rate for process (35) is two to three orders of magnitude greater than the rate for de-excitation of metastable atoms to the ground-state by electron collisions, so that as the electron density in the gas decays one may expect the relative populations of the $\text{He}({}^1\text{S})$ and $\text{He}({}^3\text{S})$ metastable states to remain in approximate thermodynamic equilibrium with each other at the electron temperature over a considerable range of conditions.

When the density of metastable atoms in helium becomes comparable to the electron density, a significant number of metastable atoms may also be removed from the gas by the Penning ionization process



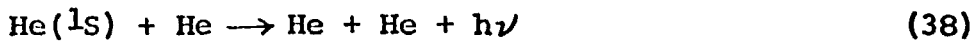
in which two metastable atoms collide and the excitation energy of one of them is transferred to ionize the other. This process has also been considered by Bates, Bell, and Kingston (ref. 57) who have shown that the reaction rate is given approximately by

$$k_f = 6.7 \times 10^{-10} T^{1/6} \text{ cm}^3/\text{sec} \quad (37)$$

when both metastable atoms are in the ${}^3\text{S}$ state, where T is the heavy-particle temperature in $^\circ\text{K}$. Their analysis may also be applied to collisions in which one or both of the metastable atoms is in the ${}^1\text{S}$ state by using the appropriate van der Waals force constant for the interaction (ref. 68) and noting that the spin conservation factor in the analysis of Bates, et. al. (ref. 57) is 1 instead of $4/9$ when either of the colliding atoms is in the ${}^1\text{S}$ state. This procedure yields the reaction rate constants given for the three Penning ionization processes (36) in Table XX (reactions 9, 10, and 11).

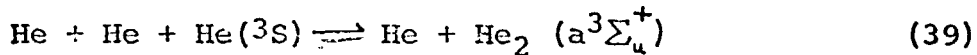
For fractional ionizations less than about 0.01 percent, collisions with ground-state neutral atoms may also make a significant contribution to the de-excitation of metastable atoms in helium. In the case of the $\text{He}({}^1\text{S})$, collisionally induced radiative transitions to the ground-state according to the

reaction



appear to be the primary de-excitation mechanism at low electron densities, where He denotes a helium atom in the ground electronic state. The reaction rate for the process (38) has been studied both experimentally and theoretically (ref. 69) and all determinations appear to be in reasonably satisfactory agreement (i.e., within a factor of about 3 or 4). For the present model, we have used an approximate curvefit to the theoretically calculated temperature dependence (ref. 69) with the value normalized at 300°K to the reaction rate $k_f = 6 \times 10^{-15} \text{ cm}^3/\text{sec}$ measured by Phelps (ref. 67).

In the case of the He^{3S} metastable atom, collisionally induced radiative transitions to the ground state of the type (38) are forbidden by spin conservation, and the metastable atom is removed from the gas at low electron densities primarily by conversion into the metastable molecular state $\text{He}_2^{\text{(a}}\text{3}\Sigma_u^+\text{)}$ according to the three body reaction (ref. 67)



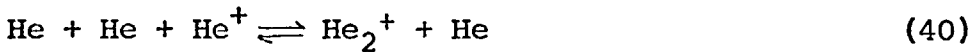
with the reaction energy presumably going primarily into translational and vibrational energy of the heavy particles. The reaction rate for this process measured by Phelps at 300°K is $k = 2.5 \times 10^{-34} \text{ cm}^6/\text{sec}$, so that the process should be negligible except at quite high gas densities. The temperature dependence of the reaction rate is unknown; however, it appears unlikely that the rate would vary greatly with temperature over the range of conditions for which the process (39) might be important, and we have arbitrarily assumed a \sqrt{T} dependence in Table XX.

Molecular species. - For pressures greater than about 1 mm Hg and low temperatures, it has been observed that atomic He^+ ions are rapidly converted into molecular ions. Although a number of different molecular ions have been observed (ref. 69) only the ground-state diatomic ion He_2^+ will be considered in the present note, since it is the ion which is formed initially by He^+ attachment and appears to be the only molecular ion which

ORIGINAL PAGE IS
OF POOR QUALITY

could be present in significant concentrations under the relatively high temperature conditions existing in an expanding plasma jet. The thermochemical properties of the He_2^+ ion now appear to be fairly well established, and are given in Table XIX. The He_2^+ dissociation energy had been rather uncertain until quite recently, but the latest experimental and theoretical results (ref. 9) now appear to strongly support a value of 2.50 ev for the electronic dissociation energy D_e of the ground-state He_2^+ ion. Since the energy differences between the various electronic states of He_2 and He_2^+ are accurately known from spectroscopic data (refs. 9, 12) the use of the above value for the He_2^+ dissociation energy, together with the available spectroscopic data (refs. 12, 70) serves to completely determine the thermochemical properties of the He_2 molecule and the He_2^+ molecular ion. The values of the lowest stable states of He_2 and He_2^+ are summarized in Table XIX.

The principal process leading to the formation of He_2^+ molecular ions at pressures above about 1 torr appears to be the three-body attachment reaction



Several independent measurements (refs. 71-73) of the reaction rate for this process have yielded values for the rate constant which agree within about a factor of two at room temperature. The temperature dependence of the rate constant is somewhat unclear, with Beatty and Patterson (ref. 71) reporting a rate constant which is approximately independent of temperature, while Niles and Robertson (ref. 72) report a T^{-1} dependence over the temperature range from 77°K to 449°K; however, this difference is perhaps not too significant in view of the rather limited temperature range for which molecular ions may be expected to be important in the gas. For the present model, we have adopted the reaction rate of Beatty and Patterson (ref. 71) for the process (40), i.e.,

$$k_1 = 1.08 \times 10^{-3} \text{ cm}^6/\text{sec}$$

independent of gas temperature.

The production of molecular ions by the associative ionization (Hornbeck-Molnar) process



has also been observed for excited He* atoms in 3p electronic states or above (ref. 74), but this reaction does not appear to be a significant source of molecular ions under the conditions existing in an expanding gas flow, and accordingly has not been included in the present model.

The primary mechanism for the recombination of He₂⁺ molecular ions again appears to be the collisional-radiative process of Bates, Kingston, and McWhirter (ref. 55) in which electrons are initially captured into highly excited molecular states and are then subsequently stabilized by collisional and radiative transitions to lower states. In spite of repeated experimental studies, the dissociative recombination process



has never been definitely observed in helium, and the reaction rate for the process appears to be almost certainly much less than 10⁻⁸ cm³/sec (ref. 75).*

The best data presently available for the He₂⁺ recombination rate appears to be that of Berlande, et. al. (ref. 77) who find a rate constant of the form

$$k_f = 5 \times 10^{-10} + 2 \times 10^{-20} n_e + 2 \times 10^{-27} n_{\text{He}} \text{ cm}^3/\text{sec} \quad (43)$$

for He₂⁺ recombination at an electron temperature of 300°K. Measurements at higher electron temperatures (ref. 78) indicate a temperature dependence at high electron densities similar to that found for atomic He⁺ ions (equation 33), so that it is consistent with the available data to treat the recombination of He₂⁺ ions at the higher electron densities as a collisional-radiative process with the rate constant

$$k_f \approx 2 \times 10^{-20} (T_e/300^\circ\text{K})^{-4.3} n_e \text{ cm}^3/\text{sec} , \quad (44)$$

*This interpretation of the data has been recently questioned by Johnson and Gerardo (ref. 76), however.

or about one fourth the rate constant found for atomic He^+ ions under similar conditions (equation 33).

Since information on the final products of the recombination process (44) is not available, it again appears reasonable to assume that the singlet and triplet molecular states are populated according to their statistical weights. The triplet states then presumably cascade down by collisional and radiative transitions to the metastable $\text{He}_2(a^3\Sigma_u^+)$ state at 17.937 ev above the He atom ground-state (see Table XIX), while the singlet states cascade down to the lowest singlet state of the He_2 molecule, namely the unstable $\text{He}_2(X^1\Sigma_g^+)$ ground-state, which then immediately dissociates into two ground-state He atoms. Since all electronic states of the He_2 molecule have approximately the same equilibrium internuclear separation r_e (ref. 12), it seems reasonable to assume that the $\text{He}_2(X^1\Sigma_g^+)$ ground-state is formed with an internuclear separation equal to the separation $r_e = 1.08 \text{ \AA}$ of the He_2^+ ground-state, corresponding to a potential energy of about 2.31 ev (ref. 79). This potential energy is then converted into kinetic energy of the dissociating helium atoms, while the remainder of the recombination energy, equal to $22.190 - 2.31 = 19.88$ ev per molecule, is converted into electronic kinetic energy and radiation by the collisional-radiative process. As with the atomic recombination process, we have not attempted to distinguish between the energy going into electronic kinetic energy and into radiation in the present note, but have simply assigned all of the excess recombination energy to the electrons in Table XX (reactions 15 and 16). Although we expect this to be a reasonable approximation for cases in which the He_2^+ recombination energy is important, this has not been definitely verified.

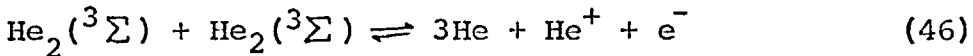
Since the first term in equation (43) appears to be much too large for a simple radiative recombination process, it has been tentatively ascribed (ref. 75) to the dissociative recombination process (42), where He^* may represent either a metastable 3S or 1S helium atom. In Table XX we have again assumed that the singlet and triplet states are populated in accordance with their statistical weights, and have taken the rate constant to be independent of temperature, although there is some theoretical evidence to indicate that it may actually be an increasing function of gas temperature (ref. 80). Although the rate constant for the process (42) is very poorly known, it represents a minor correction to the calculated net reaction rate (43) under most conditions of interest, and should thus not contribute appreciably to the overall uncertainty in the calculated gas conditions.

The final term in the observed He_2^+ recombination rate (43), which is proportional to the gas density, presumably represents the effect of stabilization by collisions with ground-state He atoms which was studied by Bates and Khare (ref. 56). Since this term becomes important only when the fraction of ionization is of the order of 10^{-7} or less, we have not included it in the reaction rate model given in Table XX.

To complete the present reaction rate model for helium, approximate rates for the destruction of the metastable He_2 molecule are included as the final two reactions in Table XX. Since the experimental studies of Collins (ref. 81) and Phelps (refs. 67, 82) indicate that the processes



and



for the destruction of metastable $\text{He}_2(^3\Sigma)$ molecules have the same rates at room temperature, within the experimental error, as do the corresponding processes for the $\text{He}(^3S)$ metastable atom, we have, for lack of any better information, simply used the reaction rates given previously for the $\text{He}(^3S)$ reactions (reactions 6 and 9 in Table XX) for the processes (45) and (46) as well. The destruction of metastable molecules by collisions with ground-state atoms appears to be negligible and is hence not included in the present model; Phelps' data (ref. 67) indicate a reaction rate for this process at least two orders of magnitude smaller than for the corresponding process (39) for metastable $\text{He}(^3S)$ atoms.

Concluding remarks - Since we have introduced a number of simplifying approximations in constructing the reaction rate model for helium presented in Tables XIX and XX, and since, moreover, several of the important reaction rates for helium are still rather uncertain, especially at the higher temperatures, it would now be desirable to verify the model by comparing its predictions with experimental data over as wide a range of conditions as possible, and, if necessary, adjust the rate constants to obtain satisfactory agreement with experiment. This has not been possible within the scope of the present study, however; and accordingly the reaction rates given in Table XX should be regarded as provisional until such time as a more complete verification of the model can be obtained.

A.2 Argon Model

The nonequilibrium argon model used in NATA is basically similar to the helium model described above, but with the parameters adjusted and a few minor modifications made to account for the difference in physical properties between helium and argon. Thus, much of the discussion given above for helium is also applicable to argon, and only the differences between the two gases need be noted here.

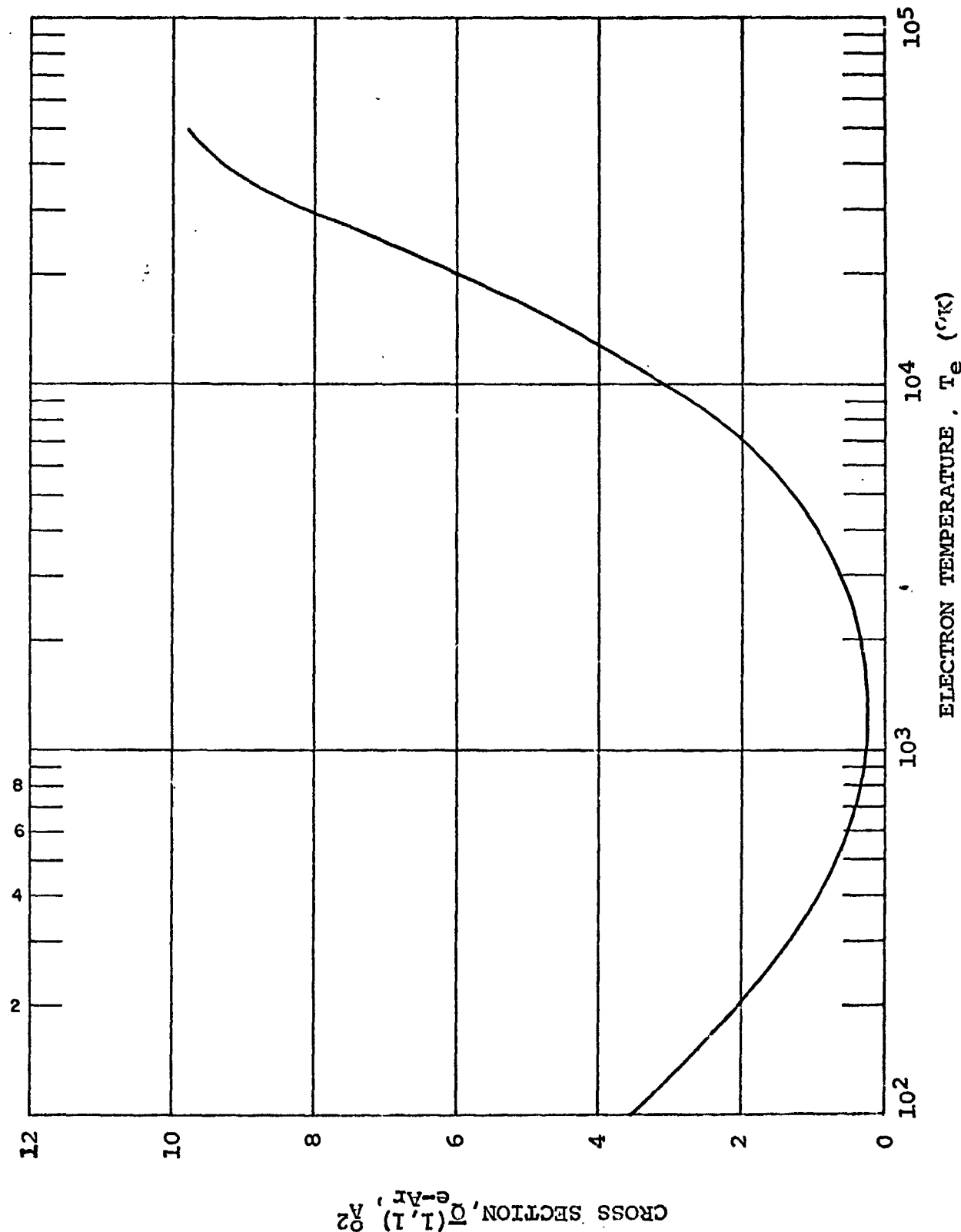
Although argon has been used extensively as a test gas in laboratory studies for various aerodynamic and arc tunnel applications, the reaction mechanisms in recombining argon have apparently not been studied in as much detail as they have for helium, and in consequence, as will be indicated in more detail in the discussion below, several of the important parameters in the argon recombination model appear to be significantly uncertain at the present time. Accordingly, the errors in the nonequilibrium model calculations for argon may be expected to be larger than for helium.

The species and parameter values for the nonequilibrium argon model used in NATA are given in Tables XXI and XXII.

Elastic collisions.—The electron energy loss due to elastic collisions in argon is again calculated from equations (25) to (30) with appropriate values of the momentum transfer cross sections for argon being used in equation (30). As in the case of helium, the approximate Coulomb cross section (31) is used in equation (30) for all electron-ion collisions.

Data on the momentum transfer cross section between electrons and ground-state argon atoms have been given by Frost and Phelps (ref. 83) and by Golden (ref. 84). For the present model, we have numerically integrated the data of Frost and Phelps over electron energy as indicated in equation (30) to obtain the Maxwell-averaged electron-argon atom cross section $\bar{Q}_{e-Ar}^{(1,1)}$ shown in figure 63 as a function of temperature. Use of the data of Golden in this computation would have given a noticeably lower cross section in the neighborhood of the Ramsauer minimum at $T = 1300^{\circ}\text{K}$; however, since the total cross section in this region is so small for either calculation, the effect of such a change on the overall electron energy balance for the gas would be negligible.

FIGURE 63 - MAXWELL AVERAGED MOMENTUM TRANSFER CROSS SECTION $\bar{\sigma}_{e-Ar}^{(1,1)}$ FOR COLLISIONS BETWEEN ELECTRONS AND GROUND STATE ARGON ATOMS



CROSS SECTION, $\bar{\sigma}_{e-Ar}^{(1,1)}$

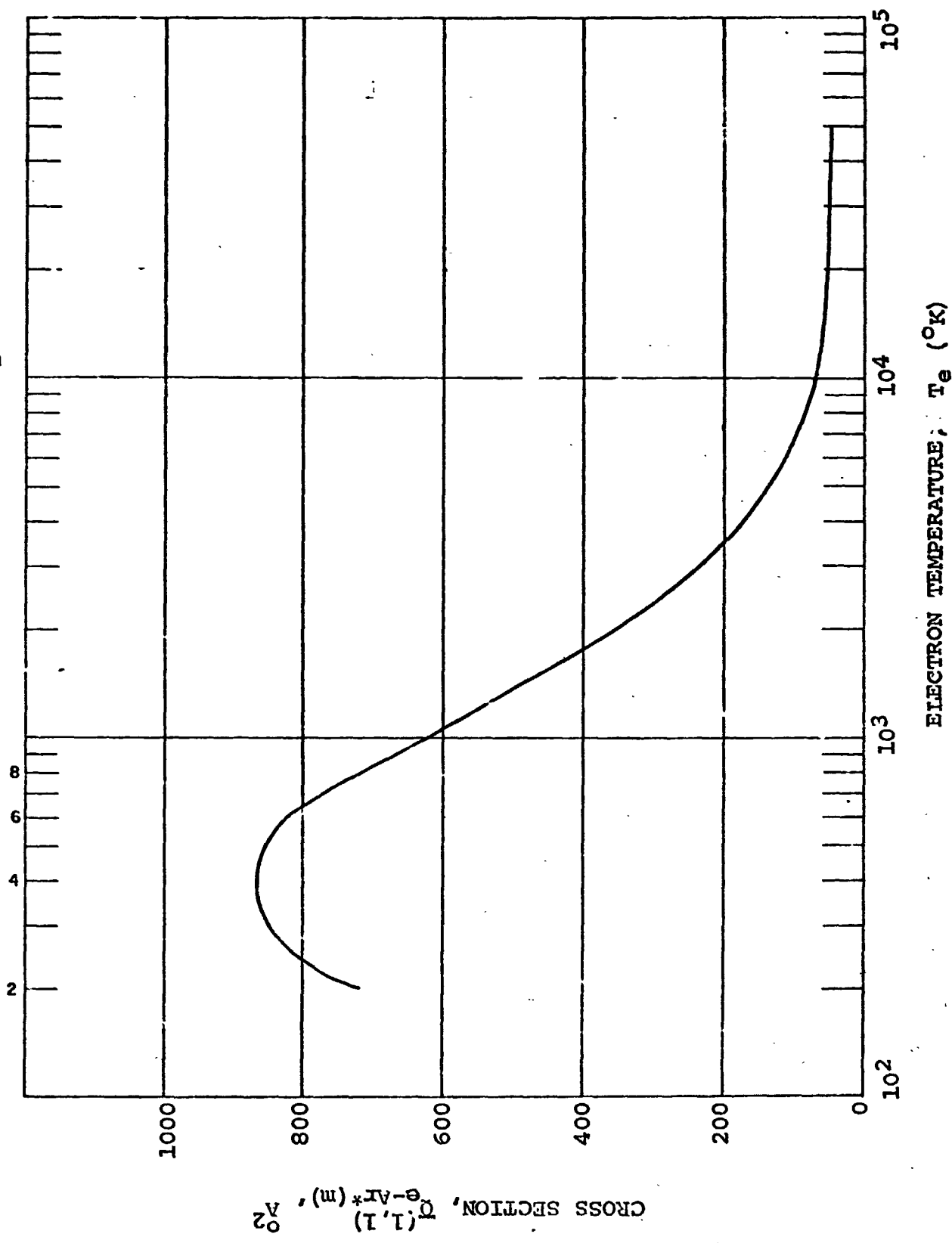
As in the case of helium, we have used the calculated electron-ground state argon atom cross section shown in figure 63 for all elastic collisions between electrons and neutral argon species. As an indication of the error involved, figure 64 shows the Maxwell-averaged cross section for collisions between electrons and metastable argon atoms which we have estimated from the available cross section data (refs. 85 and 86). One sees that the estimated metastable cross section is about two to three orders of magnitude greater than the ground state cross section over the temperature range of interest. Thus, the approximation employed in the code of using the ground-state cross sections for all neutral species should give an adequate representation of the elastic energy losses as long as the concentration of metastable species in the gas remains ≤ 0.1 percent. As noted previously in our discussion of the helium model, the elastic energy losses themselves become negligible at higher metastable concentrations, so that the error in the calculated elastic energy losses at high metastable concentrations ($\gtrsim 1$ percent) should not significantly affect the overall accuracy of the model predictions in this region.

Collisional-radiative recombinations.— Data on electronic recombination rates in argon have been reviewed recently by Biberman, et. al. (ref. 87). Although the experimental uncertainty is larger than for helium, the available data for argon again appear to be generally consistent with the collisional-radiative recombination mechanism suggested by Bates, Kingston, and McWhirter (ref. 55). Accordingly, we have followed the approximate model of collisional-radiative recombination discussed above for helium in the present treatment of argon recombination also.

As with helium, we have attempted to represent the observed recombination rate data for argon by a curvefit of the form (32). For the higher electron densities, the observed recombination rates for argon (refs. 88, 89) are found to agree with the helium data within the experimental scatter, so that the high density portion of the reaction rate curvefit for helium (equation 33) may also be used for argon.

At low electron densities, radiative recombination becomes dominant and recombination rates may be determined from available data on the argon continuum radiation. From these data (refs. 90-92) one finds that the total rate for radiative recombination into

FIGURE 64 - MAXWELL AVERAGED MOMENTUM TRANSFER CROSS SECTION FOR COLLISIONS
BETWEEN ELECTRONS AND METASTABLE $4s(3P_2)$ ARGON ATOMS



the excited states of the argon atom agrees with the corresponding rate for helium within the experimental scatter, so that the net reaction rate for recombination into an excited argon atom at low electron densities becomes

$$k_f = 2.73 \times 10^{-13} (T_e/10^4 \text{ °K})^{-0.81} \text{ cm}^3/\text{sec} \quad (47)$$

For radiative recombination directly into the argon ground state the data of Samson (ref. 93) give the recombination rate

$$k_f = 1.00 \times 10^{-13} (T_e/10^4 \text{ °K})^{-0.5} \text{ cm}^3/\text{sec} \quad (48)$$

which is somewhat lower than the corresponding rate (34c) for helium.

The data cited above indicate that the rates for electronic recombination into excited atomic states are comparable in helium and argon at both high and low electron densities. At intermediate electron densities, however, the data of Chen (ref. 94) give a recombination rate in argon which is several times higher than the corresponding helium rate and than the collisional-radiative predictions, and about an order of magnitude higher than the rate predicted from the simple curvefit (32) on the basis of the high and low electron density data.* The reason for this discrepancy is not clear. Chen suggests that the observed differences between helium and argon in his work may be due to differences in the electronic excitation and de-excitation cross sections for excited states in the two gases; however, this explanation does not appear to be consistent with the close agreement between helium and argon recombination rates at high electron densities which has been observed in other studies (refs. 88,89). In view of this apparent inconsistency and the lack of other experimental data to support the difference between helium and argon recombination rates found by Chen, the present model uses a recombination rate based only on the high and low electron density data given by equations (33), (47) and (48), and ignores the data of Chen at intermediate densities. These data should be borne in mind, however, as a possible indication of significant uncertainty in the predicted recombination rates for argon.

Because of the closed electronic p-shell in the heavier rare gas atoms, the relationship among the low-lying excited states

*Remember that the curvefit (32) gives recombination rates several times smaller than the correct collisional-radiative model at intermediate electron densities.

differs from that found in helium with the result that the decay of excited states during collisional-radiative recombination in argon follows a somewhat different pathway than that described previously for helium. Table XXIII shows the four lowest lying excited states of the argon atom, together with the three commonest designations by which they are referred to in the literature. All higher excited states of the atom can decay rapidly into one of these four low-lying excited states, so that only the populations of these four states need be followed in the collisional-radiative model. Of the four states, the 3P_2 and 3P_0 are metastable while the 3P_1 and 1P_1 can decay to the ground state by emission of resonance radiation. The decay is slow, however, because of the trapping of resonance radiation in the gas, and the two resonance states 3P_1 and 1P_1 thus behave somewhat like true metastable states under many conditions of interest.

Within the accuracy of the present model it seemed unnecessary to distinguish between all four of the low-lying excited states in Table XXIII, and accordingly we have grouped the two metastable states 3P_2 and 3P_0 into a single metastable state Ar* (m) and the two resonant states, 3P_1 and 1P_1 , into a single resonant state Ar* (r), as indicated in Table XXI. Assuming that these states are populated in proportion to their statistical weights by the recombination reactions (33) and (47) then leads to the reaction rates for electronic recombination into excited states given for reactions 1 through 4 in Table XXII. As in the case of helium, we find that an adequate fit to the total visible and infrared emission from the gas under all conditions (refs. 90-92) can be obtained by assuming that all of the recombination energy goes into the electron gas for the three-body recombinations 1 and 2 while all of the energy* goes into radiation for the two-body recombinations 3 and 4.

For radiative recombination directly into the argon atom ground state, reabsorption of the emitted recombination radiation by the gas can be effective in reducing the net recombination rate even at moderately low gas densities. An estimate of this reduction can be made by dividing the low density recombination rate

*It may be noted that in computing the electron thermal energy for the reactions in Table XXII, we have taken account of the fact that the reaction rate depends on electron energy, so that the mean energy of the electrons participating in the reaction is not the same as the mean thermal energy $3/2 k T_e$ of all the electrons in the gas. Under most conditions of interest, however, this difference will not be significant for the final results of the calculation.

TABLE XXIII
LOW-LYING EXCITED STATES OF THE ARGON ATOM

LS Designation	Paschen Designation	jL-Coupling Designation	Energy (ev)	Statistical Weight q
4s ³ P ₂	1s ₅	4s [3/2] ₂ ^o	11.545	5
4s ³ P ₁	1s ₄	4s [3/2] ₁ ^o	11.620	3
4s ³ P ₀	1s ₃	4s' [1/2] ₀ ^o	11.720	1
4s ¹ P ₁	1s ₂	4s' [1/2] ₁ ^o	11.825	3

(48) by the optical depth of the gas for the recombination radiation

$$\tau = 3.4 \times 10^{-17} n_{\text{Ar}} R, \quad (49)$$

where τ is the optical depth, n_{Ar} is the number density of ground state argon atoms in the gas in cm^{-3} , R is the channel radius in cm, and $3.4 \times 10^{-17} \text{ cm}^2$ is the absorption cross section of ground state argon atoms for the recombination radiation, as measured by Samson (ref. 93). As indicated in Table XXII (reaction 5), this reduction must be applied to the rate constant (48) whenever the optical depth (49) of the gas becomes greater than one.

Decay of excited atoms. - The de-excitation of low-lying atomic states in a decaying argon plasma appears to be due primarily to collisions with electrons and ground-state atoms, and, in the case of the resonant states, the emission of radiation. For ionization fractions greater than about 10^{-4} to 10^{-5} , electron collisions and resonance radiation will be the most important de-excitation mechanisms, while atomic collisions become important at lower fractions of ionization.

De-excitation rates for electron collisions with excited argon atoms can be obtained from experimental data on the inverse process of excitation of ground-state argon atoms by electron

impact. Rates for the latter process have been obtained both from studies of the ionization rate behind argon shocks (refs. 95-97) and from electron beam measurements of the excitation cross sections versus electron energy (refs. 98-102).

In all of the shock tube studies, it has been found that the rate determining step in the ionization process behind the shock front is the initial excitation of the ground state argon atom to a low-lying excited state, so that the excitation cross section can be determined directly from the measured ionization rates. Experimentally, the ionization is observed to proceed in two stages; first an initial induction phase in which the excitation is produced primarily by collisions with ground state atoms, followed by a second, much more rapid stage, in which the electron density has become sufficiently high for electronic collisions to contribute significantly to the observed excitation rates. Analysis of the ionization rate data for the second stage indicates that the measured rates are consistent with a linear dependence of the electronic excitation cross section on excess electron energy above the excitation threshold (~ 11.5 ev), with a slope which varies in the different experiments (refs. 95-97) over a range from about 5×10^{-18} to $7 \times 10^{-18} \text{ cm}^2/\text{ev}$. Since the experiments are not sensitive enough to determine exactly which state is being excited, this measured excitation cross section should probably be regarded as a sum over the four low-lying states of the argon atom indicated in Table XXIII.

Total cross sections for excitation of the two argon meta-stable states 3P_2 and 3P_0 by electronic collisions have been measured in electron beam studies over the energy range from threshold to ~ 200 ev (refs. 98-101). The data are in general agreement with the linear cross section dependence on electron energy assumed in the analysis of the shock tube data; however, considerable detailed structure in the cross section energy dependence is evident near threshold (refs. 98, 99) so that the cross section slope deduced from the shock tube experiments would be expected to vary somewhat with electron temperature. Using Pichanick and Simpson's relative cross section measurements near threshold (ref. 98) normalized to the absolute cross section values given by Borst (ref. 100), we find a mean cross section slope varying between about $4 \times 10^{-18} \text{ cm}^2/\text{ev}$ and $8 \times 10^{-18} \text{ cm}^2/\text{ev}$ for the range of temperatures below about $40,000^\circ\text{K}$, with the value being $\sim 8 \times 10^{-18} \text{ cm}^2/\text{ev}$ for $T \lesssim 1000^\circ\text{K}$. In the range of temperatures $T \lesssim 5000^\circ\text{K}$, it appears that a linear cross section

dependence with the slope

$$\frac{d\Omega}{dw} \approx 7 \times 10^{-18} \text{ cm}^2/\text{ev} \quad (50)$$

found by Petschek and Byron (ref. 95) should give a very satisfactory fit to the available electron beam data.

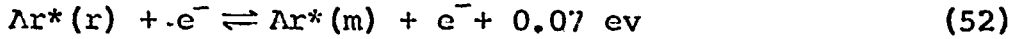
The cross section for excitation of the resonant 3P_1 and 1P_1 argon states has been measured by McConkey and Donaldson (ref. 102) in an electron beam apparatus over the energy range from threshold to about 2000 ev. In the threshold region, their results indicate a linear dependence of the total excitation cross section on electron energy with a slope

$$\frac{d\Omega}{dw} \sim 1 \times 10^{-18} \text{ cm}^2/\text{ev.} \quad (51)$$

Thus, the total excitation cross section for the argon resonant states is considerably smaller than for the metastable states at thermal energies, and the total excitation cross section for all low-lying states derived from the electron beam measurements is in excellent agreement with the shock tube results.

The reaction rates for de-excitation of the low-lying metastable and resonant excited states of atomic argon by electron collisions which are used in the present argon kinetic model are derived from the corresponding excitation cross sections (50) and (51) by detailed balance. These rates are listed as reactions 6 and 7 in Table XXII.

In addition to causing de-excitation of the low-lying excited states, electronic collisions can also result in transition between the metastable and resonant excited states according to the scheme



Although we have been unable to find any direct data, the rate for the process (52) is expected to be large (ref. 103), in analogy to the corresponding processes in helium (ref. 67) and neon (ref. 104). An approximate upper bound for the possible

reaction rate is provided by the total cross section measurements of Celotta, et. al. (ref. 85) for the inverse process of electron-metastable Ar(3P_2) collisions.

For the present model we have taken the reaction rate for the process (52) equal to the corresponding rate estimated for neon at 300°K by Phelps (ref. 104), and have assumed a $T_e^{-\frac{1}{2}}$ temperature dependence, as in the helium model, to obtain the rate constant

$$k_f = 10^{-6} \left(\frac{T_e}{300^\circ K} \right)^{-\frac{1}{2}} \text{ cm}^3/\text{sec} \quad (53)$$

for the process (52). This rate lies about an order of magnitude below the upper bound provided by the total (elastic plus inelastic) cross section measurements of Celotta, et. al.

It should be noted that the process (52) may play an important role in the decay of metastable argon atoms at low electron densities, since it can cause transitions from the relatively long-lived metastable excited states to the much shorter lived resonant states. Thus, the uncertainty in the rate constant (53) could result in significant errors in the model predictions of metastable decay rates for an argon plasma under some conditions.

In helium, all of the excited atomic states which are capable of direct radiative transitions to the ground state can also decay rapidly into one of the two metastable excited states, so that most of the excited atoms pass through one of the metastable states during the de-excitation process and only a small fraction are de-excited by direct radiative transitions to the ground state. Thus, the latter process could be neglected to a good approximation in the formulation of the helium kinetic model discussed in the preceding section. For argon, on the other hand, the low-lying 3P_1 and 1P_1 resonant excited states cannot decay radiatively to any lower excited state, so that direct radiative transitions to the ground state become the dominant decay mechanism for these states in many situations, and hence must be included in the kinetic model.

Since the mean free path of resonance radiation in a gas is typically very much shorter than usual laboratory apparatus dimensions, most of the photons emitted by the radiative decay

of excited atoms to the ground state are reabsorbed by other atoms in the gas to excite them to the resonant state, and the net rate of decay of the resonant state population density in the gas is much slower than would be predicted solely on the basis of the spontaneous emission coefficient for the state. A model to predict the net rate of decay of the population density under these conditions as a function of apparatus geometry and the absorption coefficient of the resonance line has been developed by Holstein (refs. 105, 106) and has been verified experimentally for a number of gases (refs. 104-108), including both argon (ref. 107) and neon (ref. 104).

Under the usual laboratory conditions, it is generally a good approximation to assume that the shape of the resonant radiation lines is determined by pressure broadening according to the dipole-dipole model of Fursov and Vlasov (see refs. 109, 110). With this assumption, the net decay rate for the transition to the ground state predicted by Holstein's model becomes independent of gas pressure and, for a cylindrical gas volume, reduces to the simple form

$$k_p = 0.205 A_m \left(\frac{\lambda_0}{R} \right)^{1/2} \quad (54)$$

where A_m is the probability for spontaneous emission of a resonant photon from the excited state per unit time, λ_0 is the wave-length at the center of the resonant line, and R is the cylinder radius. When the appropriate constants for the argon resonant states (ref. 111) are inserted into equation (54), one finds the reaction rates

$$k_f = \frac{8.0 \times 10^4}{\sqrt{R}} \text{ sec}^{-1} \quad (55a)$$

for the radiative decay of the Ar (3P_1) state, and

$$k_f = \frac{3.4 \times 10^4}{\sqrt{R}} \text{ sec}^{-1} \quad (55b)$$

for the Ar (1P_1) state, where R is the cylinder radius in centimeters. Equation (55a) has been verified experimentally by Ellis and Twiddy (ref. 107). Since we expect the 3P_1 state to be more highly populated than the 1P_1 state under most conditions

of interest, equation (55a) has been used for the radiative decay rate of the Ar resonant state in the present kinetic model (reaction 9 of Table XXII).

The reaction rates (55) should be valid in argon for nozzle radii $R \geq 0.1$ cm and ground state argon atom number densities $n_{Ar} \geq 10^{16}$ cm⁻³. For lower number densities than this, pressure-broadening becomes small compared to the natural line width of the resonance lines, and the effective rate constant begins to increase with decreasing number density. Eventually, at very low number densities, reabsorption of the resonance radiation of course becomes negligible, and the effective rate constant approaches the spontaneous emission coefficient $k_f = A_m$. Comparing this limit with equation (54), one sees that the net radiative decay rate for the resonant argon excited states is reduced by about three to four orders of magnitude by the trapping of resonance radiation under typical laboratory conditions.

For low fractional ionizations, the de-excitation of excited atoms by collisions with neutral atoms can become significant. Experimental data on the reaction rates are available both for the direct de-excitation process (refs. 107, 112, 113) and for the inverse excitation process (refs. 95-97, 114-117).

Several studies of the decay of excited state population densities in low temperature argon gas (refs. 107, 112, 113) have indicated that both two- and three-body de-excitation processes are significant, and have given reasonably consistent values (within about a factor of two) for the de-excitation rates. The most detailed study was that of Ellis and Twiddy (ref. 107), who gave two- and three-body reaction rates at 300°K of

$$\begin{aligned} k_2 &= (1 \pm 0.3) \times 10^{-15} \text{ cm}^3/\text{sec} \\ k_3 &= (1.7 \pm 0.2) \times 10^{-32} \text{ cm}^6/\text{sec} \end{aligned} \tag{56}$$

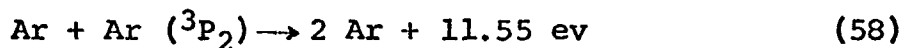
for de-excitation of the Ar (³P₂) metastable state at 11.55 ev and

$$\begin{aligned} k_2 &= (5.7 \pm 0.7) \times 10^{-15} \text{ cm}^3/\text{sec} \\ k_3 &= (1.14 \pm 0.15) \times 10^{-32} \text{ cm}^6/\text{sec} \end{aligned} \tag{57}$$

for de-excitation of the Ar (³P₀) metastable state at 11.72 ev. Futch and Grant (ref. 113) measured the Ar (³P₂) de-excitation

rates at 77°K and 300°K and their data yield a temperature dependence over this range of $k_2 \sim T^{2/3}$ for the 2-body de-excitation process (56a) and $k_3 \sim T^{-0.56}$ for the three-body process (56b).

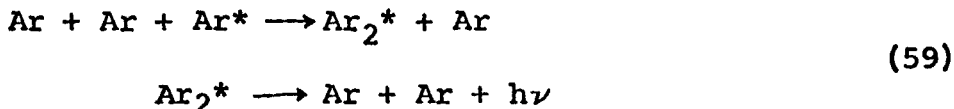
In their work, Ellis and Twiddy attribute the two-body de-excitation rate (56a) to a two-step process in which the metastable Ar (3P_2) atom is first excited to the resonant Ar (3P_1) state by collision with a ground state argon atom, and then decays radiatively to the ground state. No evidence is given to support this assignment, however, and it appears to be inconsistent with the temperature dependence observed for the two-body de-excitation process at 77°K by Futch and Grant, which suggests that the direct de-excitation process



is responsible for the observed two-body de-excitation rate.

Further evidence for the reaction (58) is provided by several shock tube studies in which excitation cross sections for collisions between ground state argon atoms were derived from the initial ionization rates behind an argon shock (refs. 95-97, 114-117). In all cases, it was found that the experimentally observed ionization rates for the initial ionization stage directly behind the shock front could be accounted for by an atom-atom excitation cross section which was (approximately) a linear function of the excess atom energy above the excitation threshold. The slope of the derived cross section energy dependence varied somewhat between the different experiments; however, all results were consistent within about an order of magnitude, with the reported values of the cross section varying from about $2.5 \times 10^{-20} \text{ cm}^2/\text{ev}$ to $2.5 \times 10^{-19} \text{ cm}^2/\text{ev}$. Using these data to derive a cross section for the inverse de-excitation reaction (58) by detailed balance, one obtains a two-body de-excitation rate, k_2 , which is proportional to \sqrt{T} and has the value $k_2 \sim 10^{-15}$ to $10^{-14} \text{ cm}^3/\text{sec}$ at 300°K, in good agreement with the measured low temperature de-excitation rates. Thus, the assignment of the observed two-body de-excitation rate (56) to the reaction (58) is verified and an approximate \sqrt{T} dependence of the de-excitation rate over the temperature range from $T = 77^\circ\text{K}$ to $\sim 10,000^\circ\text{K}$ is substantiated.

The three-body de-excitation process in equations (56) and (57) is attributed to the two-step reaction process



in which the excited argon atom combines with a ground state atom to form an excited Ar_2^* molecule, which then immediately radiates to form an unstable ground-state Ar_2 molecule which dissociates into two ground state atoms. The radiation emitted during the process (59) is observed to peak at a wavelength of about 1265 Å (ref. 118), corresponding to a mean energy of ~ 9.8 ev for the emitted photon, with the remaining ~ 1.8 ev of the excitation energy of course going into kinetic energy of the three argon atoms participating in the reaction.

For the present kinetic model, the two- and three-body de-excitation rates for the metastable $\text{Ar}^*(m)$ atom given in reactions 10 and 11 of Table XXII have been set equal to the Ar (${}^3\text{P}_2$) de-excitation rates from equation (56), since we expect that most of the metastable atoms will be in the ${}^3\text{P}_2$ state under the conditions encountered in an expanding argon plasma jet, because of this state's higher statistical weight and lower excitation energy. As noted above, the $T^{1/2}$ temperature dependence of the two-body de-excitation process appears to be well established, while we have provisionally assumed the $T^{-0.56}$ temperature dependence observed by Futch and Grant at low temperatures for the three-body process. Since collisional de-excitation rates have not been observed for the resonant excited states ${}^3\text{P}_1$ and ${}^1\text{P}_1$, we have also used the ${}^3\text{P}_2$ de-excitation rates for the resonant excited states in reactions 12 and 13 of Table XXII. This approximation should have a negligible effect on the computed population densities for the model under the conditions of interest in an expanding plasma jet, since the radiative decay rate (55) for the resonant excited states is much greater than the collisional de-excitation rate (56), except at very high gas densities.

Molecular species. - The only molecular species included in the argon kinetic model is the ground-state molecular ion Ar_2^+ . In contrast to helium, there appear to be no metastable molecular states in argon (ref. 121) so that any excited molecular states formed will decay very rapidly to the ground state, in times of the order of 0.1 μsec or less (ref. 118) and need not be considered in the kinetic model. The Ar_2 ground state molecule itself

is very weakly bound (dissociation energy $D_0 \sim 0.01$ ev (ref. 123)), and thus should be rapidly dissociated into ground-state atoms under the conditions existing in an expanding argon plasma jet.

The thermochemical properties of the argon molecular ion Ar_2^+ are still very uncertain at the present time; the values used in the present model have been taken from the recent equilibrium drift tube measurements of Teng and Conway (ref. 13) and are shown in Table XXI. The Ar_2^+ dissociation energy $D_0 \approx 1.14$ ev found by Teng and Conway is in reasonable agreement with previous experimental (refs. 119, 120) and theoretical (ref. 121) estimates obtained by less direct means. The vibrational frequency $\omega_e \sim 80 \text{ cm}^{-1}$ derived by Teng and Conway from the thermochemical data, however, is about a factor of five lower than the value estimated by O'Malley (ref. 122) on the basis of an interpretation of observed dissociative recombination rates in argon. We have accepted the value of Teng and Conway in the present work since it appears to be more directly determined from the experimental data; however, the uncertainty could be large.

As in the case of helium, the production of molecular ions in a decaying argon plasma at pressures near 1 torr or higher appears to be due primarily to the three-body conversion process



A number of measurements of the reaction rate for the process (60) at room temperature have given results in reasonably satisfactory agreement (refs. 124, 125), with the more precise determinations yielding a value

$$k_f \approx (2 \pm 1) \times 10^{-31} \text{ cm}^6/\text{sec} \quad (61)$$

for the reaction rate at 300°K. The temperature dependence of the reaction rate (61) has apparently not been accurately determined; however, available theoretical and experimental results (refs. 124, 126, 127) indicate that the rate should probably decrease somewhat with increasing temperature. As a reasonable compromise among the various estimates, we have assumed a $T^{-3/4}$ temperature dependence for the rate constant (61) in the present analysis, as predicted by the simple Thomson theory (ref. 124).

The drift tube measurements of Liu and Conway (ref. 124) indicate that the rate constant (61) applies only to reactions of the ground-state Ar^+ (${}^2\text{P}_{3/2}$) ion, and that the excited ${}^2\text{P}_{1/2}$ fine-structure component of the Ar^+ ion (at 0.18 ev above the ground-state) does not participate in the reaction (60) under the essentially electron-free conditions of their experiment. For the experiments carried out in decaying plasmas ($n_e \sim 10^{11} \text{ cm}^{-3}$) (refs. 125, 128), however, the rate of conversion between the two Ar^+ fine-structure states was apparently sufficiently rapid that no distinction between the two states was observed in the data, and the reaction rate (61) applies to the total atomic Ar^+ population density in the plasma. Since the latter experiments appear to be closer to the conditions to be expected in an argon plasma jet, we have grouped the two Ar^+ fine-structure states together into a single species for the present kinetic model (see Table XXI) and have used the experimental reaction rate (61) for the combined species in obtaining the reaction rate data given for reaction 14 in Table XXII.

The associative ionization process



is known to be rapid in argon for excited Ar^* atoms having excitation energies above a threshold of ~ 14.7 ev, with the rate constant being $k_f \sim 10^{-9} \text{ cm}^3/\text{sec}$ near room temperature (refs. 119, 129). Under conditions of collisional-radiative recombination, however, the population of excited Ar^* atoms above the 14.7 ev threshold is very small compared to the ion population, so that the associative ionization reaction (62) should not contribute appreciably to the molecular ion production rate in an expanding argon plasma at the relatively high pressures ($p \gtrsim 10^{-3} \text{ atm}$) of interest here. Thus, a detailed treatment of associative ionization has not been included in the present kinetic model.

In contrast to the situation in helium, the recombination of molecular ions in argon under most conditions occurs primarily through the dissociative recombination reaction (ref. 75)



and this process appears to be sufficiently rapid to make an important contribution to the overall recombination rates in an argon plasma even at the higher temperatures, where the molecular ion Ar_2^+ represents a relatively minor constituent of the

plasma. Dissociative recombination rates for argon have been measured in a number of independent experiments, both at room temperature and at elevated temperatures (refs. 75, 122, 127 130). The low temperature measurements (ref. 75) give a value $k_f \sim 7 \times 10^{-7}$ cm³/sec for the reaction rate of the dissociative recombination process (63) at room temperature. The measurements at elevated temperature indicate that the reaction rate for dissociative recombination depends on both the electron temperature T_e and the gas temperature T. A good fit to the data of Mehr and Biondi (ref. 130) and Cunningham and Hobson (ref. 122) has been given by O'Malley (ref. 122) in the form

$$k_f = 9.6 \times 10^{-7} (T_e/300^\circ\text{K})^{-0.67} (1 - e^{-630^\circ\text{K}/T}) \text{ cm}^3/\text{sec} \quad (64)$$

O'Malley's fit (64) does not appear to be consistent with the high temperature data of Chen (ref. 127); however, the validity of the latter data has been questioned (ref. 75).

In his original derivation of equation (64), O'Malley interpreted the observed gas temperature dependence of the dissociative recombination coefficient in terms of a model in which only the lowest vibrational state of the Ar₂⁺ molecule participates significantly in the dissociative recombination process (63) and, on the basis of this model, derived a value of $\omega_v \sim 630^\circ\text{K} \approx 440 \text{ cm}^{-1}$ for the Ar₂⁺ vibrational frequency. This interpretation of the data appears to be inconsistent with the value of the vibrational frequency $\omega_v \sim 80 \text{ cm}^{-1}$ recently derived by Teng and Conway (ref. 13) from thermodynamic data; however, other interpretations of the observed temperature dependence (64) which do not lead to this inconsistency appear to be possible. Thus, for the purposes of the present analysis, it is unnecessary to inquire into the validity of O'Malley's model in detail and we may regard equation (64) simply as a curvefit to the available experimental data on the dissociative recombination rate in argon.

The exact state of the excited Ar* atoms produced in the dissociative recombination reaction (63) is not known at present; however, it appears likely (ref. 75) to be one or more of the many excited atomic states lying in the range between about 14 ev and the molecular ion ground-state at 14.61 ev (see ref. 6). The excited atom produced in the original reaction (63) will then cascade down rapidly by the collisional-radiative process to one of

the four low-lying excited atomic states listed in Table XXIII, with the excess excitation energy being lost either by radiation or transfer to the electron gas. In setting up the reaction scheme given in Table XXII (reactions 15 and 16) we have assumed rather arbitrarily that electronic collisions will be the dominant de-excitation mechanism under the conditions existing in an argon plasma jet, so that the entire excess excitation energy is transferred to the electron gas. Lacking any detailed knowledge of the final state of the reaction products, we have simply assumed in reactions 15 and 16 that the resonant and metastable excited states will be populated in accordance with their statistical weights. Further, the rate of the inverse associative ionization process is calculated from detailed balance based on the electron temperature. This is consistent with the assumption that de-excitation of excited atoms occurs primarily by electronic collisions, since under this assumption the population of the excited Ar* atoms which can initiate the associative ionization process will be controlled primarily by the electron temperature; however, the approximation is evidently very crude and serves only to give an indication of the conditions under which associative ionization is likely to be important. To obtain a more quantitative prediction of associative ionization rates, it would be necessary to couple the associative ionization-dissociative recombination model, as suggested by Biberman, et al. (ref. 87), in order to obtain a prediction of the population densities in the various excited atomic states. Such a detailed model could perhaps explain some of the apparent anomalies which hav been observed in the measured argon recombination rates (refs. 94,127) but would be far beyond the scope of the present study.

Because of the very large dissociative recombination rate for Ar_2^+ molecular ions, the three-body collisional-radiative recombination process has apparently never been observed experimentally for Ar_2^+ ions. Nevertheless, this process would be expected to be the predominant recombination mechanism for Ar_2^+ ions at sufficiently high electron densities and has been included as the final reaction process in Table XXII, using the corresponding He_2^+ reaction rate from equation (44). Although the final state of the reaction products is not known, we have assumed in Table XXII that the recombining electron will cascade down through successive Rydberg states of the molecule to reach the unstable Ar_2 ground state, which will then dissociate into two ground state argon atoms. As in the case of helium,

it should be a good approximation, at the high electron densities for which the three-body recombination process is important, to assign all of the recombination energy to the electron gas.

APPENDIX B

DIAGNOSTIC MESSAGES

This appendix lists all of the diagnostic messages produced by NATA when error conditions are detected. For each message the following information is given:

- (1) The name of the subroutine in which the message is produced.
- (2) A brief description of any dumps or additional messages which follow the given message.
- (3) A description of the error condition indicated.
- (4) A summary of the subsequent action taken by the code.

The messages are listed in alphanumeric order for the entire code. Lower case letters appearing within the messages indicate numerical values.

Most of these diagnostics occur only very rarely. Many of them have never been observed at all with the present version of NATA, and are included in the program only to allow for unusual input errors or for programming errors which might occur during future modifications.

The Fortran variables appearing in the various dumps are to be defined in the NATA Programmer's Manual, Volume III of this final report.

BACKSTEPPING OF PERTURBATION SOLUTION TERMINATED AFTER n STEPS.
DIAGNOSTIC DATA FOLLOW.

Produced in subroutine N0NEQ.

Followed by a dump with the namelist name NEQDMP, followed in turn by "ERROR EXIT NO. 5 FROM N0NEQ."

This message is produced in the nonequilibrium solution by the perturbation method when $|\delta\chi_i|_{max}$ is greater than 1.2 C_χ and the temperature has been increased n times without finding

a flow point at which the right-hand inequality in equation (381) of Volume I (ref. 1) is satisfied.

The DUMP subroutine is called to produce a dump of common data and terminate the case.

BETA MATRIX OF INSUFFICIENT RANK

Produced in subroutine N0NEQ.

Followed by "ERROR EXIT NO. 1 FROM N0NEQ."

Indicates that the rank of the β_{ij} matrix is less than the number of dependent species ($n-c$); see Section 7.3.4 of Volume I (ref. 1). The diagnostic is encountered only when a new gas model is being used. It normally indicates that too few linearly independent chemical reactions are included in the gas model, but can also occur when an error has been made in the stoichiometric coefficients ν_{ij} , ν'_{ij} for a reaction.

The DUMP subroutine is called to produce a dump of common data and terminate the case.

BOUNDARY LAYER ITERATION NOT CONVERGED

Produced in subroutine DERIVS.

Followed by a dump with the namelist name DRVDMP.

Indicates that the self-consistent solution for the displacement thickness δ^* and the derivatives of the flow variables (Sect. 7.6 of Volume I) has not converged after three iterations.

The nonconverged δ^* value from the final iteration is used and the solution proceeds.

CONVERGENCE FAILURE IN AGSØLN AE = a DEL = d_1 d_2 X = x

Produced in subroutine AGSØLN.

Followed by a dump with the namelist name AGDMP.

Indicates failure of the iterative solution of equation (135) in Volume I. In the message, AE denotes the input value of the effective area ratio A_e , the two values following DEL are the displacement thicknesses at the current flow point, and X is the estimate of the axial coordinate from the final iteration, expressed in centimeters.

The DUMP subroutine is called to produce a dump of common data and terminate the case.

CONVERGENCE FAILURE IN RESTMP

Produced in subroutine RESTMP.

Indicates failure of the iterative solution for the conditions in the upstream reservoir, based upon either the pressure and mass flow (for ISW2B = 0) or the enthalpy and mass flow (for $ISW2B < 0$). Such failures can be caused by errors in the input data for FL \varnothing W and PRESAI or HSTAG.

The DUMP routine is called to dump common data and terminate the case.

DLOGR IS POSITIVE

Produced in subroutine N \varnothing NEQ.

Indicates that a positive value of $d \ln \rho/dx$ has been encountered in the nonequilibrium solution.

The subsequent action depends upon the value of the ratio (AFNX-DATEST)/DATEST, where AFNX is the effective area ratio and DATEST is a control parameter which is preset to 1.01. If this ratio is greater than or equal to 0.05, the message "ERROR EXIT NO. 3 FROM N \varnothing NEQ" is written and the DUMP routine is called to terminate the case. If the ratio is less than 0.05, the positive $d \ln \rho/dx$ value is taken to indicate that the nonequilibrium solution is on the subsonic branch of the downstream solution. An attempt is made to recover the desired supersonic branch of the solution by the inverse method at the previous switch point; see Section 7.4 of Volume I.

DUMP ROUTINE CALLED BY name

Produced by subroutine DUMP.

Indicates the name of the subroutine from which DUMP was called. Besides printing this message, subroutine DUMP sets a logical indicator ERR to the value .TRUE.. Tests on ERR in higher level routines then causes immediate return of control to the main program. After calling subroutine DUMPEX to print dumps (DMP1, DMP2, DMP3, DMP4) containing most of the variables in common, the main program terminates the case. Input data are then read for the next case, if any.

ERROR EXIT NO. 1 FROM NONEQ

Produced by subroutine NONEQ, following the message "BETA MATRIX OF INSUFFICIENT RANK" (see above).

ERROR EXIT NO. 2 FROM NONEQ

Produced by subroutine NØNEQ.

Indicates step failure (flunking of a validity check) in a lower level routine (DERIVS or CØMM), either in the perturbation solution or upon restart at the switch point after detection of a positive $d \ln \rho/dx$ value in the downstream solution.

The DUMP routine is called to dump common data and terminate the case.

ERROR EXIT NO. 3 FROM NONEQ

Produced by subroutine NØNEQ.

Indicates that a positive $d \ln \rho/dx$ value has been encountered in the nonequilibrium solution beyond the switch point from the inverse method to direct integration. (See message "DLOGR IS POSITIVE," above.) The present error exit message is printed if $(AFNX - DATEST)/DATEST$ is greater than or equal to 0.05.

The DUMP routine is called to dump common data and terminate the case.

ERROR EXIT NO. 4 FROM NONEQ

Produced by subroutine N \emptyset NEQ.

This message is printed if the $d \ln \rho / dx > 0$ condition is encountered when the solution has already been restarted at the switch point four times, in attempts to find the supersonic downstream solution.

The DUMP routine is called to dump common data and terminate the case.

ERROR EXIT NO. 5 FROM NONEQ

Produced by subroutine N \emptyset NEQ.

This message is printed following the "BACKSTEPPING OF PERTURBATION SOLUTION" message, discussed above.

The DUMP routine is called to dump common data and terminate the case.

ERROR EXIT NO. 6 FROM NONEQ

Produced by subroutine N \emptyset NEQ.

Indicates step failure (flunking of a validity check) in subroutine DERIVS or C \emptyset MM at the beginning of the first step of the numerical integration.

The DUMP routine is called to dump common data and terminate the case.

ERROR EXIT NO. 7 FROM NONEQ

Produced in subroutine N \emptyset NEQ.

Indicates that a temperature greater than the reservoir temperature has been computed at a point in the nonequilibrium numerical integration.

The DUMP routine is called to dump common data and terminate the case.

ERROR EXIT NO. 8 FROM NØNEQ

Produced in subroutine NØNEQ.

Indicates step failure in DERIVS or CØMM on restart of step after a step size reduction.

The DUMP routine is called to dump common data and terminate the case.

ERROR EXIT NO. 9 FROM NØNEQ

Produced in subroutine NØNEQ.

Indicates that the square of the concentration of an independent species is zero in the element conservation calculation for the nonequilibrium solution.

The DUMP routine is called to dump common data and terminate the case.

ERROR EXIT NO. 10 FROM NØNEQ

Produced in subroutine NØNEQ.

Indicates that the step size in the nonequilibrium integration has become vanishingly small. This message is printed if Δx falls below 10^{-10} cm, or if the step size has been reduced more than 30 successive times without completion of a valid step.*

*Note - if this diagnostic occurs upstream of the throat ($x < 0$), and if the terminal dump shows that $d \ln A_e / dx = DL \phi G A$ is positive, $A_e = AFNX \approx 1$, and $dT/DX = DT$ is near zero or positive, a likely cause of the failure is insufficiently rapid convergence of the nozzle profile curvefit upstream of the throat. In such cases, a successful solution can be obtained using a modified profile curvefit with a somewhat larger convergence angle in the region just upstream of the throat. The NØZFIT program (Appendix D) can be used to prepare profile curvefits.

The DUMP routine is called to dump common data and terminate the case.

ERROR IN INPUT DATA FOR NOZZLE GEOMETRY
 $X = x$ $ARATIO\theta = a$ $DERIVA = d$

Produced in subroutine GEOMAR.

Indicates that, at the axial coordinate X , the subroutine calculated either a geometric area ratio $A_g = ARATIO\theta$ less than 1 or a derivative $d A_g/dx = DERIVA$ for which $X \cdot DERIVA < 0$.

The DUMP routine is called to dump common data and terminate the case.

EXCEEDED 50 ITERATIONS IN SHOCK

Produced in subroutine SHOCK.

Indicates that the iterative solution of the cubic equation for a classical oblique shock has not converged after 50 iterations.

An error indicator in the argument list is set to inform the calling routine (WEDGE) of the failure. Wedge calculations are omitted for the angle for which the failure occurred and for all larger angles. The failure occurs because the assumed angle of attack is too high to allow an attached shock.

FINDX CALLED WITH AN AREA RATIO LESS THAN UNITY, $A = a$

Produced in subroutine FINDX.

Indicates that FINDX was called to determine the axial coordinate corresponding to a geometric area ratio A less than unity. Since the geometric area ratio cannot be less than unity, there is no solution. The error indicated by this diagnostic originates in the calling routine or in higher-level routines.

The DUMP routine is called to dump common data and terminate the case.

+++++ FIX REQUIRED IN AGSØLN

Produced in subroutine AGSØLN.

Subroutine AGSØLN solves for the geometric area ratio A_g and axial coordinate x corresponding to a specified value of the effective area ratio A_e . In channel flow problems, this requires an iterative solution of equation (135) in Volume I (ref. 1). The above message is printed if, during this iterative solution, an x value is obtained whose sign is inconsistent with that of the argument UPDØWN (which specifies whether an upstream or downstream solution is desired).

When this condition is first encountered, the programming assumes that it is a result of an unusually large separation between the throat and the sonic point (caused by rapid change of the boundary layer displacement thicknesses in the throat region). On this assumption, an attempt is made to fix the problem by resetting the assumed displacement thicknesses to their values at the throat. If the problem recurs, the message "CONVERGENCE FAILURE IN AGSØLN" (above) is printed and the case is terminated in the usual way.

GJ(i)** 2 UNDERFLOWED

Produced in subroutine NØNEQ.

Followed by message "ERROR EXIT NO. 9 FROM NØNEQ" (above).

INDEXING OR STORAGE FAILURE IN MATINV

Produced in subroutine MATINV.

Indicates that the dimension statements in arrays LPIJ and BTA are inconsistent; can occur only if someone tinkers with the programming.

The DUMP routine is called to dump common data and terminate the case.

IN NEWRAP, CAPX (k) = 0

Produced in subroutine NEWRAP.

Indicates that the mole fraction of the kth species was found to be zero.

The equilibrium solution is continued.

IN NEWRAP, P = 0

Produced in subroutine NEWRAP.

Indicates that a zero value of pressure was obtained during the iteration to determine the conditions at a point in the equilibrium solution.

The solution is continued.

INVALID INPUT DATA... NPRFLS = n

Produced in subroutine READ.

Indicates that NPRFLS was specified in the input as a value other than 1 or 2.

The job is terminated.

ITERATION TO FIND STAGNATION CONDITIONS DID NOT CONVERGE

Produced in subroutine MØDEL.

Followed by a dump with the namelist name MØDDMP.

Indicates that the iterative solution for the conditions behind the normal shock, or the solution for the stagnation conditions, did not converge within the maximum number of allowed iterations.

Conditions at the model point where the convergence failure occurred are not calculated. The solution continues.

ITERATION TO OBTAIN FREE STREAM SOLUTION AT MODEL POINT DID NOT CONVERGE X = x XMØDEL = y CM

Produced in subroutine FRØZEQ.

Followed by dump with the namelist name FRDMP2.

Indicates that the iteration to determine the free-stream conditions at a model point in the frozen or equilibrium solution has not satisfied the convergence test after the maximum allowable number of steps.

The conditions from the final iteration are used in the model condition calculations and printed out.

MATINV, MATRIX SINGULAR

Produced in subroutine MATINV.

Indicates that the square submatrix of α_{ij} defining the elemental composition of the independent species is singular. This diagnostic occurs only when a user-specified gas model is being used and indicates an error in the inputs defining the independent species. It can occur if the ISC = c species listed first are not independent, where c denotes the number of chemical elements present in the gas model.

The DUMP routine is called to dump common data and terminate the case.

MATRIX OF COEFFICIENTS IS SINGULAR

Produced in subroutine DSMSØL.

This subroutine is used throughout the program to solve systems of linear equations. The diagnostic indicates that the matrix of coefficients for such a system is singular. The preceding output, and the data in the terminal dump, should indicate the kind of calculation in which the failure occurred, i.e., reservoir conditions, frozen or equilibrium solution, nonequilibrium perturbation calculation or numerical integration.

The DUMP routine is called to dump common data and terminate the case.

MODEL PARAMETER ROUTINE CALLED FOR A MACH NUMBER LESS THAN 1.5

Produced in subroutine MØDEL.

Indicates that MØDEL was called at a point where the free-stream Mach number was less than 1.5. The method used for the

normal shock solution in MODEL does not work reliably for
 $M < 1.5$.

The model condition calculations are skipped. The solution continues.

MORE THAN 50 ITERATIONS IN FINDX, A = a
UPDWN = u IENTRY = i MBL = m

Produced in subroutine FINDX.

Followed by a dump with the namelist name DMP.

Indicates a convergence failure in subroutine FINDX, which solves for the axial coordinate x at which the geometric area ratio has the value A. According as the argument UPDWN has the value -1. or +1., the upstream or downstream solution is sought. IENTRY indicates whether the subroutine was entered at its beginning or through the entry point FINDXC, which is called to determine the x at which the MBLth profile has a half-width of A.

The DUMP routine is called to dump common data and terminate the case.

NEGATIVE CONCENTRATION ENCOUNTERED IN COMM

Produced in subroutine C₀MM.

Indicates that C₀MM found a species concentration to be negative during the nonequilibrium solution.

A step-failure indicator is set, and control is returned to the calling routine (DERIVS). Upon return to subroutine N₀EQ, the integration step size is reduced. The solution continues.

NEGATIVE OR ZERO VALUES OF XM₀DPL NOT ALLOWED. DATA IGNORED.

Produced in subroutine READ.

Indicates that the input value of XM₀DPL (the location of the first model point in a sequence) is negative.

XM₀DPL is reset to 10²⁰ and the calculations continue.

NEGATIVE RHO IN GEOM

Produced by subroutine GEOM.

Indicates that a negative density value has been encountered during the iteration to determine the density corresponding to the geometric area ratio at the current flow point during the nonequilibrium solution by the inverse method.

The DUMP routine is called to dump common data and terminate the case.

NO THERMAL PROPERTY DATA DEFINED FOR SPECIES NUMBER i IN THE CURRENT GAS MODEL (NO. m IN THE MATER LIST OF SPECIES)

Produced in subroutine READ.

Indicates that ET AJ(i) = 0. and IGJ(i) = 0 for the ith species in the gas model, because of an input error in user specification of a nonstandard species.

The job is terminated.

SU2 LESS THAN 0 IN COMM

Produced in subroutine C0MM.

Indicates that C0MM computed a total enthalpy larger than the reservoir enthalpy.

A step failure indicator is set and control is returned to the calling routine (DERIVS). After the return to N0NEQ, the step size is reduced and the calculation is continued.

TEMPERATURE GREATER THAN RESERVOIR VALUE

Produced in subroutine N0NEQ.

Followed by the message "ERROR EXIT NO. 7 FROM N0NEQ" (see above).

TOO MANY ITERATIONS IN WES0LN ZETA = z CAPGAM = c

Produced in subroutine WES0LN.

Followed by a dump with the namelist name WEDMP.

Indicates that the Newton-Raphson solution of equation (482b) in Volume I (ref. 1) for λ as a function of ζ has not converged after 20 iterations.

The final, unconverged value of λ is accepted and used. The solution continues.

TOO MANY NEWTON-RAPHSON ITERATIONS

Produced in subroutine EQCALC or in subroutine NEWRAP.

Indicates that the Newton-Raphson solution for the equilibrium mole fractions (Volume I, Sections 6.1 and 6.2) failed to converge. If the failure occurs in EQCALC during the reservoir calculations (EQCALC called by the entry INTA of subroutine INGAS), it is probably caused by an error in the input specifications of the reservoir condition (input variables ISW2B, PRESAI, CTAPI, FL δ W, HSTAG).

The DUMP routine is called to dump common data and terminate the case.

TRANSPORT PROPERTIES OF DESIRED MIXTURE CANNOT BE CALCULATED FROM AVAILABLE DATA. REVISE CROSS SECTION INPUT DATA.

Produced in subroutine XSECT.

Followed by a dump with the namelist name XSDMP.

Indicates that cross section data have not been specified for the like-like interactions of a neutral atom or molecule.

The DUMP routine is not called, but the case is terminated.

X DECREASED IN FROZEQ

Produced in subroutine FR δ ZEQ.

Indicates that the axial coordinate x decreased during a step of the frozen or equilibrium solution. Since x is calculated from the effective area ratio in these types of solution, a decrease in x could result from improper specification of the

nozzle profile (for example, a discontinuity in the profile at the point where two profile sections are joined). If the solution includes the boundary layer, rapid growth of the displacement thickness can cause the effective area ratio to decrease. A decrease in the effective area ratio downstream of the throat would lead to a decrease in x . This error condition is usually encountered only in the high Mach number region far downstream of the throat. The most common cause is instability of the coupled inviscid flow and boundary layer.

The subsequent action depends upon the circumstances. If the boundary layer is being neglected, or if the effective area ratio is less than $\frac{1}{4}$ of the geometric area ratio, a dump with the namelist name FRDMP is written and the current equilibrium or frozen flow solution is terminated. The solution of the current case continues, however. If the boundary layer is included and the effective area ratio is greater than $\frac{1}{4}$ of the geometric area ratio, the program assumes that the failure is a result of instability, and attempts to generate a valid solution by cutting the stability parameter w in equation (218) of Volume I in half, and restarting the solution in the upstream reservoir. However, if the same error occurs after three successive restarts, the dump FRDMP is written and the current (equilibrium or frozen) solution is terminated.

ZERO OR NEGATIVE STEP IN BLAYER, $X = x$ $XP = y$

Produced in subroutine BLAYER.

Followed by a dump with the namelist name DMP.

Indicates that the axial coordinate X at the current call to subroutine BLAYER is less than or equal to the value XP at the last previous call.

The RETURN is executed and the solution proceeds.

APPENDIX C

ILLUSTRATIVE TEST PROBLEMS

This appendix presents the inputs and selected portions of the output for five test problems, chosen to illustrate various features of the NATA code. Two additional test problems (nos. 1 and 1A) have already been discussed in Sections 2 and 3.

The images of the input cards for the test problems are shown in figure 65. There are four groups of data cards, each group comprising the data for a NATA run. The third run includes two cases (4A and 4B). These runs were executed on an IBM 360/75.

Test problem no. 2 illustrates NATA flow calculations for a rectangular channel. In a channel case, the problem summary includes geometric data for two profiles (figure 66). Figure 67 shows the output of reservoir conditions for this case. Figure 68 illustrates the output of the flow solution. In channel flow problems including the boundary layer, NATA prints two complete sets of boundary layer data at each flow point. The first set appears in the fourth and fifth lines of output for the flow point, the second set in the sixth and seventh lines. Each set begins with the lateral dimension ("WIDTH" or "HEIGHT") of one of the channel walls. The boundary layer data in each set pertain to the wall whose lateral dimension is included in the set. For example, at the last flow point shown in figure 68, the lateral dimensions of the channel are 2 by 18 inches. The first set of boundary layer data (including $\Theta = 0.100$ and $S_{ANTN} = 1.697D-3$) refers to the boundary layer on the walls which are 18 inches wide. The second set (including $\Theta = 0.340$ and $S_{ANTN} = 4.777D-4$) refers to the layer on the walls which are 2 inches wide. The flow points at $X = 16.000, 17.000$, and 18.000 in figure 68 are special points requested by the TSDIAM inputs in figure 65.

Test problem no. 3 illustrates a flow solution based on the larger of the two standard planetary atmosphere models. In this case, the reservoir conditions were specified by direct input of the reservoir pressure and temperature. Figures 69 through 73 show the problem summary for this case. Figure 74 shows the reservoir conditions, and figures 75 to 78 the first

FIGURE 65 - INPUT DATA FOR TEST PROBLEMS NO. 2, 3, 4A, 4B, AND 5

TEST PROBLEM NO. 2 - FROZEN AIR FLOW IN A CHANNEL

```
+INPUT  
ISW2A=0, ISW3A=0, CXMAXI=57, PRESAI=.762, FLOW=.1, ICHAN=1,  
TSDIAM=15, 16, 17, 18, 19, 20  
+END
```

TEST PROBLEM NO. 3 - PLANETARY ATMOSPHERE MODEL

```
+INPUT  
ISW1A=0, ISW3A=0, CXMAXI=50, ISW2B=1, PRESAI=1, CTAPI=10000, NOZZLE=2,  
IGAS=5  
+END
```

TEST PROBLEM NO. 4A - WEGENER EXPERIMENT C - NONSTANDARD GAS AND GEOMETRY

```
+INPUT  
ISW2B=1, NOTRAN=T, CXMAXI=5.906, TPRNTI=.001, READG=T, PRESAI=2, CTAPI=400,  
NOZZLE=0, DIAM=.5472, JDIM=0, NSECTS=2.2, ISHAPE=1.2.2.1,  
ARAMI=7.606602E-2, -.5773502, 0, 4.695442, 0, 4.0005, 4.695442, 0,  
4.0005, .6941124, 2.038825E-2, 0, ATPI=-2.000249, 0, .08154619,  
XZEROI=-10, IGAS=0, NCS=2, JCS=5.30, QPJ=.995025, .004975, ISCI=2,  
ISSI=3, ISRI=1, ICI=0, IE=5.6, IS=5.30, 29, IR=76, ISATOM=29, ISMOL=30,  
ISW4A=1,  
+END  
+EINPUT  
SP29=0.2.5.6.0.1.2.0, 4.003, -3.75E-4, 2.45E-6, 2*0, 5.945, 9586, 4*0,  
1.23*0, SP30=0.2.5.6.0.2.4.0, 3.553, .011625, -4.55E-6, 2*0, 10.028, 4473,  
4*0, 1, 23*0, RP76=3.E14, 3*0, 2.2.5.29.0.5.30.0.1.2.0.1.1, 0.0, 10*0,  
+END
```

TEST PROBLEM 4B - WEGENER EXPERIMENT F --STACKING OF CASES

```
+INPUT  
PRESAI=2.16, CTAPI=402, QPJ=.97561, .02439, ISW4A=0, READG=F  
+END
```

TEST PROBLEM NO. 5 - ELECTRONIC NONEQUILIBRIUM MODEL FOR ARGON

```
+INPUT  
ISW1A=0, ISW3A=0, ISW3B=0, CXMAXI=40, ISW6B=-1, ISW2B=1, PRFSAI=1,  
CTAPI=10000, NOZZLE=1, IGAS=3, XMODP1=20, NMODPT=3, TPRNTI=.001,  
ISW5B=-1000000  
ND
```

FIGURE 66 - FIRST PAGE OF PROBLEM SUMMARY FOR TEST PROBLEM NO. 2

RUN NO. 0 CASE 1 IN THIS JOB
RESERVOIR PRESSURE = 0.7620 ATM. TOTAL MASS FLOW = 0.10000 LB/SEC
TEST PROBLEM NO. 2 - FROZEN AIR FLOW IN A CHANNEL

NATA 11 USE OUTPUT

T12 CHANNEL (STANDARD CHANNEL NO. 1) FOR DCA = 2.0000 BY 1.0000 INCH THROAT

PROFILE NO. 1

THROAT RADIUS = 2.500 CM INLET AT -7.620 CM 6 SECTIONS IN FIT. 4 UPSTREAM OF THROAT

J	ISHAPE(J)	SHAPE	ATPI(J)	PARAM(1,J)
1	1	STRAIGHT LINE	-6.7310D 00	-1.1760D 00
2	2	CIRCLE BOTTOM	-6.0960D 00	3.8100D 00
3	1	STRAIGHT LINE	0.0	2.5400D 00
4	2	CIRCLE BOTTOM	0.0	1.0500D 02
5	2	CIRCLE BOTTOM	0.0	1.0500D 02
6	1	STRAIGHT LINE	2.5400D 00	4.0

PROFILE NO. 2

THROAT RADIUS = 1.270 CM INLET AT -7.620 CM 4 SECTIONS IN FIT. 2 UPSTREAM OF THROAT

J	ISHAPE(J)	SHAPE	ATPI(J)	PARAM(1,J)
1	1	STRAIGHT LINE	-6.7717D 00	-5.0150D-01
2	2	CIRCLE BOTTOM	0.0	1.6510D 01
3	2	CIRCLE BOTTOM	2.6464D 00	1.6510D 01
4	1	STRAIGHT LINE	1.0349D 00	1.7633D-01

STANDARD GAS NO. 2 (AIR-2)

COLD SPECIES

NO.	NAME	INDEX	MOLE FRAC.	MOL. WT.	CHEMICAL FORMULA
1	N2	5	0.78823	28.0140	(N)2
2	O2	6	0.21177	32.0000	(O)2

MEAN MOLECULAR WEIGHT OF COLD GAS = 28.4581

ELEMNT ATOM FRACTION

ELEMNT	ATOM FRACTION	ACTIVATION ENERGY	CHI TEST	THIRD BODY MATRIX
E-	0.0	5.485970D-04	1.179800D 05	0.100000 0001010
N	1.576460D 00	1.400700D 01	1.179800D 05	0.100000 0001010
O	4.235400D-01	1.600000D 01	1.179800D 05	0.100000 0001010

REACTION NO. CONSTANT FACTOR AI TEMP. POWER DEPENDENCE

1	3.599999D 14	-1.000000D 00	1.179800D 05	0.100000 0001010
2	8.999997D 15	-1.000000D 00	1.179800D 05	0.100000 0001010
3	3.200000D 15	-1.000000D 00	1.179800D 05	0.100000 0001010
4	7.200000D 14	-1.000000D 00	1.179800D 05	0.100000 0001010
5	1.900000D 15	-5.000000D-01	2.250400D 06	0.100000 0001010
6	4.100000D 16	-1.650000D 00	2.250400D 05	0.100000 0001010
7	4.700000D 15	-5.000000D-01	2.250400D 05	0.100000 0001010

ORIGINAL PAGE IS
IN POOR QUALITY

FIGURE 67 - RESERVOIR CONDITIONS OUTPUT FOR TEST PROBLEM NO. 2

RESERVOIR CONDITIONS -

GAS FLOW RATE	=	0.100	LB/SEC
CHANNEL T12	=	2.000	BY 1.000 INCH THROAT FOR D'A
PRESSURE	=	0.762	ATM
TEMPERATURE	=	5685.	DEG K
ENTHALPY	=	5765.	BTU/LB
ENTROPY	=	2.87	BTU/LB-DEG R
DENSITY	=	0.00230	LB/CU FT
VELOCITY	=	0.	FT/SEC
MASS FLUX	=	0.0	LB/SQ FT-SEC
COMPUTED FLOW	=	0.100	LB/SEC
CANNA	=	1.361	
MOLECULAR WEIGHT	=	22.54	GM/MOLE
ELECTRON DENSITY	=	1.410	1.4 ELECTRONS/CC

SPECIES MOLE FRACTIONS

E-	=	1.435D-04
N2	=	5.526D-01
O2	=	3.528D-04
N	=	1.169D-01
O	=	3.239D-01
NO	=	9.077D-03
NO2	=	1.435D-04

*****ELAPSED TIME = 0.36 MINUTES SINCE START OF RUN. 20. SECONDS SINCE LAST PRINTED TIME

RESERVOIR TRANSPORT PROPERTIES

VISCOSITY	=	9.80D-05	LBIN/FT-SEC
PRANDTL NUMBER	=	0.65960	
SIGMA	=	6.62D-01	MHD/CM
LEWIS NUMBER	=	1.013	

FIGURE 68 - FLOW-SOLUTION COMPUT FOR TEST PROBLEM NO. 2

PRREF =	0.6585	STANTN =	1.784D-03	RETH =	1.43.	RETHTR =	4.97.
DELSTR =	0.130	THETA =	0.296	ON	1.67930 00	TAUW =	1.3980-01
PRREF =	0.6585	STANTN =	5.0710-04	RETH =	471.	RETHTR =	497.

***** FROZEN *****

X =	41.094	T =	1337.	H =	3260.	P =	4.209D-03	R =	5.3980-05
ARAT =	15.303	V =	11196.	N =	4.085	S =	2.87	GAMMA =	1.415
ARATEF =	12.135	REFP =	1.886D 04	MW =	22.54	MU =	3.204D-05	SIGMA =	0.6880-01
WIDTH =	15.303	DELSTR =	0.165	THETA =	0.091	OW =	6.035D 00	TAUW =	3.844D-01
HR =	5244.	PRREF =	0.6585	STANTN =	1.7772D-03	RETH =	443.	RETHTR =	499.
HEIGHT =	2.000	DELSTR =	0.136	THETA =	0.301	OW =	1.671D 00	TAUW =	1.360D-01
HR =	5244.	PRREF =	0.6585	STANTN =	5.021D-04	RETH =	473.	RETHTR =	499.

***** FROZEN *****

X =	43.060	T =	1318.	H =	3250.	P =	4.013D-03	R =	5.220D-05
ARAT =	16.000	V =	11218.	N =	4.120	S =	2.87	GAMMA =	1.416
ARATEF =	12.524	REFP =	1.648D 04	MW =	22.54	MU =	3.173D-05	SIGMA =	0.793D-01
WIDTH =	16.000	DELSTR =	0.174	THETA =	0.093	OW =	5.791D 00	TAUW =	3.397D-01
HR =	5242.	PRREF =	0.6585	STANTN =	1.785D-03	RETH =	444.	RETHTR =	503.
HEIGHT =	2.000	DELSTR =	0.157	THETA =	0.311	OW =	1.633D 00	TAUW =	1.300D-01
HR =	5242.	PRREF =	0.6585	STANTN =	4.996D-04	RETH =	479.	RETHTR =	503.

***** FROZEN *****

X =	45.894	T =	1294.	H =	3237.	P =	3.768D-03	R =	4.992D-05
ARAT =	17.000	V =	11248.	N =	4.168	S =	2.87	GAMMA =	1.417
ARATEF =	13.061	REFP =	1.793D 04	MW =	22.54	MU =	3.133D-05	SIGMA =	0.664D-01
WIDTH =	17.000	DELSTR =	0.187	THETA =	0.097	OW =	5.442D 00	TAUW =	3.185D-01
HR =	5239.	PRREF =	0.6586	STANTN =	1.6719D-03	RETH =	445.	RETHTR =	509.
HEIGHT =	2.000	DELSTR =	0.187	THETA =	0.326	OW =	1.533D 00	TAUW =	1.200D-01
HR =	5239.	PRREF =	0.6586	STANTN =	4.653D-04	RETH =	487.	RETHTR =	509.

***** FROZEN *****

X =	45.940	T =	1294.	H =	3237.	P =	3.764D-03	R =	4.988D-05
ARAT =	17.016	V =	11248.	N =	4.169	S =	2.87	GAMMA =	1.417
ARATEF =	13.070	REFP =	1.792D 04	MW =	22.54	MU =	3.132D-05	SIGMA =	0.663D-01
WIDTH =	17.016	DELSTR =	0.188	THETA =	0.097	OW =	5.436D 00	TAUW =	3.182D-01
HR =	5239.	PRREF =	0.6586	STANTN =	1.6719D-03	RETH =	445.	RETHTR =	509.
HEIGHT =	2.000	DELSTR =	0.187	THETA =	0.326	OW =	1.534D 00	TAUW =	1.206D-01
HR =	5239.	PRREF =	0.6586	STANTN =	4.651D-04	RETH =	487.	RETHTR =	509.

***** FROZEN *****

X =	46.731	T =	1272.	H =	3225.	P =	3.655D-03	R =	4.791D-05
ARAT =	18.000	V =	11274.	N =	4.213	S =	2.87	GAMMA =	1.418
ARATEF =	13.579	REFP =	1.746D 04	MW =	22.54	MU =	3.096D-05	SIGMA =	0.543D-01
WIDTH =	18.000	DELSTR =	0.200	THETA =	0.100	OW =	5.166D 00	TAUW =	3.022D-01
HR =	5237.	PRREF =	0.6586	STANTN =	1.6597D-03	RETH =	445.	RETHTR =	514.
HEIGHT =	2.000	DELSTR =	0.216	THETA =	0.340	OW =	1.454D 00	TAUW =	1.140D-01
HR =	5237.	PRREF =	0.6586	STANTN =	4.727D-04	RETH =	487.	RETHTR =	514.

ORIGINAL PAGE IS
OF POOR QUALITY

FIGURE 69 - PROBLEM SUMMARY FOR TEST PROBLEM NO. 3 (First Page)

NATA 111 HE OUTPUT

PUN NO. 0 CASE 1 IN THIS JOB TEST PROBLEM NO. 3 - PLANETARY ATMOSPHERE MODEL

RESERVOIR PRESSURE = 1.0000 ATM. RESERVOIR TEMPERATURE = 10000.00 DEG K

STANDARD AXISYMMETRIC NOZZLE NO. 2, 1.500 INCH THROAT DIAM FOR DCA

THROAT RADIUS = 1.905 CM INLET AT -9.144 CM 6 SECTIONS IN FIT. 4 UPSTREAM OF THROAT

J	I	SHAPE(J)	SHAPE	ATPI(J)	PARAM(1,J)	PARAM(2,J)	PARAM(3,J)
1	1	STRAIGHT LINE	-9.4315D 00	-2.2739D 01	-2.7475D 00	0.0	0.0
2	2	CIRCLE BOTTOM	-8.3046D 00	3.6687D 00	-8.2381D 00	1.2700D 00	1.2700D 00
3	1	STRAIGHT LINE	-6.6470D-03	1.9048D 00	-5.2408D-02	0.0	0.0
4	2	CIRCLE BOTTOM	0.0 C	2.0320D 00	0.0	1.2700D-01	1.2700D-01
5	2	CIRCLE BOTTOM	3.2870D-02	2.0320D 00	0.0	1.2700D-01	1.2700D-01
6	1	STRAIGHT LINE		1.9005D 00	2.6793D-01	0.0	0.0

STANDARD GAS NO. 5 (CONAR)

NO.	NAME	INDEX	MOLE FRAC.	MOL. WT.	CHEMICAL FORMULA
1	CO2	13	0.75000	44.0110	(C) 1 (O) 2
2	AR	4	0.20000	39.9480	(AR) 1
3	N2	5	0.05000	28.0140	(N) 2

MEAN MOLECULAR WEIGHT OF COLD GAS = 42.3965

COLD SPECIES

ELEMENT	ATOM FRACTION	ELEMENT MOLECULAR WEIGHTS
E-	0.0	5.4859700-04
C	7.500000D-01	1.201100 01
N	9.999999D-02	1.400700 01
O	1.500000D 00	1.600000 01
AR	2.000000D-01	3.994800 01

ELEMENT	CONSTANT FACTOR AI	TEMP. POWER DEPENDENCE	ACTIVATION ENERGY	CHI TEST	THIRD BODY MATRIX
1	3.5999990 14	-1.00000D 00	1.179800D 05	0.1000000	01100101111000 0000
2	8.9966975 15	-1.00000D 00	1.179800D 05	0.1000000	
3	3.200000D 15	-1.00000D 00	1.179800D 05	0.1000000	
4	7.2000002 14	-1.00000D 00	1.179800D 05	0.1000000	
5	1.9000001 15	-5.00000D-01	2.250400D 05	0.1000000	011010111110000000
6	4.1000001 16	-1.500000D 00	2.250400D 05	0.1000000	
7	4.7000000 15	-5.00000D-01	2.250400D 05	0.1000000	
8	3.8999995 14	-1.500000D 00	1.500500D 05	0.1000000	011110001100000000
9	7.7999990 14	-1.500000D 00	1.500500D 05	0.1000000	000001110010000000
10	3.1999990 13	1.000000D 00	3.915000D 04	0.1000000	
11	7.000000 13	0.0	7.551000D 04	0.1000000	
12	6.6999990 15	-1.500000D 00	0.3	0.1000000	
13	2.2000000 22	-4.500000D 00	0.0	0.1000000	
14	2.2000001 22	-4.500000D 00	0.0	0.1000000	
15	7.9999990 15	-1.500000D 00	0.0	0.1000000	
16	7.8900000 13	5.000000D-01	0.0	0.1000000	

FIGURE 70 - PROBLEM SUMMARY FOR TEST PROBLEM NO. 3 (Second Page)

17	7.8000000	13	5.0000000-C1	0.0	0.1000000
18	1.5000000	16	-1.5000000	0.0	0.0000000
19	9.9999990	13	-2.5000000	C0	C1000000
20	2.2000000	16	-2.5000000	00	0.1000000
21	1.5000000	13	0.0	0.0	0.1000000
22	3.4000000	11	-2.0000000	00	0.1000000
23	4.7999990	14	0.0	0.0	0.1000000
24	1.6000000	15	5.0000000-D1	0.0	0.1000000
25	9.9999990	13	-2.5000000	00	0.1000000
26	d.79999960	16	-2.5000000	00	0.1000000
27	4.4800000	15	-1.0000000	00	0.1000000
28	B.8099980	14	-2.0000000	00	0.1000000
29	2.3209990	11	5.0000000-D1	1.3050000	0.1000000
30	2.7239990	13	5.0000000-D1	1.3810000	0.1000000
31	2.8599990	13	5.0000000-D1	1.0650000	0.1000000
32	4.5900000	10	5.0000000-D1	2.3970000	0.1000000
33	2.5520000	11	5.0000000-D1	7.6060000	0.1000000
34	1.0700000	14	5.0000000-D1	6.7050000	0.1000000
35	6.0330000	13	3.0000000-D1	6.3360000	0.1000000
36	6.65979990	14	5.0000000-D1	5.4160000	0.1000000
37	1.0900000	14	5.0000000-D1	9.2220000	0.1000000
38	5.4699980	14	5.0000000-D1	7.4700000	0.1000000
39	1.5000000	16	1.5000000	00	0.1000000
40	2.0000000	22	1.5000000	00	0.1000000
41	4.5899990	14	5.0000000-D1	1.0960000	0.1000000
42	4.5299990	14	5.0000000-D1	4.4490000	0.1000000
43	5.9500000	14	5.0000000-D1	3.2270000	0.1000000
44	2.2000000	22	-4.5000000	00	0.1000000
45	3.7000000	15	-1.0000000	00	1.3116000
46	4.2999980	14	5.0000000-D1	6.9670000	0.1000000
47	1.5000000	13	9.0000000-D1	5.1670000	0.1000000
48	2.0000000	14	1.0000000	00	5.5640000

SPECIES THERMAL FIT INDICATOR ALPHA MATRIX

	E-	C	N	O	AR
E-	0	0	0	0	0
AR	0	2	0	2	1
CO2	0	1	0	2	0
N2	1	0	2	0	0
O2	1	0	0	2	0
N	0	0	1	0	0
O	0	0	0	1	0
NO	0	0	1	1	0
CO	0	1	0	1	0
CN	0	1	0	1	0
C	0	0	0	1	0
N2O	1	0	1	0	0
NE	0	0	1	0	0
CS	0	0	1	0	0
N2S	1	0	2	0	0
O2S	1	0	2	0	0
CE	0	1	0	0	0
ARG	0	1	0	0	0
C3E	1	1	0	0	0

REACT NO. NU PRIME MATRIX

	E-	AR	CO2	N2	O2	N	O	CO	CN	C	NO	NC	OC	NE	CO	CE	ARG	C3E
1	0.	0.	0.	0.	0.	0.	2.	0.	0.	0.	0.	0.	0.	0.	0.	0.	0.	0.
2	0.	0.	0.	0.	0.	0.	0.	0.	0.	0.	0.	0.	0.	0.	0.	0.	0.	0.

ORIGINAL PAGE IS
OF POOR QUALITY

FIGURE 71 - PROBLEM SUMMARY FOR TEST PROBLEM NO. 3 (Third Page)

REACT NO.	NU MATRIX	E-	O-	N2	O2	CO	NO	CN	O	H2	CE	ARC	CO2
5	0	1	0	0	0	0	0	0	0	0	0	0	0
6	0	1	0	0	0	0	0	0	0	0	0	0	0
7	0	0	1	0	0	0	0	0	0	0	0	0	0
8	0	0	0	1	0	0	0	0	0	0	0	0	0
9	0	0	0	0	1	0	0	0	0	0	0	0	0
10	0	0	0	0	0	1	0	0	0	0	0	0	0
11	0	0	0	0	0	0	1	0	0	0	0	0	0
12	0	0	0	0	0	0	0	1	0	0	0	0	0
13	0	0	0	0	0	0	0	0	1	0	0	0	0
14	0	0	0	0	0	0	0	0	0	1	0	0	0
15	0	0	0	0	0	0	0	0	0	0	1	0	0
16	0	0	0	0	0	0	0	0	0	0	0	1	0
17	0	0	0	0	0	0	0	0	0	0	0	0	1
18	0	0	0	0	0	0	0	0	0	0	0	0	0
19	0	0	0	0	0	0	0	0	0	0	0	0	0
20	0	0	0	0	0	0	0	0	0	0	0	0	0
21	0	0	0	0	0	0	0	0	0	0	0	0	0
22	0	0	0	0	0	0	0	0	0	0	0	0	0
23	0	0	0	0	0	0	0	0	0	0	0	0	0
24	0	0	0	0	0	0	0	0	0	0	0	0	0
25	0	0	0	0	0	0	0	0	0	0	0	0	0
26	0	0	0	0	0	0	0	0	0	0	0	0	0
27	0	0	0	0	0	0	0	0	0	0	0	0	0
28	0	0	0	0	0	0	0	0	0	0	0	0	0
29	0	0	0	0	0	0	0	0	0	0	0	0	0
30	0	0	0	0	0	0	0	0	0	0	0	0	0
31	0	0	0	0	0	0	0	0	0	0	0	0	0
32	0	0	0	0	0	0	0	0	0	0	0	0	0
33	0	0	0	0	0	0	0	0	0	0	0	0	0
34	0	0	0	0	0	0	0	0	0	0	0	0	0
35	0	0	0	0	0	0	0	0	0	0	0	0	0
36	0	0	0	0	0	0	0	0	0	0	0	0	0
37	0	0	0	0	0	0	0	0	0	0	0	0	0
38	0	0	0	0	0	0	0	0	0	0	0	0	0
39	0	0	0	0	0	0	0	0	0	0	0	0	0
40	0	0	0	0	0	0	0	0	0	0	0	0	0
41	0	0	0	0	0	0	0	0	0	0	0	0	0
42	0	0	0	0	0	0	0	0	0	0	0	0	0
43	0	0	0	0	0	0	0	0	0	0	0	0	0
44	0	0	0	0	0	0	0	0	0	0	0	0	0
45	0	0	0	0	0	0	0	0	0	0	0	0	0
46	0	0	0	0	0	0	0	0	0	0	0	0	0
47	0	0	0	0	0	0	0	0	0	0	0	0	0
48	0	0	0	0	0	0	0	0	0	0	0	0	0

FIGURE 72 - PROBLEM SUMMARY FOR TEST PROBLEM NO. 3 (Fourth Page)

ELECTRONIC LEVELS

SPECIES	ATOMS PER MOLECULE	CHEMICAL CONSTANT	CHAR.	VIBRATIONAL TEMP.	ENTHALPY OF FORMATION	
					0.0	0.0
E-	1.0000000 00	-1.492760D-01	0.0	0.0	0.0	0.0
A ⁺	1.0000000 00	1.866300D-00	0.0	0.0	0.0	0.0
CO ₂	3.0000000 05	1.895800D-00	1.977000D-03	9.6000000 02	9.6000000 02	9.6000000 02
N2	2.0000000 00	-4.105999D-01	3.3520000 03	3.3800000 03	3.3800000 03	3.3800000 03
O2	2.0000000 00	1.140000D-01	2.2390000 03	1.125200D-01	1.125200D-01	1.125200D-01
N	1.0000000 00	2.944000D-01	6.0	5.899000D-04	5.899000D-04	5.899000D-04
O	1.0000000 00	4.938000D-01	0.0	2.699000D-03	2.146000D-04	2.146000D-04
NO	2.0000000 00	5.455000D-01	2.699000D-03	3.0830000 03	6.677000D-04	6.677000D-04
CO	2.0000000 00	3.169000D-01	3.0830000 03	2.939000D-03	1.971700D-05	1.971700D-05
CN	2.0000000 00	2.226000D-01	2.939000D-03	2.635500D-05	2.365600D-05	2.365600D-05
C	1.0000000 00	6.36996D-02	0.0	4.476000D-05	3.729400D-05	3.729400D-05
NO ₂	2.0000000 00	3.941200D-01	3.3730000 03	3.576800D-05	3.576800D-05	3.576800D-05
NS	1.0000000 00	2.943000D-01	0.0	2.860000D-05	2.860000D-05	2.860000D-05
O ₂	1.0000000 00	4.938000D-01	0.0	5.233100D-05	5.233100D-05	5.233100D-05
N2O	2.0000000 00	-3.763000D-01	3.1240000 03	3.899500D-05	3.899500D-05	3.899500D-05
O ₂ O	2.0000000 00	-3.170000D-02	2.6280000 03	2.860000D-05	2.860000D-05	2.860000D-05
CC	1.0000000 00	6.359994D-02	0.0	3.633300D-05	3.633300D-05	3.633300D-05
AC	1.0000000 00	1.866300D-00	0.0	3.1420000 03	3.1420000 03	3.1420000 03
CO ₂	2.0000000 00	2.931000D-01				

SERVOIR CONDITIONS -

FIGURE 74 - RESERVOIR CONDITION OUTPUT FOR TEST PROBLEM NO. 3

NOZZLE = DCA	= 1.500	INCH THROAT DIAMETER
PRESSURE	= 1.000	ATM
TEMPERATURE	= 1700°C	DEG K
ENTHALPY	= 19965.	BTU/LB
ENTROPY	= 3.59	BTU/LB-DEG R
DENSITY	= 0.00121	LB/CC FT
VELOCITY	= C*	FT/SFC
MASS FLUX	= C*0	LB/SO FT-SEC
COMPUTED FLOW	= 0*0	LB/SEC
GAMMA	= 1.550	
MOLECULAR WEIGHT	= 15.87	GM/MOLE
ELECTRON DENSITY	= 3.45D 16	ELECTRONS/CC

SPECIES MOLE FRACTIONS

E=	4.706D-02	
AR	7.421D-C2	
CO2	9.522D-09	
N2	6.980D-06	
O2	1.204D-05	
N	3.690D-C2	
O	5.550D-C1	
NO	1.257D-C5	
CO	1.697D-03	
CN	2.015D-05	
C	2.380D-C1	
NUC	6.978D-76	
NC	4.904D-04	
OC	4.794D-C3	
N2C	5.674D-08	
O2C	7.140D-07	
CC	4.105D-C2	
ARC	6.695D-C4	
COC	4.557D-C5	

*****ELAPSED TIME= 0.07 MINUTES SINCE START OF RUN.

2. SECONDS SINCE LAST PRINTED TIME

RESERVOIR TRANSPORT PROPERTIES

VISCOSITY	= 1.00D-C4	LBM/FT-SEC
PRANDTL NUMBER	= 0.42362	
SIGMA	= 3.13D C1	NHO/CM
LEWIS NUMBER	= C*498	

NONEQUIL. JM SOLUTION

FIGURE 75 - OUTPUT OF NONEQUILIBRIUM FLOW-SOLUTION FOR TEST PROBLEM NO. 2 (FIRST PAGE)

DCHMIN= 6.1250-C6
DCHMAX= 1.3330-02
DCHMAX= 1.6510-02
DCHMAX= 2.2640-C2

IMAX= 5
IMAX= 5
IMAX= 5
IM. X= 5

*****NONEQUILIBRIUM*****

3 STEPS*****INEQ=0

X	=	-3.484	T	=	9868.	H	=	19776.	P	=	9.189D-01	R	=	1.128D-03
DIAM	=	1.964	V	=	3C77.	M	=	0.372	S	=	3.59	GAMMA	=	1.551
ARATEF	=	1.715	REFF	=	1.17CD C4	MW	=	15.92	MU	=	1.599D-04	SIGMA	=	3.042D 01
ARAT	=	1.715	DELSTR	=	-0.019	THETA	=	0.024	QW	=	9.76D 02	TAUN	=	4.356D 00
HR	=	19918.	PREF	=	0.5455	STANTN	=	1.419D-02	RETH	=	43.	RETHTR	=	217.
E-	=	3.0360 16	AR	=	7.452D-02	C02	=	1.0A6D-08	N2	=	7.494D-06	02	=	1.209D-05
N	=	3.7C6D-02	O	=	5.57D0-01	NO	=	1.285D-05	CO	=	1.862D-03	CN	=	2.098D-05
C	=	2.4C7D-01	NOE	=	6.988D-06	NC	=	4.004D-04	OC	=	4.342D-03	N2C	=	5.4424D-06
C26	=	6.512D-C7	C5	=	3.90D0-02	ARC	=	5.671D-04	C06	=	4.579D-05			
DCHMIN=	6.5230-C6	DCHMAX=	1.003D-02	IMAX=	5									
DC4MIN=	4.761D-C6	DCHMAX=	6.697D-03	IMAX=	5									
DC5MIN=	8.091D-06	DCHMAX=	1.0C43D-02	IMAX=	5									

*****NONEQUILIBRIUM*****

3 STEPS*****INEQ=0

X	=	-2.021	T	=	9748.	H	=	19589.	P	=	8.439D-01	R	=	1.053D-03
DIAM	=	1.712	V	=	4339.	M	=	0.528	S	=	3.59	GAMMA	=	1.551
ARATEF	=	1.302	REFF	=	2.864D 04	MW	=	15.97	MU	=	1.595D-04	SIGMA	=	2.098D 01
ARAT	=	1.3C2	DELSTR	=	-0.C011	THETA	=	0.040	QW	=	5.6. > 02	TAUN	=	3.410D 00
HR	=	19956.	PREF	=	C.5474	STANTN	=	6.277D-03	RETH	=	55.	RETHTR	=	225.
E-	=	2.662D 16	AR	=	7.481D-02	C02	=	1.193D-08	N2	=	8.357D-06	02	=	1.218D-05
N	=	3.721D-C2	O	=	5.58RD-01	NO	=	1.347D-05	CO	=	2.116D-03	CN	=	2.0252D-05
C	=	2.433D-01	NOE	=	7.303D-05	NC	=	3.945C-C4	OC	=	3.924D-03	N2C	=	5.183D-06
026	=	6.118D-07	C6	=	3.697D-02	ARC	=	5.133D-04	C06	=	4.563D-05			
DCHMIN=	1.0303D-05	DCHMAX=	1.0554D-02	IMAX=	5									
DCHMIN=	2.02410-C5	DCHMAX=	2.0247D-C2	IMAX=	5									
DCHMIN=	3.1060-C5	DCHMAX=	3.0183D-02	IMAX=	5									

*****NONEQUILIBRIUM*****

3 STEPS*****INEQ=0

X	=	-0.986	T	=	9026.	H	=	194C4.	P	=	7.747D-01	R	=	9.027D-04
DIAY	=	1.0C3	V	=	5.3C3.	M	=	0.65C	S	=	3.59	GAMMA	=	1.552
ARATEF	=	1.142	REFF	=	3.283D 04	MW	=	16.01	MU	=	1.587D-04	SIGMA	=	2.065D 01
ARAT	=	1.142	DELSTR	=	-0.217	THETA	=	0.046	QW	=	4.763D 02	TAUN	=	3.894D 00
HP	=	1.912.	PREF	=	C.5493	STANTN	=	4.795D-03	RETH	=	126.	RETHTR	=	231.
E-	=	2.327D 16	AR	=	7.511D-02	C02	=	1.327D-08	N2	=	9.041D-06	02	=	1.226D-05
N	=	3.736D-02	O	=	5.0C6D-C1	NO	=	1.383D-05	CO	=	2.043D-03	CN	=	2.0358D-05
C	=	2.466D-01	N2C	=	7.0223D-C5	NC	=	3.515D-04	OC	=	3.529D-03	N2C	=	4.947D-06
028	=	5.652D-07	C6	=	7.491D-02	ARC	=	4.461C-04	C06	=	4.550D-05			
DCHMIN=	4.559D-05	DCHMAX=	6.0446D-C2	IMAX=	5									
DCHMIN=	6.353D-C1	DCHMAX=	6.0162D-02	IMAX=	5									
DCHMIN=	8.357D-05	DCHMAX=	9.0516U-C7	IMAX=	5									

*****NONEQUILIBRIUM*****

3 STEPS*****INEQ=0

X	=	-0.986	T	=	9026.	H	=	194C4.	P	=	7.747D-01	R	=	9.027D-04
DIAY	=	1.0C3	V	=	5.3C3.	M	=	0.65C	S	=	3.59	GAMMA	=	1.552
ARATEF	=	1.142	REFF	=	3.283D 04	MW	=	16.01	MU	=	1.587D-04	SIGMA	=	2.065D 01
ARAT	=	1.142	DELSTR	=	-0.217	THETA	=	0.046	QW	=	4.763D 02	TAUN	=	3.894D 00
HP	=	1.912.	PREF	=	C.5493	STANTN	=	4.795D-03	RETH	=	126.	RETHTR	=	231.
E-	=	2.327D 16	AR	=	7.511D-02	C02	=	1.327D-08	N2	=	9.041D-06	02	=	1.226D-05
N	=	3.736D-02	O	=	5.0C6D-C1	NO	=	1.383D-05	CO	=	2.043D-03	CN	=	2.0358D-05
C	=	2.466D-01	N2C	=	7.0223D-C5	NC	=	3.515D-04	OC	=	3.529D-03	N2C	=	4.947D-06
028	=	5.652D-07	C6	=	7.491D-02	ARC	=	4.461C-04	C06	=	4.550D-05			
DCHMIN=	4.559D-05	DCHMAX=	6.0446D-C2	IMAX=	5									
DCHMIN=	6.353D-C1	DCHMAX=	6.0162D-02	IMAX=	5									
DCHMIN=	8.357D-05	DCHMAX=	9.0516U-C7	IMAX=	5									

*****NONEQUILIBRIUM*****

3 STEPS*****INEQ=0

*****NONEQUILIBRIUM*****

3 STEPS*****INEQ=0

FIGURE 76 - OUTPUT OF NONEQUILIBRIUM FI' SOLUTION FOR TEST PROBLEM NO. 3 (8-second Page)

```

X = -C-44A   T = 2473.   H = 19221.   P = 7.108D-01   R = 9.173D-04
DIAM = 1.547   V = 6104.   M = 0.754   S = 3.59   GAMMA = 1.553
ARATEF = 1.063   REPF = 3.539D 04   MW = 16.06   MU = 1.562D-04
ARAT = 1.063   DELSTR = -0.040   THETA = 0.048   OW = 4.748D 02
HR = 1976.   PREF = C.5511   STANT = 4.268D-03   RETH = 141.
                                         SPECIES MOLE FRACTIONS IN THE FREE STREAM
                                         E- 7.531D-C2   CO2 = 9.513D-06   N2 = 1.233D-05
                                         V = 5.624D-01   NO = 2.927D-03   CN = 2.460D-05
                                         O = 7.051D-06   NG = 3.156D-03   N2C = 4.717D-08
                                         C6 = 3.283D-02   ARG = 3.652C-04   CUT = 4.540D-05
                                         DCMIN= 1.239D-34   DCIMAX= 1.16CD-01   IMAX= 5
                                         *****NONEQUILIBRIUM*****
```

*****NONEQUILIBRIUM*****

```

X = -0.215   T = 9372.   H = 19067.   P = 6.657D-01   R = 8.697D-04
DIAM = 1.522   V = 6631.   M = 0.622   S = 3.59   GAMMA = 1.553
ARATEF = 1.032   REPF = 3.663D 04   MW = 16.09   MU = 1.574D-04
ARAT = 1.030   DELSTR = -0.042   THETA = 0.048   OW = 4.673D 02
HR = 19724.   PREF = U.532E   STANT = 4.077D-03   RETH = 148.
                                         SPECIES MOLE FRACTIONS IN THE FREE STREAM
                                         E- 7.557D-02   CO2 = 9.926D-06   O2 = 1.237D-05
                                         V = 5.637D-01   NO = 2.682D-03   CN = 2.446D-05
                                         O = 6.921D-06   NG = 2.897D-03   N2C = 4.544D-08
                                         C6 = 3.136D-02   ARG = 3.436D-04   CG6 = 4.531D-05
                                         *****NONEQUILIBRIUM*****
```

*****NONEQUILIBRIUM*****

```

X = -0.574   T = 9270.   H = 18952.   P = 6.232D-01   R = 8.248D-04
DIAM = 1.508   V = 7122.   M = 0.887   S = 3.59   GAMMA = 1.553
ARATEF = 1.013   REPF = 3.744D C4   MW = 16.13   MU = 1.599D-04
ARAT = 1.011   DELSTR = -0.043   THETA = 0.049   OW = 4.916D 02
HR = 19687.   PREF = U.5541   STANT = 3.957C-03   RETH = 152.
                                         SPECIES MOLE FRACTIONS IN THE FREE STREAM
                                         E- 7.576D-02   CO2 = 1.039D-05   O2 = 1.243D-05
                                         V = 5.649D-01   NO = 2.844D-03   CN = 2.482D-05
                                         O = 7.093D-06   NG = 2.649D-03   N2C = 4.374D-08
                                         C6 = 2.981D-02   ARG = 3.056D-04   CG6 = 4.522D-05
                                         *****NONEQUILIBRIUM*****
```

*****NONEQUILIBRIUM*****

```

X = -0.514   T = 9163.   H = 18815.   P = 5.829D-01   R = 7.828D-04
DIAM = 1.501   V = 7336.   M = 0.949   S = 3.59   GAMMA = 1.554
ARATEF = 1.003   REPF = 3.796D 24   MW = 16.16   MU = 1.563D-04
ARAT = 1.002   DELSTR = -C.043   THETA = 0.048   OW = 4.647D 02
HR = 19650.   PREF = U.5554   STANT = 3.942D-03   RETH = 153.
                                         SPECIES MOLE FRACTIONS IN THE FREE STREAM
                                         E- 7.595D-02   CO2 = 1.065D-05   O2 = 1.246D-05
                                         V = 5.662D-01   NO = 2.943D-03   CN = 2.466D-05
                                         O = 7.116D-06   NG = 2.323D-04   N2C = 4.197D-08
                                         C6 = 2.924D-02   ARG = 2.708D-04   CG6 = 4.513D-05
                                         *****NONEQUILIBRIUM*****
```

*****NONEQUILIBRIUM*****

FIGURE 77 - OUTPUT OF NONEQUILIBRIUM FLOW SOLUTION FOR TEST PROBLEM NO. 3 (Third Page)

X	0.0C3	T	9050.	H	18	P	5.455D-01	R	7.404
DIAM	1.050	V	8C03.	M	.007	S	3.59	GAMMA	1.036
ARATEF	1.000	REFF	3.821D-04	MW	16.19	MU	1.555D-01	SIGMA	2.5260 01
ARAT	1.000	DELSTF	-0.044	THEIA	0.048	CW	4.983D-02	TAUW	9.9350 00
HR	19614.	PREF	0.5568	STANTN	4.221D-03	RETM	154.	RETTR	251.
E-	1.309D-16	AP	7.611D-02	SPECIES MOLE FRACTIONS IN THE FREE STREAM					
N	3.79CD-02	D	5.674D-01	CO2	1.717D-05	N2	1.075D-05	O2	1.241D-05
C	2.564D-01	NUC	7.204D-06	NO	1.366D-05	CO	2.977D-03	CN	2.398D-05
02C	3.971D-07	CC	2.689D-02	NC	2.126C-04	OC	2.194D-03	N2C	3.981D-06
				ARC	2.439D-04	COC	4.466D-05		

*****NONEQUILIBRIUM*****
3 STEPS*****
*****INEQn1*****

X	0.013	T	8942.	H	18556.	P	5.112D-01	R	7.052D-04
DIAM	1.5G3	V	8399.	M	1.059	S	3.59	GAMMA	1.555
ARATEF	1.005	REFF	3.834D-04	MW	16.22	MU	1.545D-04	SIGMA	2.442D 01
ARAT	1.004	DELSTF	-0.044	THETA	0.048	CW	4.977D-02	TAUW	1.036D 01
HR	19574.	PREF	0.5562	STANTN	4.230D-03	RETM	154.	RETTR	254.
E-	1.169D-16	AP	7.627D-02	SPECIES MOLE FRACTIONS IN THE FREE STREAM					
N	3.799D-02	D	5.681D-01	CO2	1.729D-08	N2	1.082D-05	O2	1.238D-05
C	2.564D-01	NUC	7.061D-06	NO	1.336D-05	CO	3.004D-03	CN	2.320D-05
02C	3.667D-07	CC	2.542D-02	NC	1.924D-04	OC	1.784D-03	N2C	3.861D-06
				ARC	2.168D-04	COC	4.438D-05		

*****TH3JAT CX= 6.0C27D-12
S1= 1.012D CC
52= 2.830D-01 AFNMX= 1.012D 00
RSA= 1.000D 00 DLOGA= 2.693D-01
DELB= -5.797D-02

*****NONEQUILIBRIUM*****
3 STEPS*****
*****INEQn1*****

X	0.028	T	8422.	H	18406.	P	4.736D-01	R	6.637D-04
DIAM	1.512	V	8635.	M	1.085	S	3.59	GAMMA	1.556
ARATEF	1.015	REFF	3.815D-04	MW	16.25	MU	1.537D-04	SIGMA	2.371D 01
ARAT	1.016	DELSTF	-0.044	THETA	0.048	CW	4.860D-02	TAUW	1.033D 01
HR	19539.	PREF	0.5568	STANTN	4.172D-03	RETM	153.	RETTR	255.
E-	1.014D-16	AP	7.644D-02	SPECIES MOLE FRACTIONS IN THE FREE STREAM					
N	3.81CD-02	D	5.7C1D-01	CO2	1.775D-08	N2	1.094D-05	O2	1.244D-05
C	2.668D-01	NUC	7.147D-06	NO	1.284D-05	CO	3.047D-03	CN	2.222D-05
02C	3.4C2D-07	CC	2.358D-02	NC	1.674D-04	OC	1.745D-03	N2C	3.613D-06
				ARC	1.639D-04	COC	4.432D-05		

1HC2081 16COM - PROGRAM INTERRUPT (P) - UNDERFLOW OLD PSW IS FFES000D8205B15C . REGISTER CONTAINED 7814B93506580000
TRACEBACK ROUTINE CALLED FROM 1SN REG. 14 REG. 15 REG. 0 REG. 1

BLAYER	0r28	02UUAFA92	00098LCB	00000001	000BAD6C
CALL	0r??	62(A4)136	003BACFB	00000001	000A3EEC
PRTA	0222	02A009C	00CA3E78	00000000	00000000
NoneQ	0791	02UUD9FA	0009F608	00000000	00000000
MAIN	0016100	01CB03738	FD00C7008	000EA7F8	

ENTRY POINT = C1CE0730

STANDARD FIXUP TAKEN . EXECUTION CONTINUING

ORIGINAL PAGE IS
OF POOR QUALITY

FIGURE 78 - OUTPUT OF NONEQUILIBRIUM FLOW-SOLUTION FOR TEST PROBLEM NO. 3 (Fourth Page)

*****NONEQUILIBRIUM*****											
1 STEPS*****INEQ01*****											
X	=	0.032	T	=	8773.	H	=	10359.	P	=	4.625D-01
DIAM	=	1.514	V	=	6966.	M	=	0.916	S	=	3.59
ARATEF	=	1.016	REFF	=	3.820D 04	MW	=	16.26	MU	=	1.556
ARAT	=	1.019	DELSTR	=	-0.044	THETA	=	0.049	QW	=	2.339D 01
HR	=	10526.	PRREF	=	0.5588	STANTN	=	1.015D-03	RETH	=	3.106D 00
SPECIES MOLE FRACTIONS IN THE FREE STREAM											
E-	=	9.774D 15	AR	=	7.652D-02	CO2	=	1.790D-08	N2	=	1.246D-05
N	=	3.812D-02	O	=	5.764D-01	NO	=	1.272D-05	CO	=	2.201D-05
C	=	2.613D-01	NOE	=	7.247D-06	NC	=	1.621D-04	OC	=	3.547D-06
D2C	=	3.324D-07	CE	=	2.318D-02	ARE	=	1.769D-04	COC	=	4.424D-05

*****NONEQUILIBRIUM*****											
2 STEPS*****INEQ01*****											
X	=	0.028	T	=	8818.	H	=	18402.	P	=	4.728D-01
DIAM	=	1.511	V	=	8844.	M	=	1.129	S	=	3.59
ARATEF	=	1.015	REFF	=	3.813D 04	MW	=	16.25	MU	=	1.556
ARAT	=	1.015	DELSTR	=	-0.044	THETA	=	0.048	QW	=	2.380D 01
HP	=	19538.	PRREF	=	0.5588	STANTN	=	4.023D-03	RETH	=	3.627D 00
SPECIES MOLE FRACTIONS IN THE FREE STREAM											
E-	=	1.011D 16	AR	=	7.648D-02	CO2	=	1.776D-08	N2	=	1.244D-05
N	=	3.810D-02	O	=	5.701D-01	NO	=	1.284D-05	CO	=	2.221D-05
C	=	2.606D-01	NOE	=	7.164D-06	NC	=	1.671D-04	OC	=	3.630D-06
D2C	=	3.406D-07	CE	=	2.355D-02	ARE	=	1.835D-04	COC	=	4.455D-05

*****NONEQUILIBRIUM*****											
3 STEPS*****INEQ01*****											
E-	=	8.973D 15	AR	=	8.043D 00	APNX	=	1.020D 00	DLOGA	=	2.697D-01
N	=	3.819D-02	O	=	5.21D 00	RSA	=	1.000D 00	DEBL	=	5.803D-02
C	=	2.627D-01	NOE	=	7.227D-06	NC	=	1.480D-04	OC	=	3.498D-06
J2C	=	3.194D-07	CE	=	2.210D-02	ARE	=	1.586D-04	COC	=	4.476D-05

*****NONEQUILIBRIUM*****											
4 STEPS*****INEQ01*****											
X	=	0.046	T	=	8716.	H	=	18279.	P	=	4.436D-01
DIAM	=	1.522	V	=	9146.	M	=	1.180	S	=	3.59
ARATEF	=	1.027	REFF	=	3.765D 04	MW	=	16.28	MU	=	1.530D-04
ARAT	=	1.029	DELSTR	=	-0.044	THETA	=	0.048	QW	=	4.576D 02
HR	=	19505.	PRREF	=	0.5601	STANTN	=	3.977D-03	RETH	=	152.
SPECIES MOLE FRACTIONS IN THE FREE STREAM											
E-	=	8.964D-02	CO2	=	1.840D-08	N2	=	1.105D-05	O2	=	1.252D-05
N	=	5.712D-01	NO	=	1.236D-05	CO	=	3.097D-03	CN	=	2.149D-05
C	=	2.617D-01	NOE	=	7.227D-06	NC	=	1.480D-04	OC	=	3.498D-06
J2C	=	3.194D-07	CE	=	2.210D-02	ARE	=	1.586D-04	COC	=	4.476D-05

*****NONEQUILIBRIUM*****											
5 STEPS*****INEQ01*****											
X	=	0.068	T	=	8616.	H	=	18162.	P	=	4.169D-01
DIAM	=	1.533	V	=	9479.	M	=	1.224	S	=	3.59
ARATEF	=	1.043	REFF	=	3.748D 04	MW	=	16.31	MU	=	1.522D-04
ARAT	=	1.044	DELSTR	=	-0.044	THETA	=	0.049	QW	=	4.505D 02
HR	=	19474.	PRREF	=	0.5613	STANTN	=	3.975D-03	RETH	=	152.
SPECIES MOLE FRACTIONS IN THE FREE STREAM											
E-	=	7.679D-02	CO2	=	1.907D-08	N2	=	1.118D-05	O2	=	1.249D-05
N	=	5.723D-01	NO	=	1.196D-05	CO	=	3.161D-03	CN	=	2.067D-05
C	=	2.645D-01	NOE	=	7.239D-06	NC	=	1.317D-04	OC	=	3.363D-06

four pages of the nonequilibrium flow solution. In this case, the switch from the inverse method to direct integration was unsuccessful on the first try, as indicated by the diagnostic "DLOGR IS POSITIVE" in figure 77. After an underflow message produced by the IBM operating system, NATA printed the conditions at the flow point where $d \ln p/dx$ was positive (top of figure 78) and restarted the solution at the previous switch point. After the restart, the switchover from the inverse method to direct integration occurred sufficiently far downstream of the throat to give the desired supersonic branch of the downstream solution, as shown in figure 78.

Test problems no. 4A and 4B simulate two of Wegener's experiments on NO_2 recombination. The NATA solutions of these cases are shown in figures 29 and 30 of Volume I (ref. 1). These problems illustrate the use of nonstandard nozzle geometry, gas species, and reactions. In the input (figure 65), the geometric data describe Wegener's wind tunnel (shown in figure 28 of Volume I). Species number 29 is NO_2 and number 30 is N_2O_4 . The recombination reaction $2\text{NO}_2 + \text{N}_2 \rightleftharpoons \text{N}_2\text{O}_4 + \text{N}_2$ is defined as reaction number 76. Figures 79 and 80 show the problem summary for case 4A. Note that the standard properties are used for N_2 . The thermal properties of NO_2 and N_2O_4 are defined by means of thermo fits; no physical model data are given for these species because NATA is not programmed to treat nonlinear triatomic molecules such as NO_2 or polyatomic species such as N_2O_4 . All transport property calculations were suppressed in this run by input of $\text{N}\theta\text{TRAN} = \text{T}$. Figure 81 shows the calculated reservoir conditions, and figure 82 the first page of the equilibrium solution.

Test problem no. 5 illustrates the use of NATA with a standard electronic nonequilibrium model (argon, IGAS = 3), together with some of the output controls. Figures 83 to 85 show the problem summary. Note that the electronically excited species AR*M and AR*R have the same alpha matrix (elemental composition) as the ground state species AR, but have different enthalpies of formation and appear in different reactions. The electron thermal nonequilibrium parameters are tabulated in figure 85. Figure 86 shows the reservoir conditions. The boundary layer was neglected in the solution. Figures 87 and 88 show two pages of the output from the nonequilibrium solution. As shown in figure 87, the code begins the solution by taking three steps using the

FIGURE 79 - PROBLEM SUMMARY TEST PROBLEM NO. 4A (First Page)

NATA III - DE OUTPUT

RUN NO. 0 CASE 1 IN THIS JOB

TEST PROBLEM NO. 4A - WEGENER EXPERIMENT C - NONSTANDARD GAS AND GEOMETRY

RESERVOIR PRESSURE= 2.0000 ATM. RESRVOIR TEMPERATURE= 400.00 DEG K

NONSTANDARD TWO-DIMENSIONAL NOZZLE. 0.547 INCH THROAT GAP FOR TEST

THROAT RADIUS= 0.695 CM INLET AT -25.400 CM 4 SECTIONS IN FIT. 2 UPSTREAM OF THROAT

J	I\$HAPE(J)	SHAPE	ATPI(J)	PARAM(1,J)
1	1	STRAIGHT LINE	-2.00002D 00	7.6065D-02
1	2	CIRCLE BOTTOM	0.0	4.695D 00
2	2	CIRCLE BOTTOM	6.1546D-02	4.695D 00
3	2	CIRCLE BOTTOM		0.0
4	1	STRAIGHT LINE		2.0368D-02

NONSTANDARD MIXTURE

COLD SPECIES

NO.	NAME	INDEX	MOLE FRACTION	MOL. WT.	CHEMICAL FORMULA
1	N2	5	0.99503	28.0140	(N)2
2	SP30	30	0.00497	92.0140	(N)2 (O) 14

MEAN MOLECULAR WEIGHT OF COLD GAS= 28.3324

ELEMENT ATOM FRACTION ELEMENT MOLECULAR WEIGHTS

N	2.00000D 00	1.40070D 01
O	1.99000D-02	1.60000D 01

REACTION NO.	CONSTANT FACTOR AI	TEMP. POWE I DEPENDENCE	ACTIVATION ENERGY	CHI TEST	THIRO BODY MATRIX
1	3.00000D 14	0.0	0.0	0.0	0.100000

SPECIES THERMAL FIT INDICATOR ALPHA MATRIX

	N	O
N2	1	0
SP30	1	2
SP29	1	1
		2

REACT NO. NU PRIME MATRIX

	N2	SP30	SP29
1	1.	1.	0.

REACT NO. NU MATRIX

	N2	SP30	SP29
1	1.	0.	2.

ORIGINAL PAGE IS
OF POOR QUALITY

FIGURE 80 - PROBLEM SUMMARY FOR TEST PROBLEM NO. 4A (Second Page)

SPECIES	ATOMS PER MOLECULE	CHEMICAL CONSTANT	CHAR. VIBRATIONAL TEMP.	ENTHALPY OF FORMATION	ELECTRONIC LEVELS
N2	2.00000D 00	-4.0105999D-01	3.3520 00D 03	0.0	5
SPECIES	(DEGENERACY-ELECTRONIC ENERGY LEVEL)				
N2	1.0 0.0	3.0 1.435400D 05	6.0 1.704800D 05	1.0 1.715000D 05	2.0 1.981100D 05

SPECIES	A	B	C	D	E	K	HEAT OF FORMATION
N2	3.451483D 00	3.088331D-04	-4.0251428D-06	2.739295D-12	-5.466319D-17	3.071268D 00	0.0
SP29	3.553000D 00	1.162500D-02	-4.0550000D-06	0.0	0.0	1.002800D 01	4.0473000D 03
SP30	4.002000D 00	-3.750000D-04	2.0450000D-06	0.0	0.0	5.945000D 00	8.586000D 03

LEWIS NUMBER CALCULATIONS BASED ON BINARY DIFFUSION COEFFICIENT FOR SP29 - SP30

BOUNDARY LAYER EFFECTS NEGLECTED

TRANSPORT PROPERTY CALCULATIONS SUPPRESSED

*****ELAPSED TIME = 0.08 MINUTES SINCE START OF RUN. 5. SECONDS SINCE LAST PRINTED TIME

SPECIFIC HEAT OF COLD GAS = 0.7476 BTU/LB-DEG R AT 300.00 DEG K

RESERVOIR CONDITIONS -

FIGURE 81 - RESERVOIR COND₁, OUTPUT FOR TEST PROBLEM NO. 4A

NOZZLE = TEST	=	0.547	INCH THROAT DIAMETER
PRESSURE	=	2.000	ATM
TEMPERATURE	=	400.	DEG K
ENTHALPY	=	183.	BTU/LB
ENTROPY	=	1.66	BTU/LB-DEG R
DENSITY	=	0.10724	LB/CU FT
VELOCITY	=	0.	FT/SFC
MASS FLUX	=	0.0	LB/SO FT-SEC
COMPUTED FLOW	=	0.0	LB/SEC
GAMMA	=	1.395	GM/MOLE
MOLECULAR WEIGHT	=	28.19	ELECTRONS/CC
ELECTRON DENSITY	=	0.0	

SPECIES MOLE FRACTIONS

N2	9. 9C1D-01
SP30	3. F86D-06
SP29	9. F93D-03

*****ELAPSED TIME = 0.09 MINUTES SINCE START OF RUN. 0. SECONDS SINCE LAST PRINTED TIME

ORIGINAL PAGE IS
OF POOR QUALITY

EQUILIBRIUM SOLUTION

FIGURE 82 - EQUILIBRIUM SOLUTION FOR TEST PROBLEM NO. 4A (First Page)

***** EQUILIBRIUM *****

X	=	-0.596	T	=	400.	H	=	183.	P	=	2.0000 00	R	=	1.0720-01	
DIAM	=	0.781	V	=	0.	H	=	0.0	S	=	1.66	GAMMA	=	1.335	
ARATEF	=	1.427	REPF	=	0.0	NW	=	28.19	MU	=	0.0	SIGMA	=	0.0	
N2	=	9.9010-01	SP30	=	3.6860-06	SP29	=	9.8930-03							

***** EQUILIBRIUM *****

X	=	-1.200	T	=	396.	H	=	182.	P	=	1.9300 00	R	=	1.0460-01	
DIAM	=	1.445	V	=	290.	H	=	0.226	S	=	1.66	GAMMA	=	1.396	
ARATEF	=	2.641	REPF	=	0.0	NW	=	28.19	MU	=	0.0	SIGMA	=	0.0	
N2	=	9.9010-01	SP30	=	4.4540-06	SP29	=	9.8920-03							

***** EQUILIBRIUM *****

X	=	-0.856	T	=	392.	H	=	180.	P	=	1.8620 00	R	=	1.0190-01	
DIAM	=	1.048	V	=	423.	H	=	0.321	S	=	1.66	GAMMA	=	1.396	
ARATEF	=	1.916	REPF	=	0.0	NW	=	28.19	MU	=	0.0	SIGMA	=	0.0	
N2	=	9.9010-01	SP30	=	5.1190-06	SP29	=	9.8910-03							

***** EQUILIBRIUM *****

X	=	-0.703	T	=	388.	H	=	178.	P	=	1.7960 00	R	=	9.9290-02	
DIAM	=	0.879	V	=	519.	H	=	0.195	S	=	1.66	GAMMA	=	1.396	
ARATEF	=	1.606	REPF	=	0.0	NW	=	28.19	MU	=	0.0	SIGMA	=	0.0	
N2	=	9.9010-01	SP30	=	5.9030-06	SP29	=	9.8900-03							

***** EQUILIBRIUM *****

X	=	-0.511	T	=	384.	H	=	176.	P	=	1.7320 00	R	=	9.9750-02	
DIAM	=	0.717	V	=	590.	H	=	0.459	S	=	1.66	GAMMA	=	1.396	
ARATEF	=	1.311	REPF	=	0.0	NW	=	28.19	MU	=	0.0	SIGMA	=	0.0	
N2	=	9.9010-01	SP30	=	6.830D-06	SP29	=	9.8870-03							

***** EQUILIBRIUM *****

X	=	-0.420	T	=	380.	H	=	175.	P	=	1.6690 00	R	=	9.4200-02	
DIAM	=	0.516	V	=	669.	H	=	0.516	S	=	1.66	GAMMA	=	1.396	
ARATEF	=	1.000	REPF	=	0.0	NW	=	28.19	MU	=	0.0	SIGMA	=	0.0	
N2	=	9.9010-01	SP30	=	7.9700-06	SP29	=	9.8800-03							

FIGURE 83 - PROBLEM SUMMARY / TEST PROBLEM NO. 5 (First Page)

NATURAL LOGUE OUTPUT

RUN NO. C CASE 1 IN THIS JOB

TEST PROBLEM NO. 5 = ELECTRONIC NONEQUILIBRIUM MODEL FOR ARGON

RESERVOIR PRESSURE= 1.0000 ATM. RESERVOIR TEMPERATURE= 10000.00 DEG K

STANDARD AXISYMMETRIC NOZZLE NO. 1. 0.750 INCH THROAT DIAM FOR DCA

THROAT RADIUS= 0.952 CM INLET AT -5.540 CM 8 SECTIONS IN FIT. 6 UPSTREAM OF THROAT

J	ISHAPE(J)	SHAPE	ATPI(J)	PARAM(1,J)	PARAM(2,J)
1	1	STRAIGHT LINE	-5.5685D 00	-1.2970D 01	-2.7475D 00
2	2	CIRCLE BOTTOM	-5.4558D 00	2.3645D 00	-5.4491D 00
3	1	STRAIGHT LINE	-1.5232D 00	1.9517D 00	-5.2408D-02
4	3	CIRCLE TOP	-1.2648D 00	1.7145D 00	-1.5398D 00
5	1	STRAIGHT LINE	-1.0999D 0C	-3.1750D-01	-1.7321D 00
6	2	CIRCLE ACTTON	0.0	2.2225D 00	0.0
7	2	CIRCLE BOTTOM	3.2870D-01	2.2225D 00	1.2700D 00
8	1	STRAIGHT LINF	9.0770D-01	9.0770D-01	1.2700D 00

STANDARD GAS NO. 3 (ARGON)

NO.	NAME	INDEX	MOLE FRAC.	MOL. WT.	CHEMICAL FORMULA
1	AR	4	1.00000	39.9480	(AR)1

MEAN MOLECULAR WEIGHT OF COLC GAS= 39.9480

ELEMENT	ATOM FRACTION	ELEMENT MOLECULAR WEIGHTS
F-	0.0	5.485970D-04
AR	1.000000 00	3.9948000 01

REACTION NO.	CONSTANT FACTOR AI	TEMP. POWER DEPENDENCE	ACTIVATION ENERGY	CHI TEST	THIRD BODY MATRIX
1	2.640C00C 21	-4.295999D 00	0.0	0.100000	
2	3.64CC0CD 21	-4.295999D 00	0.0	0.100000	
3	8.219597D 10	-8.099959D-01	0.0	0.100000	
4	8.219597D 10	-8.099959D-01	0.0	0.100000	
5	6.000CG0D 10	-5.000CG0D-01	0.0	0.100000	
6	5.000CG0D 14	5.000CG0D-01	0.0	0.100000	
7	7.199595H 13	5.000CG0D-01	0.0	0.100000	
8	A.00CC0C 04	0.0 C	0.0	0.100000	
9	C.99CC0H 16	-5.000CG0D-01	0.0	0.100000	
10	3.50000CD 09	5.000CG0D-01	0.0	0.100000	
11	8.69598H 14	-5.599959D-01	0.0	0.100000	
12	3.500CCC0 C9	5. C00CC0D-01	0.0	0.100000	
13	8.6959598D 14	-5.599959D-01	0.0	0.100000	
14	8.195579D 15	-7.50C0CG0D-01	0.0	0.100000	
15	2.80CC0CD 16	-6.700CG0D-01	1.2520000 03	0.100000	
16	2.80CC0CD 16	-6.700CG0D-01	1.2520000 03	0.100000	
17	2.000CG0D 21	-4.295999D 00	0.0	0.100000	

FIGURE 84 - PROBLEM SUMMARY FOR TEST PROBLEM NO. 5 (Second Page)

SPECIES	FRIAL I IT INDICATOR	ALPHA MATRIX
E-	0	E- AR
AR	0	1 0
AR*W	0	0 1
AR*R	0	0 1
A=Fe	C	-1 1
AR2C	C	-1 2
	O	-1

REACT NO.	NU PRIME MATRIX
1	E- 1. C. 0. 0. 0. 0. 0. 0.
2	2. 0. 0. 1. 0. 0. 0. 0.
3	3. 0. 0. 0. 1. 0. 0. 0.
4	4. 0. 0. 0. 0. 1. 0. 0.
5	5. 0. 0. 0. 0. 0. 1. 0.
6	6. 1. 0. 0. 0. 0. 0. 0.
7	7. 1. 0. 0. 0. 0. 0. 0.
8	8. 0. 1. 0. 0. 0. 0. 0.
9	9. 1. 0. 0. 0. 0. 0. 0.
10	10. 0. 0. 2. 0. 0. 0. 0.
11	11. 0. 0. 3. 0. 0. 0. 0.
12	12. 0. 0. 2. 0. 0. 0. 0.
13	13. 0. 0. 3. 0. 0. 0. 0.
14	14. 0. 0. 1. 0. 0. 0. 0.
15	15. 0. 0. 1. 0. 0. 0. 0.
16	16. 0. 1. 0. 0. 0. 0. 0.
17	17. 1. 0. 2. 0. 0. 0. 0.

REACT NO.	NU MATRIX
1	E- 2. 0. C. 0. 0. 0. 0. 0.
2	2. 2. 0. C. 0. 0. 0. 0. 0.
3	3. 1. 0. 0. C. 0. 0. 0. 0.
4	4. 1. 0. C. 0. 0. 0. 0. 0.
5	5. 1. 0. 0. C. 0. 0. 0. 0.
6	6. 1. 0. 0. 1. 0. 0. 0. 0.
7	7. 1. 0. 0. 0. C. 0. 0. 0.
8	8. 0. 0. C. 0. 0. 0. 0. 0.
9	9. 1. 0. C. 0. 0. 0. 0. 0.
10	10. 0. 0. C. 0. 0. 0. 0. 0.
11	11. 0. 0. 2. 0. 0. 0. 0. 0.
12	12. 0. 0. 1. 0. 0. 0. 0. 0.
13	13. 0. 0. 2. 0. 0. 0. 0. 0.
14	14. 0. 0. 2. 0. 0. 0. 0. 0.
15	15. 0. 1. 0. 0. 0. 0. 0. 0.
16	16. 0. 1. 0. 0. 0. 0. 0. 0.
17	17. 0. 2. 0. 0. 0. 0. 0. 0.

SPECIES	ATOMS PER MOLECULE	CHEMICAL CONSTANT	CHAR. VIBRATIONAL TEMP.	ENTHALPY OF FORMATION	ELECTRONIC LEVELS
E-	1.00000000	-1.0492760D 01	0.00	0.00	1
AR	1.00000000	1.0866300D 00	0.00	0.00	1
AR*W	0.00000000	1.0866300D 00	0.00	2.6635000 05	1
AR*R	1.00000000	1.0866300D 00	0.00	2.6797000 05	1
A=Fe	1.00000000	1.0866300D 00	0.00	3.6333000 05	2
AR2C	1.00000000	1.0866300D 00	1.1200000 00	1.1700000 05	1

FIGURE 85 - PROBLEM SUMMARY

TEST PROBLEM NO. 5 (Third Page)

SPECIES (DEGENERACY, ELECTRONIC ENERGY LEVEL)

-	2.0	C+C
	1.0	O+O
AP*W	6.0	C+C
AR*P	6.0	O+O
ARC	4.0	O+O
AR2S	2.0	C+C

ELECTRON THERMAL NONEQUILIBRIUM PARAMETERS

IR	KTF	ITR	EPAR(1,IR)	EPAR(2,IR)
1	2	5	9.657CD 0.4	0.0
2	2	5	9.536CD 0.4	0.0
3	2	1	9.697CD 0.4	7.0000D-01
4	2	0	9.536CD 0.4	7.0000D-01
5	4	1	3.6333D 0.5	1.0000D 0.0
6	2	2	2.6635D 0.5	0.0
7	2	2	2.6797D 0.5	0.0
8	5	6	2.6797D 0.5	0.0
9	2	5	1.6000D 0.3	0.0
10	1	1	0.0	0.0
11	1	0	2.2600D 0.5	0.0
12	1	1	0.0	0.0
13	1	1	2.2600D 0.5	0.0
14	1	1	0.0	0.0
15	3	2	7.0680D 0.4	0.0
16	3	2	6.9670D 0.4	0.0
17	2	5	3.37C4D 0.5	0.0

LEWIS NUMBER CALCULATIONS BASED ON BINARY DIFFUSION COEFFICIENT FOR ARC → AR (AMBIPOLAR) (NOT USED)
BOUNDARY LAYER EFFECTS NEGLECTED

INPUT DATA FOR MODEL PARAMETER CALCULATIONS

3 MODEL POINTS IN A GEOMETRIC PROGRESSION FROM X= 2.000 01 TO X= 4.000 01 INCHES BEYOND THROAT
MODEL TEMPERATURE= 300. DEG K. FLAT PLATE TEMPERATURE= 300. DEG K
BOTH EQUILIBRIUM AND FROZEN SHOCK LAYERS ON MODEL CALCULATED
SURFACE CATALYTIC FACTOR = 1.000
AXIALLY-SYMMETRIC MODEL GEOMETRY

*1*****ELAPSED TIME= 0.02 MINUTES SINCE START OF FUN. 1. SECONDS SINCE LAST PRINTED TIME
SPECIFIC HEAT OF COLD GAS= C.1244 BTU/LB-DEG R AT 300.00 DEG K

FIGURE 86 - RESERVOIR COND^TITION OUTPUT FOR TEST PROBLEM NO. 5

RESERVOIR CONDITIONS -

NCZTLE = DCA	= 0.750	INCH THROAT DIAMETER
PRESSURE	= 1.000	ATM
TEMPERATURE	= 100CC.	DEG K
ENTHALPY	= 2622.	BTU/LB
ENTROPY	= 1.39	BTU/LB-DEG R
DENSITY	= C.0025A	LB/CU FT
VELOCITY	= C.	FT/SEC
MASS LUX	= C=0	LB/SO FT-SEC
COMPUTED FLCW	= 0.C	LB/SEC
GAMMA	= 1.667	
MOLECULAR WEIGHT	= 35.14	GM/MOLE
ELECTFCN CFNSITY	= 1.48D 16	ELECTRONS/CC

SPECIES MOLE FRACTIONS

E-	2. C19D-C?
AF	9. E56D-C1
AR*M	8. E55D-C6
AR*R	8. C14D-0K
ARE	2. C18D-C2
AR2E	1. S74D-C6

*****ELAPSED TIME = 0.03 MINUTES SINCE START OF RUN.

1. SECONDS SINCE LAST PRINTED TIME

RESERVOIR TRANSFRT PROPERTIES

VISCOSITY	= 1. S6D-C4	LBM/FT-SEC
PRANDTL NUMBER	= C.26932	
SIGMA	= 2.90D C1	MHO/CM
LEVIS NUMBER	= C.145	

NONEQUILIBRIUM SOLUTION

FIGURE 87 - NONEQUILIBRIUM SOLUTION FOR TEST PROBLEM NO. 5 (First Page)

DCHMIN= 2.411D-03 DCHMAX= 2.674D 00 IMAX= 5
 DCHMIN= 6.98E-04 DCHMAX= 1.07D 00 IMAX= 5
 DCHMIN= 1.861D-04 DCHMAX= 2.234D-01 IMAX= 5
 DCHMIN= 2.022D-05 DCHMAX= 3.529D-02 IMAX= 5

*****NCNEQUILIBRIUM*****
*****INEQ=0

X = -2.174	T = 9977.	H = 2616.	P = 9.929D-01	R = 2.964D-03
DIAM = 1.0781	V = 570.	M = 0.106	S = 1.39	GAMMA = 1.666
ARATEF = 5.636	REPF = R.642D 03	NW = 39.5	MU = 1.954D-04	SIGMA = 2.894D 01
TELEC = 5.977.	QRAD = 1.103D 01	CLEFT = -1.361D 00	HS = 2.623D 03	
E- = 1.470D 16	AR = 9.599D-01	SPECIES MOLE FRACTIONS IN THE FREE STREAM		
AR2G = 1.962D-06	AR+N = 8.731D-06	ARR = 8.046D-06	ARC = 2.013D-02	

REACTION RATE DATA

PI = 1	6.3D-02	2	6.3D-02	3	5.9D-05	4	5.9D-05	5	8.1D-07	6	1.5D-04	7	2.0D-05	8	6.2D-07	
SI = 2.8D-02	10	5.1D-06	11	1.5D-08	12	4.7D-08	13	1.4D-08	14	2.1D-04	15	1.2D-04	16	1.2D-04	17	3.4D-06
CHI = 1	-5.6C-07	2	-5.6D-07	3	1.0D 00	0	1.0D 00	5	1.0D 00	6	0.0	7	0.0	8	1.0D 00	
Q = 0.0	10	0.C	11	1.0D 00	12	0.0	13	1.0D 00	14	-5.6D-07	15	0.0	16	0.0	17	0.0
PICHI = 1	-3.6D-08	2	-3.6D-08	3	5.9D-05	4	5.9D-05	5	8.1D-07	6	0.0	7	0.0	8	6.2D-07	
PI = 10	C.0	11	1.5D-08	12	0.0	13	1.4D-08	14	2.1D-04	15	0.0	16	0.0	17	0.0	
DLG	E- = -1.2D-02	AR = 2.5D-04	ARR = -2.1D-02	ARR = 2.01D-02	ARR = -2.1D-02	ARC = -1.2D-02	ARC = AR2G = -1.8D-02									
DCHMIN= 1.0461D-04	DCHMAX= 2.0234D-01	IMAX= 5	IMAX= 5	IMAX= 5	IMAX= 5	IMAX= 5	IMAX= 5	IMAX= 5	IMAX= 5	IMAX= 5	IMAX= 5	IMAX= 5	IMAX= 5	IMAX= 5	IMAX= 5	
DCHMIN= 4.433D-06	DCHMAX= 5.333D-03															
DCHMIN= 1.861D-04	DCHMAX= 2.0234D-01															
DCHMIN= 8.174D-05	DCHMAX= 9.824D-02															

*****NCNEQUILIBRIUM*****
*****INEQ=0*****NCNEQUILIBRIUM*****
*****INEQ=0

X = -0.532	T = 9948.	I = 2611.	P = 9.877D-01	R = 2.956D-03
DIAM = 1.552	V = 75.3.	M = 0.141	S = 1.39	GAMMA = 1.666
ARATEF = 4.281	REPF = 1.142D 04	NW = 39.15	MU = 1.950D-04	SIGMA = 2.886D 01
TELEC = 9.8.	QRAD = 1.084D 01	CLEFT = -1.314D 00	HS = 2.623D 03	
E- = 1.473D 16	AR = 9.599D-01	SPECIES MOLE FRACTIONS IN THE FREE STREAM		
AR2G = 1.970D-06	AR+N = 8.937D-06	ARR = 8.235D-06	ARC = 2.022D-02	

REACTION RATE DATA

PI = 1	4.7D-02	2	4.7D-02	3	4.4D-05	4	4.4D-05	5	7.0D-07	6	1.1D-04	7	1.5D-05	8	4.9D-07	
SI = 2.1D-02	1C	3.8C-08	11	1.1D-08	12	3.5D-08	13	1.0D-08	14	1.5D-04	15	8.8D-05	16	8.8D-05	17	2.5D 06
CHI = 1	1.3C-06	2	1.3D-06	3	1.0D CC	4	1.0D 00	5	1.0D 00	6	0.C	7	0.0	8	1.0D 00	
Q = 0.0	10	0.C	11	1.0D 00	12	0.0	13	1.0D 00	14	1.3D-06	15	-3.6D-15	16	-3.6D-15	17	-3.6D-15
PICHI = 1	6.1C-08	2	6.1D-08	3	4.4D-05	4	4.4D-05	5	7.0D-07	6	0.0	7	0.0	8	4.9D-07	
PI = 10	C.0	11	1.1D-08	12	0.0	13	1.0D-08	14	2.0D-10	15	-3.1D-19	16	-3.1D-19	17	-8.8D-21	
DLG	E- = -2.5D-02	AR = 5.2D-04	ARR = -4.4D-02	ARR = -4.4D-02	ARC = -2.5D-02	ARC = AR2G = -3.7D-02										
DCHMIN= 1.0661D-04	DCHMAX= 2.0234D-01	IMAX= 5	IMAX= 5	IMAX= 5	IMAX= 5	IMAX= 5	IMAX= 5	IMAX= 5	IMAX= 5	IMAX= 5	IMAX= 5	IMAX= 5	IMAX= 5	IMAX= 5	IMAX= 5	
DCHMIN= 1.028CD-04	DCHMAX= 1.246D-01															
DCHMIN= 9.248C-05	DCHMAX= 1.111D-01															

X=-1.34131C CC DELTAX= 3.455D-05 T= 9.044.015 TEP= 9.944.08 CMA= 2.08704942D 00 ODE=-4.665D 00 ICOUNT= 6

CAUSES OF STEP FAILURES Q 0 0 0 0 0 0 0 0 0 0 0 0 0 0 0 0 0 0

X=1.34127D 00 DELTAX= 3.424D-05 T= 9.044.018 TEP= 9.943.98 CMA= 2.08704931D 00 ODE= 5.125D 00 ICOUNT= 10

CAUSES OF STEP FAILURES 1.3 -3 -3 -3 -3 -3 -3 -3 -3 -3 -3 -3 -3 -3 -3 -3 -3 -3

Y=-1.34131C CC DELTAX= 3.455D-05 T= 9.044.015 TEP= 9.944.08 CMA= 2.08704942D 00 ODE=-4.665D 00 ICOUNT= 6

FIGURE 88 - NONEQUILIBRIUM SOLUTION FOR TEST PROBLEM NO. 5 (TYPICAL)

X=-3.0 DFL TAX= 6.242D-04 T= 8468.73 TEP= 8.0 .79 CHA= 2.861833E 00 QDPE=-7.661D-01 ICOUNT= 0

***** NCNE CUILLERIUM ***** 6 STEP ***** INEQ=1

X DIAW = -0.121 T = 8469. V = 4235. H = 2256. P = 6.5100-01 R = 2.291D-33
 DIAW = 0.780 REPF = 5.610D 04 N = 0.752 S = 1.39 GAMMA = 1.667
 ARATEF = C.980 ORAD = 7.36CD 0C MU = 39.18 SIGMA = 2.354D 01
 TELFC = 8615. CELET = -7.661D-01 HS = 2.615D 03

E- = 1.087D 15 AR = 9.014D-C4 AH*W = 1.683D-05 AR*R = 1.533D-05 ARC = 1.927D-02

1RF26 = 1.681D-C6

PI 1 E.6D-03 2 A.5D-03 3 6.4D-06 4 6.4D-C6 5 2.5D-07 6 2.8D-05 7 3.7D-06 8 2.4D-07
 9 5.9D-02 1G 5.7D-09 11 2.6D-09 12 3.8D-09 13 2.3D-09 14 1.8D-05 15 1.3D-05 16 1.3D-07 4.1D-07
 CHI 1 1.6D-C3 2 5.3D-C4 3 1.0D CC 4 1.0D CO 5 1.0D 00 6 9.4D-01 7 9.4D-01 8 1.0D 00
 r 1.1D-C3 10 9.5D-01 11 1.0D CC 12 9.5D-01 12 1.0D CC 14 2.0D-02 15 3.3D-04 16 7.7D-04 17 9.4D-01
 PICHI 1 1.4D-05 2 4.5D-06 3 6.4D-06 4 6.4D-06 5 2.5D-07 6 2.6D-05 7 3.4D-06 8 2.4D-07
 C 6.5D-06 10 9.2D-09 11 2.6D-C5 12 8.4D-0C 13 2.3D-C9 14 3.7D-07 15 4.4D-0C 15 1.0D-08 17 3.9D-07
 DLG E- -6.5D-02 AR 1.2D-03 AR*N 1.5D 00 AR*R 1.8D 00 AR*E -6.5D-02 AR2E -7.6D-01

X=-3.C7315C-01 DEL TAX= 6.242D-04 T= 8466.78 TEP= 8613.01 CHA= 2.8618319D 00 QDPE=-7.352D-01 ICOUNT= 0

X=-3.C66691C-C1 DFL TAX= 6.242D-04 T= 8464.83 TEP= 8611.22 CHA= 2.86183000 00 QDPE=-7.614D-01 ICOUNT= 1

X=-3.C65664C-C1 DFL TAX= 6.242D-C4 T= 8462.88 TEP= 8609.43 CHA= 2.8618281D 00 QDPE=-7.308D-01 ICOUNT= 0

X=-3.C65442D-01 DFL TAX= 6.242D-04 T= 8460.93 TEP= 8607.65 CHA= 2.8618262D 00 QDPE=-7.566D-01 ICOUNT= 0

X=-3.04618r-01 DEL TAX= 6.242D-04 T= 8458.98 TEP= 8605.85 CHA= 2.8618243D 00 QDPE=-7.265D-01 ICOUNT= 0

X=-3.C4132C-01 DFL TAX= 6.866E-04 T= 8456.83 TEP= 8603.89 CHA= 2.8618213D 00 QDPE=-7.529D-01 ICOUNT= 0

***** NCNE CUILLERIUM ***** 6 STEP ***** INEQ=1

X DIAW = -J.120 T = 8457. V = 4252. H = 2253. P = 6.486D-01 R = 2.285D-03
 DIAW = 0.779 REPF = 5.62ED C4 N = 0.755 S = 1.39 GAMMA = 1.667
 ARATEF = U.979 ORAD = 7.27E-01 CELET = -7.529D-01 MU = 1.727D-04 SIGMA = 2.349D 01
 TELFC = P6C4.

E- = 1.084D 15 AR = 9.014D-C1 AH*W = 1.694D-05 AR*R = 1.543D-05 ARC = 1.927D-02

1RF2E = 1.679D-C6

PI 1 P.6D-U3 2 8.6D-03 3 6.3D-C6 4 6.3D-06 5 2.5D-07 6 2.8U-05 7 3.7D-06 8 2.4D-07
 C 5.9r J 1C 4.6L-C9 11 2.6J-09 12 3.8D-09 13 2.3D-C9 14 1.8D-05 15 1.3D-05 16 1.3D-07 4.1D-07
 CHI 1 1.6L-C3 2 5.4D-04 3 1.0D CC 4 1.0D CO 5 1.0D 00 6 9.4U-01 7 9.4D-01 8 1.0U 00
 r 1.1L-J2 1C 6.5C-01 11 1.0D CC 12 9.5D-01 12 1.0D CC 14 2.0D-02 15 3.3D-04 16 7.3D-04 17 9.4D-C1
 PICHI 1 1.4D-05 2 4.5D-06 3 6.3D-06 4 6.3D-06 5 2.5D-07 6 2.6D-05 7 3.4D-06 8 2.4D-07
 C 6.5C-06 1C 5.27-09 11 2.6J-09 12 3.8D-09 13 2.3D-09 14 3.7D-07 15 5.6U-09 16 9.7D-09 17 3.9D-07
 DLG E- -6.5D-C2 AR 1.2D-03 AR*N 1.5D 00 AR*R 1.8D 00 AR*E -6.5L 02 AR2E -2.6U-01

X=-3.C3445C-C1 DFL TAX= 6.866E-04 T= 8454.6- TEP= 8601.92 CHA= 2.8618202D 00 QDPE=-7.167D-01 ICOUNT= 0

X=-3.C2221C-01 DEL TAX= 6.242D-L4 T= 8452.71 TEP= 8600.12 CHA= 2.8618183D 00 QDPE=-7.483D-01 ICOUNT= 1

X=-3.021 L-C1 DEL TAX= 6.212D-04 T= 845C.75 TEP= 858.33 CHA= 2.8618164D 00 QDPE=-7.127D-01 ICOUNT= 0

X=-7.031C73C-C1 DEL TAX= 6.242D-C4 T= 8446.70 TEP= 850K.54 CHA= 2.8618145D 00 QDPE=-7.167D-01 ICOUNT= 0

perturbation technique. The numerical integration then begins. Stability requirements force the use of a very small step size.

The input ISW6B = -1 in test problem no. 5 (figure 65) gives the output of reaction rate data (PI, CHI, PICHI, DIG) in each step (see Section 3.5). The input ISW5B = -1000000 gives a one-line message (X, DELTAX, T, etc.) for every completed integration step. The data included in this message are as follows:

X	Axial coordinate (cm)
DELTAX	Integration step size (cm)
T	Heavy-particle temperature (°K)
TEP	Electron temperature (°K)
CHA	Nondimensional stagnation enthalpy
QDPE	Energy transfer to the electron gas (cal/cm ³ sec)
ICOUNT	Number of step-size reductions required to achieve a successful integration step

The messages "CAUSES OF STEP FAILURE" in figures 87 and 88 are also triggered by the negative ISW5B value, and indicate the location and nature of the flunked validity check responsible for each step size reduction. The numerical code used in this message is documented in Section 4.55 of Volume III of this report.

APPENDIX D

USER'S MANUAL FOR THE NOZFIT CODE

D.1 Introduction

The geometries of nozzles and channels are specified, in NATA, by analytical curvefits to the profiles of the surfaces confining the gas flow. In these curvefits, each profile is represented by means of a sequence of straight line segments and circular arcs. The details of this system of geometric specifications have been documented in Section 4 of Volume I (ref. 1).

In order for the curvefits to be usable in NATA, the various sections must join together continuously, and with continuous slopes, to high accuracy. The NOZFIT program has been developed to facilitate the preparation of such curvefits. The main inputs to NOZFIT are geometric data, most of which can be read directly from nozzle design drawings. The outputs include

- (1) Printout of the parameters in the profile curvefit;
- (2) Punched cards, containing a Fortran DATA statement, which can be incorporated directly into NATA, to add the curvefit to the set of precoded standard profiles;
- (3) Printout of the throat region of the profile in tabular form; and
- (4) A computer-generated plot of the profile in the throat region.

Section D.2 of this appendix defines the inputs to NOZFIT, and Section D.3 discusses the various types of output. Section D.4 presents a sample run of the code with its printed and plotted output and a listing of the punched output.

D.2 Inputs to NOZFIT

The profile curvefits produced by NOZFIT consist of sections joined end to end with continuity of slope, each section being a straight line, a circular arc concave upward, or a circular arc concave downward. Array dimensions in NATA limit the

total number of sections to 12. In the analysis to determine the profile curvefit parameters, the sections are separated into two groups, those lying upstream of the throat, and those lying downstream. The analysis for each group starts at the throat and determines the sections sequentially, proceeding away from the throat. In each group, the section having a boundary at the throat ($x = 0$) is always assumed to be a circular arc concave upward with zero slope at the throat. Thus, the profile ordinate is a minimum at the throat. For the profile to be usable in NATA, it is necessary that the ordinate be a monotonically decreasing function of x upstream of the throat and a monotonically increasing function of x downstream.*

The input to a NOZFIT case begins with a card containing alphanumeric information describing and identifying the nozzle or channel whose profile is to be fitted. This card is read with an A format. The information is printed at the head of the output and reproduced as a comment card preceding the data cards produced. The first 48 characters are also used as a title for the nozzle profile plot. Finally, the first 4 characters on this header card are incorporated into the punched DATA statement and are used, by NATA, as a facility name (DCI, etc.).

The remaining inputs are all read in under the namelist name INPUT, using the usual namelist format (see Section 2.1). They are defined below:

Variable Name	Dimensions	Preset Values	Definition
NSECTS(I)	2	2*0	NSECTS(1) = number of sections in nozzle profile upstream of throat. NSECTS(2) = number of sections in nozzle profile downstream of throat.

*More precisely, the area ratio A_g must have $dA_g/dx < 0$ for $x < 0$, $dA_g/dx > 0$ for $x > 0$. In a channel, it is not necessary for both of the profiles to decrease and increase as described above, so long as the area ratio has the required behavior.

Variable Name	Dimensions	Preset Values	Definition
ISHAPE(J)	12	12*0	Index specifying shape of the Jth section (counting from the upstream inlet) 1 Straight section 2 Circular arc convex toward axis 3 Circular arc concave toward axis
PAR(I,J)	2,12	24*0	Parameter values for the Jth section: For ISHAP(E)(J) = 1, PAR(1,J) = angle of inclination to nozzle axis in degrees (positive value) For ISHAP(E)(J) = 2 or 3, PAR(1,J)= circle radius in inches (See ICOND for PAR(2,J))
DTH	1	-	Throat diameter in inches.
ICOND(J)	12	12*0	Index specifying condition defining the Jth section. ICOND(J) = 1 Throat condition* ICOND(J) = 2 Straight section (J) is tangent to adjacent circular section nearer the throat. ICOND(J) = 3 Circular section (J) is tangent to adjacent straight section (nearer the throat) at an axial distance of PAR(2,J) inches from the throat** ICOND(J) = 4 Circular section (J) is used to break a sharp angle between two straight sections which intersect at an axial distance of PAR(2,J) inches from the throat**

*Note - there are always two throat sections, one upstream and one downstream of the throat.

**Note - PAR(2,J) is negative if it represents a point upstream of the throat.

Variable Name	Dimensions	Preset Values	Definition
XSTART	1	-	Upstream limit on Z for calculation of nozzle profile (negative value, inches). The profile is calculated for a nozzle section 6 inches long.
XZERØI	1	-	Inlet position in inches above the throat (negative); for use in NATA boundary layer calculations.
NØZZLE	1	-	Nozzle index for use in NATA (integer value between 1 and 20).
CARDS	1	.TRUE.	Set to .FALSE. to suppress card output.
PLØTS	1	.TRUE.	Set to .FALSE. to suppress plot output.
ENDJ/3	1	.TRUE.	Set to .FALSE. if there is another case in the job following the current case. Set to .TRUE. in last case.

D.3 Outputs of NOZFIT

The outputs of NOZFIT are illustrated by the results for the test problem in the next section. The printed output consists of the following:

- (1) A listing of the values of all the input variables in Namelist format.
- (2) The image of the "header" card containing alphanumeric identifying information.
- (3) A table headed "nozzle profile parameters." This table contains the following five columns:

J	Nozzle section index, starting from the upstream end.
ATP	Position coordinate of the downstream boundary of the profile section (cm, positive downstream).
PARAM(1,J)	See below.
PARAM(2,J)	See below.
PARAM(3,J)	See below.

The parameter values are coefficients in the analytical expressions for the profile sections. Let $P_1 \equiv \text{PARAM}(1,J)$, $P_2 \equiv \text{PARAM}(2,J)$, and $P_3 \equiv \text{PARAM}(3,J)$. Then:

For ISHAPE(J) = 1,

$$Y = P_1 + P_2 X \quad (\text{D-1})$$

For ISHAPE(J) = 2,

$$Y = P_1 - \sqrt{P_3^2 - (X - P_2)^2} \quad (\text{D-2})$$

For ISHAPE(J) = 3

$$Y = P_1 + \sqrt{P_3^2 - (X - P_2)^2} \quad (\text{D-3})$$

where Y is the profile ordinate and X the axial coordinate. The units of P_1 , P_2 and P_3 are such as to yield Y in centimeters when X is expressed in centimeters. For ISHAPE(J) = 2 or 3, the profile section is a circular arc, P_3 is the circle radius, and the circle center is at $X = P_2$, $Y = P_1$.

- (4) Printed images of the DATA cards produced.
- (5) A two-column table headed "nozzle profile," giving the x- and y-coordinates (in inches) of points on a section of the profile 6 inches long, beginning at XSTART. These are the same data that are represented in the plot output.

The punched output consists of 12 punched cards for each case. Their format is illustrated by the printed card images in the output for the sample problem. They consist of a comment card followed by an eleven-card DATA statement defining an array ZPn, where n is the profile index (equal to the NOZFIT input NØZZLE). The newly fitted profile can be incorporated into NATA by inserting this DATA statement into the block data routine BLKD1 and recompiling the routine. Note that n must be less than or equal to 20, and must be different from the indices of all the other profiles defined in BLKD1.

All of the entries in ZPn are floating-point numbers. Some of these values represent integers. To ensure rounding-down to the correct integer values, NOZFIT increases such values by 0.1 in the DATA statement. The entries in ZPn are all defined in Section 4.7.

The plot output consists of one plot per case, showing a section of the computed profile 6 inches long in the axial direction. The coordinate scales along the x and y axes are the same so that the shape is not distorted. The plot is a little larger than full scale.

D.4 NOZFIT Test Problem

The following pages (figures 88-93) present the printed output from a NOZFIT run on the IBM 360/75 at Avco Systems Division. The values of the input variables for this test problem are listed on the first page of the output. Figure 55 shows the plot produced.

NOZZLE PROFILE PARAMETERS

J	ATP	PARAM(1,J)	PARAM(2,J)	PARAM(3,J)
1	-7.918200E 00	3.654496E 00	-1.763268E-01	0.0
2	-7.69371E 00	4.738010E 00	-7.973334E 00	3.175000E-01
3	-7.446036E 00	-8.437203E 00	-1.732050E 00	0.0
4	-5.714959E 00	5.570952E 00	-5.521296E 00	2.222500E 00
5	-1.328252E-02	2.856915E 00	-9.748853E-02	0.0
6	0.0	3.009897E 00	0.0	1.524000E-01
7	3.944400E-02	3.009897E 00	0.0	1.524000E-01
8	2.852120E 00	2.67791E-01	0.0	

DATA CARDS PRODUCED

C 10MM 2.25-1INCH NOZZLE
 DATA ZP 9 / 2.85750, -8.00100, 6+1, 2+1,
 1+1, 3+1, 1+1, 2+1, 1+1, 2+1, 1+1, 0+1, 0+1, 0+1,
 2 -7.918200, -7.698371, -7.446036, -5.714999, -0.013263, 0.0
 3 0.039444, 0.0, 0.0, 0.0, 0.0, 0.0, 0.0, 0.0, 0.0, 0.0, 0.0, 0.0
 4 3.654496, -0.176327, 0.0, 4.738010, -7.973334, 0.317500, NOZ2 9
 5 -8.437203, -1.732050, 0.0, 5.570952, -5.521296, 2.222500, NOZ2 9
 6 2.856915, -0.087489, 0.0, 3.009897, 0.0, 0.152400, NOZ2 9
 7 3.009897, 0.0, 0.152400, 2.852120, 0.267949, 0.0, NOZ2 9
 8 0.0, 0.0, 0.0, 0.0, 0.0, 0.0, 0.0, 0.0, 0.0, 0.0, 0.0, 0.0, NOZ2 9
 9 0.0, 0.0, 0.0, 0.0, 0.0, 0.0, 0.0, 0.0, 0.0, 0.0, 0.0, 0.0, NOZ2 9
 A 4H10MM/

NOZZLE PROFILE

X (INCH)	Y (INCH)
-4.00E 00	2.144E 00
-3.97E 00	2.139E 00
-3.94E 00	2.134E 00
-3.91E 00	2.128E 00
-3.88E 00	2.123E 00
-3.85E 00	2.118E 00
-3.82E 00	2.112E 00
-3.79E 00	2.107E 00
-3.76E 00	2.102E 00
-3.73E 00	2.096E 00
-3.70E 00	2.091E 00
-3.67E 00	2.086E 00
-3.64E 00	2.091E 00
-3.61E 00	2.075E 00
-3.58E 00	2.070E 00
-3.55E 00	2.065E 00
-3.52E 00	2.059E 00
-3.49E 00	2.054E 00
-3.46E 00	2.049E 00
-3.43E 00	2.044E 00
-3.40E 00	2.038E 00
-3.37E 00	2.033E 00
-3.34E 00	2.028E 00

FIGURE 91 - OUTPUT OF NOZETT TEST PROBLEM (Third page)

-3.10E 00	2.022E 00
-2.280E 00	2.017E 00
-3.2250E 00	2.012C 00
+3.220E 00	2.007E 00
-3.190E 00	2.001E 00
-3.160E 00	1.996E 00
-3.130E 00	1.991E 00
-3.100E 00	1.984E 00
-3.070E 00	1.970E 00
-3.040E 00	1.942E 00
-3.010E 00	1.892E 00
-2.980F 00	1.840E 00
-2.9C 11 0	1.788E 00
-2.920U 11 0	1.736E 00
-2.830E CC	1.691E 00
-2.860E 00	1.650E 00
-2.832E 00	1.615E 00
-2.800E 00	1.582E 00
-2.770E 00	1.553E 00
-2.740E 00	1.526E 00
-2.710E 20	1.502E 00
-2.680E 00	1.480E 00
-2.650E 00	1.459E 00
-2.620E 00	1.441E 00
-2.590E 00	1.424F 00
-2.560E 00	1.408E 00
-2.530E 00	1.394F 00
-2.500E 00	1.381E 00
-2.470E 00	1.370F 00
-2.440E U	1.360E 00
-2.410E 00	1.351F 00
-2.380E 00	1.343E 00
-2.350E 00	1.336F 00
-2.320F 00	1.331E 00
-2.290E 00	1.326E 00
-2.260E 00	1.323F 00
-2.230E 00	1.320E 00
-2.200F 00	1.317F 00
-2.170E 00	1.315E 00
-2.140E 00	1.312F 00
-2.110E 00	1.309E 00
-2.080E 00	1.307E 00
-2.050E 00	1.304E 00
-2.020E 00	1.301F 00
-1.990E 00	1.299E 00
-1.960F 00	1.296E 00
-1.930E 00	1.294C 00
-1.900F 00	1.291E 00
-1.870E 00	1.288F 00
-1.840E 00	1.286E 00
-1.810E 20	1.283E 00
-1.780F 00	1.280E 00
-1.752E 00	1.278F 00
-1.720F 00	1.275E 00
-1.690L 00	1.273E 00
-1.660E 00	1.270F 00
-1.630E 00	1.267E 00
-1.600F 00	1.265F 00
-1.570F 00	1.262E 00
-1.540F 0C	1.260E 00
-1.510F 07	1.257E 00
-1.480C 30	1.254E 00
-1.450E 00	1.252E 00

ORIGINAL PAGE IS
OF POOR QUALITY

FIGURE 92 - OUTPUT OF NDF^{***}T TEST PROBLEM (Fourth Page)

1.420E 09	1.249E 00
1.390E 00	1.246E 00
-1.360E 00	1.244E 00
-1.330E 00	1.241E 00
-1.303E 00	1.239E 00
-1.270E 00	1.236E 00
-1.240E 00	1.233E 00
-1.210E 00	1.231E 00
-1.180E 00	1.228E 00
-1.150E 00	1.225E 00
-1.120E 00	1.223E 00
-1.090E 00	1.220E 00
-1.060E 00	1.218E 00
-8.803E 00	1.215E 00
-1.030E 00	1.202E 00
-1.000E 00	1.212E 00
-9.700F -01	1.210E 00
-9.400F -01	1.207E 00
-9.100E -01	1.204E 00
-8.800E -01	1.202E 00
-8.500E -01	1.199E 00
-5.200E -01	1.197E 00
-7.900E -01	1.194E 00
-7.600F -01	1.191E 00
-7.300E -01	1.189E 00
-7.000F -01	1.186E 00
-6.700E -01	1.183E 00
-6.400E -01	1.181E 00
-6.100E -01	1.178E 00
-5.800E -01	1.176E 00
-5.500E -01	1.173E 00
-5.200E -01	1.170E 00
-4.900E -01	1.168E 00
-4.600E -01	1.165E 00
-4.300F -01	1.162E 00
-4.000E -01	1.160E 00
-3.700E -01	1.157E 00
-3.400E -01	1.155E 00
-3.100F -01	1.152E 00
-2.800F -01	1.149E 00
-2.500F -01	1.147E 00
-2.200E -01	1.144E 00
-1.900F -01	1.141E 00
-1.600E -01	1.139E 00
-1.300E -01	1.136E 00
-1.000E -01	1.134E 00
-7.000E -02	1.131E 00
-4.000E -02	1.128E 00
-1.000E -02	1.126E 00
2.000E -02	1.128E 00
5.000E -02	1.136E 00
8.000E -02	1.144E 00
1.000F -01	1.152E 00
1.400E -01	1.160E 00
1.700F -01	1.168E 00
2.000E -01	1.176E 00
2.300F -01	1.185E 00
2.600F -01	1.193E 00
2.900E -01	1.201E 00
3.200E -01	1.209E 00
3.500E -01	1.217E 00
3.800E -01	1.225E 00
4.100E -01	1.233E 00
4.400E -01	1.241E 00

FIGURE 93 - OUTPUT OF NOZFFR TEST PROBLEM (Fifth Page)

4.700E-01	1.249E 00
5.75E-01	1.257E 00
5.300E-01	1.265E 00
5.600E-01	1.273E 00
5.900E-01	1.281E 00
6.200E-01	1.289E 00
6.500E-01	1.297E 00
6.800E-01	1.305E 00
7.100E-01	1.313E 00
7.400E-01	1.321E 00
7.700E-01	1.329E 00
8.000E-01	1.337E 00
8.300E-01	1.345E 00
8.600E-01	1.353E 00
4.900E-01	1.361E 00
9.200E-01	1.369E 00
9.500E-01	1.377E 00
9.800E-01	1.385E 00
1.010E 00	1.394E 00
1.040E 00	1.402E 00
1.070E 00	1.410E 00
1.100E 00	1.418E 00
1.130E 00	1.426E 00
1.160E 00	1.434E 00
1.190E 00	1.442E 00
1.220E 00	1.450E 00
1.250E 00	1.458E 00
1.280E 00	1.466E 00
1.310E 00	1.474E 00
1.340E 00	1.482E 00
1.370E 00	1.490E 00
1.400E 00	1.498E 00
1.430E 00	1.506E 00
1.460F 00	1.514E 00
1.490E 00	1.522E 00
1.520E 00	1.530E 00
1.550E 00	1.538E 00
1.580E 00	1.546E 00
1.610E 00	1.554E 00
1.640F 00	1.562E 00
1.670E 00	1.570E 00
1.700E 00	1.578E 00
1.730F 00	1.586E 00
1.760E 00	1.594E 00
1.790E 00	1.602E 00
1.820F 00	1.611E 00
1.850E 00	1.619E 00
1.880E 00	1.627E 00
1.910E 00	1.635E 00
1.940E 00	1.643E 00
1.970E 00	1.651E 00
2.000F 00	1.659E 00

ORIGINAL PAGE IS
OF POOR QUALITY

REFERENCES

1. Bade, W. L.; and Yos, J. M.: The NATA Code - Theory and Analysis, Volume I. NASA CR-2547.
2. Anon.: UNIVAC 1108 Multi-Processor System, Fortran V Programmer's Reference Manual. UNIVAC Federal Systems Division, Sperry Rand Corp.
3. Anon.: IBM System/360, FORTRAN IV Language. IBM Corp., Programming Publications (New York).
4. Lordi, J. A.; Mates, R. E.; and Moselle, J. R.: Computer Program for the Numerical Solution of Nonequilibrium Expansions of Reacting Gas Mixtures. NASA CR-472, 1966.
5. JANAF Thermochemical Data, Dow Chemical Co., Midland, Mich.
6. Moore, C. E.: Atomic Energy Levels. Nat. Bureau of Standards Circular 467, Vol. I. U. S. Government Printing Office, 1949.
7. Hodgman, C. D., ed.: Handbook of Chemistry and Physics. Chemical Rubber Publ. Co. (Cleveland).
8. Herzberg, G.: Molecular Spectra and Molecular Structure. I. Spectra of Diatomic Molecules. D. Van Nostrand Co. (New York), 1950.
9. Ginter, W. L.; and Brown, C. M.: Dissociation Energies of $X^2\Sigma_u^+$ (He_2^+) and A $^1\Sigma_u^+$ (He_2). J. Chem. Phys., vol. 56, no. 1, 1 Jan. 1972, pp. 672-674.
10. Predvoditelev, A. S., et al.: Tables of Thermodynamic Functions of Air for the Temperature Range 6000-12000°K and Pressure Range 0.001-1000 atm. Infosearch, Ltd. (London), 1958.
11. Herzberg, G.: Molecular Spectra and Molecular Structure. III. Electronic Spectra and Electronic Structure of Polyatomic Molecules. D. Van Nostrand Co. (New York), 1966, p. 598.

12. Ginter, M. L.; and Ginter, D. S.: Spectrum and Structure of the He_2 Molecule. V. Characterization of the Triplet States Associated with the UAO's 6-17 $\mu\pi$ and 7-12 $\mu\sigma$. *J. Chem. Phys.*, vol. 48, no. 5, 1 Mar. 1968, pp. 2284-2291.
13. Teng, H. H.; and Conway, D. C.: Ion-Molecule Equilibria in Mixtures of N_2 and Ar. *J. Chem. Phys.*, vol. 59, no. 5, 1 Sept. 1973, pp. 2316-2323.
14. Kang, S.-W.; Dunn, M. G.; and Jones, W. L.: Theoretical and Measured Electron-Density Distributions for the RAM Vehicle at High Altitudes. AIAA Paper No. 72-689, 1972.
15. Dunn, M. G.: Experimental Plasma Studies. NASA CR-1958, 1972.
16. McKenzie, R. L.; and Arnold, J. O.: Experimental and Theoretical Investigations of the Chemical Kinetics and Non-equilibrium CN Radiation Behind Shock Waves in CO_2 - N_2 Mixtures. AIAA Paper No. 67-322, 1967.
17. Wray, K.L.: Chemical Kinetics of High Temperature Air. Hypersonic Flow Research, F. Riddell, ed., Academic Press, 1962, pp. 181-204.
18. Dunn, M. G.; and Treanor, C. E.: Electron and Ion Chemistry in Flow Fields, J. Defense Research, Section A (Strategic Warfare), Spring 1970, pp. 23-52.
19. Bowen, S. W.; and Park, C.: Computer Study of Nonequilibrium Excitation in Recombining Nitrogen Plasma Nozzle Flows. *AIAA J.*, vol. 9, no. 3, Mar. 1971, pp. 493-499.
20. Monchick, L.: Collision Integrals for the Exponential Repulsive Potential. *Phys. Fluids*, vol. 2, no. 6, Nov.-Dec. 1959, pp. 595-700.
21. Kihara, T; Taylor M. H.; and Hirschfelder, J. O.: Transport Properties for Gases Assuming Inverse Power Molecular Potentials. *Phys. Fluids*, vol. 3, no. 5, Sept.-Oct. 1960, pp. 715-720.
22. Yos. J. M.: Transport Properties of Nitrogen, Hydrogen, Oxygen, and Air to 30,000°K. Rep. RAD-TM-63-71 Avco Research and Advanced Development Division, Mar. 1963.

23. Yos, J. M.: Theoretical and Experimental Studies of High-Temperature Gas Transport Properties. Rep. RAD-TR-65-7, Avco Research and Advanced Development Division, 1965, Section III.
24. Massey, H. S. W.; and Burhop, E. H. S.: Electronic and Ionic Impact Phenomena. Clarendon Press (Oxford), 1952.
25. Pack, J. L.; and Phelps, A. V.: Drift Velocities of Slow Electrons in Helium, Neon, Argon, Hydrogen, and Nitrogen. Phys. Rev., vol. 121, no. 3, 1 Feb. 1961, pp. 798-806.
26. Kivel, B.: Elastic Scattering of Low Energy Electrons by Argon. Phys. Rev., vol. 116, no. 4, 15 Nov. 1959, pp. 926-927.
27. Kivel, B.: Electron Scattering by Noble Gases in the Limit of Zero Energy. Phys. Rev., vol. 116, no. 6, 15 Dec. 1959, pp. 1484-1485.
28. O'Malley, T. F.: Extrapolation of Electron-Rare Gas Atom Cross Sections to Zero Energy. Phys. Rev., vol. 130, no. 3, 1 May 1963, pp. 1020-1029.
29. Pack, J. L.; Voshall, R. E.; and Phelps, A. V.: Drift Velocities of Slow Electrons in Krypton, Xenon, Deuterium, Carbon Monoxide, Carbon Dioxide, Water Vapor, Nitrous Oxide, and Ammonia. Phys. Rev., vol. 127, no. 6, 15 Sept. 1962, pp. 2084-2089.
30. Cooper, J. W.; and Martin, J. B.: Electron Photodetachment from Ions and Elastic Cross Sections for O, C, Cl, and F. Phys. Rev., vol. 126, no. 4, 15 May 1962, pp. 1482-1488.
31. Amdur, I.; Mason, E. A.; and Jordan, J. E.: Scattering of High Velocity Neutral Particles. X. He-N₂; A-N₂. The N₂-N₂ Interaction. J. Chem. Phys., vol. 27, no. 2, Aug. 1957, pp. 527-531.
32. Amdur, I.; and Mason, E. A.: Scattering of High-Velocity Neutral Particles, III. Argon-Argon. J. Chem. Phys., vol. 22, no. 4, Apr. 1954, pp. 670-671.
33. Cloney, R. D.; Mason, E. A.; and Vanderslice, J. T.: Binding Energy of Ar₂⁺ from Ion Scattering Data. J. Chem. Phys. vol. 36, no. 4, 15 Feb. 1962, pp. 1103-1104.

34. Vanderslice, J. T.; Mason, E. A.; and Lippincott, E. R.: Interactions Between Ground State Nitrogen Atoms and Molecules. The N-N, N-N₂, and N₂-N₂ Interactions. *J. Chem. Phys.*, vol. 30, no. 1, Jan. 1959, pp. 129-136.
35. Vanderslice, J. T.; Mason, E. A.; and Maisch, W. G.: Interactions Between Oxygen and Nitrogen: O-N, O-N₂, and O₂-N₂. *J. Chem. Phys.*, vol. 31, no. 3, Sept. 1959, pp. 738-746.
36. Vanderslice, J. T.; Mason, E. A.; and Maisch, W. G.: Interactions Between Ground State Oxygen Atoms and Molecules: O-O and O₂-O₂. *J. Chem. Phys.*, vol. 32, no. 2, Feb. 1960, pp. 515-524.
37. Vanderslice, J. T.; Mason, E. A.; Maisch, W. G.; and Lippencott, E. R.: Potential Curves for N₂, NO, and O₂. *J. Chem. Phys.*, vol. 33, no. 2, Aug. 1960, pp. 614-615.
38. Fallon, R. J.; Vanderslice, J. T.; and Cloney, R. D.: Potential Curves and Rotational Perturbations of CN. *J. Chem. Phys.*, vol. 37, no. 5, 1 Sept. 1962, pp. 1097-1100.
39. Tobias, I.; Fallon, R. J.; and Vanderslice, J. T.: Potential Energy Curves for CO. *J. Chem. Phys.*, vol. 33, no. 6, Dec. 1960, pp. 1638-1640.
40. Read, S. M.; and Vanderslice, J. T.: Potential Energy Curves for C₂. *J. Chem. Phys.*, vol. 36, no. 9, 1 May 1962, pp. 2366-2369.
41. Clementi, E.: Accurate Partition Functions in the Determination of the C₂ Abundance. *Astrophys. J.*, vol. 133, no. 1, Jan. 1961, pp. 303-308.
42. Amdur, I.; and Shuler, L. M.: Diffusion Coefficients of the Systems CO-CO and CO-N₂. *J. Chem. Phys.*, vol. 38, no. 1, 1 Jan. 1963, pp. 188-192.
43. Walker, R. E.; and Westenberg, A. A.: Molecular Diffusion Studies in Gases at High Temperature. II. Interpretation of Results on the He-N₂ and CO₂-N₂ Systems. *J. Chem. Phys.*, vol. 29, no. 5, Nov. 1958, pp. 1147-1153.

44. Walker, R. E.; and Westenberg, A. A.: Molecular Diffusion Studies in Gases at High Temperature. IV. Results and Interpretation of the $\text{CO}_2\text{-O}_2$, $\text{CH}_4\text{-O}_2$, $\text{H}_2\text{-O}_2$, $\text{CO}\text{-O}_2$ and $\text{H}_2\text{O}\text{-O}_2$ Systems. *J. Chem. Phys.*, vol. 32, no. 2, Feb. 1960, pp. 436-442.
45. Ember, G.; Ferron, J. R.; and Wohl, K.: Self-Diffusion Coefficients of Carbon Dioxide at $1180^\circ\text{-}1680^\circ\text{K}$. *J. Chem. Phys.*, vol. 37, no. 4, 15 Aug. 1962, pp. 891-897.
46. Weissman, S.; and Mason, E. A.: Note on the Viscosity of $\text{N}_2\text{-CO}_2$ Mixtures. *Physica*, vol. 26, 1960, pp. 531-532.
47. Hirschfelder, J. O.; Curtiss, C. F.; and Bird, R. B.: Molecular Theory of Gases and Liquids. John Wiley and Sons, 1954.
48. Mason, E. A.; and Rice, W. E.: The Intermolecular Potentials for Some Simple Nonpolar Molecules. *J. Chem. Phys.*, vol. 22, no. 5, May 1954, pp. 843-851.
49. Blais, N. C.; and Mann, J. B.: Thermal Conductivity of Helium and Hydrogen at High Temperatures. *J. Chem. Phys.*, vol. 32, no. 5, May 1960, pp. 1459-1465.
50. Fallon, R. J.; Mason, E. A.; and Vanderslice, J. T.: Energies of Various Interactions Between Hydrogen and Helium Atoms and Ions. *Astrophys. J.*, vol. 131, no. 1, Jan. 1960, pp. 12-14.
51. Appleton, J. P.; and Bray, K. N. C.: The Conservation Equations for a Nonequilibrium Plasma. *J. Fluid Mech.*, vol. 20, no. 4, Dec. 1964, pp. 659-672.
52. Crompton, R. W.; Elford, M. T.; and Robertson, A. G.: The Momentum Transfer Cross Section for Electrons in Helium Derived from Drift Velocities at 77°K . *Austral. J. Phys.*, vol. 23, no. 5, Oct. 1970, pp. 667-681.
53. LaBahn, R. W.; and Callaway, J.: Differential Cross Sections for the Elastic Scattering of 1- to 95-ev Electrons from Helium. *Phys. Rev. A*, vol. 2, no. 2, Aug. 1970, pp. 366-369.
54. Gricm, H. R.: Plasma Spectroscopy. McGraw-Hill Book Co., 1964.

55. Bates, D. R.; Kingston, A. E.; and McWhirter, R. W. P.: Recombination Between Electrons and Atomic Ions. I. Optically Thin Plasmas. Proc. Roy. Soc., Series A, vol. 267, no. 1330, 22 May 1962, pp. 297-312.
56. Bates, D. R.; and Khare, S. P.: Recombination of Positive Ions and Electrons in a Dense Neutral Gas. Proc. Phys. Soc., vol. 85, part 2, Feb. 1965, pp. 231-243.
57. Bates, D. R.; Bell, K. L.; and Kingston, A. E.: Excited Atoms in Decaying Optically Thick Plasmas. Proc. Phys. Soc., vol. 91, part 2, June 1967, pp. 288-299.
58. Johnson, L. C.; and Hinnov, E.: Rates of Electron Impact Transitions Between Excited States of Helium. Rep. no. MATT-610, Princeton Univ. Plasma Physics Laboratory, July 1969.
59. Hinnov, E.; and Herschberg, J. G.: Electron-Ion Recombination in Dense Plasmas. Phys. Rev., vol. 125, no. 3, 1 Feb. 1962, pp. 795-801.
60. Collins, C. B.; Hicks, H. S.; Wells, W. E; and Burton, R.: Measurement of the Rate Coefficient for the Recombination of He^+ with Electrons, Phys. Rev. A, vol. 6, no. 4, Oct. 1972, pp. 1545-1558.
61. Bates, D. R.; and Kingston, A. E.: Recombination and Energy Balance in a Decaying Plasma. II. $\text{He}-\text{He}^+-\text{e}$ Plasma. Proc. Roy. Soc., Series A, vol. 279, no. 1376, 12 May 1964, pp. 32-38.
62. Bates, D. R.; and Dalgarno, A.: Electronic Recombination. Atomic and Molecular Processes, D. R. Bates, ed., Academic Press, 1962, pp. 245-271.
63. Burgess, A.; and Seaton, M. J.: A General Formula for the Calculation of Atomic Photo-Ionization Cross Sections. Monthly Not. Roy. Astron. Soc., vol. 120, no. 2, 1960, pp. 121-151.
64. Schulz, G. J.; and Fox, R. E.: Excitation of Metastable Levels in Helium Near Threshold. Phys. Rev., vol. 106, no. 6, 15 June 1957, pp. 1179-1181.

65. Moiseiwitsch, B. L.; and Smith, S. J.: Electron Impact Ionization of Atoms. *Rev. Mod. Phys.*, vol. 40, no. 2, Apr. 1968, pp. 238-353.
66. Rice, J. K.; Truhlar, D. G.; Cartwright, D. C.; and Trajmar, S.: Effect of Charge Polarization on Inelastic Scattering: Differential and Integral Cross Sections for Excitation of the 2^1S State of Helium by Electron Impact. *Phys. Rev. A*, vol. 5, no. 2, Feb. 1972, pp. 762-782.
67. Phelps, A. V.: Absorption Studies of Helium Metastable Atoms and Molecules. *Phys. Rev.*, vol. 99, no. 4, 15 Aug. 1955, pp. 1307-1313.
68. Dalgarno, A.; and Kingston, A. E.: Van der Waals Forces. *Proc. Phys. Soc.*, vol. 73, part 3, Mar. 1959, pp. 455-464.
69. Massey, H.S. W.; Burhop, E. H. S.; and Gilbody, H. B.: Electronic and Ionic Impact Phenomena. Second ed., vol. III, Clarendon Press (Oxford), 1969.
70. Ginter, M. L.: Spectrum and Structure of the He_2 Molecule. I. Characterization of the States Associated with the UAO's 3 $p\sigma$ and 3s. *J. Chem. Phys.*, vol. 42, no. 2, 15 Jan. 1965, pp. 561-568.
71. Beaty, E. C.; and Patterson, P. L.: Mobilities and Reaction Rates of Ions in Helium. *Phys. Rev.*, vol. 137, no. 2A, 18 Jan. 1965, pp. A346-A357.
72. Niles, F. E.; and Robertson, W. W.: Temperature Dependence of the Rate of Conversion of He^+ into He_2^+ . *J. Chem. Phys.*, vol. 42, no. 9, 1 May 1965, pp. 3277-3280.
73. Gerber, R. A.; Sauter, G. F.; and Oskam, H. J.: Studies of Decaying Helium Plasmas. *Physica*, vol. 32, no. 11/12, Nov.-Dec. 1966, pp. 2173-2191.
74. Wellenstein, H. F. and Robertson, W. W.: Collisional Relaxation Processes for the $n = 3$ States of Helium. II. Associative Ionization. *J. Chem. Phys.*, vol. 66, no. 3, 1 Feb. 1972.
75. Bardsley, J. N.; and Biondi, M. A.: Dissociative Recombination. *Advances in Atomic and Molecular Physics*, D. R. Bates and I. Esterman, eds., vol. 6, Academic Press, 1970, pp. 1-57.

76. Johnson, A. W.; and Gerardo, J. B.: Electronic Recombination Coefficient of Molecular Helium Ions. *Phys. Rev. Letters*, vol. 27, no. 13, 27 Sept. 1971, pp. 835-838.
77. Berlande, J.; Cheret, M.; Deloche, R.; Gonfaloni, A.; and Manus, C.: Pressure and Density Dependence of the Electron-Ion Recombination Coefficient in Helium. *Phys. Rev. A*, vol. 1, no. 3, Mar. 1970, pp. 887-896.
78. Born, G. K.: Recombination of Electrons and Molecular Helium Ions. *Phys. Rev.*, vol. 169, no. 1, 5 May 1968, pp. 155-164.
79. Jordan, J. E.; and Amdur, I.: Scattering of High-Velocity Neutral Particles. XIV. He-He Interactions Below 1.1 Å. *J. Chem. Phys.*, vol. 46, no. 1, 1 Jan. 1967, pp. 165-183.
80. Mulliken, R. S.: Rare-Gas and Hydrogen Molecule Electronic States, Noncrossing Rule, and Recombination of Electrons with Rare-Gas and Hydrogen Ions. *Phys. Rev.*, vol. 136, no. 4A, 16 Nov. 1964, pp. A962-A965.
81. Collins, C. B.: Chemistry of the Low Pressure Helium Afterglow. Ninth International Conf. on Phenomena in Ionized Gases, Bucharest, Romania, Sept. 1-6, 1969, Editura Academiei Republicii Socialiste România, p. 51.
82. Stevefelt, J.: The Decay of Optically Thick Helium Plasmas Taking Into Account Ionizing Collisions Between Metastable Atoms or Molecules. *J. Physics D: Appl. Phys.*, vol. 4, no. 7, July 1971, pp. 899-906.
83. Frost, L. S.; and Phelps, A. V.: Momentum Transfer Cross Sections for Slow Electrons in He, Ar, Kr, and Xe from Transport Coefficients. *Phys. Rev.*, vol. 136, no. 6A, 14 Dec. 1964, pp. A1538-A1545.
84. Golden, D. E.: Comparison of Low-Energy Total and Momentum Transfer Scattering Cross Sections for Electrons on Helium and Argon. *Phys. Rev.*, vol. 151, no. 1, 4 Nov. 1966, pp. 48-51.
85. Celotta, R.; Brown, H.; Molof, R.; and Bederson, B.: Measurements of the Total Cross Section for the Scattering of Low-Energy Electrons by Metastable Argon. *Phys. Rev. A*, vol. 3, no. 5, May 1971, pp. 1622-1628.

86. Robinson, E. J.: Electron Scattering by the Metastable Rare Gases. *Phys. Rev.*, vol. 182, no. 1, 5 June 1969, pp. 169-200.
87. Biberman, L. M.; Yakubov, I. T.; and Vorobev, V. S.: Kinetics of Collisional-Radiation Recombination and Ionization in Low-Temperature Plasma. *Proc. IEEE*, vol. 59, no. 4, April 1971, pp. 555-572.
88. Funahashi, A.; and Takeda, S.: Three-Body Electron-Ion Recombination in Argon Plasmas. *J. Phys. Soc. Japan*, vol. 25, no. 1, July 1968, pp. 298-299.
89. Gusinow, M. A.; Gerado, J. B.; and Kerdey, J. T.: Investigation of Electronic Recombination in Helium and Argon Afterglow Plasmas by Means of Laser Interferometric Measurements. *Phys. Rev.*, vol. 149, no. 1, 9 Sept. 1966, pp. 91-96.
90. Lee, J. B.; and Incropera, F. P.: Spectral Distribution of Radiation from the Cascade Arc Plasma. *J. Quant. Spectrosc. Radiat. Transfer*, vol. 13, no. 12, Dec. 1973, pp. 1539-1552.
91. Morris, J. C.; and Yos, J. M.: Radiation Studies of Arc Heated Plasmas. ARL 71-0317, Dec. 1971.
92. Dobbins, R. A.: Precursor Photoexcitation and Photoionization of Argon in Shock Tubes. *AIAA J.*, vol. 8, no. 3, Mar. 1970, pp. 407-414.
93. Samson, J. A. R.: Experimental Photoionization Cross Sections in Argon from Threshold to 280 Å. *J. Opt. Soc. Am.*, vol. 54, no. 3, Mar 1964, pp. 420-421.
94. Chen, C. J.: Collisional-Radiative Electron-Ion Recombination Rate in Rare-Gas Plasmas. *J. Chem. Phys.*, vol. 50, no. 4, 15 Feb. 1969, pp. 1560-1566.
95. Petschek, H.; and Byron, S.: Approach to Equilibrium Ionization Behind Strong Shock Waves in Argon. *An. Phys.*, vol. 1, no. 3, June 1957, pp. 270-315.
96. Wong, H.; and Bershadsky, D.: Thermal Equilibration Behind an Ionizing Shock. *J. Fluid Mech.*, vol. 26, part 3, Nov. 1966, pp. 459-480.
97. Merila, M.; and Morgan, E. J.: Total Ionization Times in Shock-Heated Noble Gases. *J. Chem. Phys.*, vol. 52, no. 2, 1 Mar. 1970, pp. 2192-2198.

98. Pichanick, F. M. J.; and Simpson, J. A.: Resonances in the Total Cross Sections for Metastable Excitation of Noble Gases by Electron Impact. *Phys. Rev.*, vol. 168, no. 1, 5 Apr. 1968, pp. 64-70.
99. Olmstead, J.; Newton, A. S.; and Street, K.: Determination of the Excitation Functions for Formation of Metastable States of Some Rare Gases and Diatomic Molecules by Electron Impact. *J. Chem. Phys.*, vol. 42, no. 7, Apr. 1965, pp. 2321-227.
100. Borst, W. L.: Excitation of Metastable Argon and Helium Atoms by Electron Impact. *Phys. Rev. A*, vol. 9, no. 3, Mar. 1974, pp. 1195-1200.
101. Lloyd, C. R.; Weigold, E.; Teubner, P. J. O.; and Hood, S. T.: Excitation Functions for the Formation of Metastable He and Ar by Electron Impact. *J. Phys. B*, vol. 5, no. 9, Sept. 1972, pp. 1712-1718.
102. McConkey, J. W.; and Donaldson, F. G.: Excitation of the Resonance Lines of Ar by Electrons. *Can. J. Phys.*, vol. 51, no. 9, 1 May 1973, pp. 914-921.
103. LeCalvé, J. ; and Bourène, M.: Pulse Radiolysis Study of Argon-Nitrogen Mixtures. Measurement of the Rate Constant of Metastable Argon De-excitation by Nitrogen. *J. Chem. Phys.*, vol. 58, no. 4, 15 Feb. 1973, pp. 1446-1451.
104. Phelps, A. V.: Diffusion, De-excitation, and Three-Body Collision Coefficients for Excited Neon Atoms. *Phys. Rev.*, vol. 114, no. 4, 15 May 1959, pp. 1011-1025.
105. Holstein, T.: Imprisonment of Resonance Radiation in Gases. *Phys. Rev.*, vol. 72, no. 12, 15 Dec. 1947, pp. 1212-1233.
106. Holstein, T.: Imprisonment of Resonance Radiation in Gases. II. *Phys. Rev.*, vol. 83, no. 6, 15 Sept. 1951, pp. 1159-1168.
107. Ellis, E.; and Twiddy, N. D.: Time-Resolved Optical Absorption Measurements of Excited-Atom Concentrations in the Argon Afterglow. *J. Phys. B (Atom. Molec. Phys.)*, vol. 2, no. 12, Dec. 1969, pp. 1366-1377.

108. Phelps, A. V.; and McCoubrey, A. O.: Experimental Verification of the "Incoherent Scattering" Theory for the Transport of Resonance Radiation. *Phys. Rev.*, vol. 118, no. 6, 15 June 1960, pp. 1561-1565.
109. Breene, R. G., Jr.: Line Width. *Handbuch der Physik*, S. Flugge, ed., vol. XXVII, Springer-Verlag, 1964, pp. 1-79.
110. Copley, G. H.; and Camm, D. M.: Pressure Broadening and Shift of Argon Emission Lines. *J. Quant. Spectroscop. Radiat. Transfer*, vol. 14, no. 9, Sept. 1974, pp. 899-907.
111. Wiese, W. L.; Smith, M. W.; and Miles, B. M.: Atomic Transition Probabilities, Vol. II. Sodium Through Calcium. *Nat. Bur. Stand. (U.S.)*, NSRDS-NBS 22, Oct. 1969.
112. Phelps, A. V.; and Molnar, J. P.: Lifetimes of Metastable States of Noble Gases. *Phys. Rev.*, vol. 89, no. 6, 15 Mar. 1953, pp. 1202-1208.
113. Futch, A. H.; and Grant, F. A.: Mean Life of the 3P_2 Metastable Argon Level. *Phys. Rev.*, vol. 104, no. 2, 15 Oct. 1956, pp. 356-361.
114. Harwell, K. E.; and Jahn, R. G.: Initial Ionization Rates in Shock-Heated Argon, Krypton and Xenon. *Phys. Fluids.*, vol. 7, no. 2, Feb. 1964, pp. 214-222.
115. Kelly, A. J.: Atom-Atom Ionization Cross Sections of the Noble Gases - Argon, Krypton, Xenon. *J. Chem. Phys.*, vol. 45, no. 5, 1 Sept. 1966, pp. 1723-1732.
116. McLaren, T. I.; and Hobson, R. M.: Initial Ionization Rates and Collision Cross Sections in Shock-Heated Argon. *Phys. Fluids*, vol. 11, no. 10, Oct. 1968, pp. 2162-2172.
117. Schneider, K. P.; and Gronig, H.: Ionization Measurements Behind Shocks in Argon with Microwaves and a Pulsed Langmuir Probe. *Z. Naturforsch.*, vol. 27A, no. 12, Dec. 1972, pp. 1717-1730.
118. Kochler, H. A.; Forderher, L. J.; Redhead, D. L.; and Ebert, P. J.: Vacuum-Ultraviolet Emission from High-Pressure Xenon and Argon Excited by High-Current Relativistic Electron Beams. *Phys. Rev. A*, vol. 9, no. 2, Feb. 1974, pp. 768-781.

119. Huffman, R. E.; and Katayama, D. H.: Photoionization Study of Diatomic-Ion Formation in Argon, Krypton, and Xenon. *J. Chem. Phys.*, vol. 45, no. 1, 1 July 1966, pp. 138-146.
120. Kebarle, P.; Haynes, R. M.; and Searles, S. K.: Mass-Spectrometric Study of Ions in Xe, Kr, Ar, Ne at Pressures up to 40 Torr: Termolecular Formation of the Rare-Gas Molecular Ions. Bond Dissociation Energy of Ar_2^+ and Ne_2^+ . *J. Chem. Phys.*, vol. 47, no. 5, 1 Sept. 1967, pp. 1684-1691.
121. Mulliken, R. S.: Potential Curves of Diatomic Rare-Gas Molecules and Their Ions, with Particular Reference to Xe_2 . *J. Chem. Phys.*, vol. 52, no. 10, 15 May 1970, pp. 5170-5180.
122. O'Malley, T. F.; Cunningham, A. J.; and Hobson, R. M.: Dissociative Recombination at Elevated Temperatures. II. Comparison Between Theory and Experiment in Neon and Argon Afterglows. *J. Phys. B*, vol. 5 no. 11, Nov. 1972, pp. 2126-2133.
123. LeRoy, R. J.: Improved Spectroscopic Dissociation Energy for Ground-State Ar_2 . *J. Chem. Phys.*, vol. 57, no. 1, 1 July 1972, pp. 573-574.
124. Liu, W. F.; and Conway, D. C.: Ion-Molecule Reaction Rates in Ar at 293°K. *J. Chem. Phys.*, vol. 60, no. 3, 1 Feb. 1974, pp. 784-792.
125. Bhattacharya, A. K.: Mass Spectrometric Study of Argon Afterglow Plasmas. *J. Appl. Phys.*, vol. 41, no. 5, 15 Mar. 1970, pp. 1707-1710.
126. Smith, D.; Dean, A. G.; and Plumb, I. C.: Three-Body Conversion Reactions in Pure Rare Gases. *J. Phys. B*, vol. 5, no. 11, Nov. 1972, pp. 2134-2142.
127. Chen, C. J.: Temperature Dependence of Dissociative Recombination and Molecular-Ion Formation in He, Ne, and Ar Plasmas. *Phys. Rev.*, vol. 177, no. 1, 5 Jan. 1969, pp. 245-254.
128. Smith, D.; and Cromey, P. R.: Conversion Rates and Ion Mobilities in Pure Neon and Argon Afterglow Plasmas. *J. Phys. B*, vol. 1, no. 4, July 1968, pp. 638-649.
129. Becker, P. M.; and Lampe, F. W.: Mass-Spectrometric Study of the Bimolecular Formation of Diatomic Argon Ion. *J. Chem. Phys.*, vol. 42, no. 11, 1 June 1965, pp. 3857-3863.

30. Mehr, F. J.; and Biondi, M. A.: Electron-Temperature Dependence of Electron-Ion Recombination in Argon. Phys. Rev., vol. 176, no. 1, 5 Dec. 1968, pp. 322-326.

ORIGINAL PAGE IS
OF POOR QUALITY